

Dissertation ETH No. 18617

**Ruthenium(IV) Catalyzed Allylation Using Allyl Alcohols as  
Substrates**

A dissertation submitted to the  
SWISS FEDERAL INSTITUTE OF TECHNOLOGY ZURICH

for the degree of  
Doctor of Sciences

presented by

**Stefan Gruber**

M.Sc. ETH in Chemie

born on February 14<sup>th</sup>, 1982

citizen of St. Niklaus, VS

accepted on the recommendation of

Prof. Dr. P. S. Pregosin, examiner

Prof. Dr. A. Togni, co-examiner

Zurich, 2009



Für meine Freundin und meine Eltern



“Inmitten der Schwierigkeiten liegt die Möglichkeit“

*Albert Einstein*



## Acknowledgments

Thanks are given to all the people who have helped and supported me during the completion of this thesis.

I am grateful to my supervisor, *Prof. Dr. Paul S. Pregosin*, for giving me the opportunity to carry out my Ph.D. in his group. I thank him for his guidance and patience, I feel well prepared for everything that I will encounter in the future.

I wish to thank *Prof. Dr. Antonio Togni* for agreeing to be my co-examiner.

I thank all present and former members of the Pregosin group (*Alexey, Nacho, Aitor, René, Danièle, Deva* and *Helen*) for the great time we shared and for the assistance everyone gave me during my Ph.D.

Several parts of the projects described in this thesis were carried out as teamwork. Consequently, I am deeply indebted to *Dr. Alexey Zaitsev* for the collaboration and helpful discussions.

I am grateful to *Dr. Heinz Rügger* (†) for all the practical and theoretical support with respect to NMR techniques.

I thank *Dr. Michael Würle* for the introduction and the assistance in solving X-ray structures.

Thanks to *Prof. Dr. Luis F. Veiros* for performing the DFT calculations.

I also thank my colleagues *Roger* and *Martin* for the mainly not chemistry based discussions during lunch time.

*Meinen Eltern* danke ich für die moralische und finanzielle Unterstützung während meines gesamten Studiums.

Und zu guter Letzt danke ich meiner Freundin *Corinne* für ihre bedingungslose Unterstützung und für die abwechslungsreiche Zeit ausserhalb der ETH.





## Publications and Presentations

### Publications

“Allylic Alcohols as Substrate for Ruthenium-Catalyzed C-C Coupling Allylation Reactions.” I. F. Nieves, D. Schott, S. Gruber, P. S. Pregosin, *Helvetica Chimica Acta*, **2007**, *90*, 271-276.

“Fast, efficient Ru(IV)-catalysed regioselective allylation of indoles using allyl alcohol (without additives) under mild conditions.” A. B. Zaitsev, S. Gruber, P. S. Pregosin, *Chem. Commun.*, **2007**, *44*, 4692-4693.

“Facile Ruthenium(IV)-Catalyzed Single and Double Allylation of Indole Compounds using Alcohols as Substrates: Aspects of Ruthenium(IV) Allyl Chemistry.” S. Gruber A. B. Zaitsev, M. Wörle, P. S. Pregosin, L. F. Veiros, *Organometallics*, **2008**, *27*, 3796-3805.

“Fast and Highly Regioselective Allylation of Indole and Pyrrole Compounds by Allyl Alcohols Using Ru-Sulfonate Catalysts.” A. B. Zaitsev, S. Gruber, P. A. Plüss, P. S. Pregosin, L. F. Veiros, M. Wörle, *J. Am. Chem. Soc.*, **2008**, *130*, 11604-11605.

“Rapid Selective Ru-Sulfonate-Catalyzed Allylation of Indoles Using Alcohols as Substrates.” S. Gruber, A. B. Zaitsev, M. Wörle, P. S. Pregosin, *Organometallics*, **2009**, *28*, 3437-3448.

“Ruthenium Catalyzed Selective Regio- and Mono-Allylation of 1,3-Diketones Using Allyl Alcohols as Substrates.” S. Gruber, P. S. Pregosin, *Adv. Synth. Catal*, **2009**, submitted.

### Contributions in form of an oral presentation

Minisymposium of the Laboratory of Inorganic Chemistry 2008, Zurich, Switzerland, “Ruthenium(IV)-Catalyzed Allylation of Indoles with Allyl Alcohols and Related Ruthenium(IV) Organometallic Complexes”, S. Gruber, A. B. Zaitsev and P. S. Pregosin.

## **Contributions in form of poster presentations**

9<sup>th</sup> FIGIPAS Meeting in Inorganic Chemistry 2007, Vienna, Austria, "Efficient Ruthenium(IV)-Catalyzed Allylation of Indoles with Allyl Alcohols", S. Gruber, A. B. Zaitsev and P. S. Pregosin.

Swiss Chemical Society Fall Meeting 2007, Lausanne, Switzerland, "Efficient Ruthenium(IV)-Catalyzed Allylation of Indoles with Allyl Alcohols", S. Gruber, A. B. Zaitsev and P. S. Pregosin.

Swiss Chemical Society Fall Meeting 2008, Zurich, Switzerland, "Ruthenium(IV)-Catalyzed Allylation of Indoles. A New Unexpected Ruthenium(IV) S-shaped Allyl Complex", S. Gruber, A. B. Zaitsev and P. S. Pregosin.

2<sup>nd</sup> EuChMS Chemistry Congress 2008, Torino, Italy, "Ruthenium(IV)-Catalyzed Allylation of Indoles. A New Unexpected Ruthenium(IV) S-shaped Allyl Complex", S. Gruber, A. B. Zaitsev and P. S. Pregosin.

# Table of Contents

Summary	i
Zusammenfassung	iii
<b>1. Introduction</b>	
1.1. History and Characteristics of Ruthenium	2
1.2. Organometallic Chemistry of Ruthenium	2
1.2.1. Hydrogenation and Transfer Hydrogenation	3
1.2.2. Metathesis	6
1.2.3. C-C Bond Formation	8
1.2.4. Hydroamination	9
1.2.5. Isomerisation	10
1.2.6. Kinetic Resolution	11
1.3. Transition-Metal Catalyzed Allylations	12
1.3.1. Ruthenium Catalyzed Allylations	16
1.3.2. Ruthenium-Cp* Catalyzed C-C Bond Allylations	18
1.4. Objective of this thesis	22
1.5. References	23
<b>2. Synthesis and Characterisation of new Ruthenium-Cp* Complexes</b>	
2.1. Introduction	28
2.2. Results and Discussion	30
2.2.1. Ruthenium-Cp* Complexes with an $\eta^3$ -C <sub>3</sub> H <sub>5</sub> Moiety	30
2.2.2. Ruthenium-Cp* Complexes with an $\eta^3$ - or $\eta^5$ -Pentadienyl Moiety	35
2.3. Conclusions	48
2.4. References	50
<b>3. Allylation of Phenol Derivatives</b>	
3.1. Introduction	54
3.2. Results and Discussion	56
3.2.1. Allylation of 6-Bromonaphthalen-2-ol with Several Allyl Alcohols	56
3.2.2. Allylation of 2,6-Dimethylphenol with Several 1,3-Di-Aryl	

Allyl Alcohols	59
3.3. Conclusions	62
3.4. References	63
<b>4. Allylation of Indoles</b>	
4.1. Introduction	66
4.2. Results and Discussion	68
4.2.1. Catalysis Using $[\text{Ru}(\eta^3\text{-C}_3\text{H}_5)(\text{Cp}^*)(\text{MeCN})_2](\text{PF}_6)_2$	68
4.2.2. Catalysis Using Trost's Catalyst in Combination with Acids	76
4.2.3. Catalysis Using Several Isolated Complexes	86
4.2.4. NMR Measurement Experiments	87
4.2.5. Oxidative Addition Reactions to form Ruthenium(IV)-Allyl Complexes	89
4.2.6. DFT Studies	93
4.3. Conclusions	98
4.4. References	100
<b>5. Allylation of Cyclic 1,3-Diketones</b>	
5.1. Introduction	104
5.2. Results and Discussion	106
5.2.1. Allylation of Cyclic 1,3-Diketones with Allyl Alcohol	106
5.2.2. Allylation of Dimedone with Several Aryl Allyl Alcohols	109
5.3. Conclusions	112
5.4. References	114
<b>6. Experimental</b>	
6.1. General	116
6.1.1. Techniques and Chemicals	116
6.1.2. Analytical Techniques and Instruments	116
6.1.3. Synthesis of Substrates	117
6.2. Chapter 2: Synthesis and Characterisation of new Ruthenium-Cp* Complexes	123
6.3. Chapter 3: Allylation of Phenol Derivatives	129
6.4. Chapter 4: Allylation of Indoles	131

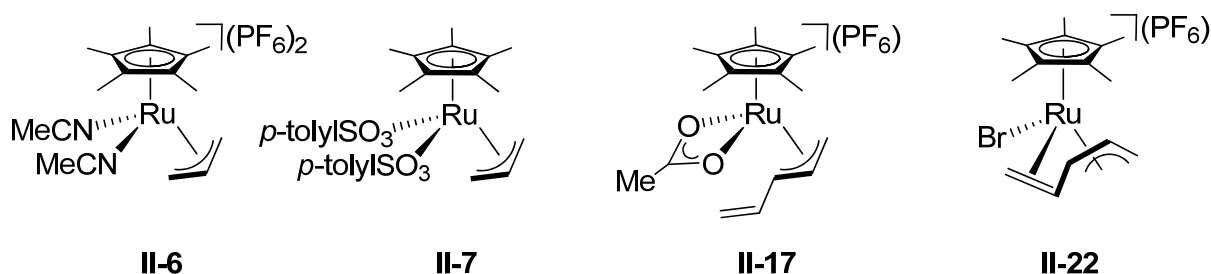
6.5.	Chapter 5: Allylation of Cyclic 1,3-Diketones	142
6.6.	NMR Tables	148
6.7.	References	158
<b>7. Appendix</b>		
7.1.	Abbreviations	162
7.2.	Crystallographic Data and Tables	164
7.3.	Curriculum Vitae	185



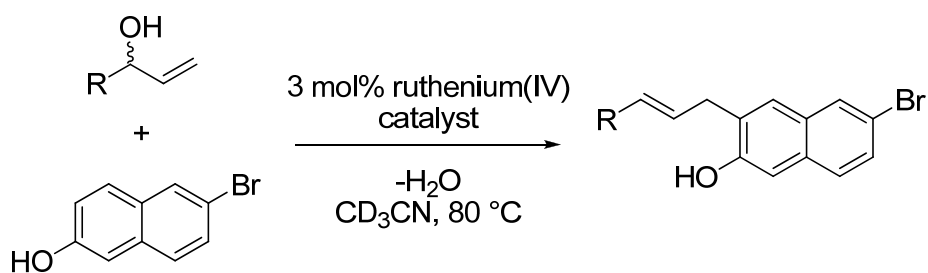
## Summary

This thesis describes the development and application of new ruthenium(IV)-allyl catalysts in several allylation reactions. These complexes are capable of employing allyl alcohols as substrates such that the leaving group is water. This avoids the production of unnecessary by-products by a “green chemistry reaction”.

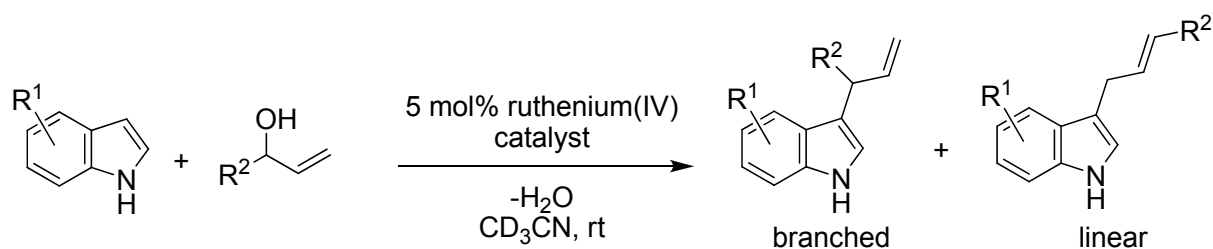
Specifically the syntheses and characterisation of new ruthenium(IV)-allyl complexes with  $\eta^3$ -C<sub>3</sub>H<sub>5</sub>,  $\eta^3$ -pentadienyl and  $\eta^5$ -pentadienyl moieties, such as **II-6**, **II-7**, **II-17** and **II-22**, respectively, are reported.



One of these complexes was found to catalyze the Friedel-Crafts type allylation of phenol derivatives using allyl alcohol substrates. The reactions are fairly rapid and often complete in less than 10 min with excellent regioselectivity.



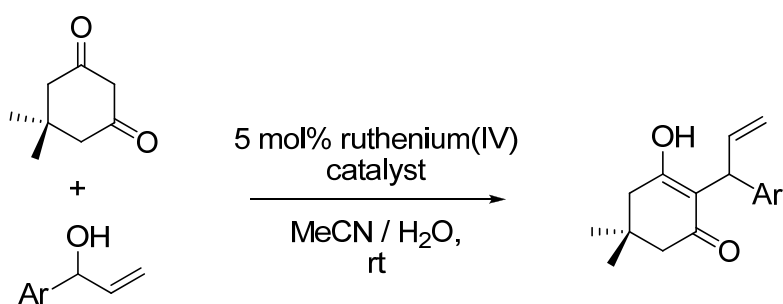
In addition, the allylation of different indoles with several substituted allyl alcohols is readily achieved with excellent branched to linear ratios.



We postulate a mechanism which reveals how the catalyst converts allyl alcohols and the nucleophiles to the desired products with water as the leaving group. Based on this finding, it is shown that  $[\text{Ru}(\text{Cp}^*)(\text{MeCN})_3](\text{PF}_6)$  plus a sulfonic acid can serve as an alternative catalyst to a ruthenium(IV)-allyl precursor.

NMR experiments and DFT calculations provide a rationale for the observed excellent branched to linear ratios based on structural distortions due to the presence of bulky substituents in the allyl alcohols.

Furthermore the rapid and regioselective mono-allylation of dimedone with substituted aryl allyl alcohols to the branched products is reported. These reactions proceed without acid, base or other additives.



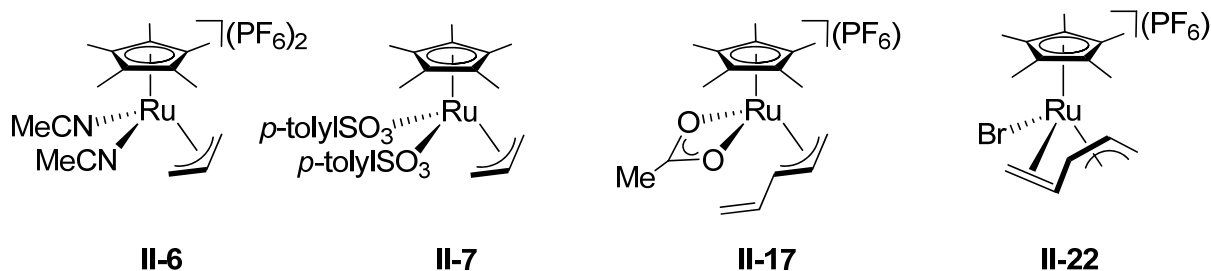
Finally the mono and double allylation of several cyclic 1,3-diketones using allyl alcohol as substrate is given. These reactions proceed in almost quantitative yield, rapidly and under mild conditions.



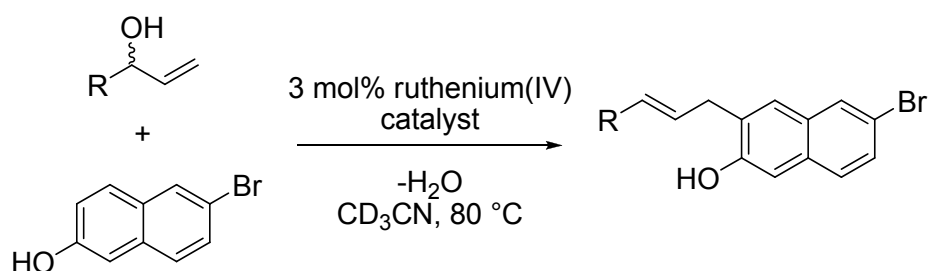
## Zusammenfassung

In dieser Dissertation wird die Entwicklung, Reaktivität und Anwendung neuer Ruthenium(IV)-Allyl Katalysatoren diskutiert. Diese Komplexe ermöglichen die direkte Verwendung von Allyl Alkoholen als Substrate in Allylierungsreaktionen. Durch den Gebrauch von Wasser als Abgangsgruppe wird die Entstehung unnötiger Nebenprodukte vermieden und eine besonders ökonomische bzw. ökologische Reaktionsführung ermöglicht.

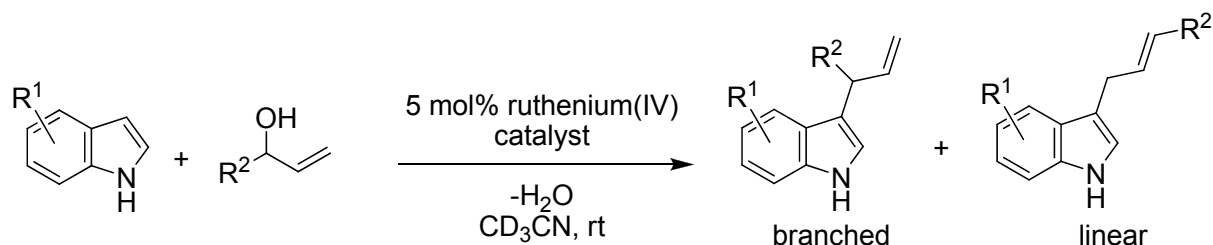
Besonders über die Synthese und Charakterisierung dieser neuer Ruthenium(IV)-Allyl Komplexe, welche  $\eta^3$ -C<sub>3</sub>H<sub>5</sub>-,  $\eta^3$ -Pentadienyl- und  $\eta^5$ -Pentadienyl-Liganden enthalten, wird berichtet. Beispiele sind die Komplexe **II-6**, **II-7**, **II-17** und **II-22**.



Es wurde festgestellt, dass einer dieser Komplexe die Friedel-Crafts Allylierung von Phenol Derivaten mit Allyl Alkoholen als Substrate katalysiert. Die Reaktionen verlaufen schnell, mit exzellenter Regioselektivität und sind oft in weniger als 10 min beendet.

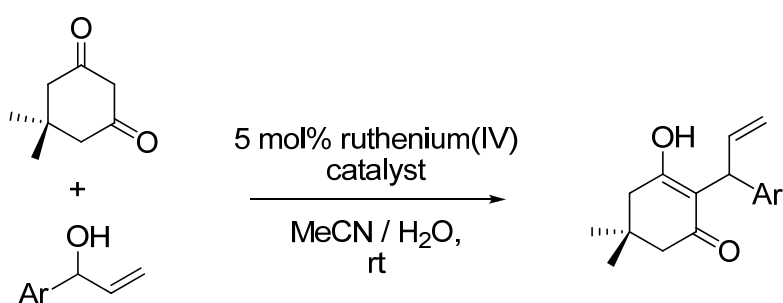


Des weiteren wird die Allylierung verschiedener Indole mit mehreren substituierten Allyl Alkoholen beschrieben. Die Produkte werden schnell und mit beachtlichen Verhältnissen von verzweigt zu linear erzeugt.



Der postulierte Reaktionsmechanismus liefert einen tieferen Einblick in die untersuchte Katalyse. Hierbei verwandelt der Katalysator die Allyl Alkohole und die Nucleophile zu den gewünschten Produkten unter Abspaltung von Wasser als Abgangsgruppe. Auf der Grundlage dieser Annahme zeigen wir, dass man als Alternative zu einem Ruthenium(IV)-Allyl Vorläufer auch  $[\text{Ru}(\text{Cp}^*)(\text{MeCN})_3](\text{PF}_6)$  und eine zusätzliche Sulfonsäure als Katalysator verwenden kann. Unter Verwendung von NMR spektroskopischen Experimenten und DFT Berechnungen geben wir eine Erklärung für das beobachtete Verhältnis von verzweigten zu linearen Produkten. Komplextiert ein sterisch anspruchsvoller Allyl Alkohol an den Rutheniumkomplex, kommt es zu strukturellen Verzerrungen, welche die Entstehung des verzweigten Produktes begünstigen.

Darüber hinaus wird von einer schnellen und regioselektiven Reaktion von Dimedon und Aryl-Allyl Alkoholen zu den verzweigten mono-allylierten Produkten berichtet. Diese Reaktion verläuft ohne Zugabe von Säuren, Basen oder anderen Zusatzstoffen.



Die Mono- und Doppel-Allylierung von verschiedenen zyklischen 1,3-Diketonen mit Allyl Alkoholen wird ebenfalls beschrieben. Diese Reaktionen verlaufen schnell, unter milden Bedingungen und mit beinahe quantitativer Ausbeute.



**1.**

# **Introduction**

## 1.1. History and Characteristics of Ruthenium

Ruthenium was discovered and isolated by Karl Ernst Claus in 1844. He showed that a part of crude platinum is insoluble in aqua regia, which contains a new element. In 1827 ruthenium was nearly discovered by Jöns Jakob Berzelius and Gottfried Osann. They examined residues that were left over after dissolving crude platinum from the Ural Mountains in aqua regia. Berzelius did not find any unusual metals, but Osann thought that he had found three new metals and named one of them ruthenium. The name ruthenium derives from the Latin Ruthenia: "Russia".<sup>[1]</sup>

Ruthenium is generally found in ores with the other platinum group metals in North and South America and in the Ural Mountains. This metal is commercially isolated through a complex chemical process in which hydrogen is used to reduce ammonium ruthenium chloride yielding a metallic ruthenium powder.<sup>[2]</sup>

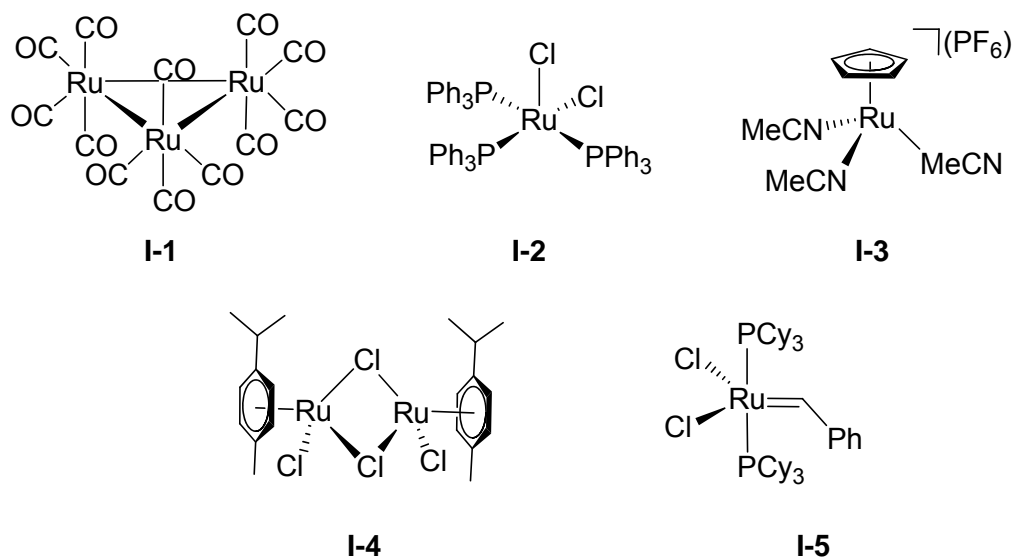
Ruthenium is the 74<sup>th</sup> most abundant metal on earth<sup>[3]</sup>, it has the symbol Ru and the atomic number 44, with an electron configuration  $[\text{Kr}]4d^75s^1$ . It exhibits at least eight oxidation states: -2:  $[\text{Ru}(\text{CO})_4]^{2-}$ , 0:  $[\text{Ru}(\text{PPh}_3)_3(\text{MeCN})]$ , +1:  $[\text{RuCl}(\text{dppp})_2]$ , +2:  $[\text{RuCl}_2(\text{PPh}_3)_3]$ , +3:  $[\text{RuCl}_3]$ , +4:  $[\text{RuCl}_4(\text{bipy})]$ , +5:  $[\text{RuF}_6]^-$ , +6:  $[\text{RuO}_4]^{2-}$ , +7:  $[\text{RuO}_4]^-$ , +8:  $[\text{RuO}_4]$ , but the +2, +3 and +4 states are the most common.<sup>[1]</sup>

Ruthenium is used in platinum and palladium alloys to make them harder and wear-resistant. Ruthenium complexes are being investigated for possible anticancer properties. They act more selectively on tumours and show a greater resistance to hydrolysis than *cis*-platinum complexes. Ruthenium complexes are also versatile catalysts in organic chemistry and chemical industry.

## 1.2. Organometallic Chemistry of Ruthenium

During the last decade ruthenium catalysts have provided a variety of novel activation processes leading to powerful new organic synthetic methods. This is due to the availability of a large number of well-defined and stable ruthenium precursors. These complexes have a variety of useful characteristics including high electron transfer ability, Lewis acid activity, low redox potentials, unique selectivity and they can easily form compounds with carbon ruthenium bonds.

Organometallic ruthenium complexes can be divided into five groups according to their coordinating ligands: carbonyl **I-1**, tertiary phosphines **I-2**, cyclopentadienyl **I-3**, arene/dienes **I-4** and carbenes **I-5** (Scheme 1.1). These ligands serve effectively to activate and stabilize reactive intermediates. The liberation of ligands generates coordinatively unsaturated species which can undergo further reactions.<sup>[4]</sup>



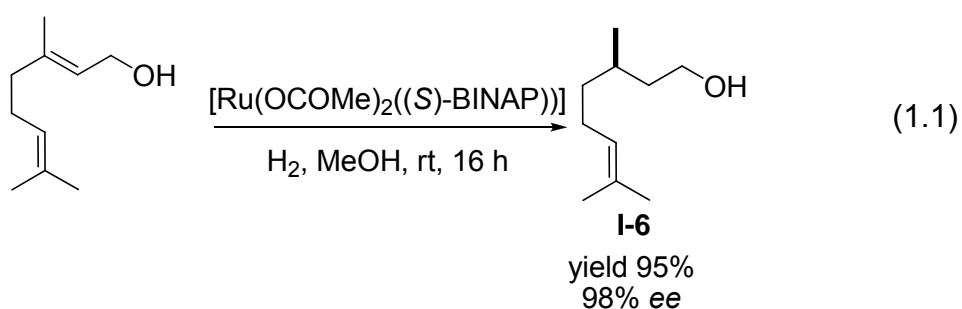
**Scheme 1.1.** Shows a selection of ruthenium complexes of the five different groups according to their ligand coordination.

New ruthenium catalysts make possible carbon-carbon, carbon-hydrogen and carbon-heteroatom bond formation. They can provide activation modes like a metathesis reaction. Hydrogenation, metathesis reaction, a variety of multiple C-C bond making reactions, hydroamination, isomerisation, kinetic resolution and allylic alkylation will be discussed in sub-Chapters 1.2.1-1.2.6 and 1.3.1-1.3.2.

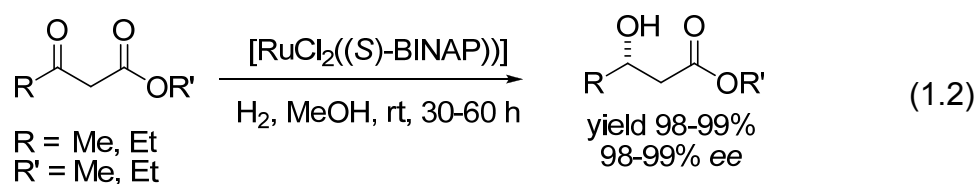
### 1.2.1. Hydrogenation and Transfer Hydrogenation

The asymmetric hydrogenation and transfer hydrogenation reactions provide access to chiral building blocks of biological interest. The reduction of C=O, C=N or C=C bonds with hydrogen can be catalysed by a number ruthenium complexes. In 2001 R. Noyori together with W. S. Knowles received the Chemistry Nobel Prize for the study of enantioselectively catalyzed hydrogenations.<sup>[5, 6]</sup> The Ru(II)-BINAP catalysts developed by Noyori find applications in industrial processes. For example, the syntheses of naproxen<sup>[7]</sup>, citronellol<sup>[8]</sup> and  $\beta$ -methylcarbapenem intermediate<sup>[9]</sup>.

Equation 1.1 shows the selective hydrogenation of one of the two double bonds from geraniol to give (*S*)-citronellol (**I-6**), catalysed by Noyori's Ru(II)-BINAP complex.<sup>[8]</sup>

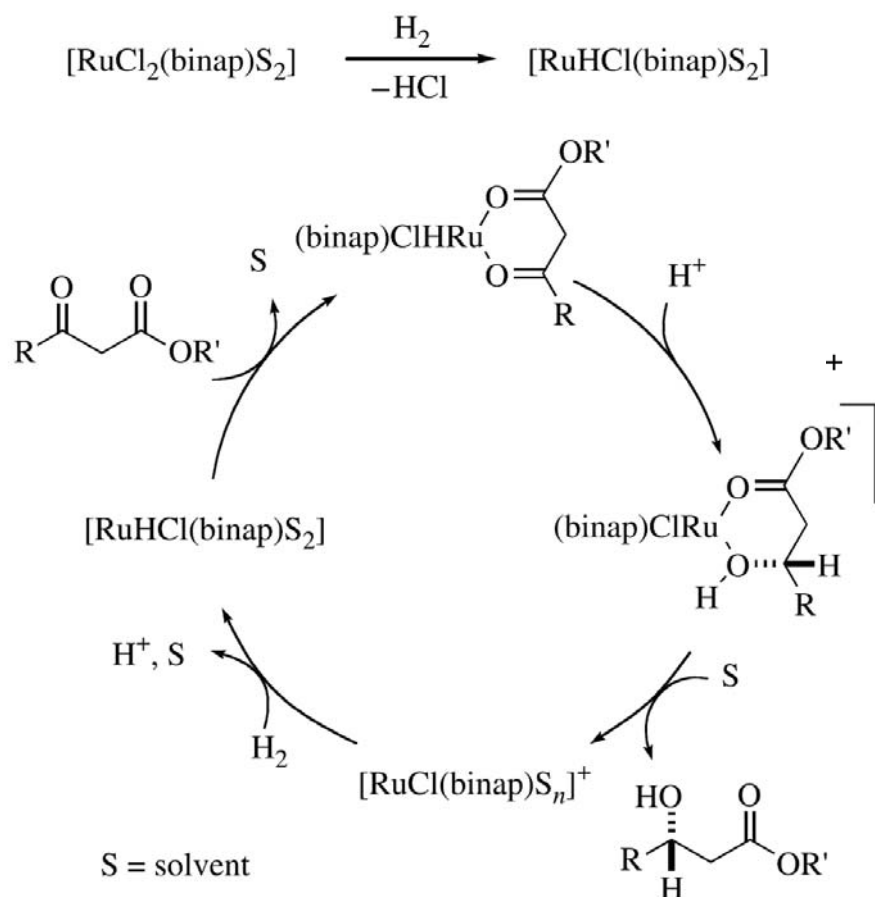


The slightly modified halogen-containing complex  $[\text{RuCl}_2((S)\text{-BINAP})]$  catalyses the hydrogenation of  $\beta$ -keto esters in excellent enantioselectivity (Equation 1.2).<sup>[10]</sup>



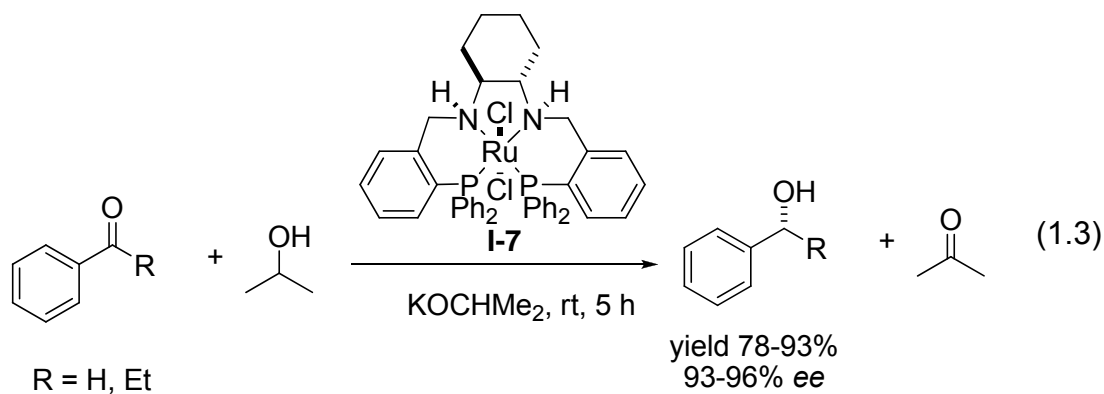
Functionalized ketones such as  $\beta$ -keto esters have coordinating oxygen atoms, which direct the stereochemical outcome and the reactivity. Simultaneous coordination of both carbonyl oxygen atoms to the ruthenium atom generates a six-membered chelate ring, with different enantiofaces (Scheme 1.2).





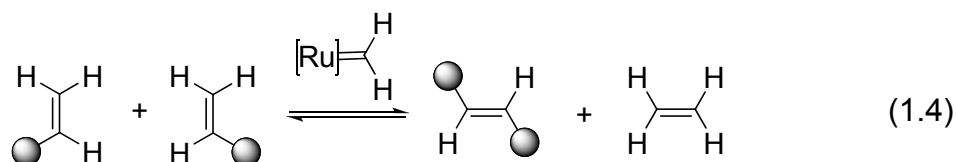
**Scheme 1.2.** Literature mechanism of the asymmetric hydrogenation of  $\beta$ -keto esters catalysed by a  $[\text{RuCl}_2((S)\text{-BINAP})]$  complex. <sup>[11]</sup>

The reaction which uses alcohols as an alternative to molecular hydrogen is called transfer hydrogenation. 2-Propanol is a conventional hydrogen source having favourable properties and acetone as by-product is easily removed. The ruthenium PNP complex **I-7** in Equation 1.3 is an effective catalyst for transfer hydrogenation of aromatic ketones and aldehydes, respectively, with 2-propanol. <sup>[12]</sup>

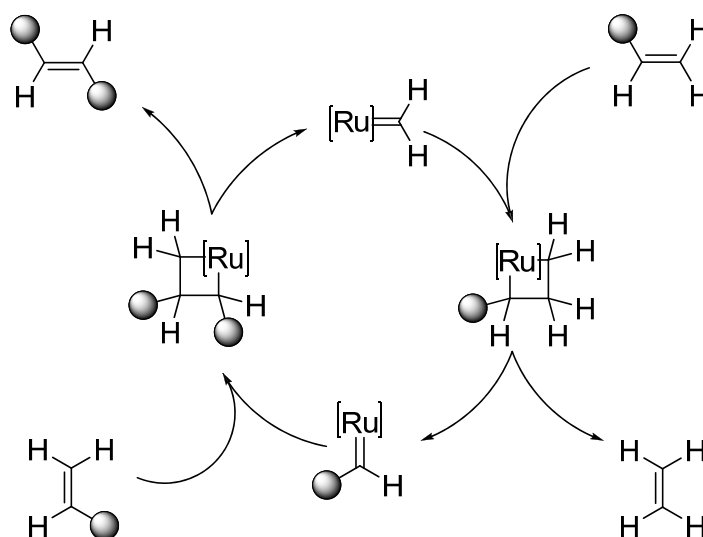


### 1.2.2. Metathesis

In 2005 the Chemistry Nobel Prize was awarded to Yves Chauvin, Robert H. Grubbs and Richard R. Schrock for the development of the metathesis method in organic synthesis.<sup>[13-15]</sup> Their contributions have already assumed major significance in the chemical industry: e.g. production of pharmaceuticals, plastics and other materials. The metathesis reaction is catalyzed by several transition metals such as ruthenium, molybdenum, tungsten and titanium. The word metathesis means “change places”. In olefin metathesis the two double-bonded atom groups will change places with one another (Equation 1.4). Generally the metathesis reaction can be divided into four types of sub reactions: cross metathesis (CM), ring closing metathesis (RCM), acyclic diene metathesis (ADMET) and ring opening metathesis polymerization (ROMP).

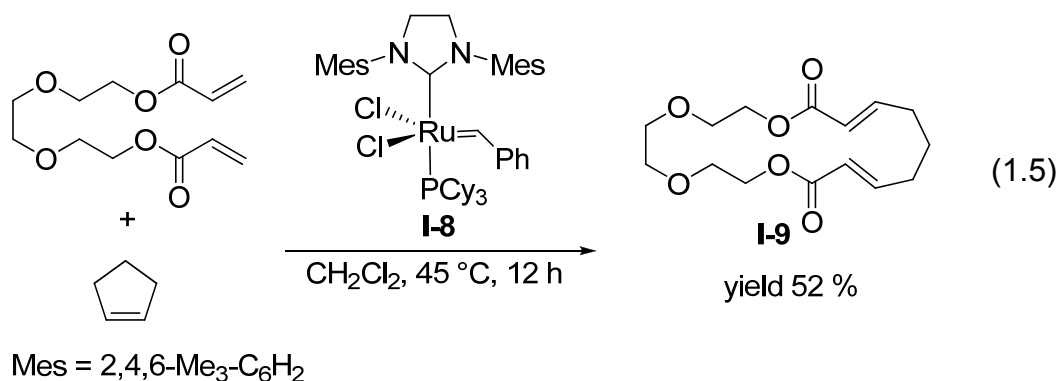


Metathesis chemistry is relatively old, in 1971 Chauvin suggested a mechanism, which allows producing much more efficient metathesis catalysts (Scheme 1.3).<sup>[16]</sup>

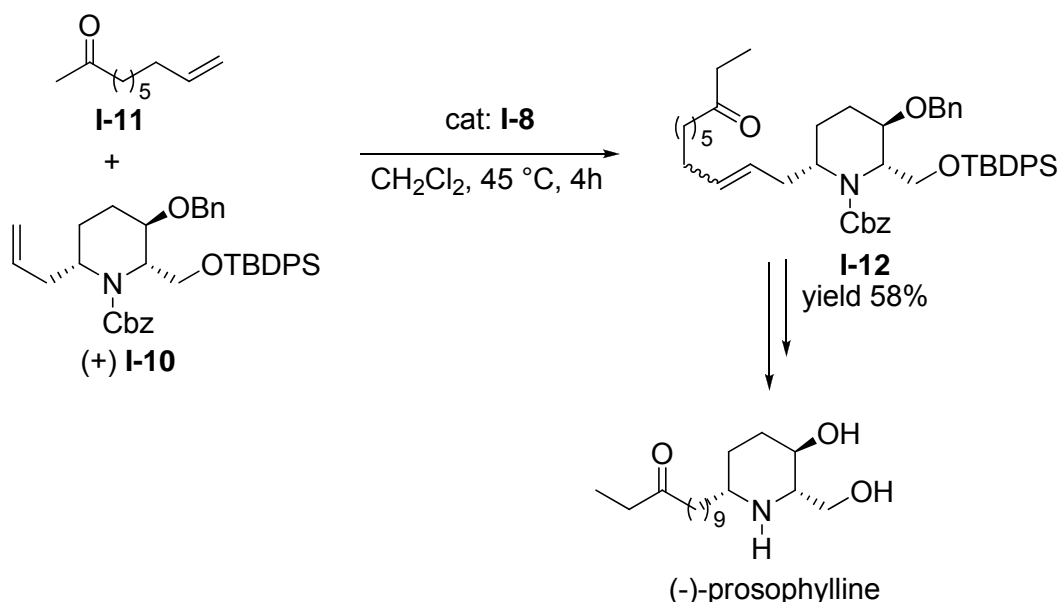


**Scheme 1.3.** Chauvin's mechanism for the olefin metathesis catalyzed by a metal carbene complex.

In recent years the group of Grubbs has synthesized a variety of ruthenium metathesis catalysts such as complex **I-8**. This catalyst can perform three different types of metathesis reactions at once: ROMP followed by CM and RCM produces the macrocycle **I-9** in moderate yield (Equation 1.5).<sup>[17]</sup>



Cossy<sup>[18]</sup> et al have applied CM to the synthesis of the alkaloid (-)-prosophylline (isolated from the leaves of *Prosopis africana*<sup>[19]</sup>, which possesses antibiotic and anesthetic properties<sup>[20]</sup>). Reaction of the alkene piperidine substrate **I-10** with ketone **I-11** catalyzed by complex **I-8** gives intermediate **I-12**, which then can be transformed to (-)-prosophylline after a hydrogenation and deprotection step (Scheme 1.4).

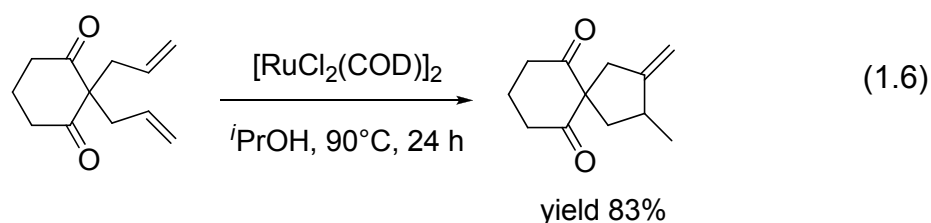


**Scheme 1.4.** CM reaction step in the synthesis of (-)-prosophylline.

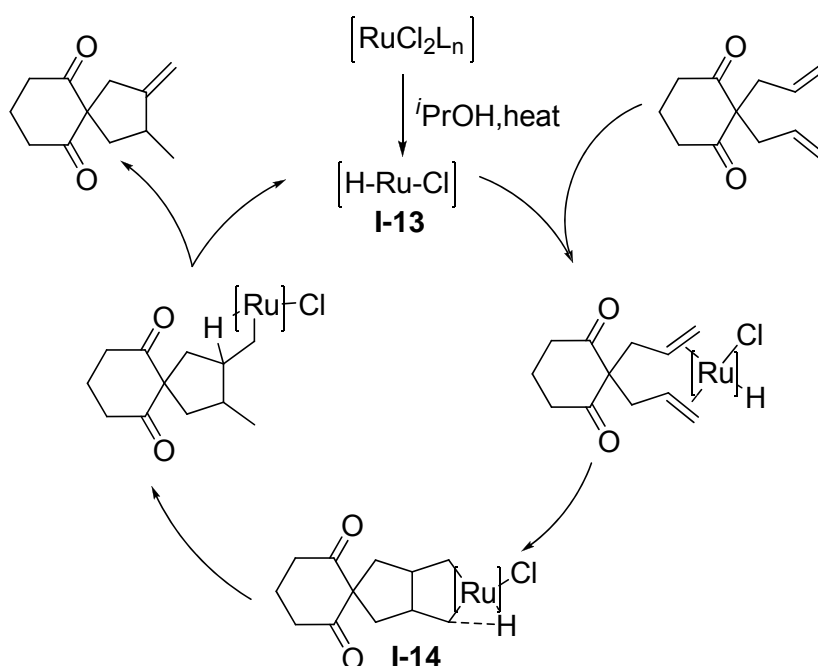
### 1.2.3. C-C Bond Formation

In the last decade ruthenium catalysts have helped to create a large number of reactions for selective C-C bond formation. Coupling of two C=C bonds, cross-coupling of a C=C bond with allene and C-H bond activation represent examples of this kind of chemistry (these will be discussed on the next pages).

The intramolecular coupling of two adjacent allyl double bonds catalyzed by a ruthenium complex leads to *exo*-methylenecyclopentane substrate (Equation 1.6).<sup>[21]</sup>

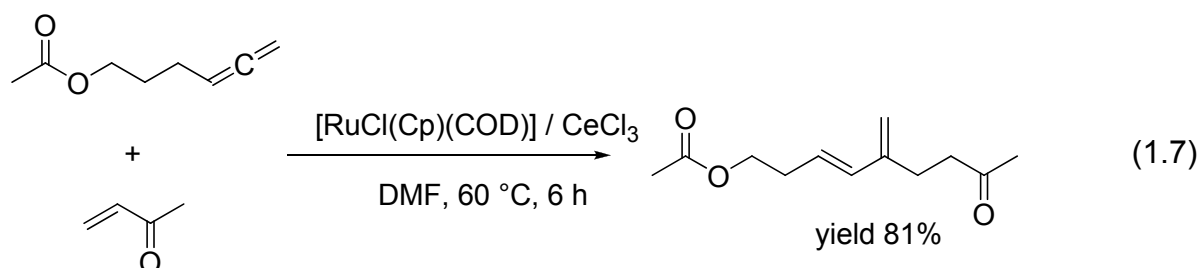


The authors suggest that the active catalyst is a coordinatively unsaturated ruthenium-chloro-hydrido species **I-13**. Complexation of the double bonds and oxidative cyclization leads to ruthenacyclopentane-hydrido complex **I-14**, which undergoes a reductive elimination followed by a  $\beta$ -hydride elimination to the product (Scheme 1.5).

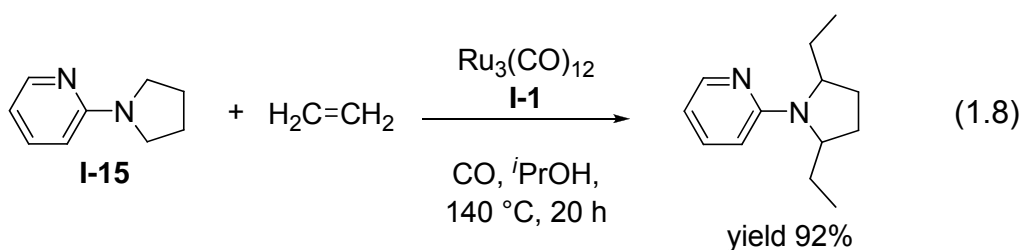


**Scheme 1.5.** Postulated mechanism for the formation of *exo*-methylenecyclopentane substrates catalyzed by  $[\text{RuCl}_2(\text{COD})]_n$ .

1,3-Dienes can be obtained by a selective two component coupling of an allene and an activated olefin in good yields (Equation 1.7). In the reaction for the formation of *exo*-methylene-cyclopentane, a ruthenacyclopentane has been proposed as an intermediate (see Scheme 1.5).<sup>[22]</sup>

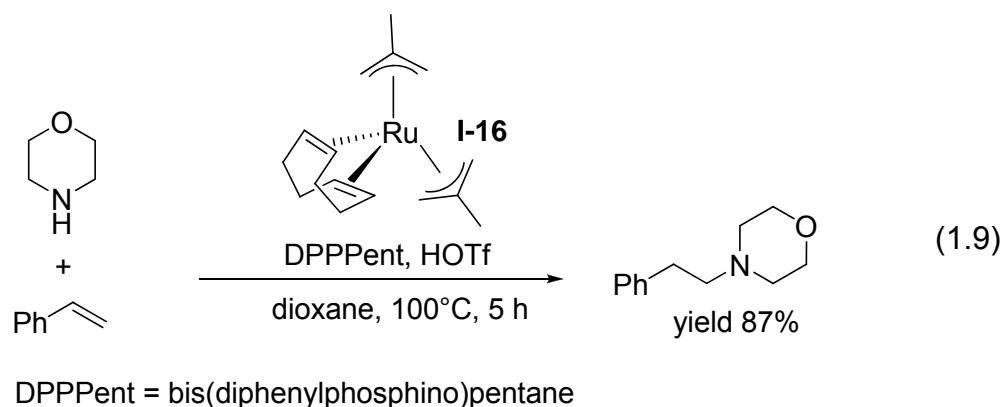


In the early literature C-H bond activation catalyzed by ruthenium complexes was limited to aromatic compounds, where C-C bond formation occurs at the *ortho* position. In recent years the development of catalytic reactions which involve the cleavage of unreactive C-H bonds (e.g. on  $sp^3$  carbons) has been a subject of considerable interest. It is noteworthy that complexation of the nitrogen atom of the substrate to a ruthenium metal **I-1** can even activate the C-H bond of neighbouring  $sp^3$  carbons (such as in substrate **15**) and the reaction proceeds in excellent yield (Equation 1.8).<sup>[23]</sup>



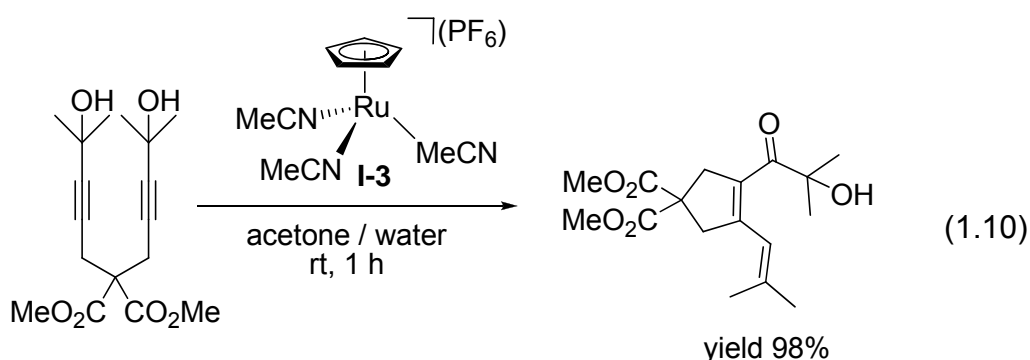
#### 1.2.4. Hydroamination

The hydroamination reaction represents a highly atom economical method of preparing substituted amines from alkenes or alkynes. The product amines are attractive building blocks for organic synthesis and the pharmaceutical industry. For example, the  $[Ru(2\text{-methylallyl})_2(COD)]$  precursor (**I-16**) together with DPPent allows control of the regiochemistry. The hydroamination of styrene and morpholine gives exclusively the anti-Markovnikov product (Equation 1.9).<sup>[24]</sup>

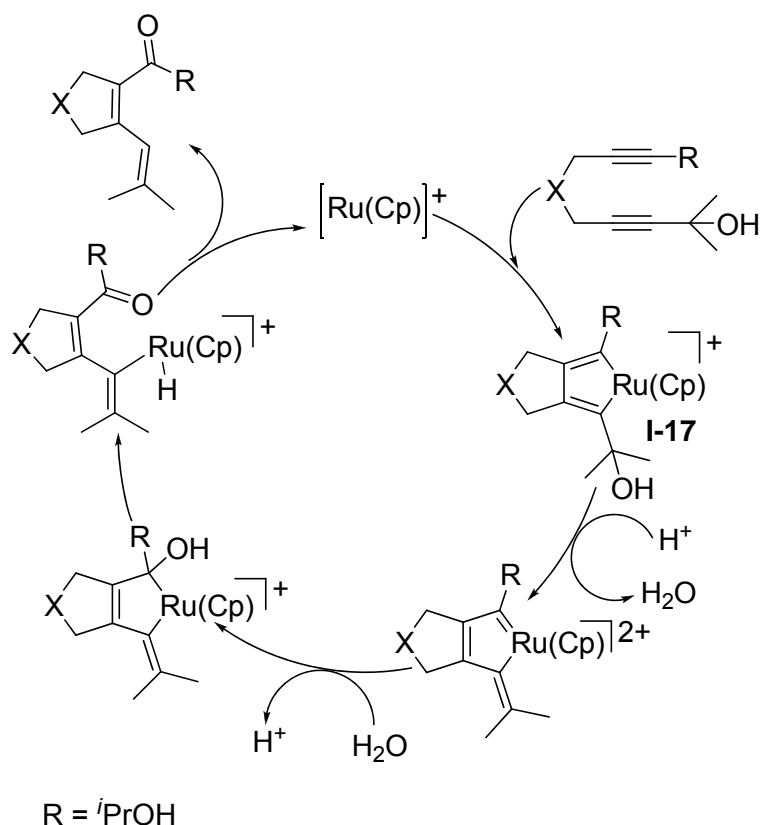


### 1.2.5. Isomerisation

Isomerisation of easily accessible starting materials can create highly functionalized ring structures through addition reactions that allow building molecular complexity while preserving atom economy. The ruthenium catalyzed cycloisomerisation of a diynol substrate to a dienone derivative is shown in Equation 1.10. <sup>[25]</sup>



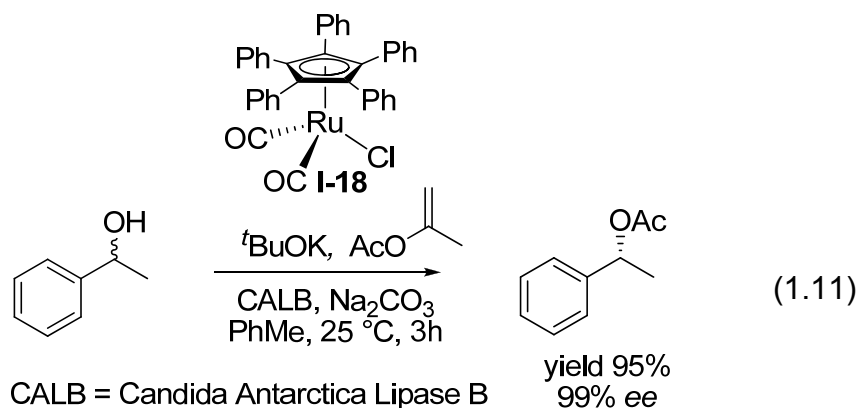
Trost and co-workers have proposed a mechanism for this reaction based on the formation of a ruthena-cyclopentadiene species **I-17**, which then eliminates a water molecule. Re-addition of water to the other side of the ruthenacycle, followed by a  $\beta$ -H elimination and a reductive elimination leads to the product (Scheme 1.6). <sup>[26]</sup>



**Scheme 1.6.** Suggested mechanism for the cycloisomerisation of diynol derivatives.

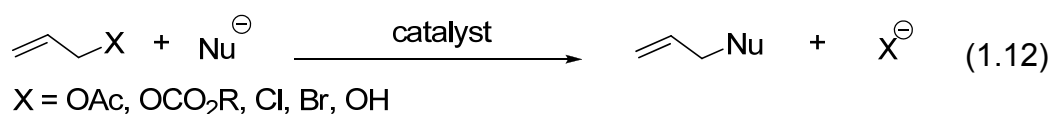
### 1.2.6. Kinetic Resolution

The subject of kinetic resolution uses the fact that two enantiomers can show different reaction rates. Asymmetric ruthenium complexes can be used to resolve racemic compounds into optically active substrates with excellent enantioselectivities. The group of Bäckvall has shown, that the ruthenium complex **I-18** together with the enzyme CALB (Candida Antarctica Lipase B) catalyzes the dynamic kinetic resolution of racemic 1-phenylethanol to (*R*)-1-phenylethanol, which is trapped by an acyl donor in excellent yield and enantioselectivity (Equation 1.11).<sup>[27]</sup>

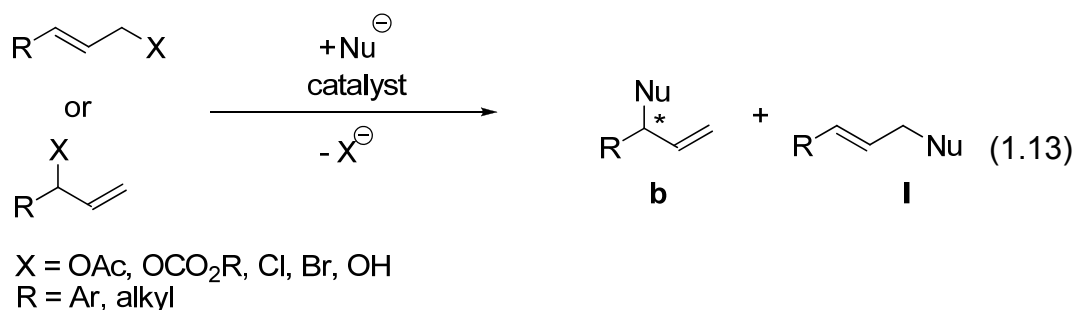


### 1.3. Transition-Metal Catalyzed Allylations

The nucleophilic substitution of allylic substrates catalyzed by transition-metal complexes represents a powerful method in organic synthesis. Equation 1.12 shows a general reaction scheme for the allylation with C<sub>3</sub>-allyl substrates and a nucleophile catalyzed by a transition metal. The leaving group X is mainly an acetate or carbonate, but sometimes a chloride or bromide and in the recent years occasionally a water molecule. The nucleophile can be a carbon or heteroatom substrate, which has been deprotonated by an additional base or the leaving group.

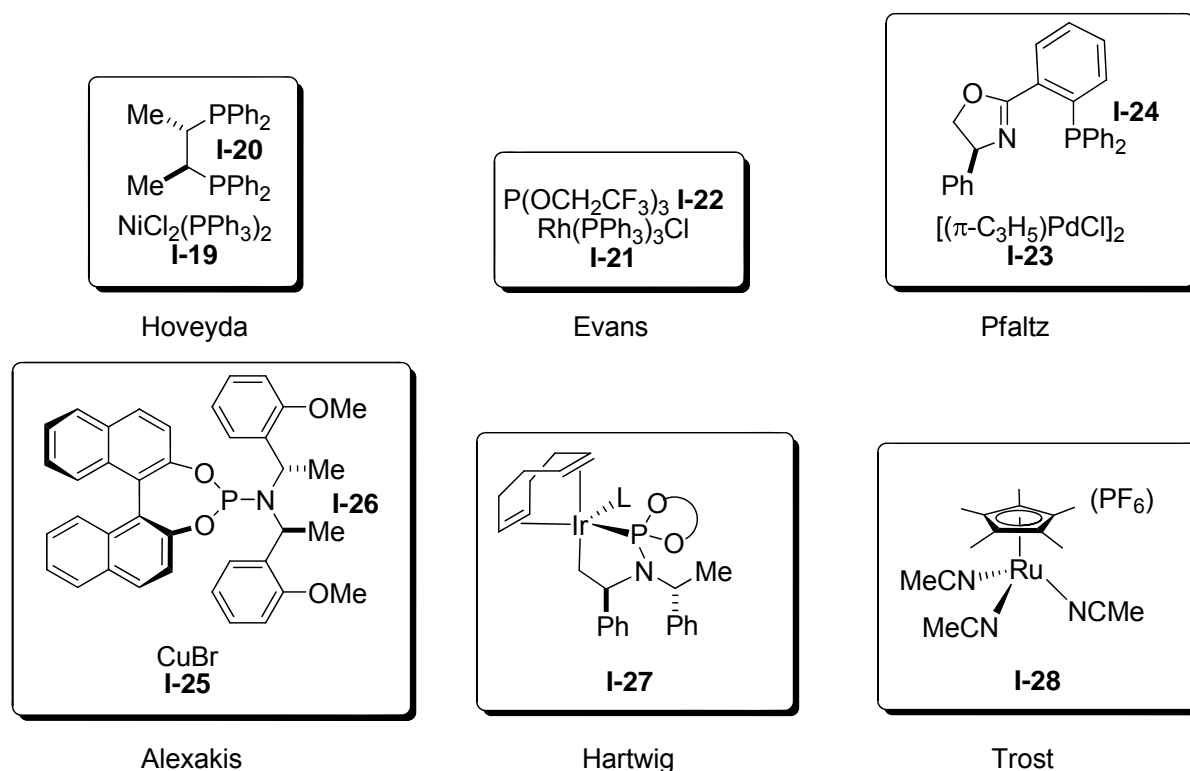


A substituted allyl substrate leads to branched (**b**) and / or linear (**I**) regioisomers (Equation 1.13). The branched product can contain a stereogenic centre (indicated by \*), and therefore many catalyst systems use chiral ligands to achieve the branched product in enantiomeric excess.



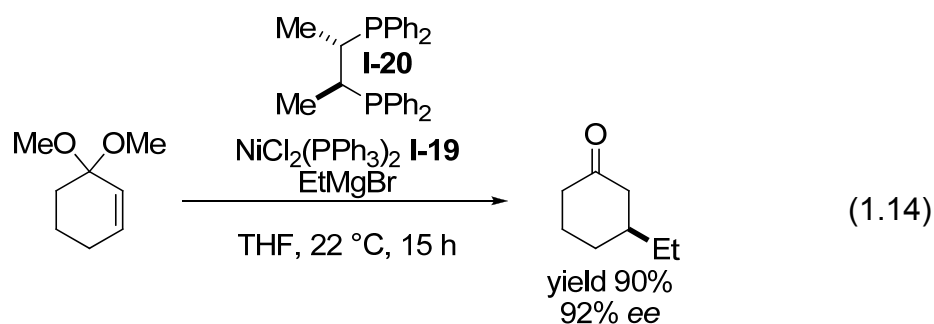
Scheme 1.7 gives a selection of allylation catalyst systems or precursors with different types of metal centres.



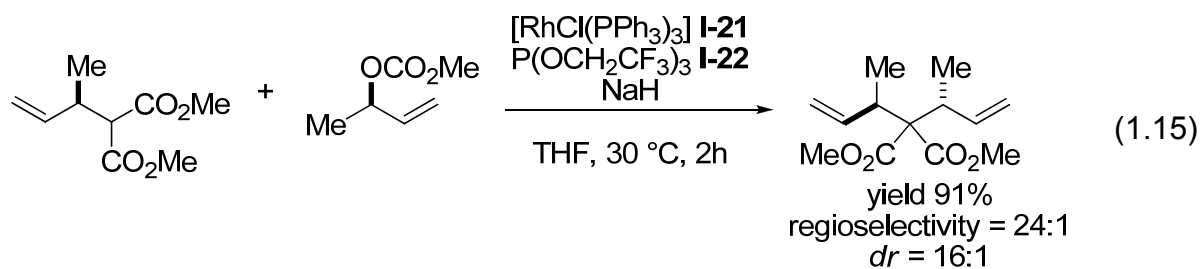


**Scheme 1.7.** A selection of allylation catalyst systems or precursors with different types of metal centres.

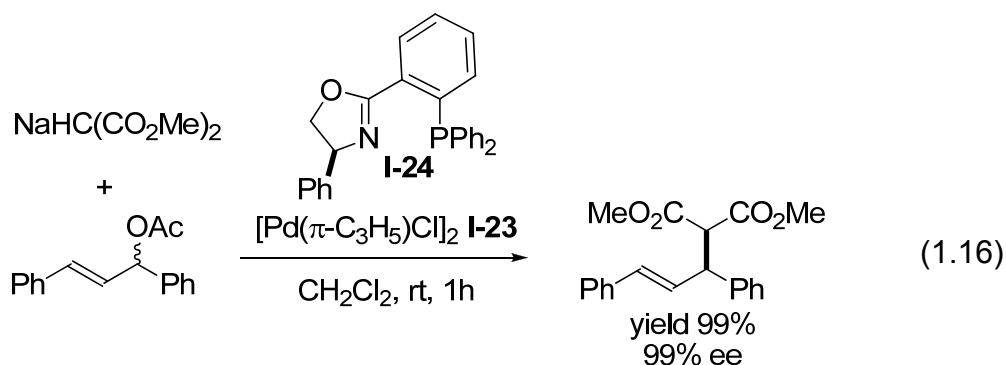
Nickel catalysts have been shown to promote allylic substitutions with hard organometallic nucleophiles and allylic substrates. Hoveyda has reported a catalyst system based on a nickel(II) salt (**I-19**) together with (*S,S*)-chiraphos (**I-20**) for the conversion of an acetal with a Grignard reagent into a cyclohexanone with excellent enantiomeric excess (Equations 1.14).<sup>[28]</sup>



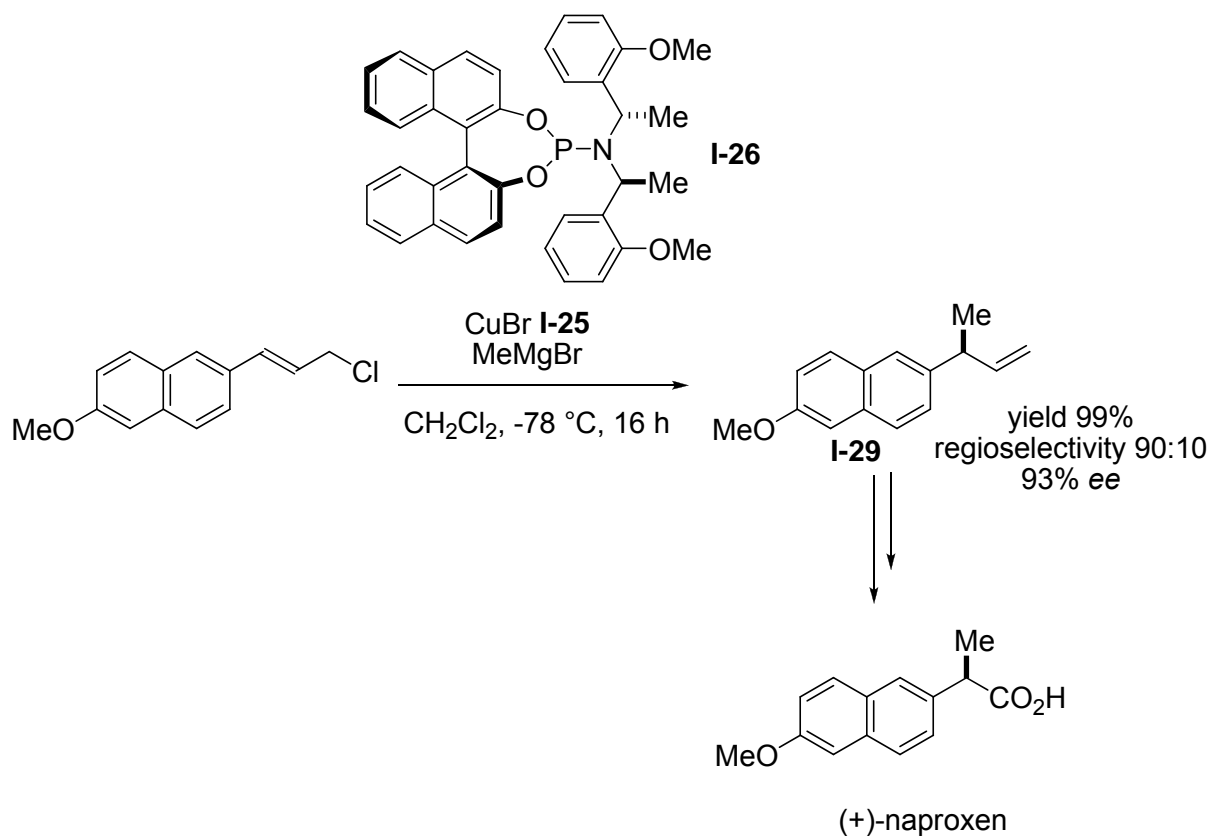
Rhodium catalyzed allylic substitution processes generally proceed in a stereospecific manner. Equation 1.15 shows an allylation catalyzed by Wilkinson's catalyst (**I-21**) in the presence of phosphites **I-22**, which affords the product in good regio- and diastereoselectivity.<sup>[29]</sup>



The palladium catalyzed allylic substitution represents a versatile, widely used process in organic synthesis. The group of Pflatz has reported an allylic alkylation catalyzed by palladium(II)-allyl precursor (**I-23**) together with a phosphinooxazoline ligand (**I-24**) (Equation 1.16). The reaction works fast, under mild conditions and the product is obtained in excellent yield and enantioselectivity.<sup>[30]</sup>

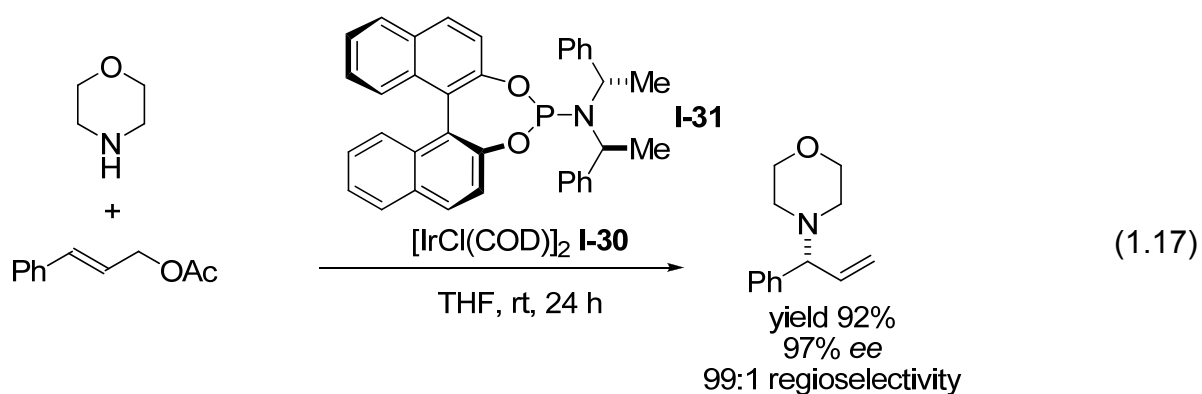


Chiral phosphoramidite ligands derived from BINOL have shown excellent potential in copper-catalyzed asymmetric  $S_N2'$  substitutions. Alexakis and co-workers have found that phosphoramidite ligand **I-26** in the presence of CuBr (**I-25**) affords the methylated compound **I-29**, which is a precursor in the synthesis of (+)-naproxen (Scheme 1.8).<sup>[31]</sup>

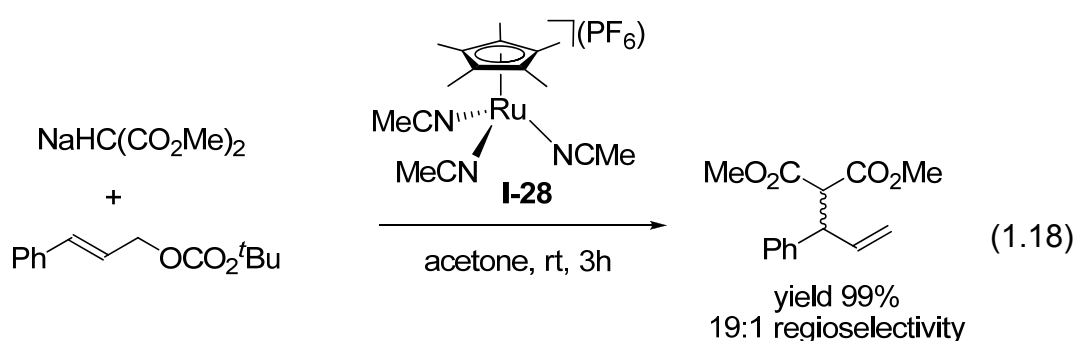


**Scheme 1.8.** Shows the synthesis of substrate **I-29** as precursor in the synthesis of (+)-naproxen.

Hartwig has reported that an iridium(I) precursor, **I-30**, in combination with two phosphoramidite ligands, **I-31**, affords the catalyst, **I-27**, that mediates the conversion of allylic carbonates into allylic amines with excellent regio- and enantioselectivity (Equation 1.17 and Scheme 1.7).<sup>[32]</sup> He identified the activated cyclometalated complex **I-27** with two coordinating phosphoramidites (see Scheme 1.7) as the active catalyst in these kind of reaction.<sup>[33]</sup>

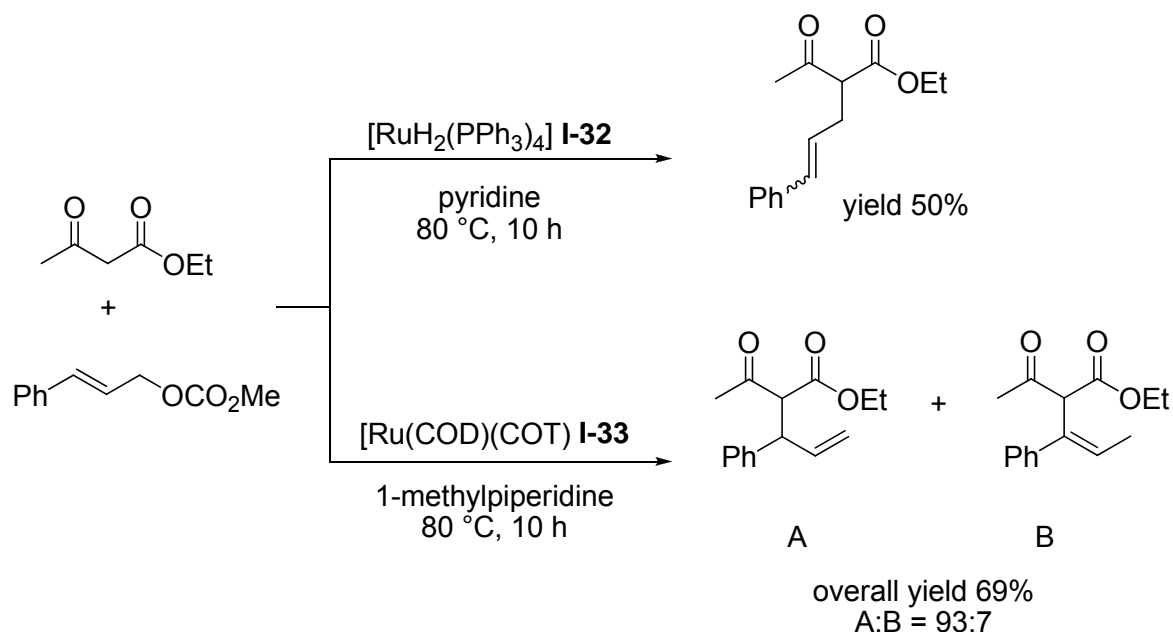


In 2002 Trost and co-workers reported on “a stereospecific ruthenium-catalyzed allylic alkylation”, using the simple pentamethylcyclopentadienyl ruthenium(II) salt (**I-28**). This catalyst favors the attack of the nucleophile at the more substituted carbon atom, regardless of the regioisomeric nature of the substrate (Equation 1.18).<sup>[34]</sup> In contrast, palladium catalyzed allylic alkylations normally prefer nucleophilic addition to the less substituted allyl terminus, although ligands can influence this selectivity. Further literature reviews of ruthenium catalyzed allylation and especially with ruthenium-Cp\* as catalyst will be discussed in sub-Chapters 1.3.1 and 1.3.2, respectively.



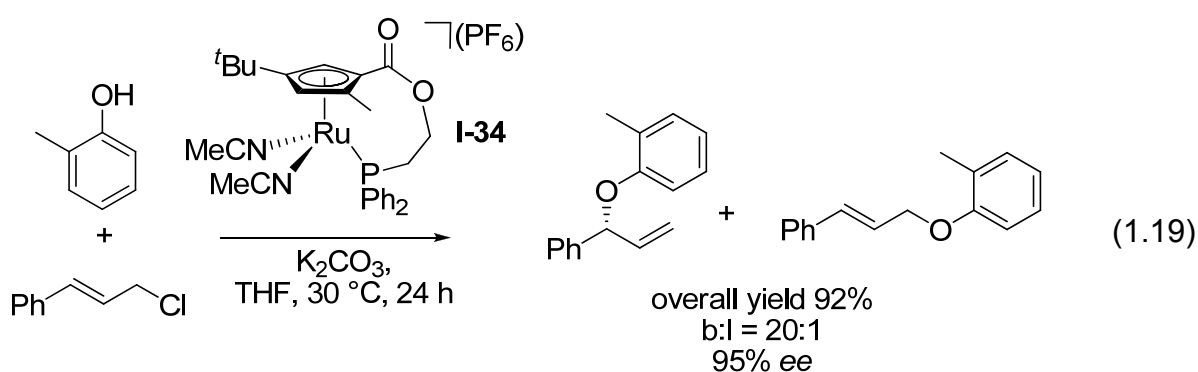
### 1.3.1. Ruthenium Catalyzed Allylations

Ruthenium complexes often show catalytic activity and product selectivity quite different from those with palladium or other transition metal complexes. Further Scheme 1.9 shows, how the change from a ruthenium(II) precursor **I-32** to a ruthenium(0) catalyst **I-33** can affect the product selectivity under approximately the same conditions.<sup>[35]</sup>

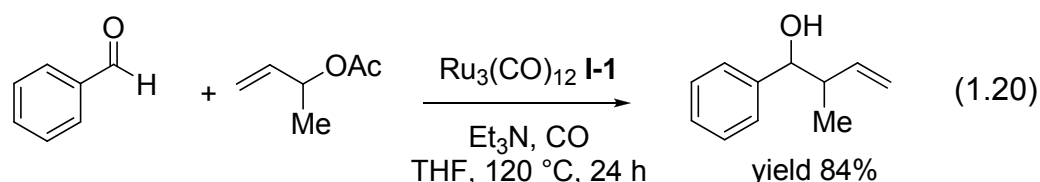


**Scheme 1.9.** Shows the different product selectivity catalyzed by a Ru(II) and Ru(0) catalyst, respectively.

Onitsuka and co-workers have documented a stereoselective reaction of cinnamyl chloride and *o*-cresol with good regioselectivity and enantioselectivity up to 95% (Equation 1.19). They use a cyclopentadiene-phosphine ruthenium complex **I-34** with planar-chirality.<sup>[36]</sup>

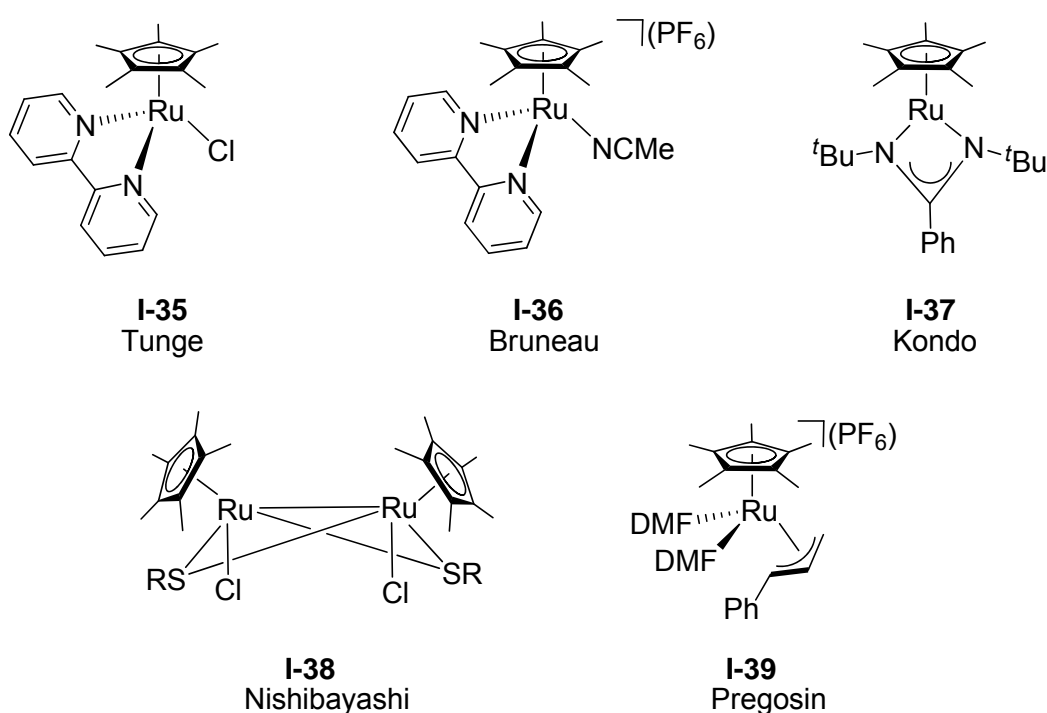


It is noteworthy that the easily prepared ruthenium complex **I-1** is also active for the allylation of electrophiles such as benzaldehyde with allylacetate and proceeds in a highly regioselective manner (see Equation 1.20).<sup>[37]</sup>



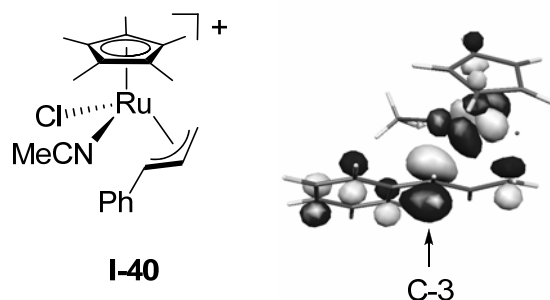
### 1.3.2. Ruthenium-Cp\* Catalyzed C-C Bond Allylations

In recent years there has been a significant effort to explore and expand the allylic alkylation reactions with pentamethylcyclopentadienyl-ruthenium catalysts. These ruthenium(II) complexes efficiently perform the activation of allylic carbonates and halides to generate cationic and dicationic ruthenium(IV) complexes (e.g. **I-39**). Aside from Trost-catalyst (**I-28**) discussed in sub-chapter 1.3, Scheme 1.10 shows a selection of the ruthenium-Cp\* catalysts currently in use.



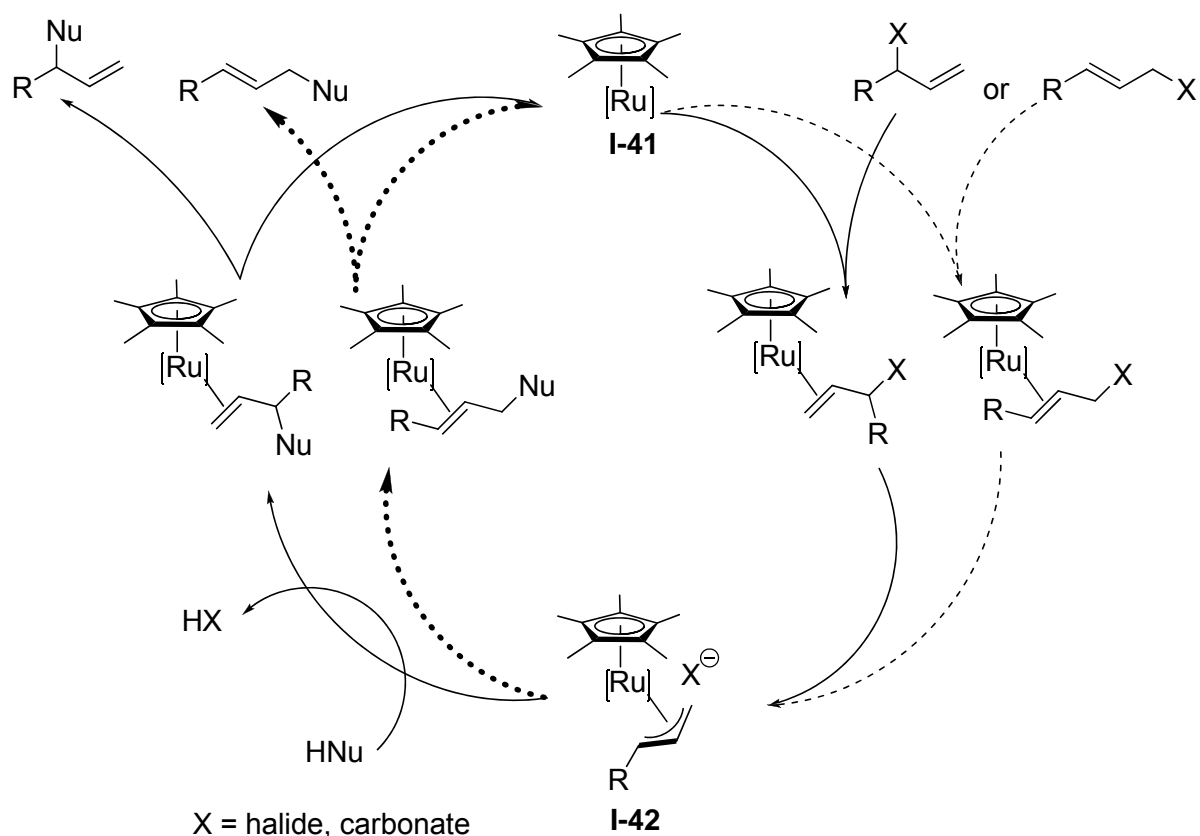
**Scheme 1.10.** Ruthenium-Cp\* allylation catalysts currently in use.

The structural and electronic properties of the ruthenium(IV)-allyl moieties can lead to the regioselective formation of branched products resulting from nucleophilic addition to their most substituted terminus. Pregosin and co-workers have recently suggested that the regioselectivity of the ruthenium-Cp\* catalyzed allylation reactions derives from orbital control (see Figure 1.1).<sup>[38]</sup>



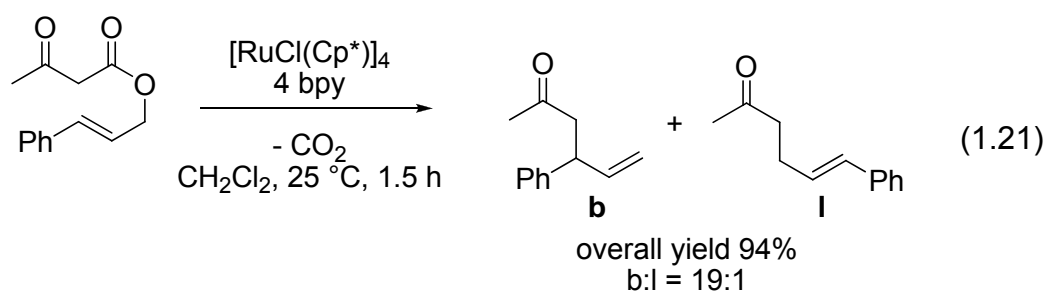
**Figure 1.1.** View of the LUMO (picture on the right side) of cation **I-40**, showing the preferred location of nucleophilic attack at the C-3 carbon.

Scheme 1.11 shows a postulated mechanism for ruthenium-Cp\* catalyzed allylation of nucleophiles with asymmetric allyl substrates. The ruthenium(II) complex **I-41** carries out an oxidative addition to form the ruthenium(IV)- $\pi$ -allyl intermediate **I-42**. The attack of the nucleophile on the intermediate **I-42** leads to branched and/or linear allylic product.

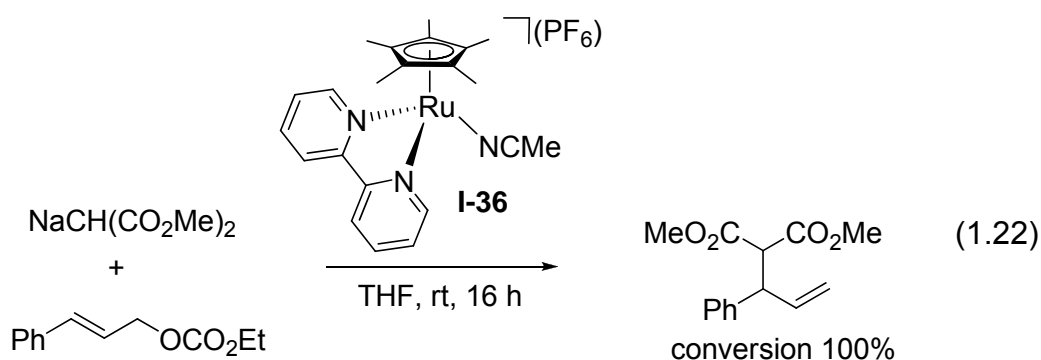


**Scheme 1.11.** Postulated mechanism for asymmetric allylation reactions catalyzed by ruthenium(II)-Cp\* complexes.

Tunge and co-workers have reported a Carroll rearrangement of allyl- $\beta$ -ketoesters catalyzed by  $[\text{RuCl}(\text{Cp}^*)(\text{bpy})]$  (**I-35**), which is generated during the reaction by  $[\text{RuCl}(\text{Cp}^*)]_4$  and four equivalents of bipyridine (Equation 1.21). The reaction proceeds under mild conditions via the formation of a ruthenium- $\pi$ -allyl intermediate which is attacked by freely diffusing enolates, with good regioselectivity. The branched (**b**) and linear (**l**) products are formally generated after decarboxylation by a [3,3] rearrangement and a [1,3] rearrangement, respectively.<sup>[39]</sup>

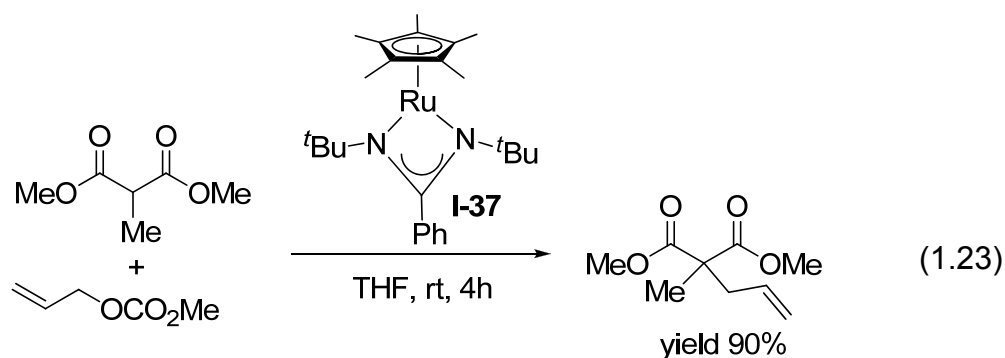


The group of Bruneau has documented a modified catalyst for the reaction shown in Equation 1.18 above. The change from catalyst **I-28** to complex **I-36** and the solvent from acetone to THF, respectively, gives exclusively the branched product (Equation 1.22).<sup>[40]</sup>

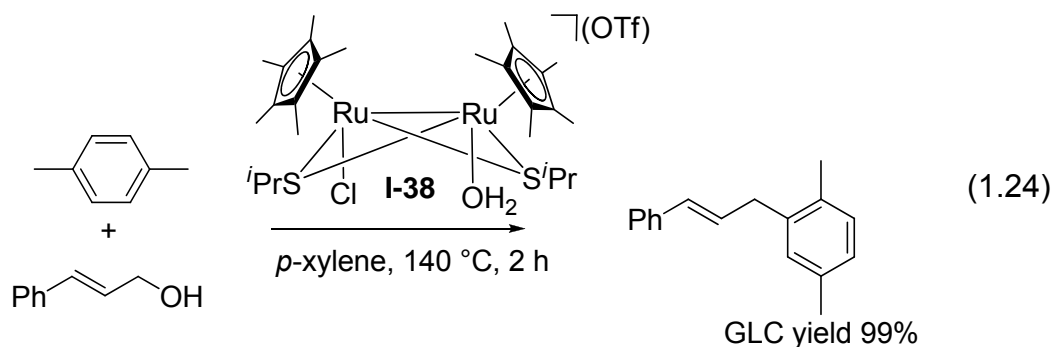


Kondo has found that the coordinatively unsaturated  $[\text{Ru}(\text{Cp}^*)(\text{amidinate})]$  complex **I-37** successfully catalyzes the reaction of allyl methyl carbonate with dimethyl methyl malonate (Equation 1.23).<sup>[41]</sup>

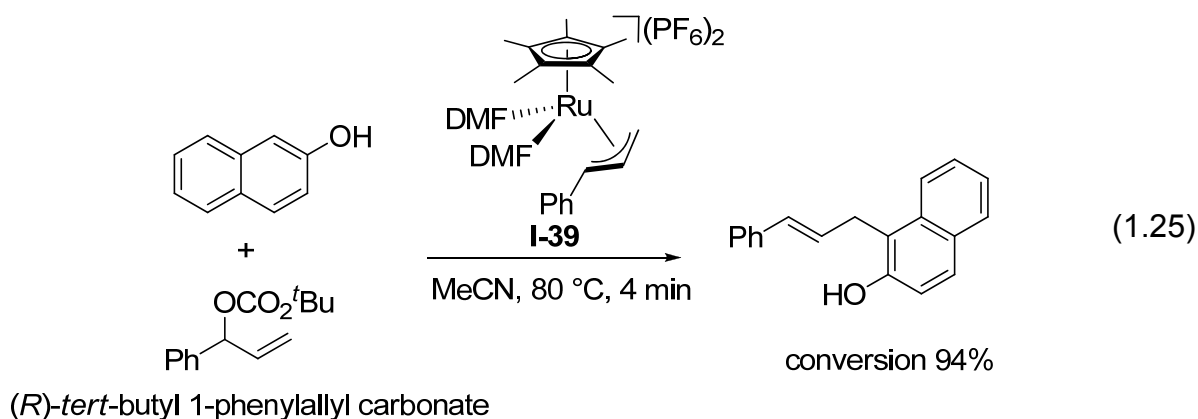




The cationic thiolate-bridged diruthenium(III,III) complex **I-38** catalyzes the Friedel-Crafts type allylation of *p*-xylene and cinnamyl alcohol (see Equation 1.24)<sup>[42]</sup>. The use of alcohols instead of allyl carbonates and halides, respectively, is an improvement because no leaving group is wasted.



Pregosin and co-workers have directly applied a ruthenium(IV) complex **I-39** for the Friedel-Crafts type allylation of 2-naphthol with *tert*-butyl 1-phenylallyl carbonate (Equation 1.25).<sup>[43]</sup> It is noteworthy that the reaction is extremely fast (about 4 min), with excellent regioselectivity and only the linear product is observed.



#### **1.4. Objective of this thesis**

The aim of this thesis is to synthesise and characterize some new, efficient ruthenium(IV)-allyl complexes for the allylation of different carbon-nucleophiles.

Further the catalyst should be capable of employing allyl alcohols instead of carbonates, acetates and halides. The catalyst should be competent modifying the substrate such that the leaving group is water. This would avoid the production of an unnecessary by-product by a “green” chemistry reaction.

As one can see in sub-chapter 1.3.2 allylation reactions catalyzed by ruthenium-Cp\* complexes are slow and/or require elevated temperatures. Therefore the new catalyst should be able to perform these reactions under mild conditions and rapidly with high yields.

## 1.5. References

- [1] E. A. Seddon, K. R. Seddon, *The Chemistry of Ruthenium*, Elsevier, **1984**.
- [2] H. H. Binder, *Lexikon der chemischen Elemente*, S. Hirzel Verlag Stuttgart-Leipzig, **1999**.
- [3] J. Emsley, *Nature's Building Block*, Oxford University Press, **2001**.
- [4] S. I. Murahashi, *Ruthenium in Organic Synthesis*, Wiley-VCH: Weinheim, **2004**.
- [5] [http://nobelprize.org/nobel\\_prizes/chemistry/laureates/2001/noyori-lecture.pdf](http://nobelprize.org/nobel_prizes/chemistry/laureates/2001/noyori-lecture.pdf).
- [6] [http://nobelprize.org/nobel\\_prizes/chemistry/laureates/2001/kowalski-lecture.pdf](http://nobelprize.org/nobel_prizes/chemistry/laureates/2001/kowalski-lecture.pdf).
- [7] T. Ohta, H. Takaya, M. Kitamura, K. Nagai, R. Noyori, *The Journal of Organic Chemistry* **1987**, *52*, 3174-3176.
- [8] H. Takaya, T. Ohta, S. Inoue, M. Tokunaga, M. Kitamura, R. Noyori, *Organic Syntheses* **1995**, *72*, 74-85.
- [9] S. Murahashi, T. Naota, T. Kuwabara, T. Saito, H. Kumobayashi, S. Akutagawa, *Journal of the American Chemical Society* **1990**, *112*, 7820-7822.
- [10] R. Noyori, T. Ohkuma, M. Kitamura, H. Takaya, N. Sayo, H. Kumobayashi, S. Akutagawa, *Journal of the American Chemical Society* **1987**, *109*, 5856-5858.
- [11] R. Noyori, C. A. Sandoval, K. Muñiz, T. Ohkuma, *Philosophical Transactions of the Royal Society A: Mathematical, Physical and Engineering Sciences* **2005**, *363*, 901-912.
- [12] R. Noyori, S. Hashiguchi, *Accounts of Chemical Research* **1997**, *30*, 97-102.
- [13] [http://nobelprize.org/nobel\\_prizes/chemistry/laureates/2005/grubbs-lecture.pdf](http://nobelprize.org/nobel_prizes/chemistry/laureates/2005/grubbs-lecture.pdf).
- [14] [http://nobelprize.org/nobel\\_prizes/chemistry/laureates/2005/schrock-lecture.pdf](http://nobelprize.org/nobel_prizes/chemistry/laureates/2005/schrock-lecture.pdf).
- [15] [http://nobelprize.org/nobel\\_prizes/chemistry/laureates/2005/chauvin-lecture.pdf](http://nobelprize.org/nobel_prizes/chemistry/laureates/2005/chauvin-lecture.pdf).
- [16] P. J.-L. Hérisson, Y. Chauvin, *Die Makromolekulare Chemie* **1971**, *141*, 161-176.
- [17] C. W. Lee, T.-L. Choi, R. H. Grubbs, *Journal of the American Chemical Society* **2002**, *124*, 3224-3225.

- [18] J. Cossy, C. Willis, V. Bellosta, S. BouzBouz, *The Journal of Organic Chemistry* **2002**, *67*, 1982-1992.
- [19] G. Ratle, X. Monseur, B. C. Das, J. Yassi, Q. Khuong-Huu, R. Goutarel, *Bull. Soc. Chim. Fr.* **1966**, 2945.
- [20] P. Bourinet, A. Quevauviller, *Ann. Pharm. Fr.* **1968**, *26*, 787.
- [21] Y. Yamamoto, Y.-i. Nakagai, N. Ohkoshi, K. Itoh, *Journal of the American Chemical Society* **2001**, *123*, 6372-6380.
- [22] B. M. Trost, A. B. Pinkerton, M. Seidel, *Journal of the American Chemical Society* **2001**, *123*, 12466-12476.
- [23] N. Chatani, T. Asaumi, S. Yorimitsu, T. Ikeda, F. Kakiuchi, S. Murai, *Journal of the American Chemical Society* **2001**, *123*, 10935-10941.
- [24] J. Takaya, J. F. Hartwig, *Journal of the American Chemical Society* **2005**, *127*, 5756-5757.
- [25] B. M. Trost, M. T. Rudd, *Journal of the American Chemical Society* **2005**, *127*, 4763-4776.
- [26] B. M. Trost, M. T. Rudd, *Journal of the American Chemical Society* **2001**, *123*, 8862-8863.
- [27] B. Martin-Matute, M. Edin, K. Bogar, F. B. Kaynak, J.-E. Backvall, *Journal of the American Chemical Society* **2005**, *127*, 8817-8825.
- [28] E. Gomez-Bengoa, N. M. Heron, M. T. Didiuk, C. A. Luchaco, A. H. Hoveyda, *Journal of the American Chemical Society* **1998**, *120*, 7649-7650.
- [29] P. A. Evans, L. J. Kennedy, *Journal of the American Chemical Society* **2001**, *123*, 1234.
- [30] P. von Matt, A. Pfaltz, *Angewandte Chemie International Edition in English* **1993**, *32*, 566-568.
- [31] K. Tissot-Croset, A. Alexakis, *Tetrahedron Letters* **2004**, *45*, 7375-7378.
- [32] T. Ohmura, J. F. Hartwig, *Journal of the American Chemical Society* **2002**, *124*, 15164-15165.
- [33] C. A. Kiener, C. Shu, C. Incarvito, J. F. Hartwig, *Journal of the American Chemical Society* **2003**, *125*, 14272-14273.
- [34] B. M. Trost, P. L. Fraise, Z. T. Ball, *Angewandte Chemie International Edition* **2002**, *41*, 1059-1061.
- [35] S.-W. Zhang, T.-a. Mitsudo, T. Kondo, Y. Watanabe, *Journal of Organometallic Chemistry* **1993**, *450*, 197-207.

- [36] K. Onitsuka, H. Okuda, H. Sasai, *Angewandte Chemie International Edition* **2008**, *47*, 1454-1457.
- [37] Y. Tsuji, T. Mukai, T. Kondo, Y. Watanabe, *Journal of Organometallic Chemistry* **1989**, *369*, C51-C53.
- [38] R. Hermatschweiler, I. Fernandez, P. S. Pregosin, E. J. Watson, A. Albinati, S. Rizzato, L. F. Veiros, M. J. Calhorda, *Organometallics* **2005**, *24*, 1809-1812.
- [39] E. C. Burger, J. A. Tunge, *Organic Letters* **2004**, *6*, 2603-2605.
- [40] D. M. Mbaye, B. Demerseman, J.-L. Renaud, T. Bruneau, Loïc, B. Christian, *Angewandte Chemie International Edition* **2003**, *42*, 5066-5068.
- [41] H. Kondo, Y. Yamaguchi, H. Nagashima, *Chemical Communications* **2000**, 1075-1076.
- [42] G. Onodera, H. Imajima, M. Yamanashi, Y. Nishibayashi, M. Hidai, S. Uemura, *Organometallics* **2004**, *23*, 5841-5848.
- [43] I. Fernández, R. Hermatschweiler, F. Breher, P. S. Pregosin, L. F. Veiros, M. J. Calhorda, *Angewandte Chemie International Edition* **2006**, *45*, 6386-6391.



# 2.

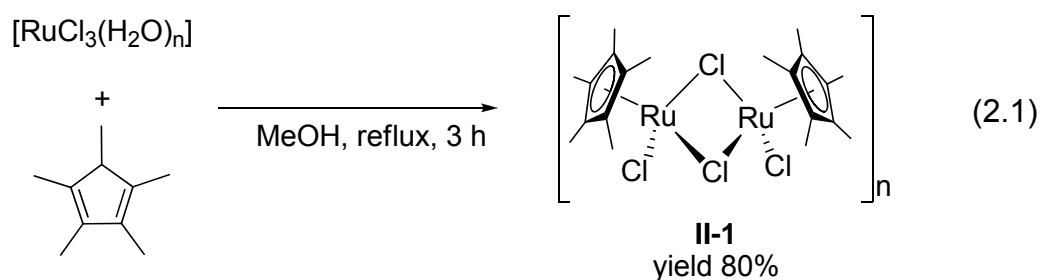
## **Synthesis and Characterisation of new Ruthenium- Cp\* Complexes**

## 2.1. Introduction

This chapter will deal with the synthesis and characterisation of new ruthenium(IV)-allyl-Cp\* complexes. Their application as catalysts and behaviour in the regioselective product transformation will be discussed in Chapters 3-5.

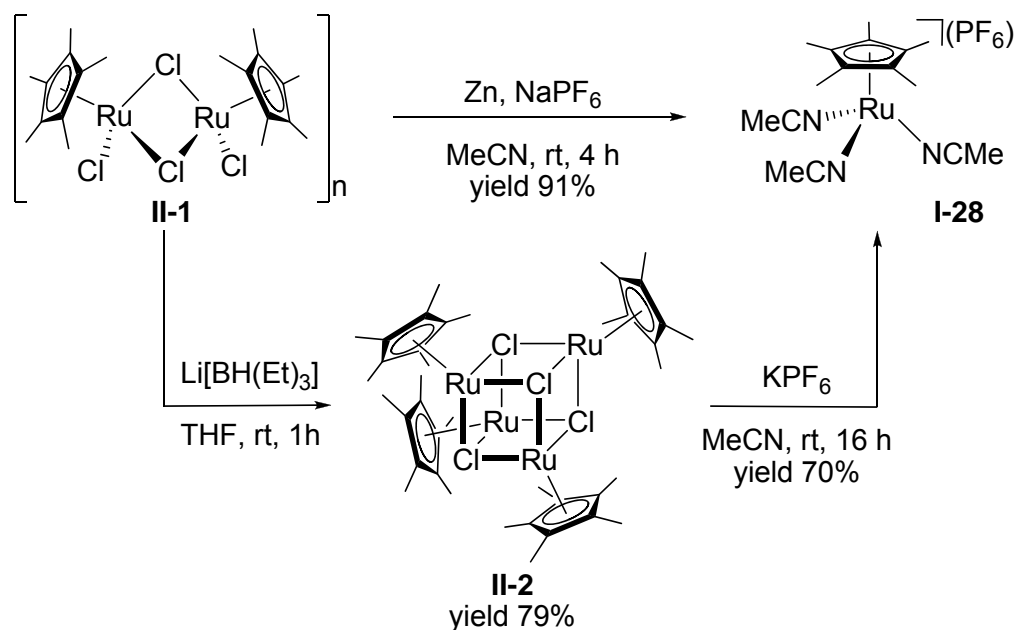
In recent years ruthenium complexes containing Cp\* ligands are finding increasing applications in homogenous catalysis (see sub-Chapter 1.3.2).<sup>[1]</sup> These complexes are mainly derived from the polymer  $[\text{RuCl}_2\text{Cp}^*]_n$ , **II-1** or Trost's catalyst,  $[\text{Ru}(\text{Cp}^*)(\text{MeCN})_3]\text{PF}_6$  (**I-28**), respectively.

Reaction of commercially available  $[\text{RuCl}_3(\text{H}_2\text{O})_n]$  with pentamethylcyclopentadiene in boiling methanol affords the polymer **II-1** in good yield (Equation 2.1).<sup>[2]</sup>



Reduction of this polymer with  $\text{Li}[\text{BHEt}_3]$  gives a ruthenium(II) tetramer<sup>[3]</sup>, **II-2**, which upon ligand addition and abstraction of chloride atoms yields in Trost catalyst.<sup>[4]</sup> In 1999 Schenk and co-workers<sup>[5]</sup> reported that this catalyst can be directly prepared by a zinc reduction of the polymer in acetonitrile in excellent yield (Scheme 2.1).

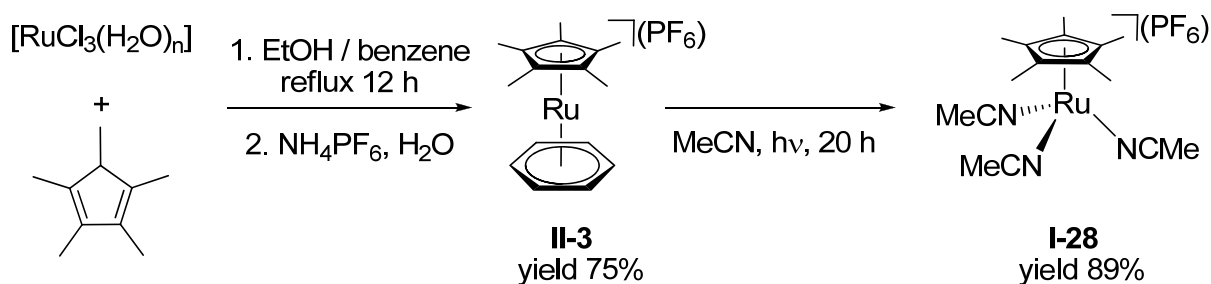




**Scheme 2.1.** Synthesis of the Trost catalyst starting from  $[\text{RuCl}_2\text{Cp}^*]_n$ .

An alternative synthetic approach involves the formation of the sandwich complex<sup>[6]</sup>, **II-3**, that exchanges the arene moiety slowly with acetonitrile ligands after irradiation (Scheme 2.2).<sup>[7]</sup>

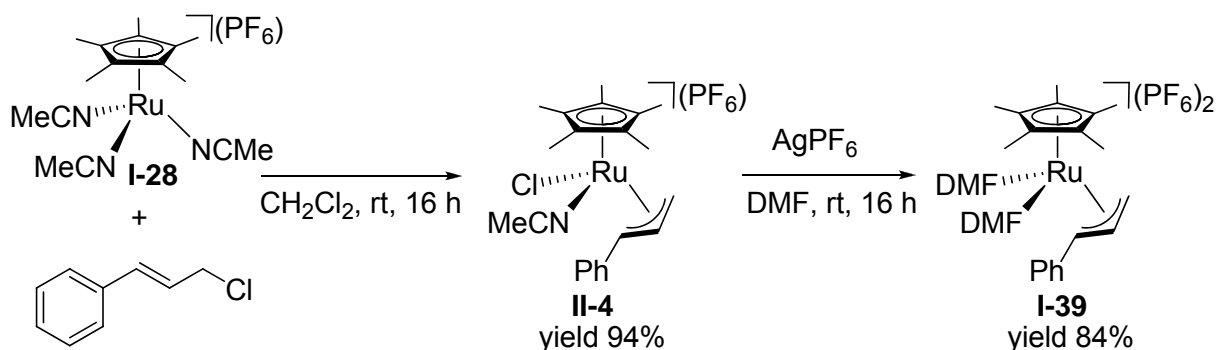
$[\text{RuCl}_2\text{Cp}^*]_n$  and  $[\text{Ru}(\text{Cp}^*)(\text{MeCN})_3]\text{PF}_6$  are commercially available. However in the synthesis on a large scale it is financially advantageous using the direct transformation of the polymer to Trost catalyst's is a straight forward reaction (Trost's catalyst is relatively expensive).



**Scheme 2.2.** Synthesis of the catalyst **I-28** via irradiation of the sandwich complex **II-3**.

The dicationic ruthenium(IV)-allyl complex **I-39** was recently prepared in the group.<sup>[8]</sup> This salt is a catalytic precursor in C-C bond allylation reactions, as discussed in sub-Chapter 1.3.2 in Equation 1.25.

The oxidative addition reaction of Trost's catalyst with cinnamyl chloride affords the ruthenium(IV)-chloride complex **II-4**,<sup>[9]</sup> which is further transformed via halogen abstraction to this dicationic ruthenium(IV) salt, **I-39** in good yield (Scheme 2.3).<sup>[8]</sup>



**Scheme 2.3.** Synthesis of the dicationic ruthenium(IV) salt **I-39**.

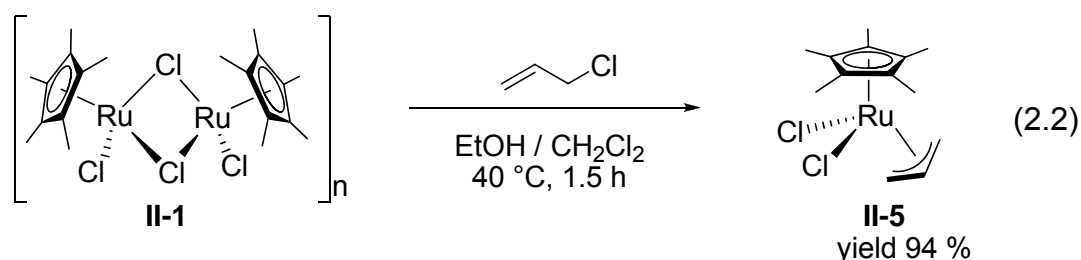
This dicationic ruthenium(IV) salt is the corner stone for this thesis and was used at the beginning for the allylation of phenol derivatives with allyl alcohols (Chapter 3). These C-C allylation reactions are relatively slow and need elevated temperatures; therefore we investigated the preparation of some new ruthenium(IV)-allyl-Cp\* catalysts.

## 2.2. Results and Discussion

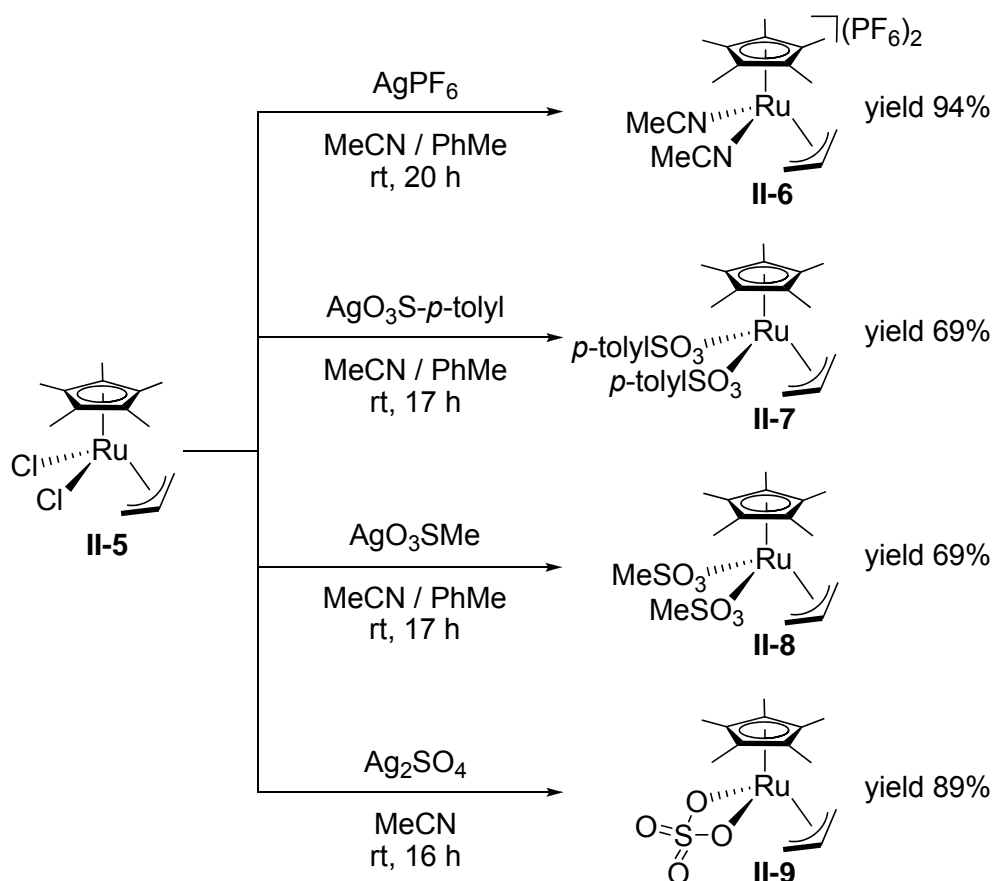
We were particularly interested in preparing labile ruthenium(IV)-allyl precursors, with the goal of accelerating the rates of existing reactions and finding new and more selective applications.

### 2.2.1. Ruthenium-Cp\* Complexes with an $\eta^3$ -C<sub>3</sub>H<sub>5</sub> Moiety

As an alternative to the preparation of ruthenium(IV)-allyl-Cp\* complexes starting from Trost's catalyst (see Scheme 2.3) one can prepare a known literature ruthenium(IV)-allyl complex **II-5** directly from the polymer **II-1** (Equation 2.2).<sup>[10]</sup>



This dichloro ruthenium(IV) complex served as starting point for a set of new ruthenium(IV)-allyl complexes (Scheme 2.4).



**Scheme 2.4.** Shows the synthesis of the new ruthenium(IV)-allyl-Cp\* complexes **II-6**, **II-7**, **II-8** and **II-9**.

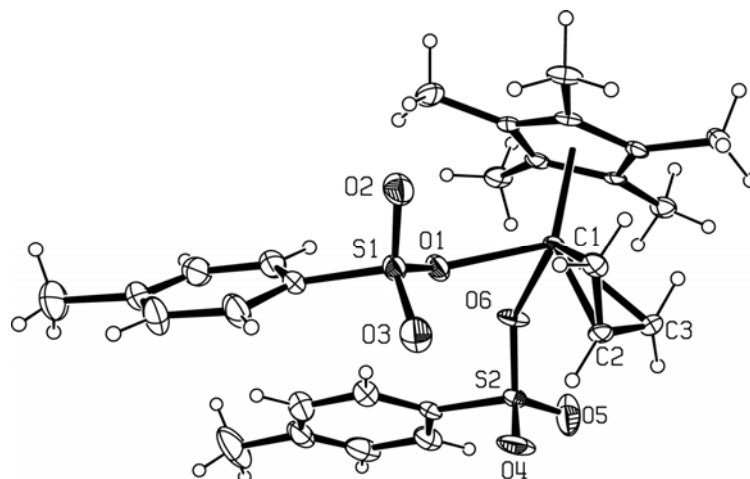
The slightly modified catalyst, [Ru( $\eta^3$ -C<sub>3</sub>H<sub>5</sub>)(Cp\*)(MeCN)<sub>2</sub>](PF<sub>6</sub>)<sub>2</sub> (**II-6**) can be prepared more readily and in higher yield than [Ru( $\eta^3$ -Ph-C<sub>3</sub>H<sub>4</sub>)(Cp\*)(DMF)<sub>2</sub>](PF<sub>6</sub>)<sub>2</sub> (**I-39**) (see Scheme 2.3). Starting from the polymer, only two instead of three reaction steps are necessary and the overall yield increases from 72% to 88%.

The allylation of indoles (see Chapter 4) works with Trost's catalyst in combination with sulfonic acids. Therefore we prepared two sulfonate complexes, **II-7**, **II-8** and a sulfate complex, **II-9** starting from **II-5**, in 69% and 89% yields, respectively.

Crystals of complexes **II-7** and **II-9** suitable for X-ray diffraction were obtained from ether/acetone and ether/dichloromethane solutions, respectively. Figures 2.1 and 2.2

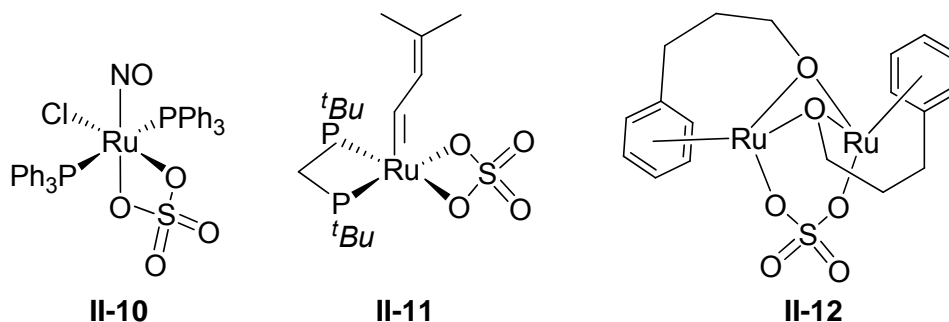
show an ORTEP view of the two complexes, and the captions give a selection of bond lengths and bond angles.

In structure **II-7**, the immediate coordination sphere contains the Cp\*, the  $\eta^3$ -C<sub>3</sub>H<sub>5</sub>, and two coordinated *p*-tolylsulfonate anions. The  $\eta^3$ -allyl ligand has the central C-H vector pointing away from the Cp\*, and all of the Ru-O and Ru-C(allyl) separations are consistent with the literature. The six S-O separations do not differ much and fall in narrow range of ca. 1.42-1.48 Å.



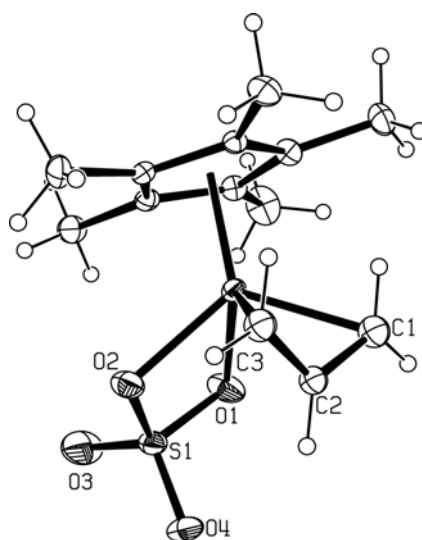
**Figure 2.1.** ORTEP view of complex **II-7** showing the  $\eta^3$ -allyl coordination as well as the *p*-tolylsulfonate ligands. Selected bond lengths (Å) and bond angles (°): Ru(1)-O(1), 2.154(4); Ru(1)-O(6), 2.144(3); Ru(1)-C(1), 2.185(4); Ru(1)-C(2), 2.135(3); Ru(1)-C(3), 2.213(4); S(1)-O(1), 1.474(4); S(1)-O(2), 1.454(3); S(1)-O(3), 1.434(3); S(2)-O(4), 1.446(4); S(2)-O(5), 1.413(5); S(2)-O(6), 1.490(3); C(1)-C(2), 1.396(6); C(2)-C(3), 1.402(6); O(1)-Ru(1)-O(6), 77.69(12); O(1)-S(1)-O(2), 111.4(2); O(1)-S(1)-O(3), 113.6(2); O(2)-S(1)-O(3), 113.2(3); O(4)-S(2)-O(5), 114.4(3); O(4)-S(2)-O(6), 111.1(2); O(5)-S(2)-O(6), 113.1(3).

There are not many structures<sup>[11-16]</sup> of sulfato ligands in connection with ruthenium chemistry (see for example **II-10**, **II-11**, **II-12**). The study by Volland<sup>[14]</sup> et al., which includes structure **II-10**, also includes ruthenium complexes whose structures possess coordinated CF<sub>3</sub>SO<sub>3</sub><sup>-</sup> and CF<sub>3</sub>CO<sub>2</sub><sup>-</sup>.



The immediate coordination sphere of **II-9** contains the Cp\*, the  $\eta^3$ -C<sub>3</sub>H<sub>5</sub>, and the chelated sulfate anion. Again the allyl ligand has the central carbon C-H vector pointing away from the Cp\*, and the Ru-Cp\* bonding is slightly asymmetric. The two Ru-O bond lengths Ru(1)-O(1), 2.108(3) Å and Ru(1)-O(2), 2.103(3) Å are marginally longer than those for **II-10**, Ru-O 2.079(7) Å, but not quite as long as the Ru-O(*p*-tolylsulfonate) separations (Ru(1)-O(1), 2.154(4); Ru(1)-O(6), 2.144(3)) in **II-7**. The three Ru-C(allyl) distances are normal and very close to those found for **II-7**.

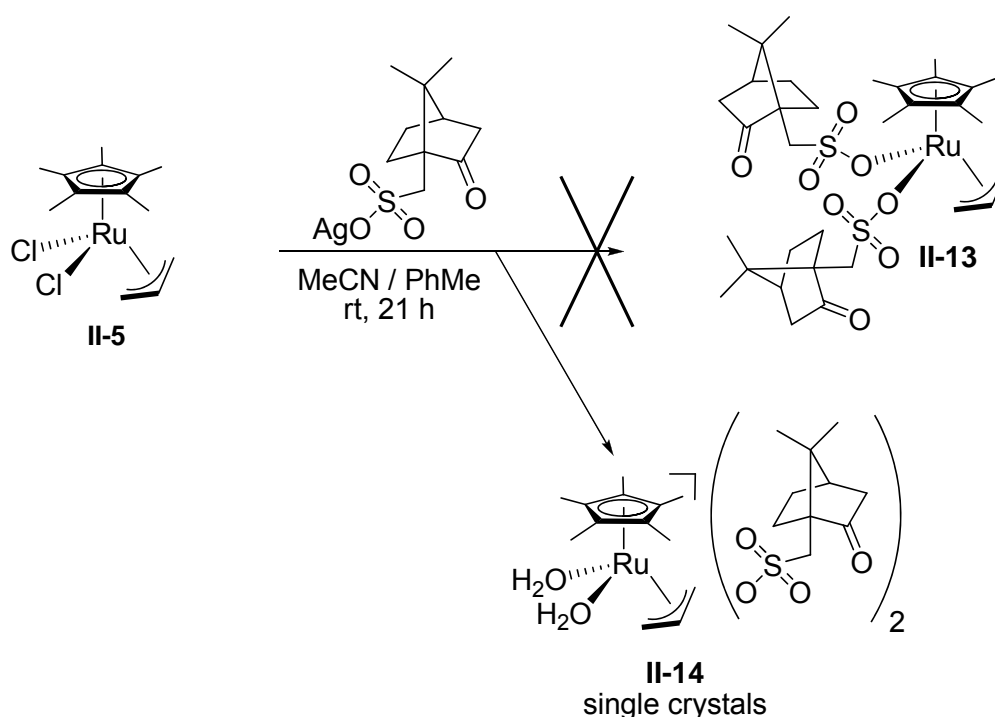
The four sulfate S-O bond lengths, S(1)-O(1) 1.518(3), S(1)-O(2) 1.527(3), S(1)-O(3) 1.429(3) and S(1)-O(4) 1.437(3), suggest localized bonding in that the two S-O bonds associated with the metal, at ca 1.52 Å, are significantly longer than the remaining two S-O distances at ca 1.43 Å. The O(1)-Ru(1)-O(2) angle at 66.86(10) is small (as is the analogous bond angle in **II-10**, ca 69°).



**Figure 2.2.** ORTEP view of complex **II-9** showing the  $\eta^3$ -allyl coordination as well as the bidentate coordination of the sulfate ligand. Selected bond lengths (Å) and bond angles (°): Ru(1)-O(2), 2.103(3); Ru(1)-O(1), 2.108(3); Ru(1)-C(3), 2.279(7); Ru(1)-C(2), 2.163(6); Ru(1)-C(1), 2.181(8); S(1)-O(1), 1.518(3); S(1)-O(2), 1.527(3); S(1)-O(3), 1.429(3); S(1)-O(4), 1.437(3); O(2)-Ru(1)-O(1), 66.86(10); O(3)-S(1)-O(4), 113.54(19); O(3)-S(1)-O(1), 111.3(2); O(4)-S(1)-O(1), 110.9(2); O(3)-S(1)-O(2), 110.7(2); O(4)-S(1)-O(2), 110.3(2); O(1)-S(1)-O(2), 99.26(14). Only one orientation of the disordered allyl-molecule (C1, C2, C3) is shown.

Both species show that the sulfonate and sulfate anions, respectively, are capable of oxygen coordination to the ruthenium atom.

We were not able to obtain an analogous product with coordinated camphorsulfonate anions (**II-13**); however, after more than one month at ambient temperature crystals of the bis-aquo complex **II-14** were grown from an acetone solution layered by ether (Scheme 2.5). We presume that the water derives from the acetone solvent.

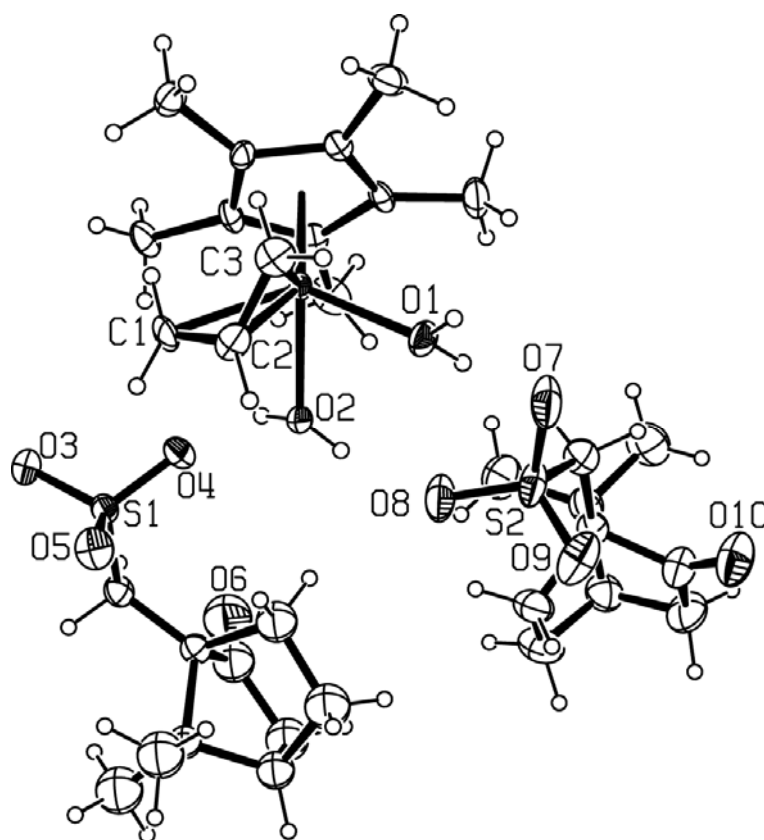


**Scheme 2.5.** Shows the obtained bis-aquo ruthenium(IV)-allyl-Cp\* complexes **II-14**.

Figure 2.3 shows an ORTEP view of complex **II-14** with a selection of bond lengths and bond angles. Although Ru(H<sub>2</sub>O) complexes are known<sup>[17-21]</sup>, this is the first such structure with camphorsulfonate anions and supports the view that this bulky anion will not be a strong ligand. The immediate coordination sphere contains the Cp\*, the  $\eta^3$ -C<sub>3</sub>H<sub>5</sub> an two water molecules. Again the central allyl proton is pointing away from the Cp\* and all of the Ru-O and Ru-C(allyl) bond lengths are consistent with the literature.

The O(1)-Ru-O(2) angle associated with the water molecules is ca 79°, whereas the various O-S-O angles from the two anions fall in the range ca 110°-115°. The six S-O separations do not differ much and fall in narrow range of ca. 1.42-1.47 Å. The

positions of the two anions are consistent with H-bonding interactions between the coordinated water and the oxygen atoms of the sulfonate anions.



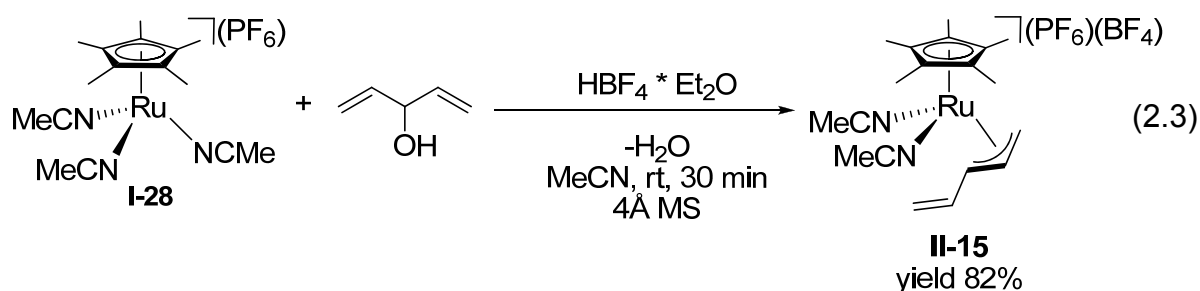
**Figure 2.3.** ORTEP view of complex **II-14** showing the  $\eta^3$ -allyl coordination as well as the coordination of the two water molecules and the un-coordinated camphor-sulfonate counterions. Selected bond lengths (Å) and bond angles (°): Ru(1)-O(1), 2.119(3); Ru(1)-O(2), 2.141(3); Ru(1)-C(1), 2.199(5); Ru(1)-C(2), 2.114(4); Ru(1)-C(3), 2.183(4); S(1)-O(5), 1.446(4); S(1)-O(4), 1.452(3); S(1)-O(3), 1.461(4); S(2)-O(9), 1.419(5); S(2)-O(8), 1.457(4); S(2)-O(7), 1.471(5); O(1)-Ru(1)-O(2), 79.02(13); O(5)-S(1)-O(4), 112.9(2); O(5)-S(1)-O(3), 112.6(2); O(4)-S(1)-O(3), 112.4(2); O(9)-S(2)-O(8), 114.8(3); O(9)-S(2)-O(7), 112.9(3); O(8)-S(2)-O(7), 110.6(2). Only one orientation of the disordered camphor-sulfonate counterion is shown.

### 2.2.2. Ruthenium-Cp\* Complexes with an $\eta^3$ - or $\eta^5$ -Pentadienyl Moiety

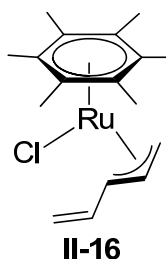
The allylation of indoles (see Chapter 4) with  $\text{CH}_2=\text{CHCH}(\text{OH})\text{CH}=\text{CH}_2$  gives exclusively linear, rather than the branched, product. Therefore we considered it useful to study the reaction of this allyl alcohol in oxidative addition reactions together with Trost's catalyst and an acid. It is usually assumed that a ruthenium(II) complex

and an allyl substrate is converted into a ruthenium(IV)-allyl intermediate via an oxidative addition, which is then attacked by a nucleophile. However, relatively little is known about the structure, stability and dynamics of these ruthenium(IV)-allyl species under acidic conditions and when isomeric allyl complexes can be formed.

The product of the stoichiometric reaction of this dienol with  $[\text{Ru}(\text{Cp}^*)(\text{MeCN})_3](\text{PF}_6)$  in the presence of  $\text{HBF}_4 \cdot \text{Et}_2\text{O}$  is shown in Equation 2.3.



Structure **II-15** was confirmed by NMR experiments ( $^1\text{H}$ -,  $^{13}\text{C}$ -, 2-D-NMR spectra) and is consistent with the  $\eta^3$ -vinyl-allyl organometallic complex **II-16**, which has been reported previously by Stryker and co-workers.<sup>[22]</sup>

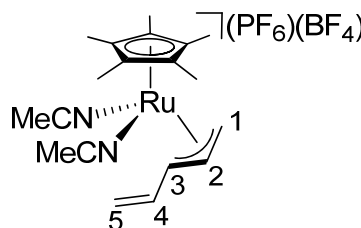


However, **II-16** is a neutral ruthenium(II) complex, whereas our salt contains ruthenium(IV). On the basis of NOE data we determined, that our product has the central allyl proton remote from the  $\text{Cp}^*$ . This observation is consistent with the literature<sup>[23]</sup> and with the crystal structures shown in Figures 2.1 and 2.2. Table 2.1 shows the  $^1\text{H}$ -NMR data for the seven non-equivalent protons of the allyl fragment, three of which appear in the region of a non-coordinating double bond. The  $^{13}\text{C}$ -NMR spectrum clearly reveals that the allyl carbon atoms C1, C2 and C3 are coordinated and the two vinyl carbons C4 and C5 appear at the expected high frequency.



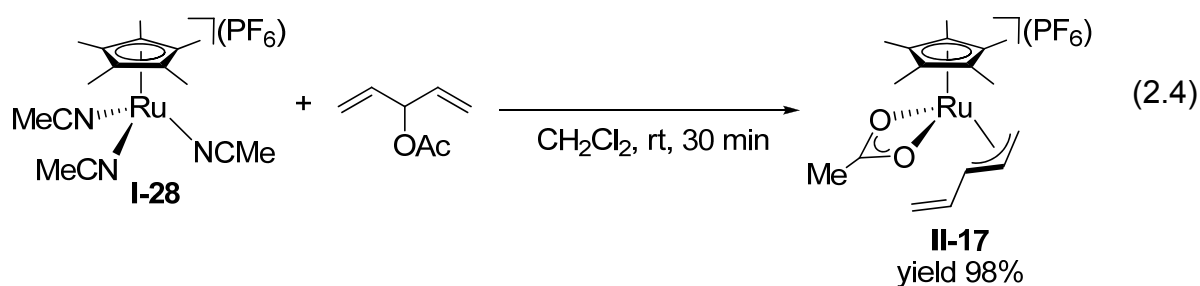
**Table 2.1.**  $^1\text{H}$ - and  $^{13}\text{C}$ -NMR Data for **II-15** in  $\text{CD}_3\text{CN}$  at rt.

Position	$\delta(^1\text{H})$ [ppm]	$\delta(^{13}\text{C})$ [ppm]
1 <sub>syn</sub>	4.54	67.4
1 <sub>anti</sub>	2.94	67.4
2	5.86	97.0
3	4.29	98.6
4	6.39	135.7
5 <sub>cis</sub>	6.04	129.1
5 <sub>trans</sub>	5.99	129.1



The crude product, **II-15**, contained a second component which could not be completely identified. From the  $^1\text{H}$ -NMR spectrum, this unknown component contains two  $\text{Cp}^*$ 's and an  $\eta^5\text{-C}_5\text{H}_7$  fragment with 7 protons in the ratio 2:2:2:1 and may be a dinuclear triple-decker *U*-shaped sandwich complex.<sup>[24]</sup>

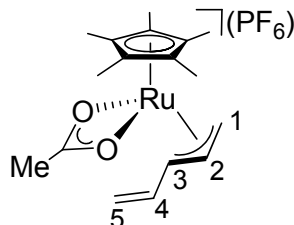
The reaction of 1,4-pentadien-3-yl acetate with  $[\text{Ru}(\text{Cp}^*)(\text{MeCN})_3](\text{PF}_6)$  affords a related ruthenium(IV)-allyl complex **II-17** with a chelated acetate anion in almost quantitative yield (Equation 2.4).



$^1\text{H}$ - and  $^{13}\text{C}$ -NMR chemical shifts for the organometallic allyl fragment are given in Table 2.2.

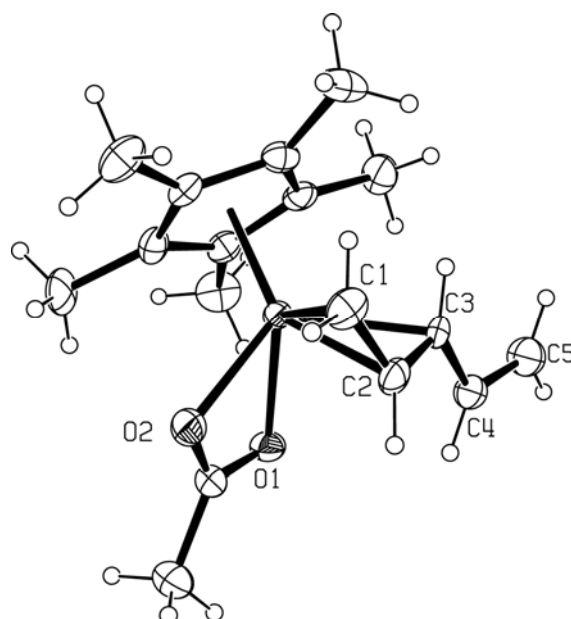
**Table 2.2.**  $^1\text{H}$ - and  $^{13}\text{C}$ -NMR Data for **II-17** in  $\text{CD}_2\text{Cl}_2$  at rt.

Position	$\delta(^1\text{H})$ [ppm]	$\delta(^{13}\text{C})$ [ppm]
$1_{syn}$	4.46	66.7
$1_{anti}$	3.01	66.7
2	5.47	103.6
3	4.05	88.5
4	6.08	135.6
$5_{cis}$	5.75	124.1
$5_{trans}$	5.71	124.1



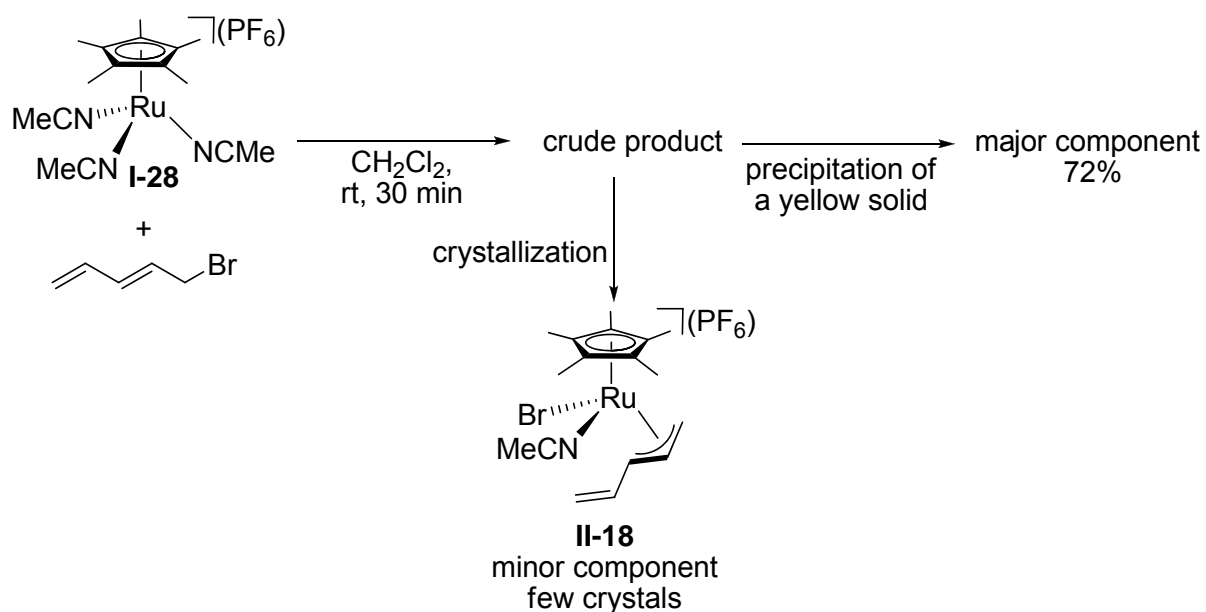
Crystals of complex **II-17** suitable for X-ray diffraction were obtained from an ether/dichloromethane solution. Figure 2.4 shows an ORTEP view of the complex, and the caption gives a selection of bond lengths and bond angles. Again the central allyl proton is pointing away from the  $\text{Cp}^*$  and all of the Ru-O(acetate) distances are consistent with the literature. The most interesting aspect of this structure involves the two markedly different terminal Ru-C bond distances, Ru(1)-C(1) and Ru(1)-C(3), at 2.195(8) Å and 2.260(7) Å, respectively. Routine Ru-C(allyl) separations are on the order of 2.1-2.2 Å. However, the distortion in allyl bonding for this vinyl allyl complex is not quite so marked as in that for a related  $[\text{Ru}(\eta^3\text{-PhCHCHCH}_2)(\text{Cp}^*)(\text{MeCN})_2](\text{PF}_6)_2$  complex<sup>[9]</sup>.

Assuming that such a distortion favors attack at the branched carbon, these results partly rationalize the observation that the allyl intermediate from  $\text{CH}_2=\text{CH}-\text{CH}(\text{OH})\text{CH}=\text{CH}_2$  affords only linear products, whereas the allyl intermediate from  $\text{PhCH}(\text{OH})\text{CH}=\text{CH}_2$  results in more branched product.



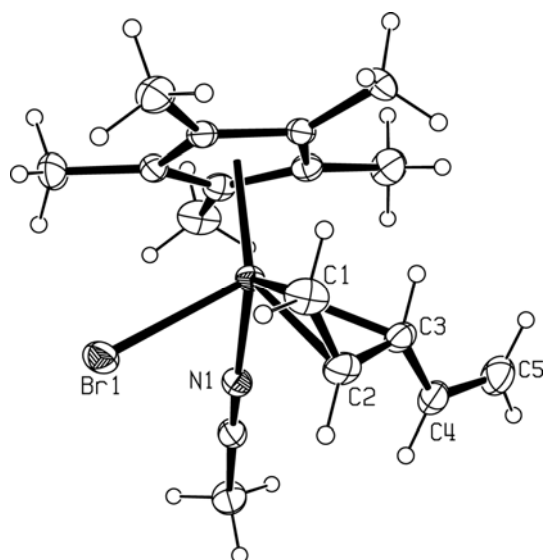
**Figure 2.4.** ORTEP view of complex **II-17** showing the  $\eta^3$ -allyl coordination as well as the bidentate coordination of the acetate ligand. Selected bond lengths (Å) and bond angles ( $^\circ$ ): Ru(1)-C(1) 2.195(8); Ru(1)-C(2), 2.123(6); Ru(1)-C(3), 2.260(7); Ru(1)-O(2), 2.139(4); Ru(1)-O(1), 2.147(3); C(1)-C(2), 1.409(12); C(2)-C(3), 1.397(12); C(3)-C(4), 1.500(9); C(4)-C(5), 1.338(9); O(2)-Ru(1)-O(1), 61.29(19).

Scheme 2.6 shows the two products which are observed from the oxidative addition reaction of 5-bromo-1,3-pentadiene with  $[\text{Ru}(\text{Cp}^*)(\text{MeCN})_3](\text{PF}_6)$ .



**Scheme 2.6.** Overview of the oxidative addition reaction of 5-bromo-1,3-pentadiene with  $[\text{Ru}(\text{Cp}^*)(\text{MeCN})_3](\text{PF}_6)$  in  $\text{CH}_2\text{Cl}_2$ .

From the crude product a few orange-red single crystals of the *minor* component **II-18** could be isolated from an ether/dichloromethane solution. The structure was solved by X-ray diffraction methods and Figure 2.5 shows an ORTEP view of the complex, and the caption gives a selection of bond lengths and bond angles. Again the central allyl proton is pointing away from the Cp\* and all of the Ru-Br and Ru-N(acetonitrile) distances are consistent with the literature. Once more, this  $\eta^3$ -vinyl-allyl structure shows two markedly different terminal Ru-C bond distances, Ru(1)-C(1) and Ru(1)-C(3), at 2.220(4) Å and 2.299(4) Å, respectively.

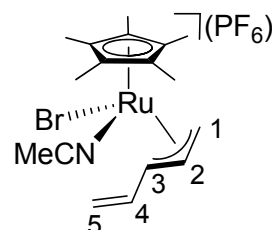


**Figure 2.5.** ORTEP view of the cation of salt **II-18** showing the  $\eta^3$ -allyl coordination as well as the acetonitrile and bromide ligands. Selected bond lengths (Å) and bond angles (°): Ru(1)-Br(1), 2.5522(5); Ru(1)-N(1), 2.080(3); Ru(1)-C(1), 2.220(4); Ru(1)-C(2), 2.159(4); Ru(1)-C(3), 2.299(4); C(1)-C(2), 1.404(6); C(2)-C(3), 1.404(6); C(3)-C(4), 1.455(6); C(4)-C(5), 1.315(7); N(1)-Ru(1)-Br(1), 82.45(9).

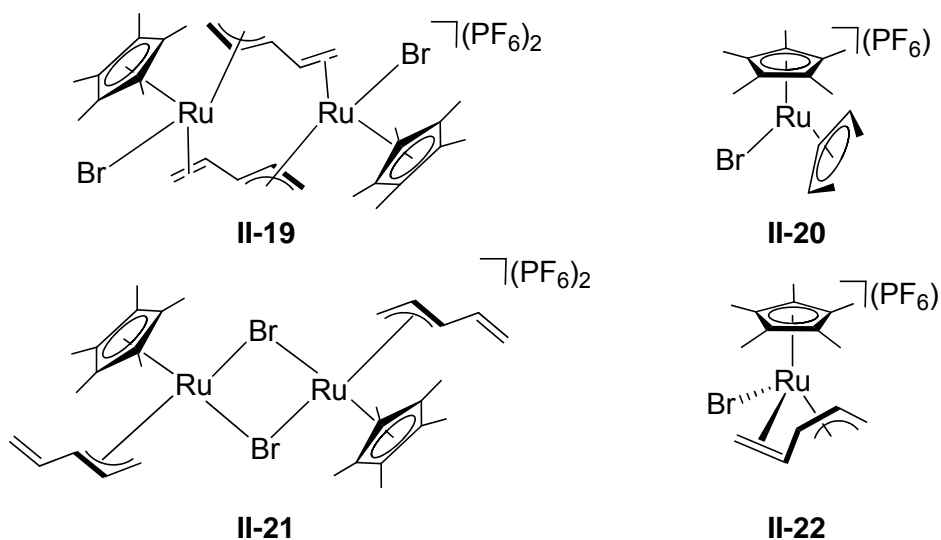
If one redissolves the few crystals of **II-18** in CD<sub>3</sub>NO<sub>2</sub>, a mixture of the *minor* and *major* components is obtained. Despite the low signal-to-noise ratio we were able to assign the structure of the organometallic allyl fragment of the *minor* component to **II-18** (see Table 2.3).

**Table 2.3.**  $^1\text{H}$ - and  $^{13}\text{C}$ -NMR data for **II-18** in  $\text{CD}_3\text{NO}_2$  at rt.

Position	$\delta(^1\text{H})$ [ppm]	$\delta(^{13}\text{C})$ [ppm]
$1_{syn}$	4.54	65.8
$1_{anti}$	2.56	65.8
2	5.43	95.8
3	3.82	87.4
4	6.27	136.2
$5_{cis}$	5.82	124.3
$5_{trans}$	5.79	124.3

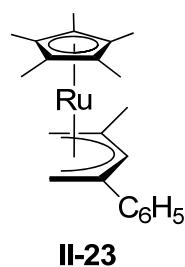


The structure of the major component (obtained by precipitating a yellow solid from the crude product), was not immediately obvious. Given the elemental analysis ( $\text{C}_{15}\text{H}_{22}\text{BrF}_6\text{PRu}$ ) and the seven non-equivalent protons in the  $^1\text{H}$ -NMR spectrum, we suggest, that the *major* component contains an asymmetric allyl coordinated structure. Several possibilities are indicated in Scheme 2.7.

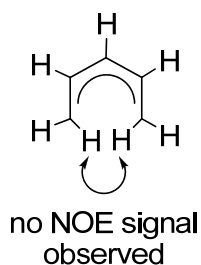
**Scheme 2.7.** Possible structures of the major component.

The dinuclear species **21**, containing an  $\eta^3$ -vinyl-allyl ligand, was dismissed on the basis of its  $^1\text{H}$ - and  $^{13}\text{C}$ -NMR properties, since all five carbons (and the seven associated protons) show marked high-frequency shifts (see Table 2.4).

The bridged  $\eta^5$ -pentadienyl coordinated complex **II-19**, was eliminated by PGSE diffusion studies, which indicate that this *major* component is a mononuclear species. Therefore we had to distinguish between species **II-20** and **II-22**. Ernst and co-workers<sup>[25]</sup> have reported a number of *U*-shaped  $\eta^5$ -pentadienyl coordinated sandwich complexes, e.g. **II-23**.

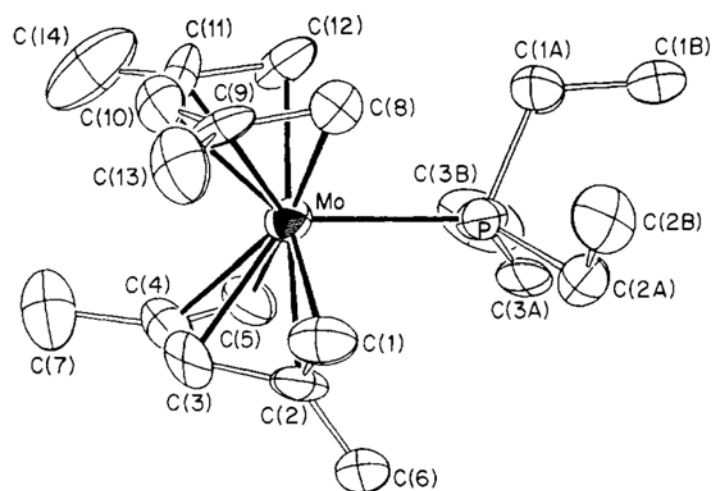


For the possible species **II-20**, a rotated *U*-shaped  $\eta^5$ -pentadienyl could explain the observed lack of symmetry. This possibility was dismissed on the basis of Overhauser studies, which should show a strong NOE signal between the two terminal anti protons (see Figure 2.6), and this was not observed.



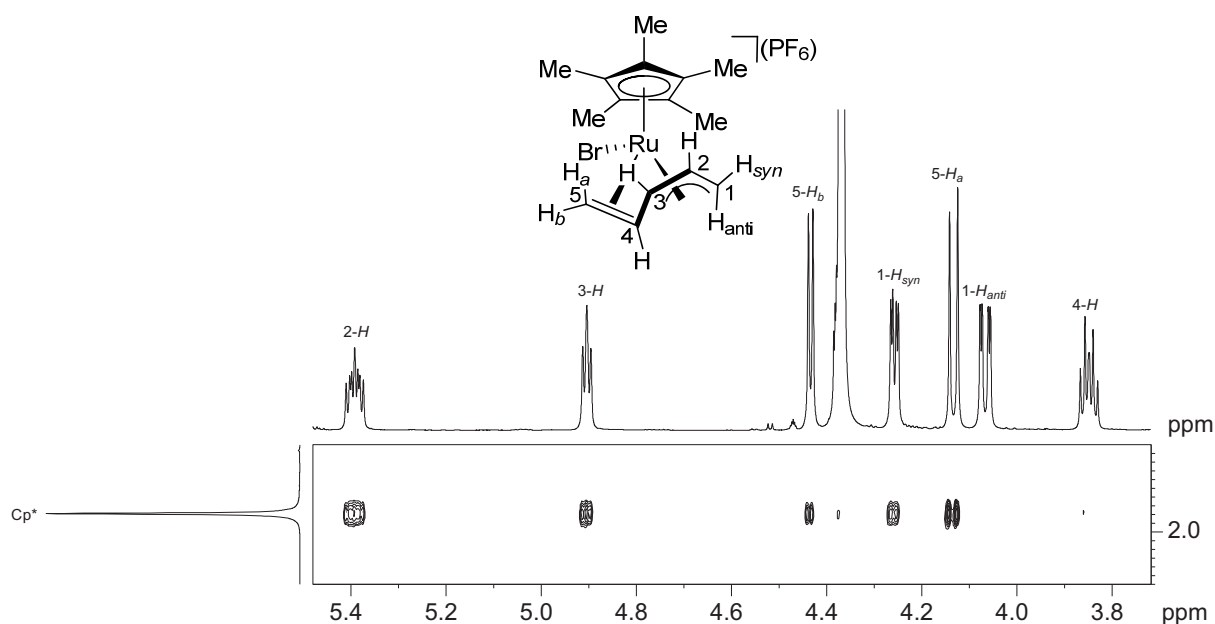
**Figure 2.6.** A *U*-shaped pentadienyl fragment, which could not be verified by Overhauser studies.

There are several reports<sup>[26-28]</sup> on molybdenum(II) complexes which show the *S*-shaped  $\eta^5$ -pentadienyl coordination of **II-22** rather than an *U*-shaped of **II-20** (see Scheme 2.8).



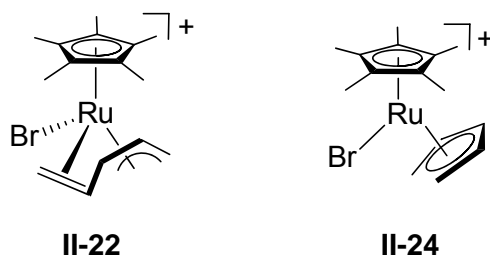
**Scheme 2.8.** Literature structure which shows a S-shaped  $\eta^5$ -pentadienyl coordination (atoms C(1)-C(5)).

The proposed species **II-22** could be verified by  $^1\text{H-NMR}$  Overhauser studies at  $-30$  °C. Figure 2.7 shows a slice through the 2-D NOESY spectrum. The Cp\* methyl groups reveal strong cross-peaks to the allyl protons 1- $\text{H}_{\text{syn}}$ , 2-H, 3-H, 5- $\text{H}_a$  and 5- $\text{H}_b$ . Further the absence of significant contacts to 1- $\text{H}_{\text{anti}}$  and 4-H support the proposed structure.



**Figure 2.7.** Section of the 2-D NOESY spectrum for salt **II-22** showing the contacts from the Cp\* methyl groups to the various  $\text{C}_5\text{H}_7$  protons. Note that 4-H and 1- $\text{H}_{\text{anti}}$  show no- and very weak-contacts, respectively ( $-30$  °C, 700 MHz,  $\text{CD}_2\text{Cl}_2$ ).

DFT calculations<sup>[29]</sup> were performed by Prof. Veiros in order to evaluate the relative stability of the two isomers **II-22** and **II-24** of the cation  $[\text{Ru}(\eta^5\text{-C}_5\text{H}_7)\text{Br}(\text{Cp}^*)]^+$ . We were especially interested in understanding the driving force for the observation of the “S” versus the “U” shaped conformations of the pentadienyl-ligand, that is, molecules with structures **II-22** and **II-24**, respectively. The geometries calculated for both isomers are represented in Figure 2.8.

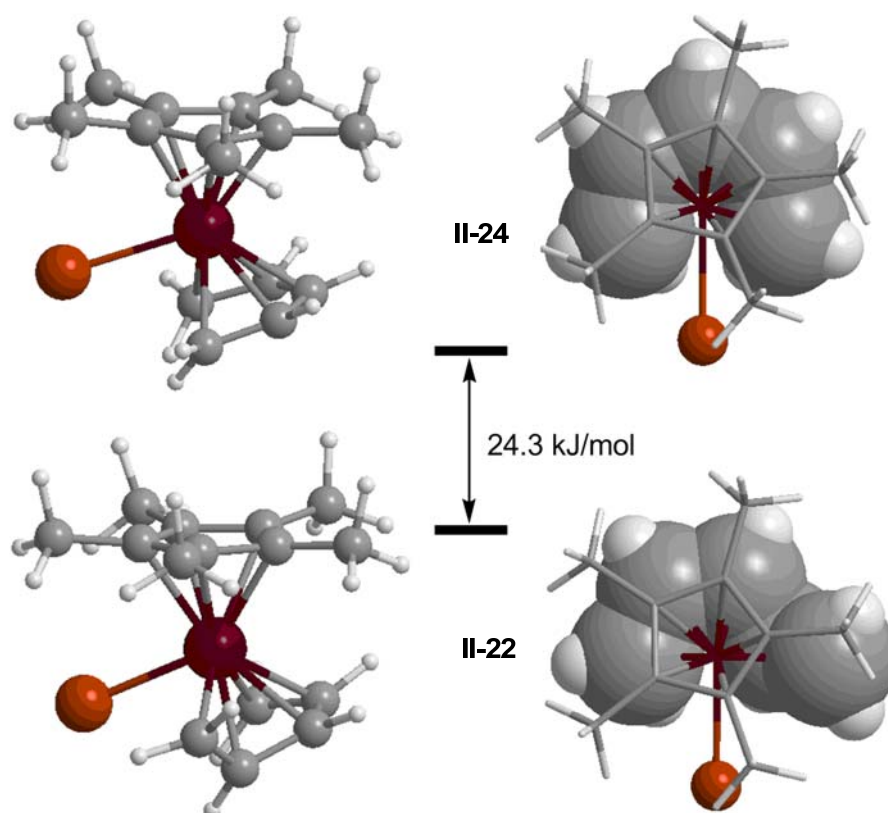


The calculations indicate that the most stable isomer (by 24.3 kJ/mol) corresponds to the complex with the “S” shaped pentadienyl ligand (**II-22**), in agreement with the conclusions based on the NMR results. In this cation, the pentadienyl-ligand adopts an allyl-ene coordination mode with the coordinated C4-C5 double bond making a 55° angle with the plane of the C1–C2–C3 allyl moiety. The C2-H bond is directed towards the Cp\* ligand, corroborating the data from the NOESY spectrum.

Despite several attempted initial geometries with an asymmetric coordination of the pentadienyl ligand (such as **II-20**), the structure obtained for the complex with a “U” shaped pentadienyl ligand, **II-24** has a symmetric coordination geometry with the central C-atom pointing towards the Cp\* ligand. In the optimized structure **II-24**, the pentadienyl-ligand presents a planar coordination geometry with the five carbon atoms within bonding distances from the metal (2.21–2.31 Å) and a Ru–C mean distance of 2.26 Å. This value is 0.03 Å longer than the Ru–C(pentadienyl) mean distance in **II-22**. Although a slightly shorter Ru–C mean distance suggests a stronger coordination of the pentadienyl-moiety in complex **II-22**, no clear electronic reason could be found to explain the stability difference calculated for the two isomers. The metal charge, obtained by means of a Natural Population Analysis (NPA),<sup>[30-36]</sup> is within 0.01 in both species, indicating similar electron density at both metal centers.



From a structural point of view, the main difference between the two isomeric species is the Ru–Br distance, which is considerably longer in the complex **II-24**, 2.59 Å (assuming a symmetric pentadienyl), compared with the isomer **II-22**, 2.55 Å (with an “S” shaped conformation). In addition, the  $X_{\text{Cp}^*}\text{--Ru--Br}$  angle ( $X_{\text{Cp}^*}$  being the  $\text{Cp}^*$  ring centroid) is significantly smaller in the case of complex **II-24**,  $109^\circ$ , than in **II-22**,  $114^\circ$ . In other words, the Br ligand is somewhat more remote from the pentadienyl fragment in **II-24**, relative to **II-22**. When the pentadienyl adopts a symmetric “U” shaped arrangement, there is less space left for the Br in the metal coordination sphere, as illustrated by the space filling representations in Figure 2.8, and shown by the closest Br–C(pentadienyl) distances in both complexes: 2.99/3.02 Å in **II-24**, and 3.10/3.22 Å in **II-22**. Taken together, these computational results indicate that the stability difference between both isomers is mainly due to inter-ligand repulsion between the Br and pentadienyl ligands.

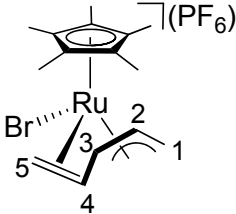


**Figure 2.8.** Optimized geometry of  $[\text{Ru}(\eta^5\text{-C}_5\text{H}_7)\text{Br}(\text{Cp}^*)]^+$  with two configurations of the pentadienyl ligand, a) the “U” shaped (structure **II-24**, top), and b) the “S” shaped (structure **II-22**, bottom). Left: side view of the optimized structures; right: top view of the molecules with space filling representations of the pentadienyl ligand. The energy difference (kJ/mol) is indicated.

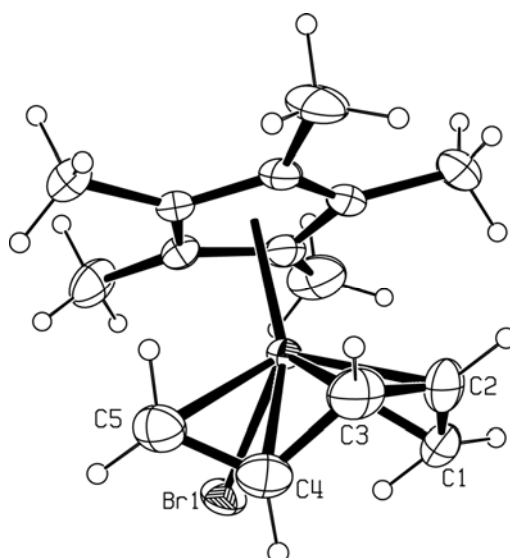
Consequently, we assign the major component to structure **II-22**, as this proposal fits all of the observed NMR and analytical data and is in agreement with the DFT calculations.  $^1\text{H}$ - and  $^{13}\text{C}$ - NMR chemical shifts for the organometallic allyl fragment are given in Table 2.4.

**Table 2.4.**  $^1\text{H}$ - and  $^{13}\text{C}$ -NMR Data for **II-22** in  $\text{CD}_3\text{NO}_2$  at  $-30\text{ }^\circ\text{C}$ .

Position	$\delta(^1\text{H})$ [ppm]	$\delta(^{13}\text{C})$ [ppm]
1 <sub>syn</sub>	4.26	68.6
1 <sub>anti</sub>	4.07	68.6
2	5.39	107.4
3	4.90	90.9
4	3.86	100.6
5 <sub>syn</sub>	4.43	78.0
5 <sub>anti</sub>	4.13	78.0

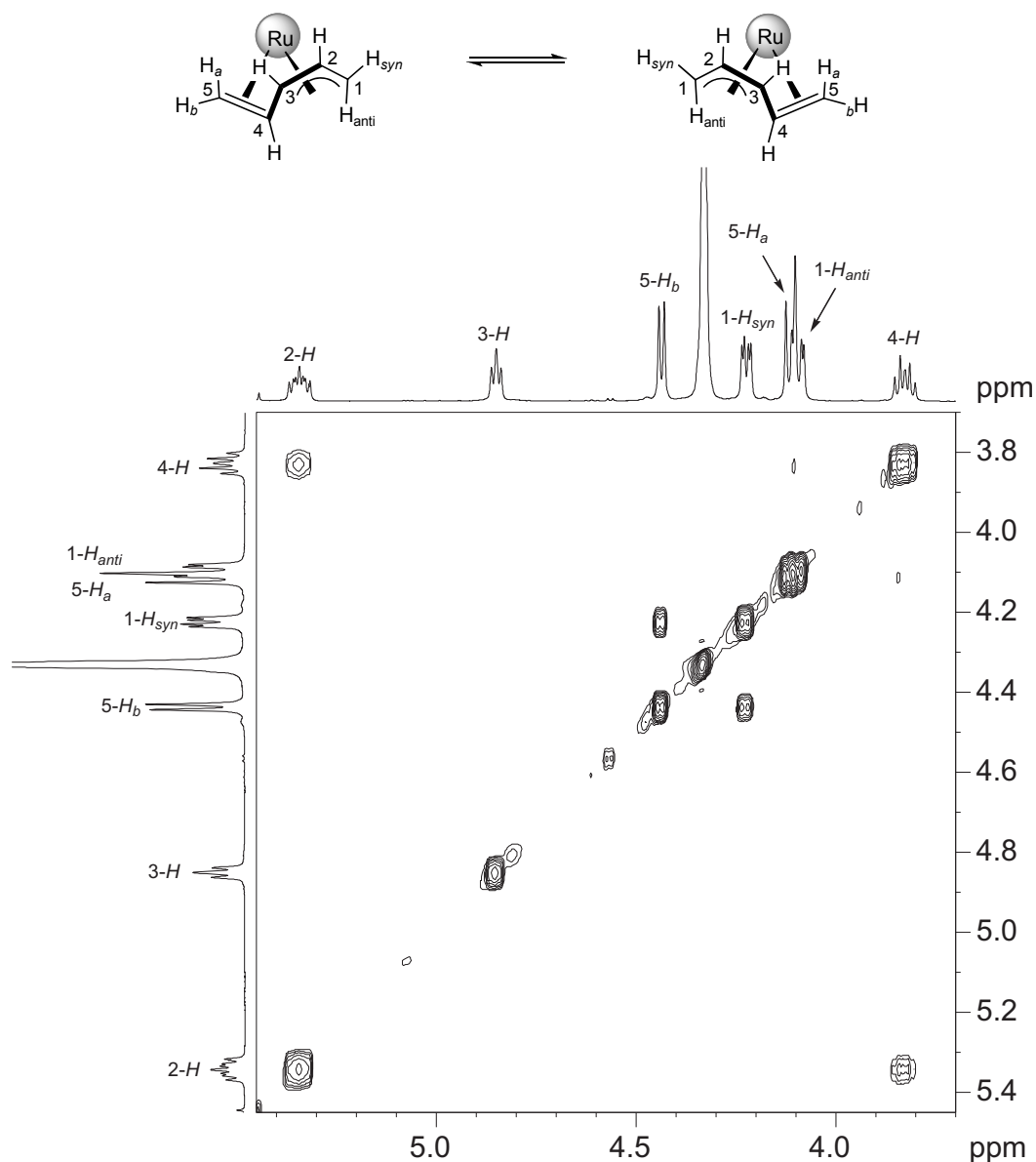


Approximately half a year later, we were able to grow crystals of **II-22** suitable for X-ray diffraction. The ORTEP structure given in Figure 2.9 represents additional proof for our proposed structure. The Ru-Br distance is consistent with the literature. The five Ru-C(allyl) bond lengths are on the order of ca 2.15-2.30 Å. The dihedral angles of C(1)-C(2)-C(3)-C(4) and C(2)-C(3)-C(4)-C(5) are ca.  $4^\circ$  and ca.  $126^\circ$ , respectively. Therefore the C-atoms C(1)-C(2)-C(3)-C(4) seem to lie in one plane. This type of  $\eta^5$ -pentadienyl moiety results when the vinyl group in a *U*-shaped orientation is rotated around the C3-C4 bond and then complexed.



**Figure 2.9.** ORTEP view of the cation of salt **II-22** showing the  $\eta^5$ -allyl-S-shaped coordination as well as the bromide ligands. Selected bond lengths (Å): Ru(1)-Br(1), 2.5288(8); Ru(1)-C(1), 2.258(7); Ru(1)-C(2), 2.216(7); Ru(1)-C(3), 2.152(8); Ru(1)-C(4), 2.152(7); Ru(1)-C(5), 2.302(7); C(1)-C(2), 1.429(12); C(2)-C(3), 1.385(13); C(3)-C(4), 1.465(11); C(4)-C(5), 1.344(11).

The room temperature NOESY spectrum of complex **II-22**, shows a selective exchange process (see Figure 2.10). The observed pair wise exchange of 2-H with 4-H, 1- $H_{anti}$  with 5- $H_b$  and 1- $H_{syn}$  with 5- $H_a$  is consistent with the equilibrium exchange of carbons C1 with C5 and C2 with C4.



**Figure 2.10.** Section of the 2-D NOESY spectrum for salt **II-22** showing the selective exchange cross-peaks between 2-H and 4-H as well as between 1- $H_{syn}$  and 5- $H_b$ . The exchange between 1- $H_{anti}$  and 5- $H_a$  is present but not well resolved (rt., 500 MHz,  $CD_2Cl_2$ ).

### 2.3. Conclusions

Summarizing, substitution reactions starting from  $[Ru(\eta^3-C_3H_5)Cl_2(Cp^*)]$  and stoichiometric oxidative addition reactions of  $CH_2=CHCH(OH)CH=CH_2$ ,  $CH_2=CHCH(OAc)CH=CH_2$ , or  $CH_2=CHCH=CHCH_2Br$  with  $[Ru(Cp^*)(MeCN)_3](PF_6)$  afford new ruthenium(IV)-allyl complexes.

Six of these complexes **II-7**, **II-9**, **II-14**, **II-17**, **II-18** and **II-22** have been studied by X-ray diffraction methods. The analyses include several 2-D NMR experiments.

In addition to the ruthenium(IV)- $\eta^3$ -vinyl-allyl bonding mode observed for **II-15**, **II-17** and **II-18**, we also find an isomer of **II-18**, with structure **II-22**, which reveals a dynamic ruthenium(IV) *S*-shaped (rather than *U*-shaped)  $\eta^5$ -pentadienyl moiety.

To the best of our knowledge this species **II-22** is the first *S*-shaped pentadienyl fragment complexed to a ruthenium(IV) center.

DFT computational results indicate that the *S* form rather than the *U* form is the most stable ruthenium(IV) species and that the stability difference between both isomers is mainly due to interligand repulsion between the Br and pentadienyl ligands.

## 2.4. References

- [1] C. Bruneau, J.-L. Renaud, B. Demerseman, *Chemistry - A European Journal* **2006**, *12*, 5178-5187.
- [2] T. D. Tilley, R. H. Grubbs, J. E. Bercaw, *Organometallics* **2002**, *3*, 274-278.
- [3] P. J. Fagan, M. D. Ward, J. C. Calabrese, *Journal of the American Chemical Society* **2002**, *111*, 1698-1719.
- [4] D. M. Mbaye, B. Demerseman, J.-L. Renaud, L. Toupet, C. Bruneau, *Advanced Synthesis & Catalysis* **2004**, *346*, 835-841.
- [5] B. Steinmetz, W. A. Schenk, *Organometallics* **1999**, *18*, 943-946.
- [6] A. R. Kudinov, M. I. Rybinskaya, Y. T. Struchkov, A. I. Yanovskii, P. V. Petrovskii, *Journal of Organometallic Chemistry* **1987**, *336*, 187-197.
- [7] J. L. Schrenk, A. M. McNair, F. B. McCormick, K. R. Mann, *Inorganic Chemistry* **2002**, *25*, 3501-3504.
- [8] I. Fernández, R. Hermatschweiler, F. Breher, P. S. Pregosin, L. F. Veiros, M. J. Calhorda, *Angewandte Chemie International Edition* **2006**, *45*, 6386-6391.
- [9] R. Hermatschweiler, I. Fernandez, P. S. Pregosin, E. J. Watson, A. Albinati, S. Rizzato, L. F. Veiros, M. J. Calhorda, *Organometallics* **2005**, *24*, 1809-1812.
- [10] H. Nagashima, K. Mukai, Y. Shiota, K. Ara, K. Itoh, H. Suzuki, N. Oshima, Y. Morooka, *Organometallics* **2002**, *4*, 1314-1315.
- [11] J. Reed, S. L. Soled, R. Eisenberg, *Inorganic Chemistry* **2002**, *13*, 3001-3005.
- [12] X.-D. He, B. Chaudret, F. Lahoz, J. A. Lopez, *J. Chem. Soc. Chem. Commun.* **1990**, 958-959.
- [13] R. Flügel, B. Windmüller, O. Gevert, H. Werner, *Chemische Berichte* **1996**, *129*, 1007-1013.
- [14] M. A. O. Volland, S. M. Hansen, F. Rominger, P. Hofmann, *Organometallics* **2004**, *23*, 800-816.
- [15] E. Nakatani, Y. Takai, H. Kurosawa, *Journal of Organometallic Chemistry* **2007**, *692*, 278-285.
- [16] J. C. Toledo, B. dos Santos Lima Neto, D. W. Franco, *Coordination Chemistry Reviews* **2005**, *249*, 419-431.
- [17] H. Asano, K. Katayama, H. Kurosawa, *Inorganic Chemistry* **1996**, *35*, 5760-5761.

- [18] D. L. Davies, J. Fawcett, S. A. Garratt, D. R. Russell, *Organometallics* **2001**, *20*, 3029-3034.
- [19] H. Kurosawa, H. Asano, Y. Miyaki, *Inorganica Chimica Acta* **1998**, *270*, 87-94.
- [20] L. Dadci, H. Elias, U. Frey, A. Hoernig, U. Koelle, A. E. Merbach, H. Paulus, J. S. Schneider, *Inorganic Chemistry* **2002**, *34*, 306-315.
- [21] M. F. Mahon, M. K. Whittlesey, P. T. Wood, *Organometallics* **1999**, *18*, 4068-4074.
- [22] A. Ramirez-Monroy, M. A. Paz-Sandoval, M. J. Ferguson, J. M. Stryker, *Organometallics* **2007**, *26*, 5010-5024.
- [23] S. Bi, A. Ariafard, G. Jia, Z. Lin, *Organometallics* **2005**, *24*, 680-686.
- [24] H. W. Bosch, H. U. Hung, D. Nietlispach, A. Salzer, *Organometallics* **2002**, *11*, 2087-2098.
- [25] G. C. Turpin, A. L. Rheingold, R. D. Ernst, *Journal of Organometallic Chemistry* **2003**, *672*, 109-114.
- [26] M. Green, K. R. Nagle, C. M. Woolhouse, D. J. Williams, *J. Chem. Soc., Chem. Commun.* **1987**, 1793-1795.
- [27] G. H. Lee, S. M. Peng, T. W. Lee, R. S. Liu, *Organometallics* **2002**, *5*, 2378-2380.
- [28] L. Stahl, J. P. Hutchinson, D. R. Wilson, R. D. Ernst, *Journal of the American Chemical Society* **1985**, *107*, 5016-5018.
- [29] R. G. Parr, W. Yang, *Density Functional Theory of Atoms and Molecules*, Oxford University Press: New York, **1989**.
- [30] J. E. Carpenter, Ph.D. thesis, University of Wisconsin, Madison WI, **1987**.
- [31] J. E. Carpenter, F. Weinhold, *Journal of Molecular Structure: THEOCHEM* **1988**, *169*, 41-62.
- [32] F. Weinhold, J. E. Carpenter, *The Structure of Small Molecules and Ions*, Plenum NY, **1988**.
- [33] J. P. Foster, F. Weinhold, *Journal of the American Chemical Society* **1980**, *102*, 7211-7218.
- [34] A. E. Reed, F. Weinhold, *The Journal of Chemical Physics* **1983**, *78*, 4066-4073.
- [35] A. E. Reed, R. B. Weinstock, F. Weinhold, *The Journal of Chemical Physics* **1985**, *83*, 735-746.
- [36] A. E. Reed, L. A. Curtiss, F. Weinhold, *Chemical Reviews* **2002**, *88*, 899-926.





# 3.

## **Allylation of Phenol Derivatives**

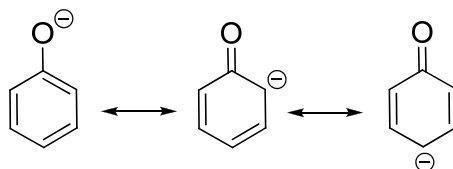
### 3.1. Introduction

This chapter involves the ruthenium(IV) catalyzed C-C bond allylation of phenol derivatives with substituted allyl alcohols. The first challenge was to perform the reaction directly with allyl alcohols as substrates instead of allyl carbonates.

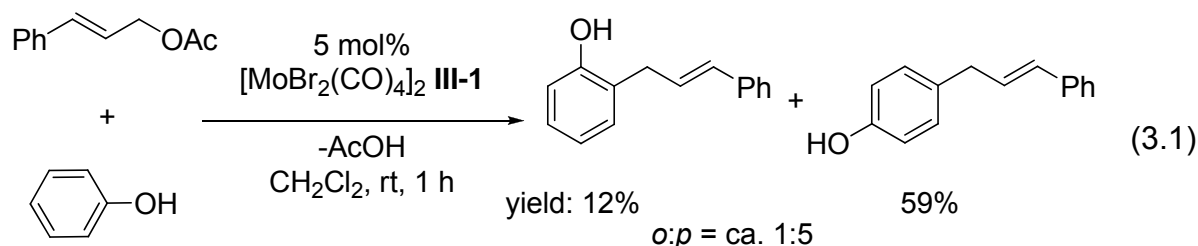
An increasing variety of metal-mediated catalytic transformations involving allyl compounds have been developed, and these tools are rapidly becoming indispensable in organic synthesis. Typically allyl carbonates, acetates and halides have been employed as allyl sources, however, the direct use of an allyl alcohol is both economically and environmentally preferable, in that the leaving group is not wasted. One finds only a modest number of reports, discussing allyl alcohols as substrates. Since the OH moiety is a poor “leaving group”, such reactions often require additives and/or elevated temperatures; otherwise a drastic loss in the conversion is not unusual.

Aromatic systems, such as phenols, are naturally activated to electrophilic substitution reactions. *Friedel-Crafts* alkylation is one of the greatest discoveries that allows the placement of a carbon substituent on an arene ring.<sup>[1, 2]</sup>

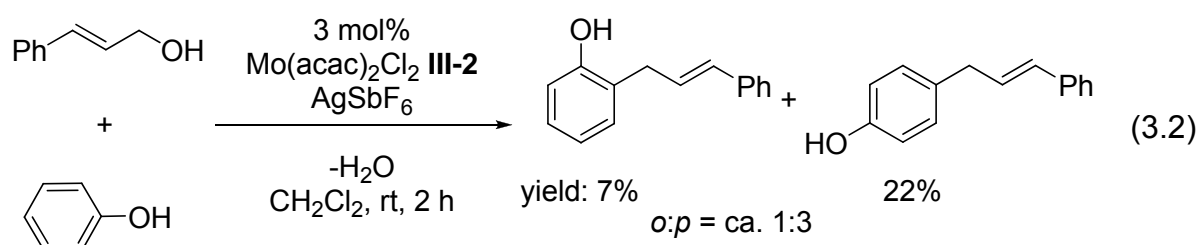
Since phenol is slightly acidic in water, therefore it has weak tendencies to lose the  $H^+$  from the OH group, resulting in the phenolate anion  $C_6H_5O^-$ . The negative charge on oxygen is shared by the *ortho*- and *para*- carbon atoms (see resonance structures). For this reason, phenol derivatives can undergo either O- and/or C-allylation.



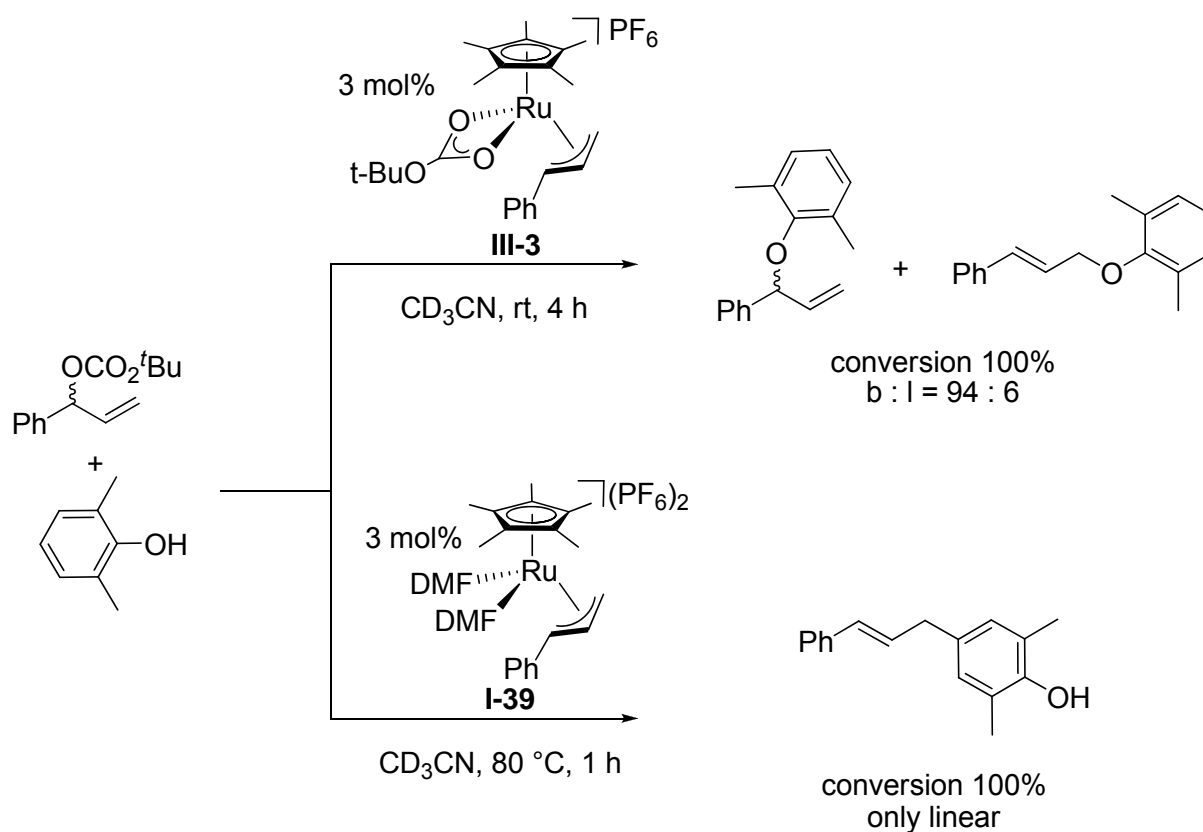
The *Friedel-Crafts* type allylation of phenol with cinnamyl acetate catalyzed by molybdenum(II) precursor **III-1** is shown in Equation 3.1.<sup>[3]</sup> The reaction proceeds rapidly (1 hour) in 71% overall yield.



The change from cinnamyl acetate to cinnamyl alcohol under approximately the same conditions (a molybdenum(IV) precursor **III-2** was used) shows a reduction of the overall yield from 71% to 29% and a decrease in the regioselectivity (Equation 3.2).<sup>[4]</sup> As one can see, the effort made to avoid wasting a leaving group results in the reduced product yield.



It is known that the monocationic ruthenium(IV)-carbonate complex **III-3** is an excellent catalyst for the phenolation of allyl carbonates. Only the C-O bond making product is observed, mainly with the branched regiochemistry under ambient temperatures (Scheme 3.1).<sup>[5]</sup> By heating the reaction mixture and changing this monocationic ruthenium(IV)-carbonate catalyst **III-3** to the dicationic ruthenium(IV) catalyst **I-39** different products are observed. Instead of a C-O bond making reaction the C-C bond *Friedels-Crafts* type products are obtained. It is noteworthy that the regioselectivity of this reaction is inverted, in that the linear C-C bond products were observed.<sup>[6]</sup>



**Scheme 3.1.** Shows the C-O and C-C bond allylation of 2,6-dimethylphenol.

For more examples of transition metal catalyzed allylation of phenol derivatives see Kuntz<sup>[7]</sup> et al. and Vercauteren<sup>[8]</sup> and co-workers.

### 3.2. Results and Discussion

In an attempt not to waste a leaving group we have continued the ruthenium(IV) catalyzed allylation of phenols using allyl alcohol substrates.

#### 3.2.1. Allylation of 6-Bromonaphthalen-2-ol with Several Allyl Alcohols

An extension of the C-C bond making reaction of Scheme 3.1 is given in Equation 3.3<sup>[9]</sup>. Different allyl alcohols were applied for the allylation of 6-bromonaphthalen-2-ol catalyzed by **I-39**.

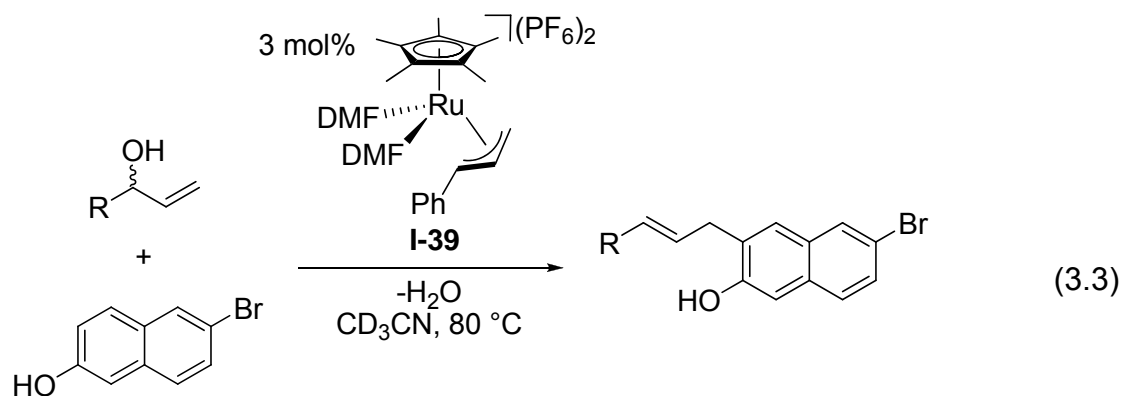
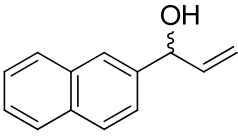
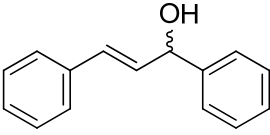
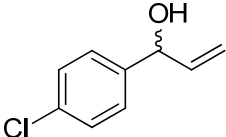
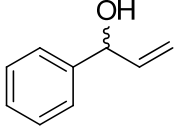
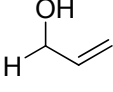
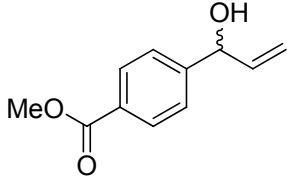


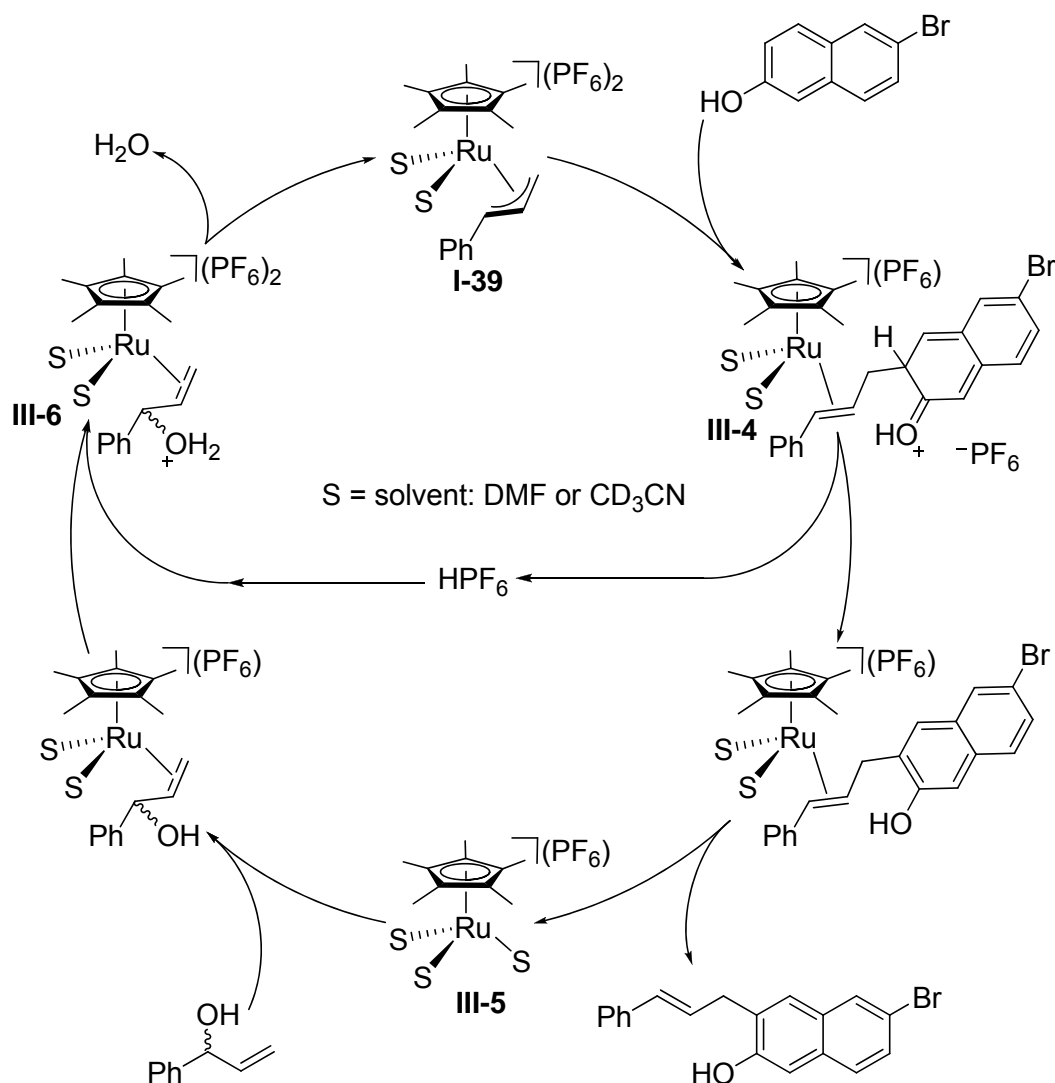
Table 3.1 gives a list of the allyl alcohols tested in the C-C bond allylation reactions. The reactions were fairly rapid and often complete in less than 10 min. Only allyl alcohol and methyl-*p*-(hydroxyallyl)benzoate (entries 5 and 6) were slower, 125 min and 310 min, respectively. Nevertheless the conversion was higher than 60%. The reaction proceeds regioselectively in that only the linear product with allylation at position C-3 of 6-bromonaphthalen-2-ol was observed.

**Table 3.1.** Allylation of 6-bromonaphthalen-2-ol with allyl alcohols using **I-39**.

Entry <sup>[a]</sup>	Nucleophile	Reaction time [min]	Conversion [%] <sup>[b]</sup>
1		1	92
2		1	90
3		6	96
4		8	94
5		125	ca. 60
6		310	100

[a] Reaction conditions: CD<sub>3</sub>CN (0.5 ml), 6-bromonaphthalen-2-ol (0.21 mmol), allyl alcohol (0.07 mmol), **I-39** (0.002 mmol = 3 mol%), 80 °C. [b] The reaction was monitored via <sup>1</sup>H-NMR.

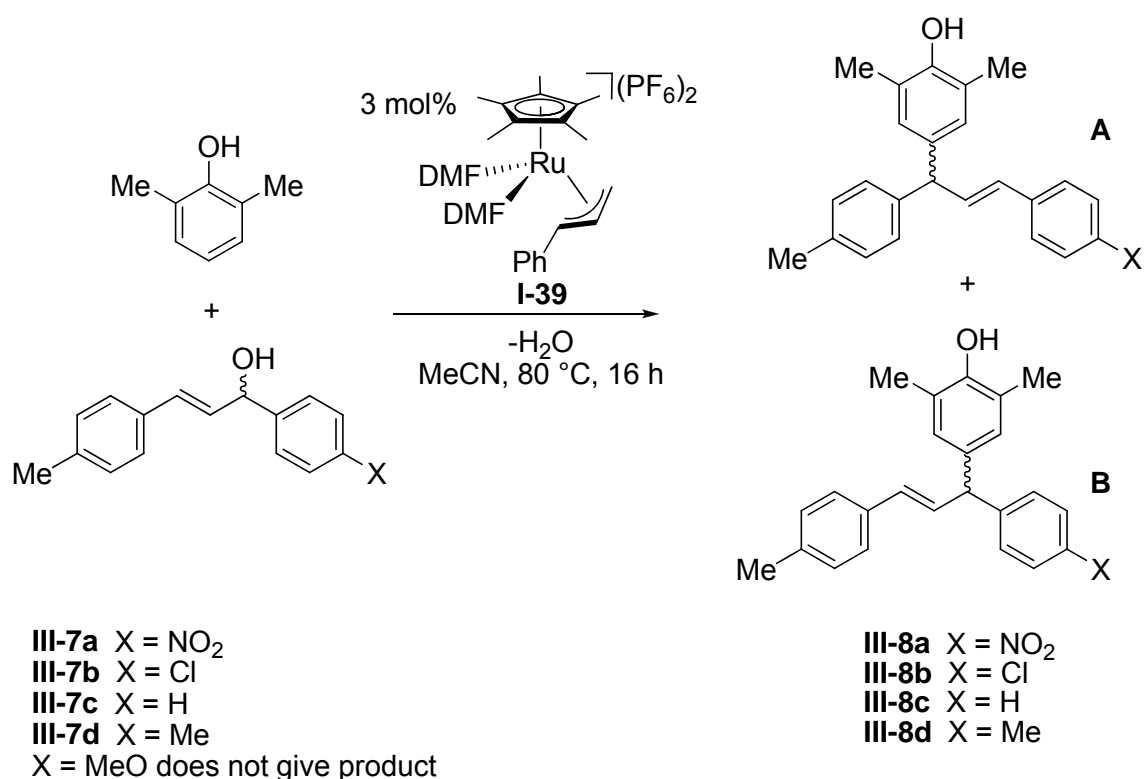
We propose that this catalytic reaction proceeds so smoothly with allyl alcohols, in that the ruthenium(IV) catalyst releases exactly one proton per catalytic cycle, as indicated in Scheme 3.2. The ruthenium(IV) catalyst will be reductively attacked by the phenol substrate and forms the ruthenium(II) species **III-4**. The loss of HPF<sub>6</sub> and the product leads to complex **III-5**, which is the equivalent of Trost's catalyst if the solvent is acetonitrile. Double bond complexation of a new allyl alcohol substrate and protonation of the hydroxy group by HPF<sub>6</sub> affords intermediate **III-6**. Finally the oxidative addition reaction with water as the leaving groups generates the starting ruthenium(IV) catalyst.



**Scheme 3.2.** Plausible mechanism for the allylation of 6-bromonaphthalen-2-ol with vinylbenzyl alcohol.

### 3.2.2. Allylation of 2,6-Dimethylphenol with Several 1,3-Di-Aryl Allyl Alcohols

In addition to this reaction, we studied the allylation of bis-*para*-substituted 1,3-di-arene-allyl alcohols with 2,6-dimethylphenol. We were interested in determining the influence of electron withdrawing and donating groups on the arene in connection with the regioselective product outcome. The arene fragment connected to the allyl double bond was fixed as a *para*-tolyl group. The other arene fragment varied as shown in the Scheme 3.3. The allylation reaction affords a mixture of the two expected regioisomeric products **A** and **B** as indicated in Scheme 3.3. The products were isolated, purified and fully characterized by 2-D NMR experiments and mass spectroscopy.



**Scheme 3.3.** Allylation of 2,6-dimethylphenol with different 1,3-di-arene-allyl alcohols.

For X equal methoxy no product was isolated. For substrate **III-7d** only one allylation product is possible in 47% yield. The other products **III-8a-c** were isolated in the ratios **A:B** of 2.30:1, 1.38:1, and 0.87: 1 and an overall yield of 72%, 81% and 72% respectively.

We conclude that the electronic influence of the substrate is slightly significant in that the ratio of **A:B** for NO<sub>2</sub> and H varies of a factor ca. 2.6. The experiments reveal that substrates with electron withdrawing groups afford the products in higher yields.

Table 3.2 gives an overview of the allyl chemical shifts and coupling constants of the isolated products, as well as the isomeric ratios.



**Table 3.2.** Allyl chemical shifts and coupling constants of the isolated products.

Product	Regioisomer	Ratio	$\delta$ [ppm] / J [Hz] of H <sub>a</sub>	$\delta$ [ppm] / J [Hz] of H <sub>b</sub>	$\delta$ [ppm] / J [Hz] of H <sub>c</sub>
<b>III-8a</b>		2.30	6.40 / d, 15.8	6.86 / dd, 15.8 & 7.4	4.80 / d, 7.4
	major				
<b>III-8a</b>		1.00	4.87 / d, 7.5	6.56 / dd 15.9 & 7.5	6.33 / d, 15.9
	minor				
<b>III-8b</b>		1.38	6.29 / d, 15.6	6.64 / dd, 15.6 & 7.6	4.75 / d, 7.6
	major				
<b>III-8b</b>		1.00	4.75 / d, 7.2	6.56 / dd, 15.8 & 7.2	6.30 / d, 15.8
	minor				
<b>III-8c</b>		0.87	6.32 / d, 15.8	6.63 / dd, 15.8 & 7.4	4.79 / d, 7.4
	minor				
<b>III-8c</b>		1.00	4.76 / d, 7.7	6.66 / dd, 15.9 & 7.7	6.36 / d, 15.9
	major				
<b>III-8d</b>		-	6.34 / d, 15.8	6.63 / dd, 15.8 & 7.5	4.77 / d, 7.5

### 3.3. Conclusions

Concluding, the ruthenium(IV)-allyl complex **I-39** permits the use of the economically and environmentally more favorable allyl alcohol substrate (rather than a carbonate or acetate) in the C-C coupling reaction described.

A mechanism, with water as the leaving in the oxidative addition step, has been proposed.

In addition, the influence of electron withdrawing and donating groups in the allylation of 2,6-dimethylphenol with bis-*para*-substituted 1,3-di-arene-allyl alcohols has been studied. The products obtained were isolated and characterized by 2-D NMR methods.

### 3.4. References

- [1] R. M. Roberts, A. A. Khalaf, *Friedel-Crafts Alkylation Chemistry: A Century of Discovery*, M. Dekker: New York, **1984**.
- [2] M. Bandini, A. Umani-Ronchi, *Catalytic Asymmetric Friedel-Crafts Alkylations*, Wiley-VCH, Weinheim, **2009**.
- [3] A. V. Malkov, S. L. Davis, I. R. Baxendale, W. L. Mitchell, P. KociÅovský, *The Journal of Organic Chemistry* **1999**, *64*, 2751-2764.
- [4] B. Nay, M. Collet, M. Lebon, C. Chèze, J. Vercauteren, *Tetrahedron Letters* **2002**, *43*, 2675-2678.
- [5] R. Hermatschweiler, I. Fernandez, P. S. Pregosin, F. Breher, *Organometallics* **2006**, *25*, 1440-1447.
- [6] I. Fernández, R. Hermatschweiler, F. Breher, P. S. Pregosin, L. F. Veiros, M. J. Calhorda, *Angewandte Chemie International Edition* **2006**, *45*, 6386-6391.
- [7] E. Kuntz, A. Amgoune, C. Lucas, G. Godard, *Journal of Molecular Catalysis A: Chemical* **2006**, *244*, 124-138.
- [8] B. Nay, J.-F. Peyrat, J. Vercauteren, *European Journal of Organic Chemistry* **1999**, *1999*, 2231-2234.
- [9] I. Fernández, D. Schott, S. Gruber, P. S. Pregosin, *Helvetica Chimica Acta* **2007**, *90*, 271-276.



# 4.

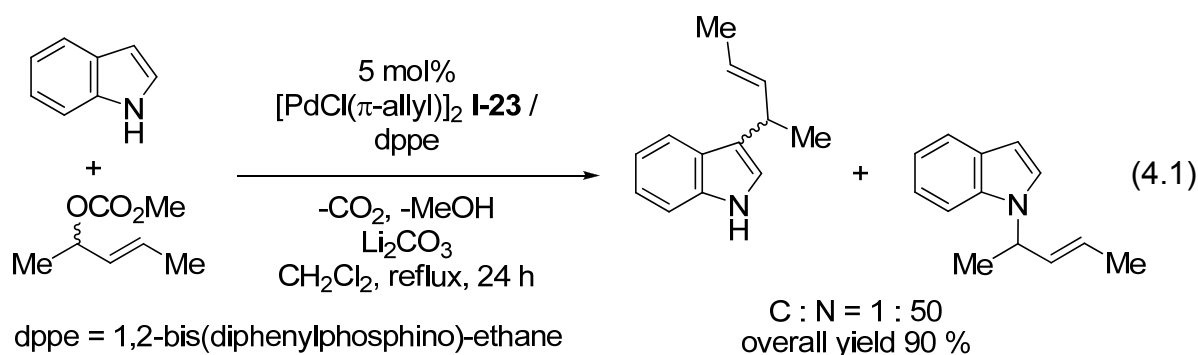
## **Allylation of Indoles**

## 4.1. Introduction

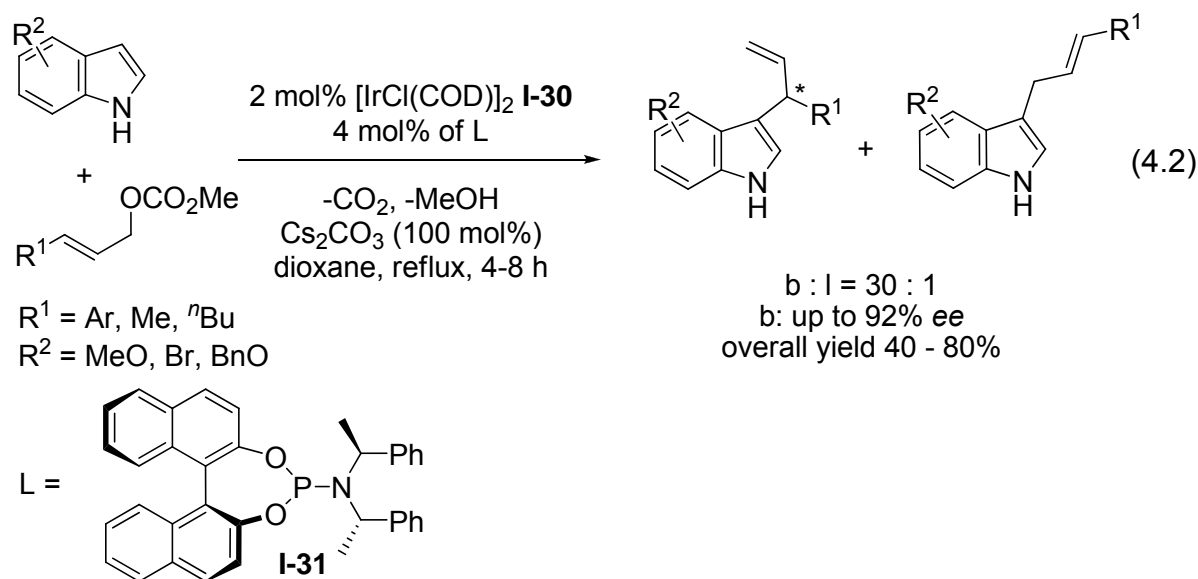
This chapter deals primarily with the ruthenium(IV) catalyzed allylation of indoles and pyrroles. In addition stoichiometric oxidative addition reactions and DFT calculations were performed to explore the regioselectivity of these reactions.

Indole is widely recognized as a key motif in the synthesis of complex molecules with numerous applications in material science, pharmaceuticals and agrochemicals.<sup>[1]</sup> For this reason, the functionalization of such a compound has captured the attention of the chemical community over the past decades. Indole serves as an ambient nucleophile, and it can undergo either N-allylation and/or C-allylation.

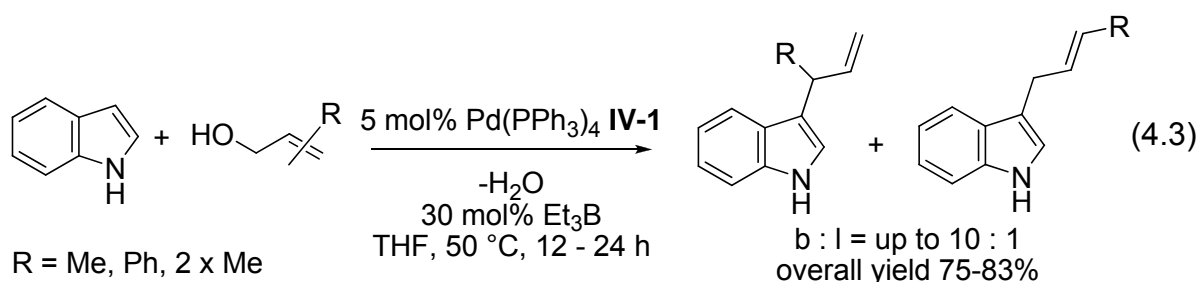
The allylation of indole with methyl pent-3-en-2-yl carbonate catalyzed by a palladium(II)-allyl precursor **I-23** is shown in Equation 4.1.<sup>[2]</sup> The reaction proceeds relatively slow (24 hours under reflux) and a stoichiometric amount of an additional base is needed. The regioselectivity of the reaction, C- versus N-allylation, and the yield are excellent.



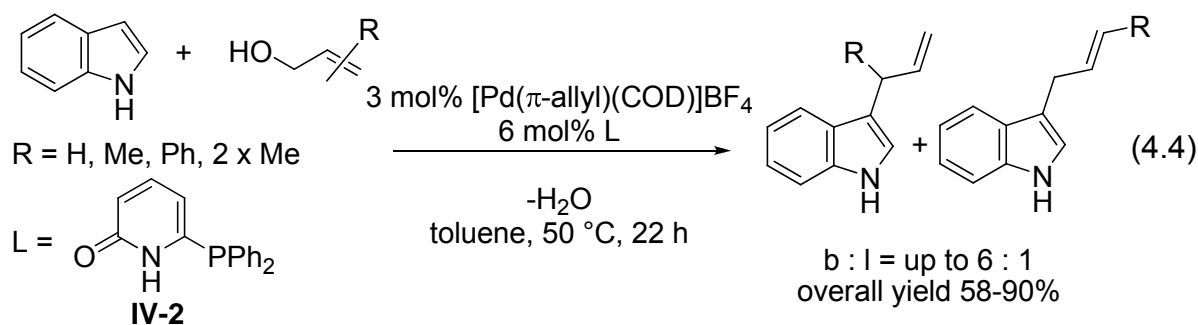
After our initial report<sup>[3]</sup> on ruthenium(IV) catalyzed allylation of indoles, Young and co-workers have reported an enantioselective allylation of different indole compounds with an iridium(I) precursor **I-30** in combination with a phosphoramidite ligand **I-31** (Equation 4.2).<sup>[4]</sup> The reaction proceeds in a highly regio- and stereoselective manner (b:l = 30:1; ee up to 92%). Nevertheless allyl acetates, an additional base and elevated temperature are required to obtain the products in moderate yields.



Equation 4.3 shows a literature example that uses allyl alcohol substrates.<sup>[5]</sup> The reaction takes place with a commercially available tetrakis(triphenylphosphine)-palladium(0) catalyst (**IV-1**), but long reaction times under refluxing conditions and a boron co-catalyst are required to activate the allyl alcohols.



The use of allyl alcohols can be promoted by additional ligands such as **IV-2** (Equation 4.4).<sup>[6]</sup> The authors suggest that hydrogen bonding between the self-assembling ligands and allyl alcohols assist the hydroxy group to become a better leaving group.



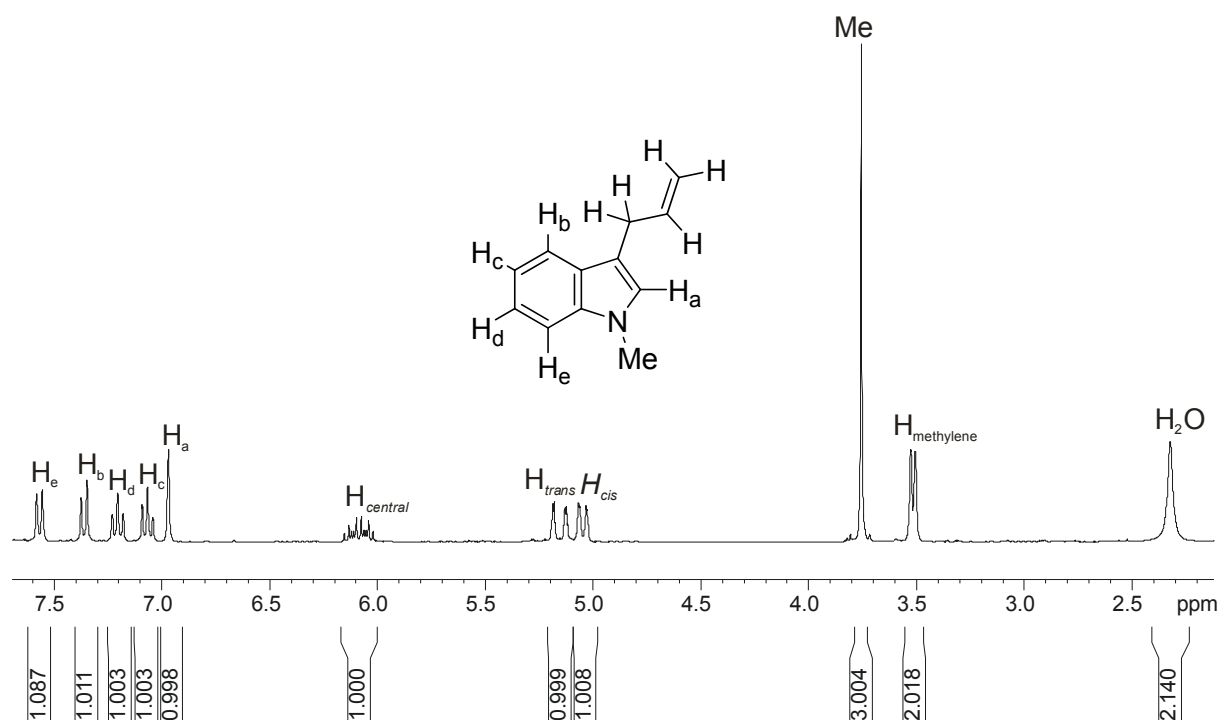
Further examples of transition metal catalyzed allylation of indoles have been reported by Chan<sup>[7]</sup>, Mayr<sup>[8]</sup> and Trost<sup>[9]</sup>.

## 4.2. Results and Discussion

Given the efficiency of our ruthenium(IV)-allyl precursors we have investigated the allylation of a number of indoles using allyl alcohols.

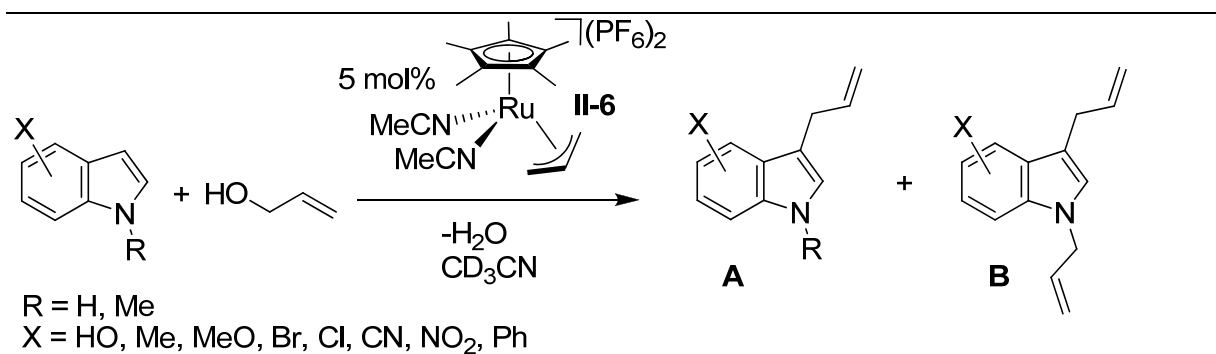
### 4.2.1. Catalysis Using $[\text{Ru}(\eta^3\text{-C}_3\text{H}_5)(\text{Cp}^*)(\text{MeCN})_2](\text{PF}_6)_2$

The reaction of allyl alcohol with substituted indole compounds catalysed by the dicationic ruthenium(IV)-allyl catalyst **II-6** was followed by <sup>1</sup>H-NMR spectroscopy (see Table 4.1 and Figure 4.1). The major product is the 3-substituted allyl indole **A** with the double allylation product **B** as the minor component. Using an excess (four equivalents) of the alcohol results in complete conversion to the double allylation product (entry 2). The use of 2-phenylindole as substrate (entry 11) slows the reaction only slightly and the product, 3-allyl-2-phenylindole, is obtained in excellent yield. The reactions of N-substituted indoles (entries 12 and 13) afford exclusively the 3-allyl product **A**. The observed regioselectivity at the indole 3-position is consistent with known literature.<sup>[2, 10]</sup>



**Figure 4.1.** Shows the recorded spectrum of the reaction mixture for the formation of 3-allyl-1-methylindole after 1 hour at room temperature in CD<sub>3</sub>CN.



**Table 4.1.** Allylation of indole compounds with allyl alcohol catalyzed by **II-6**.

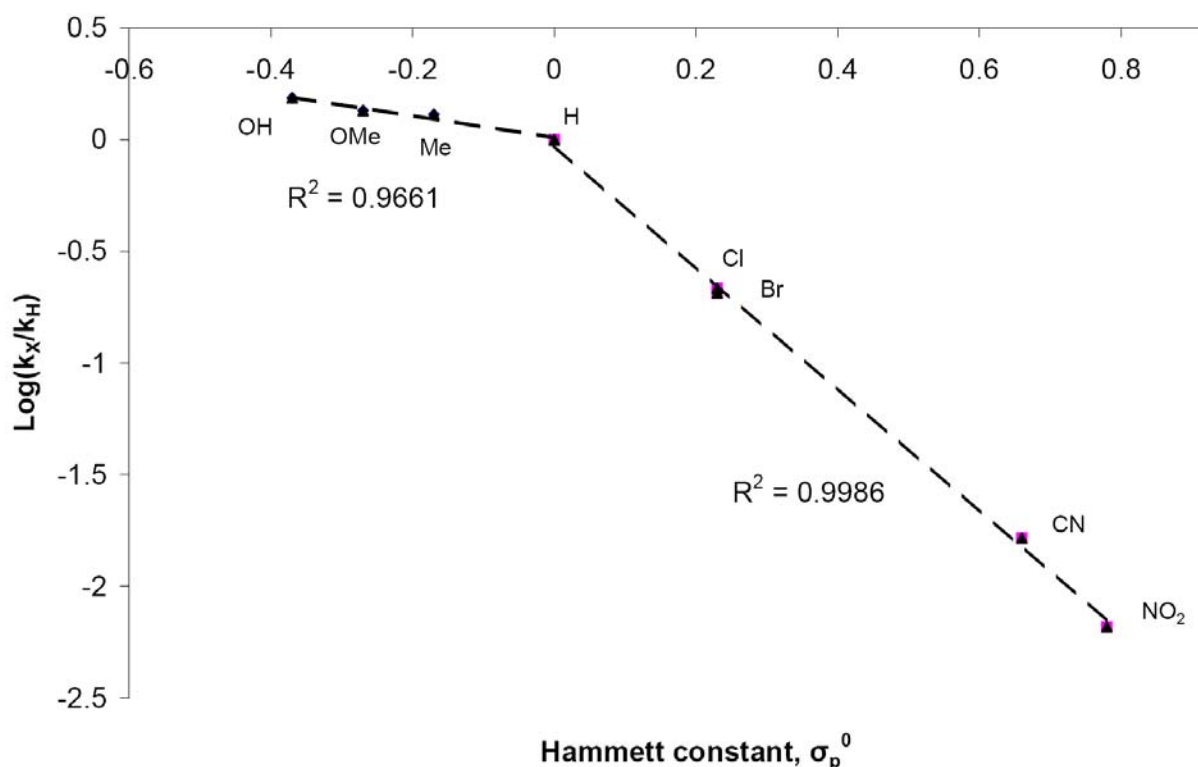
Entry <sup>[a]</sup>	Indole	Reaction time [h]	Conversion [%] <sup>[b]</sup>	A : B ratio
1	Indole	0.5	100	8 : 1
2	Indole	12	100	only B <sup>[c]</sup>
3	5-HO-indole	0.5	100	8 : 1
4	5-Me-indole	0.5	100	7 : 1
5	5-MeO-indole	0.5	100	7 : 1
6	5-Br-indole	3	100	6 : 1
7	5-Cl-indole	5.5	100	6 : 1
8	5-CN-indole	27	100	8 : 1
9	5-NO <sub>2</sub> -indole	96	100	8 : 1
10	4-MeO-indole	0.5	100	5 : 1
11	2-Ph-indole	0.9	100	11 : 1
12	1-Me-indole	1	100	only A <sup>[d]</sup>
13	1-Me-2-Ph - indole	0.5	100	only A <sup>[d]</sup>

[a] Reaction conditions: allyl alcohol (0.07 mmol), indole (0.07 mmol), catalyst (0.0035 mmol) in CD<sub>3</sub>CN (0.5 ml), rt. [b] The reaction was monitored via <sup>1</sup>H-NMR. [c] Four equivalents of allyl alcohol (with respect to indole) were used to induce complete conversion to B. [d] N-allylation blocked.

Using the dicationic ruthenium(IV) catalyst **II-6** is advantageous, in that the reactions are rapid, do not require additives such as bases and/or phosphine containing ligands and are completed at ambient temperature. The only side-product of the catalytic transformation is water.

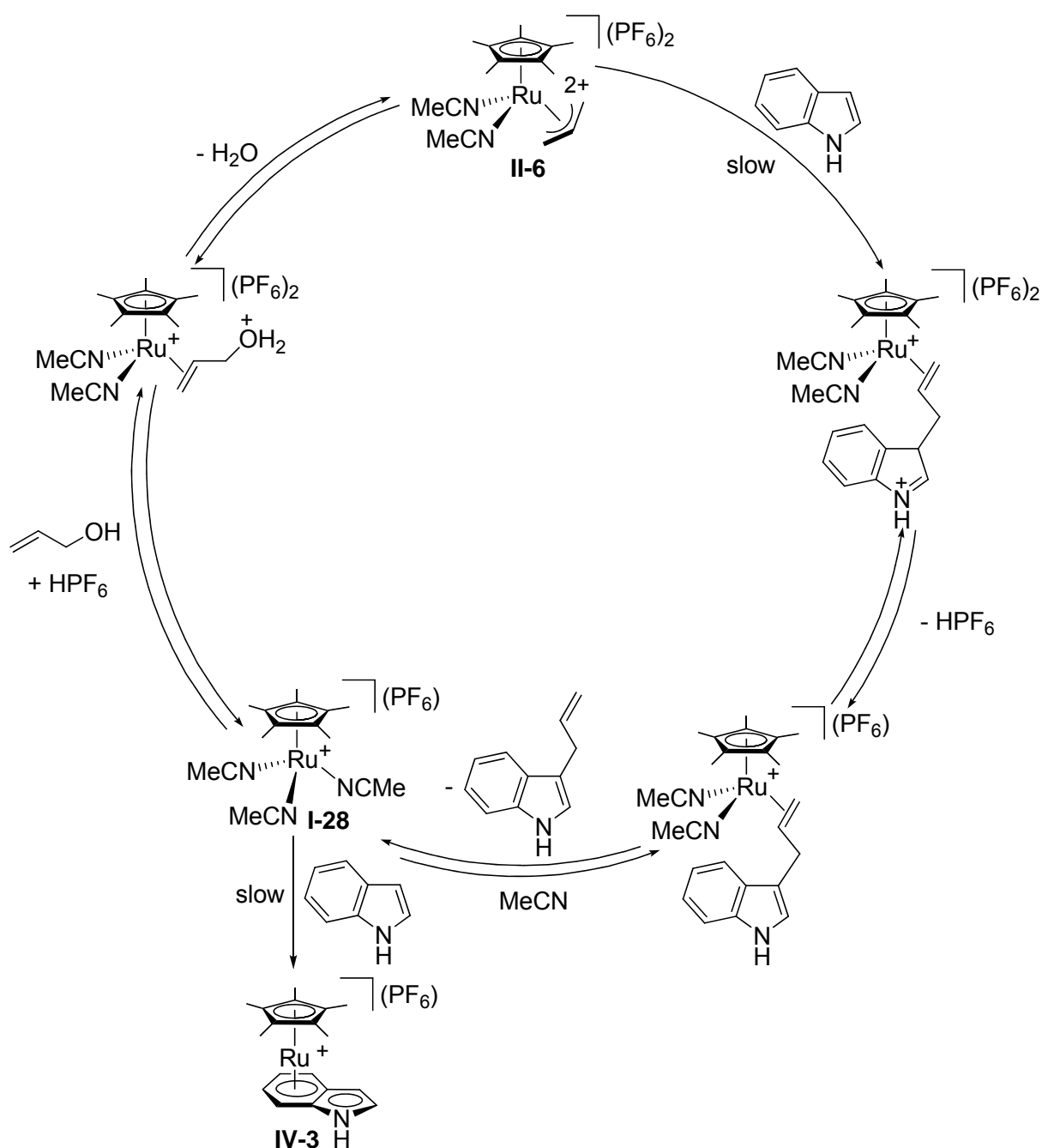
Preparative experiments, on the 1 mmol scale, using the indole substrates in entries 12 and 13 afforded 93% and 96% yields of the new products, respectively.

Concentration dependent rate studies, using either indole or 5-hydroxyindole as reagent, reveal that this reaction is zero order in the alcohol, first order in the ruthenium catalyst and first order in the indole compound. A plot of the logarithm of the relative rate versus the Hammett substitution constant is given in Figure 4.2. This reveals that electron withdrawing groups at the 5-position of indole decreases the allylation reaction rate whereas electron donating groups accelerate the reaction slightly.



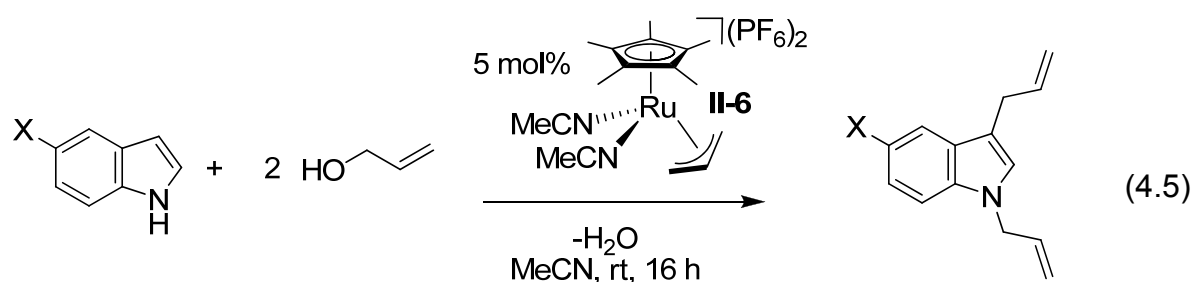
**Figure 4.2.** Hammett plot for the allylation of 5-substituted indoles. The reactions were monitored via <sup>1</sup>H-NMR spectroscopy: after 4-5 min for X = HO, MeO, Me and H; after 10 min for X = Cl and Br; and after 2 h for X = CN and NO<sub>2</sub>.

Scheme 4.1 shows a suggested mechanism which is similar to the mechanism proposed in Chapter 3, Scheme 3.2. The rate determining step is the attack of the indole nucleophile on the ruthenium(IV)-allyl catalyst (emphasized with *slow*). We believe that liberating a catalytic amount of H<sup>+</sup> per cycle permits the use of the alcohol as substrate. This *controlled release* of acid, due to the nucleophilic attack on the ruthenium(IV) catalyst precursor, eventually results in water as the leaving group in the oxidative addition reaction (this can be verified by a closer look at the spectrum shown in Figure 4.1 by the appearance of a broad signal at 2.32 ppm). The proposed mechanism suggests that the use of Trost's catalyst, [Ru(Cp\*)(MeCN)<sub>3</sub>]PF<sub>6</sub> (**I-28**) plus an additional acid should afford an active catalyst. We have carried out this experiment and, indeed, the catalysis works well. This experiment and several related reactions will be discussed later in sub-Chapter 4.2.2. However, the use of **II-6** guarantees a controlled release of exactly one proton per catalytic cycle, whereas adding acid can result in either too much or not enough plus an unnecessary additional anion. We have prepared the  $\eta^6$ -arene complex **IV-3**<sup>[11]</sup> according to a literature procedure and find that this complex does not catalyze the allylation reaction.



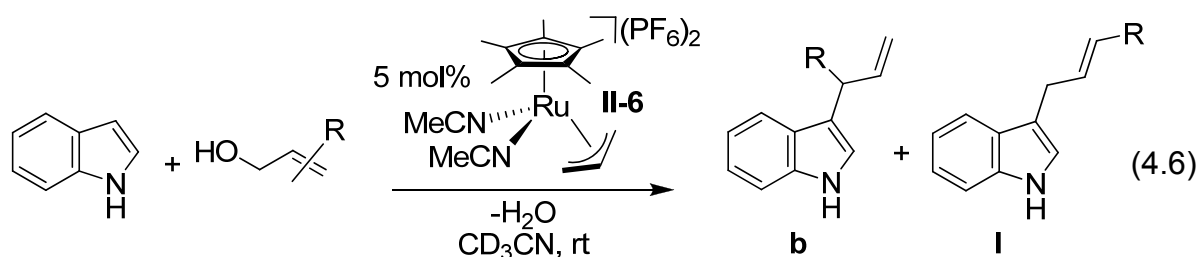
**Scheme 4.1.** Proposed mechanism derived from the data obtained from concentration studies.

Preparative experiments for the double allylation of different indole compounds are shown in Equation 4.5. Two equivalents of allyl alcohol and a reaction time of 16 hours are required to achieve the products **IV-4**, **IV-5** and **IV-6** in 86%, 79% and 76% yield, respectively. This chemistry is relatively slow, and given the fast reaction with one equivalent of allyl alcohol, the N-allylation (rather than the C-allylation) is clearly much slower (see Table 4.1). We believe this is the first example of such a controlled one-pot double allylation of indole.<sup>[12]</sup>



Isolated yield for: X = Me (**IV-4**): 86%  
 MeO (**IV-5**): 79%  
 H (**IV-6**): 76%

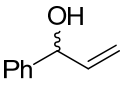
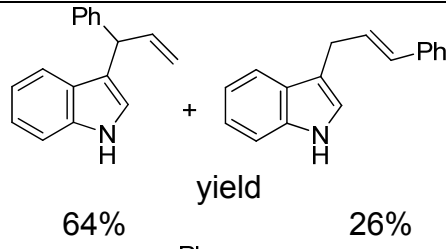
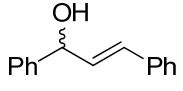
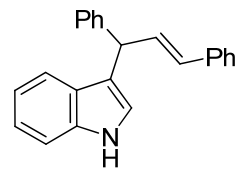
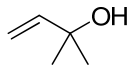
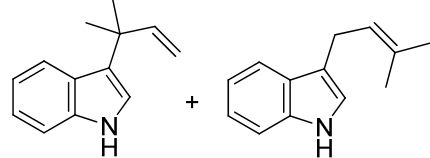
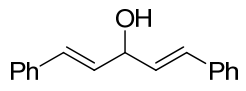
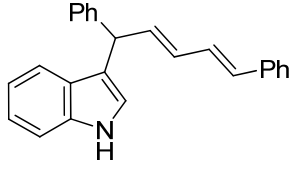
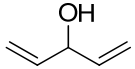
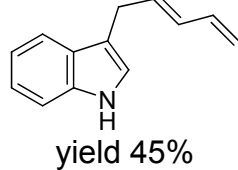
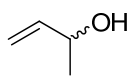
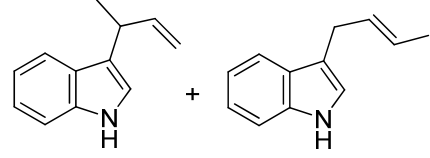
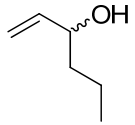
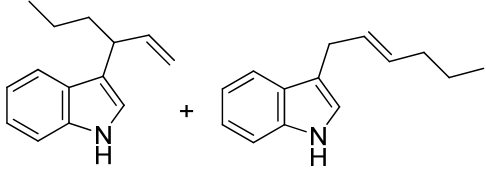
We have allowed indole to react with several substituted allyl alcohols in the presence of the dicationic ruthenium(IV)-allyl catalyst **II-6** (Equation 4.6 and Table 4.2). Several reactions were performed on a preparative scale (entries 1-5) and the products were isolated by column chromatography. The reactions in entries 6-7 were followed by  $^1\text{H-NMR}$  spectroscopy.



In general, our reaction times compare very favorably with related literature reports, and a factor of 10, in time, is not unusual.<sup>[2]</sup> Furthermore, the branched to linear (b/l) ratios vary considerably. The best b/l ratio was obtained for  $\text{CH}_2=\text{CHC}(\text{OH})\text{Me}_2$  with a value of 13: 1.

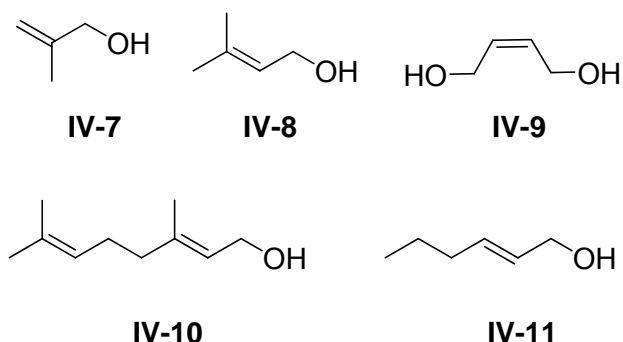
A comparison of the two dienol substrates  $\text{PhCH}=\text{CHCH}(\text{OH})\text{CH}=\text{CHPh}$  (entry 4) and  $\text{CH}_2=\text{CHCH}(\text{OH})\text{CHCH}_2$  (entry 5) shows that the former substrate gives the product within 25 min and a yield of 85%, whereas the latter requires heating at 60 °C for 3 hours with a moderate yield (45%). It is noteworthy that using  $\text{CH}_2=\text{CHCH}(\text{OH})\text{CH}=\text{CH}_2$  (a discussion of pentadienyl complexes is given in Chapter 2) affords exclusively the linear product, whereas  $\text{PhCH}(\text{OH})\text{CH}=\text{CH}_2$  and  $\text{CH}_2=\text{CHC}(\text{OH})\text{Me}_2$  (entries 1 and 3) give mainly the branched product.

**Table 4.2.** Allylation of indole with different substituted allyl alcohols catalyzed by **II-6**.

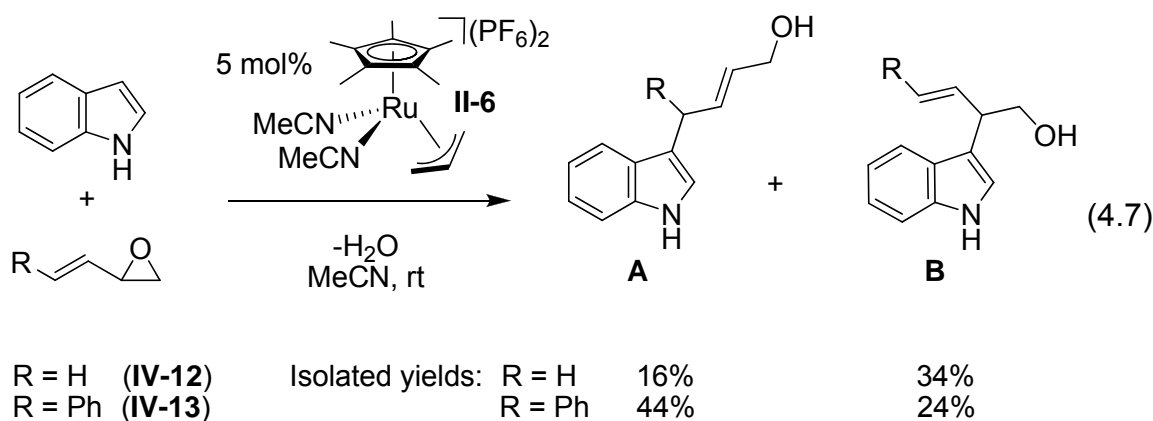
Entry	Allyl substrate	Reaction time [h]	Conversion [%]	Product
1 <sup>[a]</sup>		4.5	100	 yield 64%                      26%
2 <sup>[a]</sup>		1.3	100	 yield 91%
3 <sup>[a]</sup>		5	100	 mixture: overall yield 75% b : l = 13 : 1
4 <sup>[a]</sup>		25 min	100	 yield 85%
5 <sup>[a][b]</sup>		3	100	 yield 45%
6 <sup>[c]</sup>		2.75	100	 not isolated b : l = 1 : 1
7 <sup>[c]</sup>		6	75	 not isolated b : l = 0.43 : 1

[a] Reaction conditions: allyl alcohol (1 mmol), indole (1 mmol), **II-6** (0.05 mmol) in MeCN (5 ml). [b] 60 °C. [c] Reaction conditions: allyl alcohol (0.07 mmol), indole (0.07 mmol), **II-6** (0.0035 mmol) in CD<sub>3</sub>CN (0.5 ml), rt; the reaction was monitored via <sup>1</sup>H-NMR.

Allyl alcohols **IV-7**, **IV-8**, **IV-9**, **IV-10** and **IV-11** that were substituted on the allyl double bond gave no conversion to the product after 3 hours at ambient temperature, suggesting that steric hindrance to olefin complexation may be important.



The vinyl epoxides **IV-12** and **IV-13** were tested as an allyl source for the alkylation of indole (Equation 4.7). The reaction using **IV-12** is finished in ca. 40 min, whereas with **IV-13**, the reaction is complete in ca. 5 min. The isolation of the products on the 1 mmol scale and separation of the isomeric products results in a drop in the overall yield for **IV-12** and **IV-13** to 50% and 68%, respectively. For R = H the ratio of A:B is in the order of 1:2, whereas for R = Ph the ratio is inverted to ca. 2:1.



For comparison with the allyl alcohols, we have carried out related reactions for several 5-substituted indoles using *tert*-butyl-1-phenylallyl carbonate catalyzed by **II-6** (Table 4.3). The experiments reveal a decrease in the selectivity for indoles with an increasing electron withdrawing ability of the 5-substituent. The reaction rates are slow (up to 48 hours), however 5-methoxy indole requires less than 1 hour for complete conversion to the product. There is not much advantage in using and

wasting the carbonate leaving group which has to be prepared from the alcohol in an additional reaction step.

**Table 4.3.** Allylation of indole compounds with *tert*-butyl-1-phenylallyl carbonate catalyzed by **II-6**.

$\text{X} = \text{MeO, H, Br, CN, NO}_2$

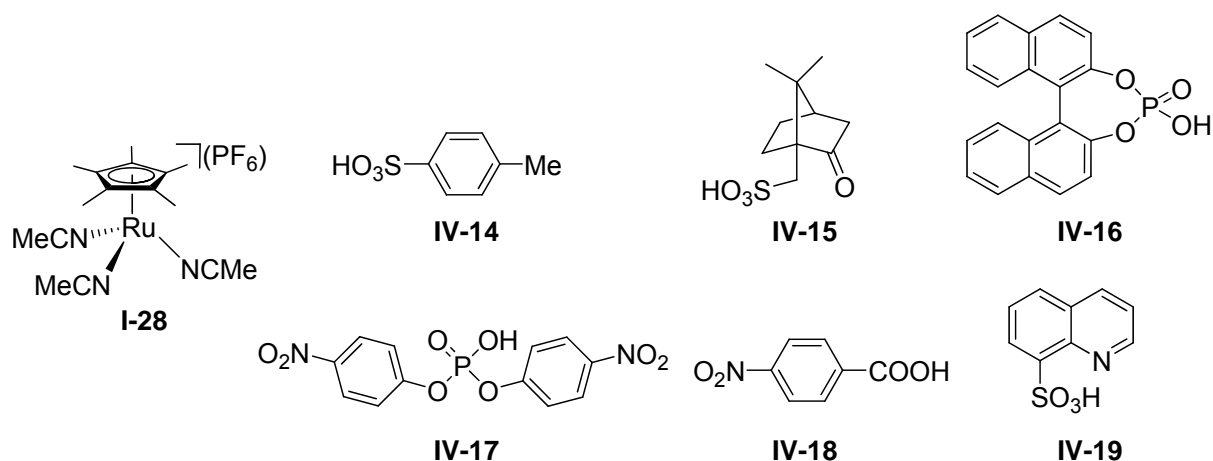
Entry <sup>[a]</sup>	X	Reaction time [h]	Conversion [%] <sup>[b]</sup>	b : I ratio
1	MeO	0.67	100	3.4 : 1
2	H	3	100	2.6 : 1
3	Br	20	100	2 : 1
4	CN	19	100	2.1 : 1
5	NO <sub>2</sub>	48	100	0.8 : 1

[a] Reaction conditions: *tert*-butyl-1-phenylallyl carbonate (0.07 mmol), indole (0.07 mmol), catalyst (0.0035 mmol) in CD<sub>3</sub>CN (0.5 ml), rt. [b] The reaction was monitored via <sup>1</sup>H-NMR at rt.

#### 4.2.2. Catalysis Using Trost's Catalyst in Combination with Acids

Given that [Ru(Cp\*)(MeCN)<sub>3</sub>]PF<sub>6</sub> (**I-28**) plus an additional acid should afford an active catalyst (see our proposed mechanism in Scheme 4.1 and the conclusions) we have carried out related experiments with different acids and studied the influence of these on the reaction rate and product regioselectivity (Table 4.4).





Without the addition of a catalytic amount of acid (entry 1) no conversion to the product was obtained after 3 hours. The sulfonic acids (entries 2-4) each afford rapid reactions (25-40 min) and favorable b/l ratios (up to 9:1 for camphorsulfonic acid). Triflic acid,  $\text{CF}_3\text{SO}_3\text{H}$  and  $\text{HBF}_4$  (entries 5 and 6) induce a rapid allylation reaction (30 and 50 min) but are less selective than the sulfonic acids. Sulfuric acid,  $\text{H}_2\text{SO}_4$ , phosphoric acid,  $\text{H}_3\text{PO}_4$  (entries 7-8), several carboxylic acids (entries 13-16) and quinoline-8-sulfonic acid (entry 17) are poor co-catalysts in that the reactions proceed slowly or not at all. Several hydrogen phosphates (entries 9-12) were employed, although all of these reactions are slower (4-6 hours) than the allylation with the sulfonic acids. These hydrogen phosphates are not very soluble in acetonitrile, so an additional co-solvent such as  $\text{D}_2\text{O}$  or  $\text{DMF-d}_7$  was necessary. Entry 9 seemed promising with a b/l ratio of 9.8:1.

**Table 4.4.** Effect of the acid on the allylation of indole with PhCH(OH)CH=CH<sub>2</sub>.

Entry	acid	Reaction time [min]	Conversion [%] <sup>[d]</sup>	b : I ratio
1 <sup>[a]</sup>	no acid	3 h	0	
2 <sup>[a]</sup>	<b>IV-14</b>	40	100	6 : 1
3 <sup>[a]</sup>	<b>IV-15</b>	25	100	9 : 1
4 <sup>[a]</sup>	MeSO <sub>3</sub> H	30	100	8.4 : 1
5 <sup>[a]</sup>	CF <sub>3</sub> SO <sub>3</sub> H	32	100	ca. 1 : 1
6 <sup>[a]</sup>	HBF <sub>4</sub> •Et <sub>2</sub> O	50	100	ca. 1 : 3
7 <sup>[a]</sup>	H <sub>2</sub> SO <sub>4</sub>	80	< 50	4.5 : 1
8 <sup>[a]</sup>	H <sub>3</sub> PO <sub>4</sub>	60	Ca. 18	ca. 0.7 : 1
9 <sup>[b]</sup>	<b>IV-16</b>	5 h	100	9.8 : 1
10 <sup>[c]</sup>	<b>IV-16</b>	4 h	100	5 : 1
11 <sup>[b]</sup>	<b>IV-17</b>	6 h	100	7.2 : 1
12 <sup>[c]</sup>	<b>IV-17</b>	4 h	100	3.2 : 1
13 <sup>[a]</sup>	CF <sub>3</sub> CO <sub>2</sub> H	20 h	45	8 : 1
14 <sup>[a]</sup>	HO <sub>2</sub> CCO <sub>2</sub> H	20 h	28	3.9 : 1
15 <sup>[a]</sup>	CH <sub>3</sub> COOH	25	0	
16 <sup>[a]</sup>	<b>IV-18</b>	25	0	
17 <sup>[a]</sup>	<b>IV-19</b>	25	0	

[a] Reaction conditions: allyl alcohol (0.07 mmol), indole (0.07 mmol), **I-28** (0.0035 mmol) acid (0.0035 mmol) in CD<sub>3</sub>CN (0.5 ml), rt. [b] Reaction conditions: allyl alcohol (0.09 mmol), indole (0.09 mmol), **I-28** (0.0046 mmol) acid (0.0046 mmol) in CD<sub>3</sub>CN (0.48 ml), DMF-d<sub>7</sub> (0.02 ml), rt. [c] Reaction conditions: allyl alcohol (0.09 mmol), indole (0.09 mmol), **I-28** (0.0046 mmol) acid (0.0046 mmol) in CD<sub>3</sub>CN (0.40 ml), D<sub>2</sub>O (0.1 ml), rt. [d] The reaction was monitored via <sup>1</sup>H-NMR.

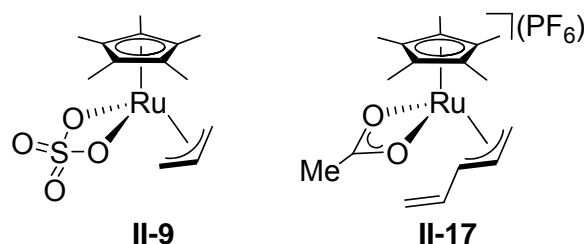
We have tested the allylation of indole with several aromatic allyl alcohols catalyzed by  $[\text{Ru}(\text{Cp}^*)(\text{MeCN})_3](\text{PF}_6)$  (**I-28**) in combination with a catalytic amount of 1,1'-binaphthyl-2,2'-diyl hydrogen phosphate (**IV-16**) (Table 4.5). The odd entry numbers represent reactions with  $\text{D}_2\text{O}$  as co-solvent and the even numbers with  $\text{DMF-d}_7$ , respectively. The data reveal that the reactions with  $\text{DMF-d}_7$  as co-solvent are a factor of ca. 3-5 slower than the appropriate reaction with  $\text{D}_2\text{O}$ , but the b/l ratios are higher. Entries 3 and 10 are notable for their excellent b/l ratios, 36:1 and 22:1, respectively.

**Table 4.5.** Allylation of indole using aromatic allyl alcohols catalyzed by **I-28** and 1,1'-binaphthyl-2,2'-diyl hydrogen phosphate (**VI-16**).

Entry	Ar	Reaction time [min]	Conversion [%] <sup>[c]</sup>	b : l ratio
1 <sup>[a]</sup>		25	100	5 : 1
2 <sup>[b]</sup>		90	93	12 : 1
3 <sup>[a]</sup>		45	100	36 : 1
4 <sup>[b]</sup>		225	~50	> 95% branched
5 <sup>[a]</sup>		30	100	0.7 : 1
6 <sup>[b]</sup>		80	100	4 : 1
7 <sup>[a]</sup>		50	100	2.9 : 1
8 <sup>[b]</sup>		210	~90	4.5 : 1
9 <sup>[a]</sup>		60	100	0.4 : 1
10 <sup>[b]</sup>		190	100	22 : 1

[a] Reaction conditions: allyl alcohol (0.09 mmol), indole (0.09 mmol), **I-28** (0.0046 mmol) acid (0.0046 mmol) in  $\text{CD}_3\text{CN}$  (0.4 ml),  $\text{D}_2\text{O}$  (0.1 ml), rt. [b] Reaction conditions: allyl alcohol (0.09 mmol), indole (0.09 mmol), **I-28** (0.0046 mmol) acid (0.0046 mmol) in  $\text{CD}_3\text{CN}$  (0.48 ml),  $\text{DMF-d}_7$  (0.02 ml), rt. [c] The reaction was monitored via  $^1\text{H-NMR}$ .

Since sulphuric acid and acetic acid are poor co-catalysts we attempted to prepare possible ruthenium(IV) intermediates containing  $\text{SO}_4^{2-}$  and  $\text{AcO}^-$ . The resulting sulfate and acetate complexes **II-9** and **II-17** (for detailed discussions of these complexes see Chapter 2) are not active allylation catalysts at room temperature. It would seem that filling up the two coordination positions with chelating ligands<sup>[13, 14]</sup> has an unfavorable effect on the allylation rate.



Given that camphorsulfonic acid **IV-15** represents the best co-catalyst with respect to both the reaction rate and selectivity, we have performed several allylation reactions with  $[\text{Ru}(\text{Cp}^*)(\text{MeCN})_3](\text{PF}_6)$  (**I-28**) in combination with **IV-15** (Tables 4.6-4.9).

Table 4.6 summarizes the relative rates and the observed regioselectivity for the allylation of substituted indoles with  $\text{PhCH}(\text{OH})\text{CH}=\text{CH}_2$ . These indole derivatives undergo fast allylation (usually < 30 min for 100% conversion) at ambient temperature in the presence of **II-28** + sulfonic acid **IV-15** as catalyst. The branched products are favored and the catalyst is selective in that we do not find either N-allylation or di-allyl ether products. As noted previously (see Table 4.1) electron-withdrawing substituents in the 5-position of the indole, slow the reaction considerably. From entries 6 and 9 it is clear that the catalyst is also active in allylation of N-substituted indoles.

**Table 4.6.** Allylation of indoles with PhCH(OH)CH=CH<sub>2</sub> catalyzed by **I-28** / **IV-15**.

Entry <sup>[a]</sup>	Indole	Reaction time [min]	Conversion [%] <sup>[b]</sup>	b : i ratio
1	Indole	25	100	9 : 1
2	5-HO-indole	6	100	7 : 1
3	5-MeO-indole	14	100	10 : 1
4	5-Me-indole	12	100	9 : 1
5	5-Br-indole	105	100	6.5 : 1
6	1-Me-indole	14	100	8 : 1
7	2-Ph-indole	16	100	1 : 1
8	2-Me-indole	8	100	7 : 1
9	1-Me-2-Ph-indole	8	100	only branched

[a] Reaction conditions: allyl alcohol (0.07 mmol), indole (0.07 mmol), **I-28** (0.0035 mmol) **IV-15** (0.0035 mmol) in CD<sub>3</sub>CN (0.5 ml), rt. [b] The reaction was monitored via <sup>1</sup>H-NMR.

The allylation of indole with different aryl allyl alcohols catalyzed by **I-28** and **IV-15** was followed by <sup>1</sup>H-NMR spectroscopy (Table 4.7). The reactions proceed quickly (less than 55 min) and with excellent regioselectivity. Reaction of indole with PhCH(OH)CH=CH<sub>2</sub> (entry 1) afforded 100% conversion to the products after 25 min with a b/i ratio of 9:1. For the same reaction, the dicationic [Ru( $\eta^3$ -C<sub>3</sub>H<sub>5</sub>)(Cp\*)(MeCN)<sub>2</sub>](PF<sub>6</sub>)<sub>2</sub> catalyst (**II-6**) (Table 4.2, entry 1) requires 4.5 hours and gives a b/i ratio of 2:1. A possible explanation for the observed change in the product selectivity of these two catalysts is given in sub-Chapters 4.2.6. Notable for their excellent b/i ratios (up to 49:1) are the bulky aryl allyl alcohols (Ar = *o*-tolyl, mesityl and 1-naphthyl) given in entries 6-8.

**Table 4.7.** Allylation of indole by different aryl allyl alcohols catalyzed by **I-28** / **IV-15**.

Entry <sup>[a]</sup>	Ar	Reaction time [min]	Conversion [%] <sup>[b]</sup>	b : l ratio
1	Ph	25	100	9 : 1
2	<i>p</i> -Cl-C <sub>6</sub> H <sub>4</sub> -	40	100	5 : 1
3	<i>p</i> -MeO-C <sub>6</sub> H <sub>4</sub> -	40	100	11.5 : 1
4	<i>o</i> -Cl-C <sub>6</sub> H <sub>4</sub> -	20	100	24 : 1
5	<i>o</i> -MeO-C <sub>6</sub> H <sub>4</sub> -	55	100	24 : 1
6	<i>o</i> -Me-C <sub>6</sub> H <sub>4</sub> -	20	100	49 : 1
7	mesityl	55	100	32 : 1
8	1-naphtyl	15	100	49 : 1
9	2-naphtyl	35	100	8 : 1
10	2-furyl	20	100	2.3 : 1

[a] Reaction conditions: allyl alcohol (0.07 mmol), indole (0.07 mmol), **I-28** (0.0035 mmol) **IV-15** (0.0035 mmol) in CD<sub>3</sub>CN (0.5 ml), rt. [b] The reaction was monitored via <sup>1</sup>H-NMR.

The best selectivities were obtained by allylating sterically hindered allyl alcohols with different substituted indoles (Table 4.8). The increased bulkiness of the aryl substituent a) significantly improves the observed branched to linear (b/l) ratio from ca 7-10 (see Table 4.6) to ca 40-60 and b) leads to somewhat faster reactions. However, as indicated by entries 4 and 9, a phenyl substituent at the 2-position of the indole results in much more linear product.

**Table 4.8.** Allylation of indoles with two bulky aromatic allyl alcohols catalyzed by **I-28** / **IV-15**.

Entry <sup>[a]</sup>	Indole	Allyl substrate	Reaction time [min]	Conversion [%] <sup>[b]</sup>	b : I ratio
1			20	100	49 : 1
2			9	100	only b
3			60	100	41 : 1
4			120	100	1.7 : 1
5			9	100	only b
6			15	100	49 : 1
7			12	100	only b
8			60	100	57 : 1
9			≤ 150	100	1.7 : 1

[a] Reaction conditions: allyl alcohol (0.07 mmol), indole (0.07 mmol), **I-28** (0.0035 mmol) **IV-15** (0.0035 mmol) in CD<sub>3</sub>CN (0.5 ml), rt. [b] The reaction was monitored via <sup>1</sup>H-NMR.

We have also tested the **I-28** / **IV-15** mixture as catalyst for a series of pyrroles and show these catalytic results in Table 4.9. Since the allylation reaction of pyrrole affords mixtures of mono- and di-allylated linear and/or branched products we tested specific substituted pyrroles. For these few substrates the reactions are even faster,

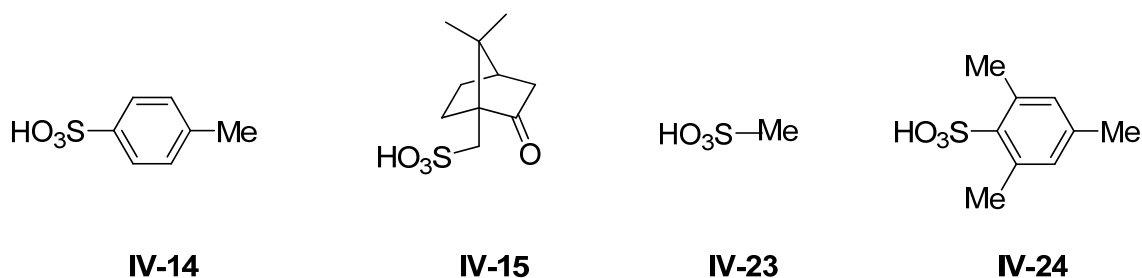
and, for entries 1-5, using 2-ethyl pyrrole, afford impressive b/l ratios. Further, no N-allylation of the pyrrole derivatives was observed.

**Table 4.9.** Allylation of pyrroles by different allyl alcohols catalyzed by **I-28** / **IV-15**.

Entry <sup>[a]</sup>	Ar	R <sup>1</sup>	R <sup>2</sup>	R <sup>3</sup>	Reaction time [min]	Conversion [%] <sup>[b]</sup>	b : l ratio
1	<i>o</i> -Me-C <sub>6</sub> H <sub>4</sub> -	Et	H	H	5	100	only b
2	mesityl	Et	H	H	≤ 7	100	only b
3	1-naphthyl	Et	H	H	≤ 7	100	only b
4	<i>o</i> -MeO-C <sub>6</sub> H <sub>4</sub> -	Et	H	H	≤ 7	100	71 : 1
5	<i>o</i> -Cl-C <sub>6</sub> H <sub>4</sub> -	Et	H	H	≤ 7	100	38 : 1
6	Ph	Et	H	H	7	100	13 : 1
7	Ph	Me	Et	Me	35	100	22 : 1
8	Ph	Me	H	Me	12	100	12 : 1

[a] Reaction conditions: allyl alcohol (0.07 mmol), indole (0.07 mmol), **I-28** (0.0035 mmol) **IV-15** (0.0035 mmol) in CD<sub>3</sub>CN (0.5 ml), rt. [b] The reaction was monitored via <sup>1</sup>H-NMR.

Since the sulfonic acids **IV-14**, **IV-15** and **IV-23** represent the best co-catalysts, indole was allowed to react with the more sterically hindered alcohol substrates **IV-20**, **IV-21** and **IV-22** (see Table 4.10).





The reaction rates are comparable to those found for **IV-14**, **IV-15** and **IV-23** in Table 4.4; however, in many runs markedly increased b/l ratios (often > 40:1) are observed. Entry 4 shows that changing the aryl sulfonic acid from **IV-15** to the mesityl analog **IV-24** can be advantageous with respect to the observed regioselectivity.

**Table 4.10.** Catalysis with sulfonic acid co-catalyst and bulky alcohol substrates.

**IV-20:** X = Me  
**IV-21:** X = MeO  
**IV-22:** X = Cl

Entry <sup>[a]</sup>	X	Sulfonic acid	Reaction time [min]	Conversion [%] <sup>[b]</sup>	b : l ratio
1	Me	<b>IV-14</b>	18	100	16 : 1
2	Me	<b>IV-15</b>	20	100	49 : 1
3	Me	<b>IV-23</b>	25	100	77 : 1
4	Me	<b>IV-24</b>	20	100	39 : 1
5	MeO	<b>IV-14</b>	26	100	9 : 1
6	MeO	<b>IV-15</b>	55	100	24 : 1
7	MeO	<b>IV-23</b>	29	100	19 : 1
8	Cl	<b>IV-14</b>	21	100	22 : 1
9	Cl	<b>IV-15</b>	20	100	24 : 1
10	Cl	<b>IV-23</b>	18	100	20 : 1

[a] Reaction conditions: allyl alcohol (0.09 mmol), indole (0.09 mmol), **I-28** (0.0046 mmol) acid (0.0046 mmol) in CD<sub>3</sub>CN (0.5 ml), rt. [b] The reaction was monitored via <sup>1</sup>H-NMR.

### 4.2.3. Catalysis Using Several Isolated Complexes.

Given the varying rates and observed b/l ratios as a function of the acid in the catalytic reactions, it seemed that the sulfonate anion is involved in the ruthenium coordination sphere. Although we were not able to obtain evidence for the existence of sulfonate complexes from the catalytic solutions, several stoichiometric reactions in acetonitrile / toluene solvent mixtures led to isolable sulfonate complexes **II-7** and **II-8** (synthesis see Chapter 2 Scheme 2.4). We were not able to obtain an analogous complex with camphor sulfonic acid.

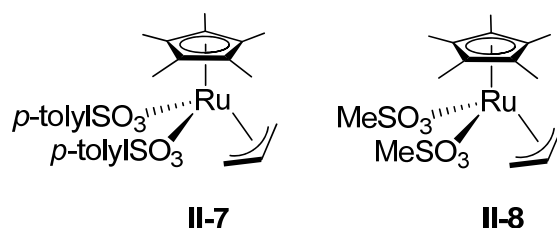


Table 4.11 shows the catalytic data stemming from reactions using *isolated* ruthenium(IV)-allyl catalysts **II-7** and **II-8** (without added acid) and confirms that the presence of the complexed sulfonate anion has a strong positive effect on the observed b/l ratios. The Table gives data for reactions using the ruthenium(IV) catalyst  $[\text{Ru}(\eta^3\text{-C}_3\text{H}_5)(\text{Cp}^*)(\text{MeCN})_2](\text{PF}_6)_2$  (**II-6**) i.e. without the complexed sulfonate (see entries 3 and 6). Clearly, in terms of both the b/l ratios and the reaction rate, **II-7** and **II-8** are far superior.

To distinguish between the steric and electronic effects associated with these complexed anions, one can compare the catalytic reactions with catalyst **II-8** and **II-7**. The reactions with  $\text{PhCH}(\text{OH})\text{CH}=\text{CH}_2$  are finished for both **II-8** and **II-7** in less than 40 min with a b/l ratio of 10.5:1 and 9.5:1, respectively (entries 1 and 2).

For  $o\text{-MeC}_6\text{H}_4\text{CH}(\text{OH})\text{CH}=\text{CH}_2$  the reactions are finished in 20 minutes with a b/l ratio of 93:1 for **II-8** and 56:1 for **II-7** (entries 4 and 5). The smaller sulfonate affords a larger and unprecedented regioselectivity, and consequently, it would appear that this improved selectivity is based on an electronic rather than a steric effect. This point will be discussed later by the study of DFT calculations in sub-Chapter 4.2.6.

**Table 4.11.** Allylation of indole by PhCH(OH)CH=CH<sub>2</sub> and its *o*-methyl-substituted analogue **IV-20** using preformed ruthenium(IV)-allyl catalysts **II-6**, **II-7** and **II-8**.

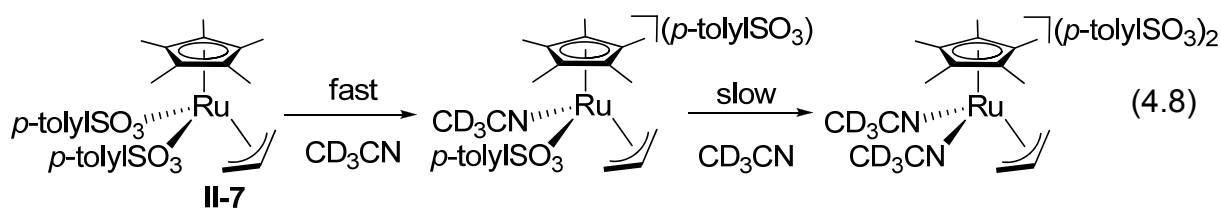
Entry <sup>[a]</sup>	Allyl substrate	Catalyst	Reaction time [min]	Conversion [%] <sup>[b]</sup>	b : l ratio
1			35	100	10.5 : 1
2			40	100	9.5 : 1
3			4.5	100	2 : 1
4			20	100	93 : 1
5			20	100	56 : 1
6			50	100	15 : 1

[a] Reaction conditions: allyl alcohol (0.07 mmol), indole (0.07 mmol), complex (0.0035 mmol) in CD<sub>3</sub>CN (0.5 ml), rt. [b] The reaction was monitored via <sup>1</sup>H-NMR.

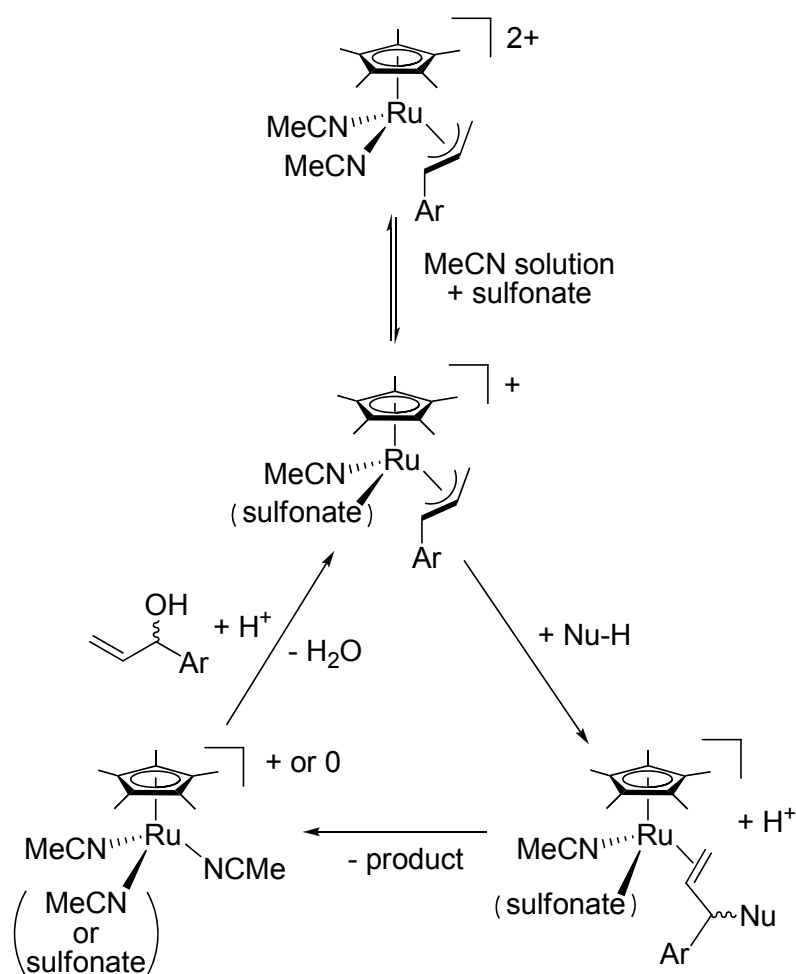
#### 4.2.4. NMR Measurement Experiments

The catalytic results are informative; however there is still the question of the number of complexed sulfonate ligands in acetonitrile solution. To shed light on this question we have carried out a series of NMR measurement experiments. Immediately after dissolving the bis-sulfonate complex **II-7** (2 mmol/L) in CD<sub>3</sub>CN, one can observe a set of <sup>1</sup>H-NMR signals that can be assigned to a species formed by dissociation of one *p*-toluene sulfonate ligand. The <sup>1</sup>H-NMR of this freshly prepared CD<sub>3</sub>CN solution revealed five non-equivalent η<sup>3</sup>-C<sub>3</sub>H<sub>5</sub> allyl resonances (δ = 6.13 ppm, 4.60 ppm, 4.43 ppm, 3.27 ppm and 2.82 ppm) plus resonances for two separate *p*-toluene sulfonate

methyl groups ( $\delta = 2.40$  ppm and 2.36 ppm), in addition to a singlet for the five equivalent Cp\* methyl groups ( $\delta = 1.67$  ppm). Pulsed gradient spin-echo (PGSE) diffusion measurements<sup>[15-20]</sup> gave *different* diffusion constants (D values) for the two *p*-toluene sulfonate methyl groups ( $D = 16.91 \times 10^{-10} \text{ m}^2\text{s}^{-1}$  for the signal at  $\delta = 2.36$  ppm and  $D = 13.16 \times 10^{-10} \text{ m}^2\text{s}^{-1}$ , for the signal at  $\delta = 2.40$  ppm). The latter value is identical to the diffusion constant derived from the Cp\* methyl groups at  $\delta = 1.67$  ppm, ( $D = 13.08 \times 10^{-10} \text{ m}^2\text{s}^{-1}$ ) suggesting that these two ligands are attached to the same ruthenium atom. Based on these data we assign the sulfonate moiety with the larger D-value to an un-complexed anion, and the sulfonate group with smaller D-value to a coordinated *p*-toluene sulfonate ligand. The intensity of the un-complexed methyl signal at  $\delta = 2.36$  ppm slowly increases in time, over hours, with concomitant decrease in the intensity of the signal of the coordinated sulfonate at  $\delta = 2.40$  ppm. At the same time a new set of *three*  $\eta^3$ -allyl resonances signals grow-in (in the ratio 2:2:1). Based on these observations, we propose the sequence shown in Equation 4.8.



When complex **II-7** was allowed to react with indole in  $\text{CD}_2\text{Cl}_2$  only a modest amount of allylation product was found. Addition of  $\text{CD}_3\text{CN}$  to this reaction solution gave rapid conversion to the organic product, 3-allyl indole. Consequently, given that the catalytic reactions are rapid, we assume that the mono-sulfonate cation is likely to be catalytic relevant. A mechanism for the formation of the branched allyl product, consistent with all of these observations, is given in Scheme 4.2.

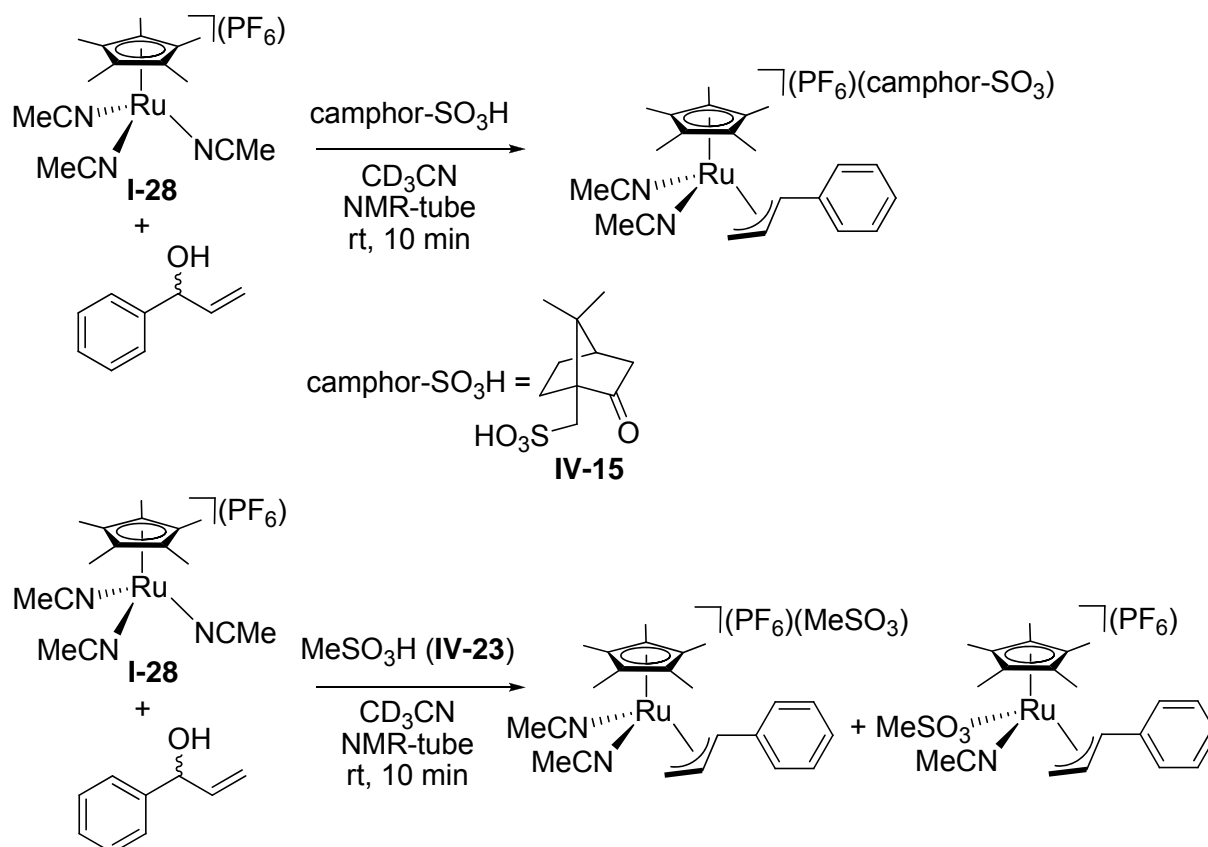


**Scheme 4.2.** Plausible mechanism for the appearance of the branched product in the allylation reaction.

#### 4.2.5. Oxidative Addition Reactions to form Ruthenium(IV)-Allyl Complexes

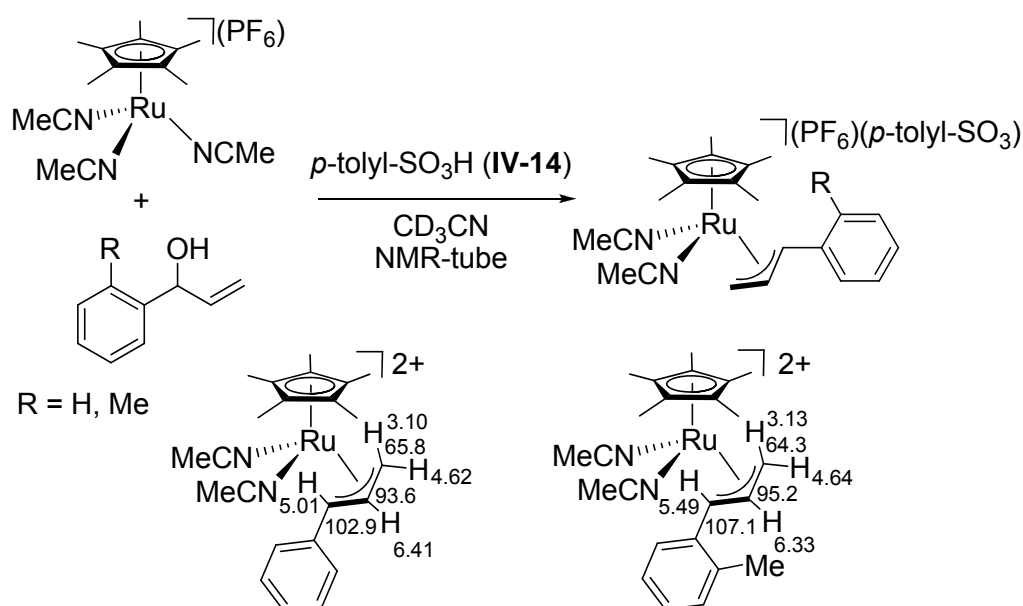
A mixture of one equivalent of **I-28**, PhCH(OH)CH=CH<sub>2</sub> and acid **IV-15** led to fast (less than 10 min) formation of an  $\eta^3$ -C<sub>3</sub>H<sub>5</sub> ruthenium(IV)-allyl complex (Scheme 4.3). Further, rapid formation of a ruthenium(IV)-allyl complex was also observed on allowing one equivalent each of **I-28**, PhCH(OH)CH=CH<sub>2</sub> and methane sulfonic acid, **IV-23**, to react in CD<sub>3</sub>CN solution. The new product in this case is assigned to an equilibrium mixture of the two ruthenium(IV) species shown, based on PGSE diffusion measurements. The observed D-value for the sulfonate methyl group found at  $\delta = 2.58$  ppm ( $14.92 \times 10^{10} \text{ m}^2\text{s}^{-1}$ ) is larger than that for the Cp\* methyl groups ( $11.76 \times 10^{10} \text{ m}^2\text{s}^{-1}$ ), but smaller than the D-value found for a solution of the model triethyl ammonium methane sulfonate salt in CD<sub>3</sub>CN ( $19.33 \times 10^{10} \text{ m}^2\text{s}^{-1}$ ), prepared for comparison purposes. This intermediate D-value is consistent with rapid exchange of the methyl sulfonate ligand on the NMR time scale. <sup>1</sup>H-NMR

measurements on a mixture of **I-28** and PhCH(OH)CH=CH<sub>2</sub> in CD<sub>3</sub>CN, *without* acid, show this complex does not react with the alcohol. We conclude that, as expected, the presence of strong acid facilitates the oxidative addition step by converting the (presumably complexed) allyl alcohol into a substrate with water as the leaving group.



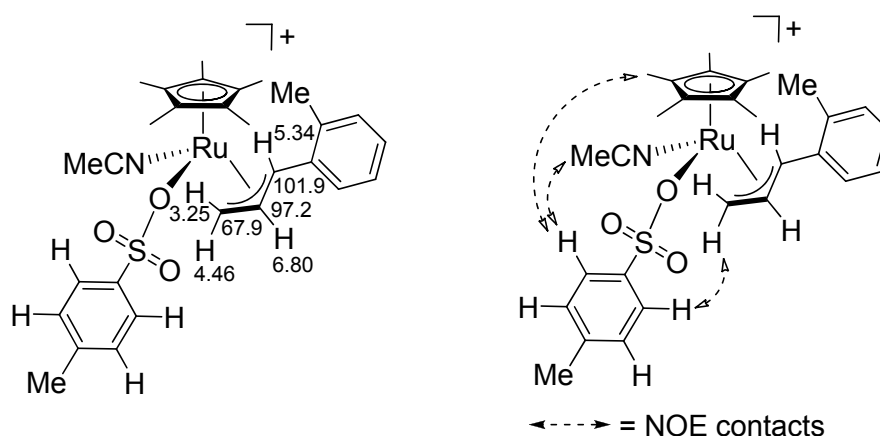
**Scheme 4.3.** Oxidative addition reactions of **I-28** and PhCH(OH)CH=CH<sub>2</sub> and an appropriate acid.

To obtain data with respect to the observed difference in the b/l ratio when the alcohol substrate has a bulky *ortho*-substituent, we have allowed one equivalent of either PhCH(OH)CH=CH<sub>2</sub> or *o*-MeC<sub>6</sub>H<sub>4</sub>CH(OH)CH=CH<sub>2</sub> to react with a mixture of one equivalent each of **I-28** and *p*-MeC<sub>6</sub>H<sub>4</sub>SO<sub>3</sub>H (**IV-14**) at ambient temperature in CD<sub>3</sub>CN solution. <sup>1</sup>H- and <sup>13</sup>C-NMR data for the bis-nitrile products, that form, [Ru(η<sup>3</sup>-PhCHCHCH<sub>2</sub>)(Cp\*)(MeCN)<sub>2</sub>]<sup>2+</sup> and [Ru(η<sup>3</sup>-*o*-MeC<sub>6</sub>H<sub>4</sub>-CHCHCH<sub>2</sub>)(Cp\*)(MeCN)<sub>2</sub>]<sup>2+</sup>, are given in Scheme 4.4. We note that the two substituted terminal allyl carbon resonances appear at δ = 102.9 ppm and δ = 107.1 ppm, for the Ph and *o*-tolyl analogues, respectively. This difference may have some significance since a higher frequency <sup>13</sup>C-allyl resonance is often associated with a weaker bond.<sup>[21]</sup>



**Scheme 4.4.** Oxidative additions of aryl allyl alcohols with **I-28**. At the bottom the difference in  $^1\text{H}$ - and  $^{13}\text{C}$ -NMR chemical shifts between the phenyl allyl complex and the *o*-tolyl analogue is shown.

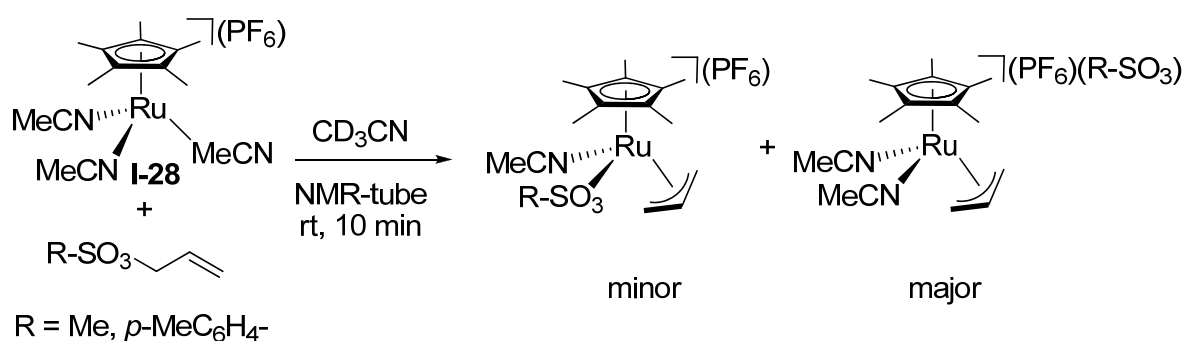
In a separate preparative experiment, the acetonitrile solvent from the reaction with  $o\text{-MeC}_6\text{H}_4\text{CH}(\text{OH})\text{CH}=\text{CH}_2$  was evaporated and the resulting crude solid suspended in  $\text{CD}_2\text{Cl}_2$ . The major product in solution is now the mono-sulfonate complex,  $[\text{Ru}(\eta^3\text{-}o\text{-MeC}_6\text{H}_4\text{-CHCHCH}_2)(\text{Cp}^*)(p\text{-MeC}_6\text{H}_4\text{SO}_3)(\text{MeCN})]^+$ , and  $^1\text{H}$ -,  $^{13}\text{C}$ - and NOE NMR details for this species are given in Scheme 4.5.



**Scheme 4.5.** Shows allyl chemical shifts of  $[\text{Ru}(\eta^3\text{-}o\text{-MeC}_6\text{H}_4\text{-CHCHCH}_2)(\text{Cp}^*)(p\text{-Me-C}_6\text{H}_4\text{SO}_3)(\text{MeCN})]^+$  and NOE contacts in  $\text{CD}_2\text{Cl}_2$ .

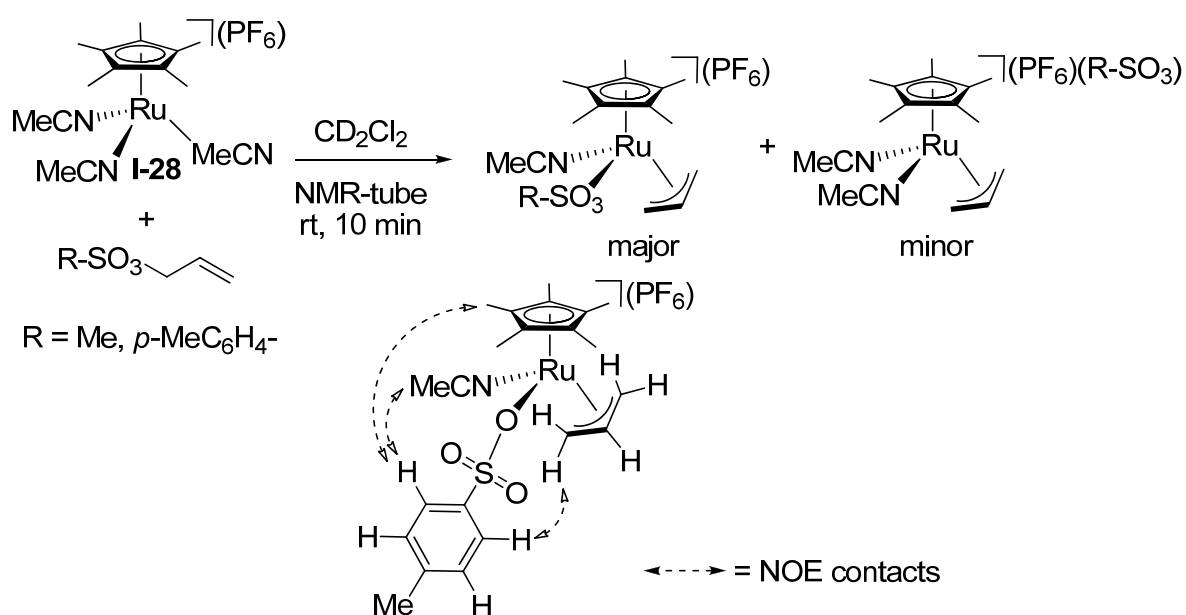
In a further attempt to characterize ruthenium(IV)-mono-sulfonate complexes, we have allowed one equivalent of **I-28** to react with one equivalent of either

$\text{MeSO}_3\text{CH}_2\text{CH}=\text{CH}_2$  or  $p\text{-MeC}_6\text{H}_4\text{SO}_3\text{CH}_2\text{CH}=\text{CH}_2$  at ambient temperature, first in  $\text{CD}_3\text{CN}$  (Scheme 4.6), and then in a separate experiment for each substrate, in  $\text{CD}_2\text{Cl}_2$  solution in an NMR tube (Scheme 4.7). In both cases, oxidative addition reactions proceed rapidly. In  $\text{CD}_3\text{CN}$ , the major product is the known<sup>[3]</sup>  $[\text{Ru}(\eta^3\text{-C}_3\text{H}_5)(\text{Cp}^*)(\text{bis-nitrile})\text{dication}]$ ; however there are several minor products and we assign one of these to  $[\text{Ru}(\eta^3\text{-C}_3\text{H}_5)(\text{Cp}^*)(p\text{-MeC}_6\text{H}_4\text{SO}_3)(\text{MeCN})]^+$  and  $[\text{Ru}(\eta^3\text{-C}_3\text{H}_5)(\text{Cp}^*)(\text{MeSO}_3)(\text{MeCN})]^+$ , respectively.



**Scheme 4.6.** Shows the products of the oxidative addition reaction of **I-28** and  $\text{RSO}_3\text{CH}_2\text{CH}=\text{CH}_2$  in  $\text{CD}_3\text{CN}$  at rt.

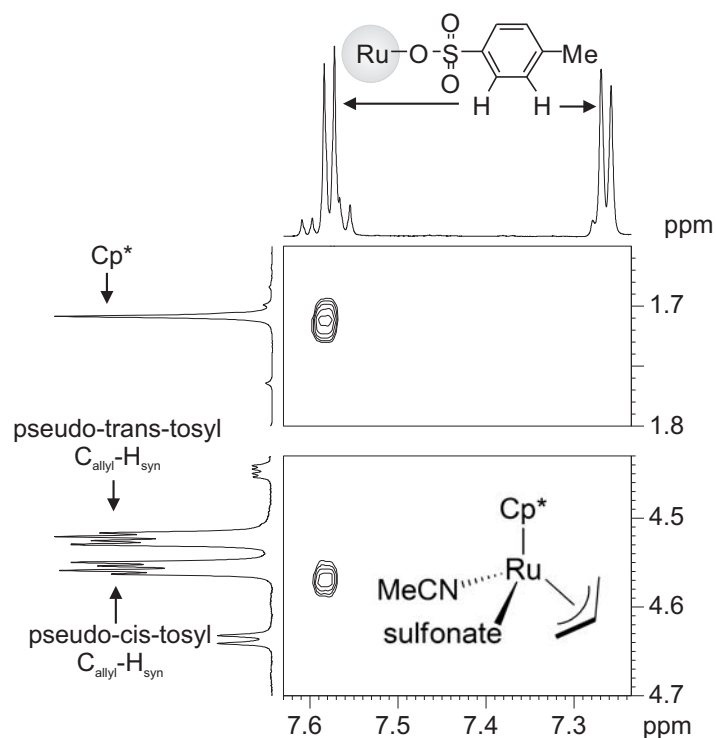
In  $\text{CD}_2\text{Cl}_2$ , the major product is now the mono-sulfonate salt. The bis nitrile is also present along with very minor amounts of unidentified species.



**Scheme 4.7.** Shows the products of the oxidative addition reaction of **I-28** and  $\text{RSO}_3\text{CH}_2\text{CH}=\text{CH}_2$  in  $\text{CD}_2\text{Cl}_2$  at rt and NOE contacts of  $[\text{Ru}(\eta^3\text{-CH}_2\text{CHCH}_2)(\text{Cp}^*)(p\text{-MeC}_6\text{H}_4\text{SO}_3)(\text{MeCN})]^+$ .



NOESY data in  $\text{CD}_2\text{Cl}_2$  solution show selective contacts from the  $p\text{-MeC}_6\text{H}_4\text{SO}_3^-$  ligand to both the  $\text{Cp}^*$  and the allyl group thereby confirming that this ligand is complexed (Fig. 4.3).



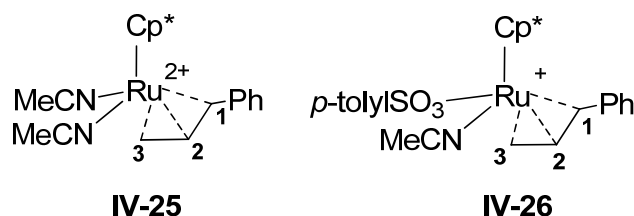
**Figure 4.3.** Sections of the 700 MHz  $^1\text{H}$ - 2-D NOESY for the cation  $[\text{Ru}(\eta^3\text{-C}_3\text{H}_5)(\text{Cp}^*)(p\text{-MeC}_6\text{H}_4\text{SO}_3)(\text{MeCN})]^+$  in  $\text{CD}_2\text{Cl}_2$  solution showing selective contacts from the coordinated sulfonate to the  $\text{Cp}^*$  methyl groups (upper section) and to the *syn* allyl proton closest to the complexed sulfonate (lower section).

These reactions support a) the idea that mono-sulfonate complexes are relatively stable, b) that the oxidative addition step is facile, and c) reasonably enough, that the sulfonate anion cannot compete favorably for the ruthenium center in the presence of a large excess of acetonitrile.

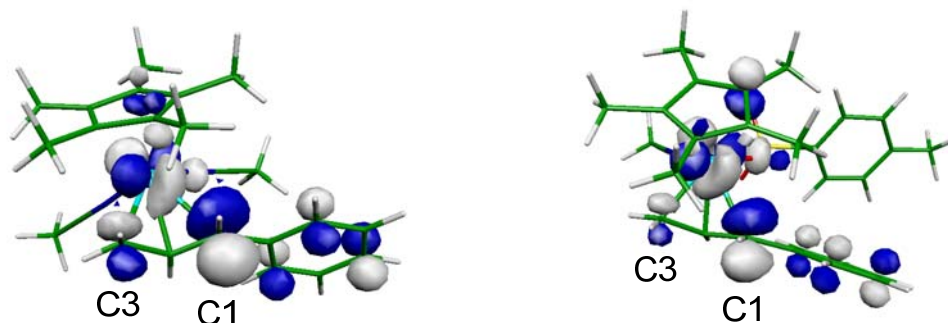
#### 4.2.6. DFT Studies

The various catalytic and NMR experiments described above suggest the involvement of one complexed sulfonate anion. DFT calculations<sup>[22]</sup> carried out in Lisbon by Prof. Veiros, were performed on the two ruthenium(IV) complexes, **IV-25** and **IV-26** in order to probe the observed regioselectivity. The calculated complexes show increasing Ru–allyl backdonation with the number of sulfonate anions in the complex, resulting in stronger and less asymmetric allyl coordination (*i.e.*, with

shorter Ru–C1 distances). Relevant metric and electronic parameters are provided in Chapter 7 Table A.13. These results are in contrast to the regioselectivity observed for the allylation reaction. The calculations indicate that the presence of sulfonate ligands produce similar Ru–C3 bonds and more negative C1 atoms.



Thus, the selectivity is not due to attack on a weaker Ru–C(allyl) moiety, and is certainly not charge driven. The LUMO of the complexes offers a clue to the observed selectivity. Figure 4.4 shows the LUMO for **IV-25**, the bis(nitrile) and **IV-26**, the species with one sulfonate ligand, suggested by the experimental results as the possible active species.



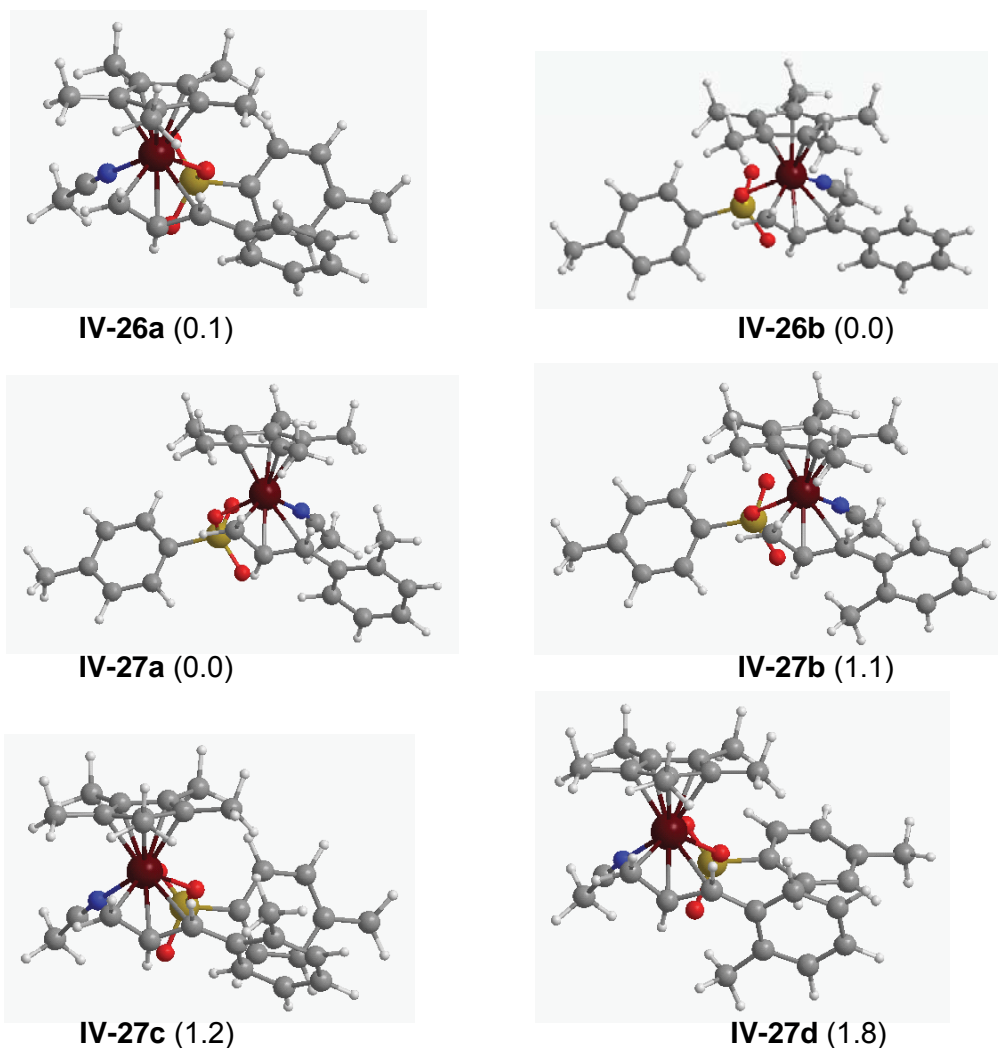
**Figure 4.4.** LUMO of  $[\text{Ru}(\eta^3\text{-CH}_2\text{CHCHC}_6\text{H}_5)(\text{Cp}^*)(\text{MeCN})_2]^{2+}$  (**IV-25**, left) and of  $[\text{Ru}(\eta^3\text{-CH}_2\text{CHCHC}_6\text{H}_5)(\text{Cp}^*)(p\text{-MeC}_6\text{H}_4\text{SO}_3)(\text{MeCN})]^+$  (**IV-26**, right). Note the difference in the C3 contributions.

Both orbitals are essentially equivalent in their general features, and represent a Ru–allyl  $\pi^*$  orbital. In both cases there is an important contribution from C1, the substituted allyl carbon. However, there is a major difference in the *relative weight of the contribution for the two terminal allyl C-atoms*. For the sulfonate complex, **IV-26**, the contribution of C3 is much diminished when compared to the contribution of C3,

in the bis(nitrile) species, **IV-25**. Thus, the preference for a nucleophilic attack on C1, yielding the branched product, appears to be related to the *relative contribution* of these two terminal C-atoms on the LUMO of the complex. The reaction is driven by orbital control, and the selectivity is dictated by the topology of the LUMO of the corresponding ruthenium(IV) complexes.

However, since the metal is a stereogenic center, a cation with the empirical formula  $[\text{Ru}(\eta^3\text{-PhCHCHCH}_2)(\text{Cp}^*)(\text{RSO}_3)(\text{MeCN})]^+$  can exist as a number of different diastereomers. To shed further light on this chemistry we have carried out further DFT calculations on the two isomers of  $[\text{Ru}(\eta^3\text{-PhCHCHCH}_2)(\text{Cp}^*)(p\text{-MeC}_6\text{H}_4\text{SO}_3)(\text{MeCN})]^+$  **IV-26a,b**, and the four isomeric forms of  $[\text{Ru}(\eta^3\text{-(}o\text{-MeC}_6\text{H}_4\text{)CHCHCH}_2)(\text{Cp}^*)(p\text{-MeC}_6\text{H}_4\text{SO}_3)(\text{MeCN})]^+$ , **IV-27a-d**.

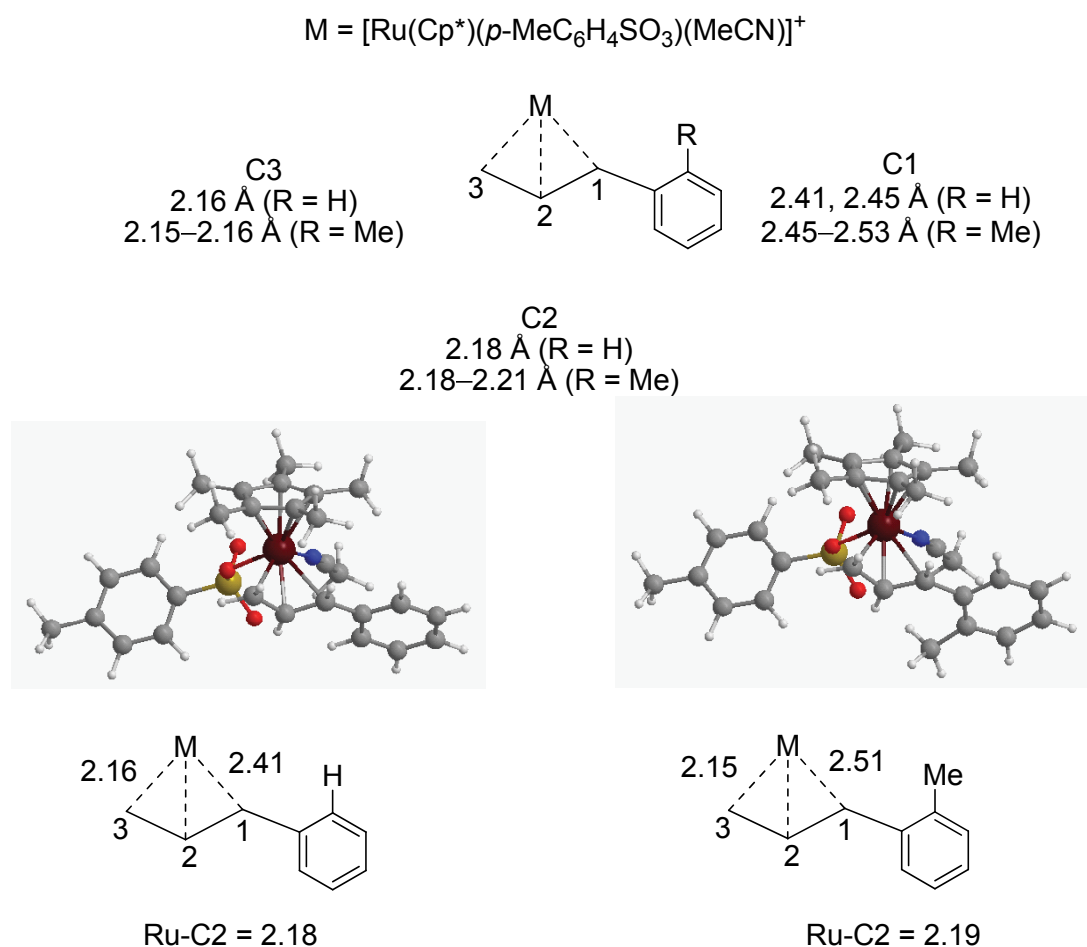
In Figure 4.5 we show the optimized geometries for these six species along with the relative energies between the isomers. Note that, in **IV-27**, we show isomers which differ only in that the *o*-Me substituent of the tolyl-group is either close to C2 or remote from this atom and directed towards the Cp\* ligand (see **IV-27a** and **IV-27b**). Although one might have expected that the relative position of the sulfonate with respect to the allyl aryl group would markedly affect the energy, this is not the case. The sterically less favored structures having the aryl sulfonate ligand pseudo-*cis* to the aryl group of the allyl ligand are only slightly less stable.



**Figure 4.5.** Structures and Energies (kcal/mol) for  $[\text{Ru}(\eta^3\text{-PhCHCHCH}_2)(\text{Cp}^*)(p\text{-MeC}_6\text{H}_4\text{SO}_3)(\text{MeCN})]^+$ , **IV-26a,b**, and  $[\text{Ru}(\eta^3\text{-(}o\text{-MeC}_6\text{H}_4\text{)CHCHCH}_2)(\text{Cp}^*)(p\text{-MeC}_6\text{H}_4\text{SO}_3)(\text{MeCN})]^+$ , **IV-27a-d**, containing complexed  $p\text{-MeC}_6\text{H}_4\text{SO}_3$  ligands.

Figure 4.6 presents a summary of the Ru–C(allyl) bond distances (Å) for **IV-26** and **IV-27**. As expected, based on previous studies,<sup>[21, 23-26]</sup> the Ru–C3 allyl separation is not very sensitive to the various changes in structure, and remains at about 2.15–2.16 Å. However, the Ru–C1 separation is both longer than the Ru–C3 distance, and sensitive to whether the allyl has a phenyl or a *o*-tolyl group. For example, considering the most stable diastereomer of each complex, **IV-26b** and **IV-27a** (see the bottom of Figure 4.6), one finds a 0.1 Å difference in the Ru–C1 bond length, while the Ru–C3 distances are within 0.01 Å in the two molecules. These geometric differences are corroborated by the Wiberg indices (WI)<sup>[27]</sup> of the corresponding bonds (see Chapter 7, Tables A.13–14), confirming an electronic reason for the changes observed. The Wiberg index associated with the Ru–C1 bond drops from WI

= 0.34, in **IV-26b**, to WI = 0.30, in **IV-27a**, whereas for the Ru-C3 bonds the WI values are within 0.01, for both species. These results suggest a larger distortion, for the allyl ligand with the *o*-tolyl group, in **IV-27a**, than for the allyl with the phenyl group, in **IV-26b**, due to a weaker Ru-C1 bond in the former complex.



**Figure 4.6.** Calculated bond lengths (Å) for the allyl carbons.

The charges calculated via a Natural Population Analysis (NPA)<sup>[28-34]</sup> reflect the differences in the Ru-allyl bond strength discussed above (see Chapter 7). Stronger Ru-allyl bonds are associated with enhanced back donation from Ru to allyl,<sup>[21]</sup> and correspond to electron richer ligands. This is reflected in the total charges associated with the allyl ligand, +0.35 in **IV-26b** and +0.38 in **IV-27a**, indicating a less positive ligand, and, thus, a stronger Ru-allyl interaction, in **IV-26b**. This structural dissimilarity is accompanied by differences in the atomic charges calculated for the allyl carbon C1: -0.17 for the phenyl analog, **IV-26b**, and -0.15 for the *o*-tolyl derivative, **IV-27a**. The charges at the CH<sub>2</sub> terminus, C3, are quite similar for both

complexes (-0.42 in **IV-26b** and -0.43 in **IV-27a**) and much more negative than the values calculated for C1. Consequently, in the *o*-tolyl set the Ru-C1 bond is weaker and the C-atom is more positive (less negative), and therefore more likely to attract the incoming nucleophile and yield the branched product. Summarizing, the calculations for the presumed to be important sulfonate salts  $[\text{Ru}(\eta^3\text{-C}_3\text{H}_5)(\text{Cp}^*)(\text{RSO}_3)(\text{MeCN})]^+$ , suggest that the changes in the observed b/l ratios are likely to arise from structural distortions due to the presence of the *o*-substituent.

### 4.3. Conclusions

Summarizing we have shown that our new ruthenium(IV)-allyl complex, **II-6**, is an excellent catalyst for the C-allylation of different selected indoles and pyrroles using allyl alcohols as substrates. Several products have been isolated in good yields. A mechanism has been established and involves the controlled release of one proton per catalytic cycle.

As an alternative, the combination of  $[\text{Ru}(\text{Cp}^*)(\text{MeCN})_3](\text{PF}_6)$  (**I-28**) and one of the sulfonic acids **IV-14**, **IV-15**, and **IV-23** can be used. Several acids (such as  $\text{H}_2\text{SO}_4$ ,  $\text{CF}_3\text{SO}_3$ ,  $\text{HBF}_4$  and carboxylic acids) are either poorer or inefficient co-catalysts. 1,1'-Binaphthyl-2,2'-diyl hydrogen phosphate (**IV-16**) is an excellent co-catalyst; however, it requires co-solvents to become soluble in acetonitrile.

By using allyl alcohol it is not necessary to waste a leaving group (such as acetates and carbonates), and no additives (such as bases) are required. The branched products are favored, and a number of examples, with only branched products are observed. The catalyst is selective in that there is no N-allylation (for substituted allyl alcohols) or di-allyl ether formation. Addition of excess of C3-allyl alcohols results in N- and C-double allylation of substituted indoles in good yields. Further, preliminary experiments suggest that selected vinyl epoxides may be used as an alternative allyl source.

$[\text{Ru}(\eta^3\text{-C}_3\text{H}_5)(\text{Cp}^*)(\text{RSO}_3)_2]$  is an efficient catalyst precursor; however, the NMR data suggest that one of the active species is the mono-sulfonate cationic complex  $[\text{Ru}(\eta^3\text{-C}_3\text{H}_5)(\text{Cp}^*)(\text{RSO}_3)(\text{MeCN})]^+$ . Stoichiometric oxidative addition reaction are shown to

be relatively rapid. The NMR studies reveal that the mono-sulfonate complexes are formed. These salts are not very stable in acetonitrile solution; however they are readily characterized in dichloromethane.

The DFT calculations have provided a rationale for the relatively large observed b/l ratios based on structural distortions due to the presence of the bulky *o*-methyl-substituent in the alcohol substrate.

#### 4.4. References

- [1] R. J. Sundberg, *Indoles*, Academic Press: San Diego, **1996**.
- [2] M. Bandini, A. Melloni, A. Umani-Ronchi, *Organic Letters* **2004**, *6*, 3199-3202.
- [3] A. B. Zaitsev, S. Gruber, P. S. Pregosin, *Chem. Commun.* **2007**, 4692-4693.
- [4] W.-B. Liu, H. He, L.-X. Dai, S.-L. You, *Organic Letters* **2008**, *10*, 1815-1818.
- [5] M. Kimura, M. Futamata, R. Mukai, Y. Tamaru, *Journal of the American Chemical Society* **2005**, *127*, 4592-4593.
- [6] I. Usui, S. Schmidt, M. Keller, B. Breit, *Organic Letters* **2008**, *10*, 1207-1210.
- [7] H. Y. Cheung, W.-Y. Yu, F. L. Lam, T. T. L. Au-Yeung, Z. Zhou, T. H. Chan, A. S. C. Chan, *Organic Letters* **2007**, *9*, 4295-4298.
- [8] M. Westermaier, H. Mayr, *Organic Letters* **2006**, *8*, 4791-4794.
- [9] B. M. Trost, J. Quancard, *Journal of the American Chemical Society* **2006**, *128*, 6314-6315.
- [10] M. Yasuda, T. Somyo, A. Baba, *Angewandte Chemie International Edition* **2006**, *45*, 793-796.
- [11] S. P. Nolan, K. L. Martin, E. D. Stevens, P. J. Fagan, *Organometallics* **1992**, *11*, 3947-3953.
- [12] G. J. Bodwell, J. Li, *Organic Letters* **2001**, *4*, 127-130.
- [13] D. M. Mbaye, B. Demerseman, J.-L. Renaud, L. Toupet, C. Bruneau, *Angewandte Chemie International Edition* **2003**, *42*, 5066-5068.
- [14] J.-L. Renaud, C. Bruneau, B. Demerseman, *Synlett* **2003**, *2003*, 0408-0410.
- [15] P. Stilbs, *Progress in Nuclear Magnetic Resonance Spectroscopy* **1987**, *19*, 1-45.
- [16] C. Zuccaccia, N. G. Stahl, A. Macchioni, M.-C. Chen, J. A. Roberts, T. J. Marks, *Journal of the American Chemical Society* **2004**, *126*, 1448-1464.
- [17] D. Zuccaccia, A. Macchioni, *Organometallics* **2005**, *24*, 3476-3486.
- [18] P. S. Pregosin, P. G. A. Kumar, I. Fernandez, *Chemical Reviews* **2005**, *105*, 2977-2998.
- [19] P. S. Pregosin, *Progress in Nuclear Magnetic Resonance Spectroscopy* **2006**, *49*, 261-288.
- [20] P. G. A. Kumar, *Australian Journal of Chemistry* **2006**, *59*, 78-78.
- [21] R. Hermatschweiler, I. Fernandez, P. S. Pregosin, E. J. Watson, A. Albinati, S. Rizzato, L. F. Veiros, M. J. Calhorda, *Organometallics* **2005**, *24*, 1809-1812.



- [22] R. G. Parr, W. Yang, *Density Functional Theory of Atoms and Molecules*, Oxford University Press: New York, **1989**.
- [23] R. Hermatschweiler, I. Fernández, F. Breher, P. S. Pregosin, L. F. Veiros, M. J. Calhorda, *Angewandte Chemie International Edition* **2005**, *44*, 4397-4400.
- [24] I. Fernandez, R. Hermatschweiler, P. S. Pregosin, A. Albinati, S. Rizzato, *Organometallics* **2005**, *25*, 323-330.
- [25] R. Hermatschweiler, I. Fernandez, P. S. Pregosin, F. Breher, *Organometallics* **2006**, *25*, 1440-1447.
- [26] I. Fernández, R. Hermatschweiler, F. Breher, P. S. Pregosin, L. F. Veiros, M. J. Calhorda, *Angewandte Chemie International Edition* **2006**, *45*, 6386-6391.
- [27] K. B. Wiberg, *Tetrahedron* **1968**, *24*, 1083-1096.
- [28] J. E. Carpenter, F. Weinhold, *Journal of Molecular Structure: THEOCHEM* **1988**, *169*, 41-62.
- [29] J. E. Carpenter, Ph.D. thesis, University of Wisconsin, Madison WI, **1987**.
- [30] J. P. Foster, F. Weinhold, *Journal of the American Chemical Society* **1980**, *102*, 7211-7218.
- [31] A. E. Reed, F. Weinhold, *The Journal of Chemical Physics* **1983**, *78*, 4066-4073.
- [32] A. E. Reed, R. B. Weinstock, F. Weinhold, *The Journal of Chemical Physics* **1985**, *83*, 735-746.
- [33] A. E. Reed, L. A. Curtiss, F. Weinhold, *Chemical Reviews* **2002**, *88*, 899-926.
- [34] F. Weinhold, J. E. Carpenter, *The Structure of Small Molecules and Ions*, Plenum NY, **1988**.



# 5.

**Allylation of Cyclic**

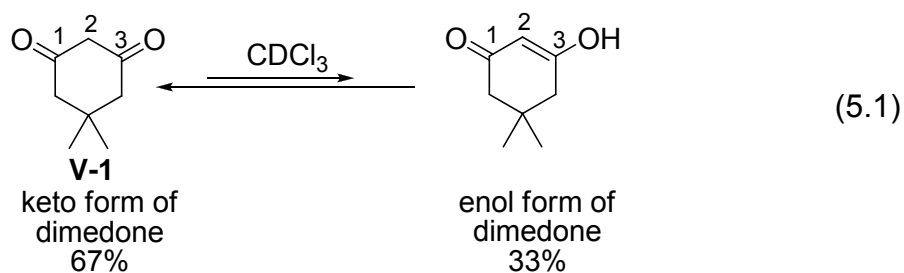
**1,3-Diketones**

## 5.1. Introduction

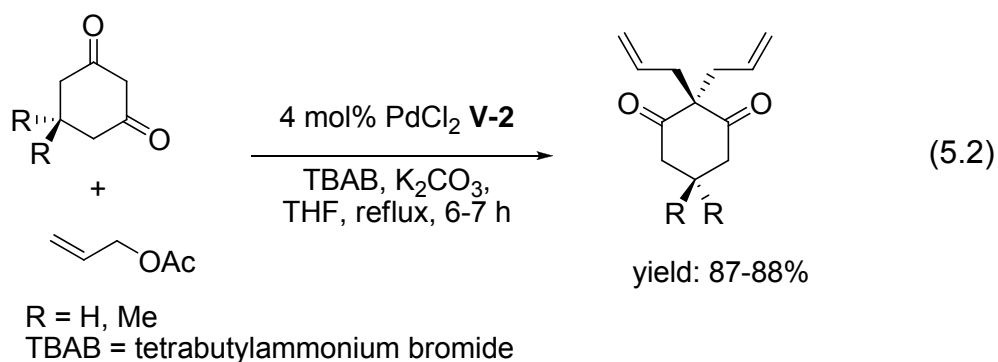
This chapter concerns the ruthenium(IV) catalyzed allylation of cyclic 1,3-diketones using allyl alcohols as substrates.

In the literature it has been shown that cyclic 1,3-diketones can serve as substrates for substitution reactions.<sup>[1, 2]</sup> Since 1,3-diketones are acidic at the C-2 position, they serve as excellent nucleophiles for several reactions such as allylation and halogenation.

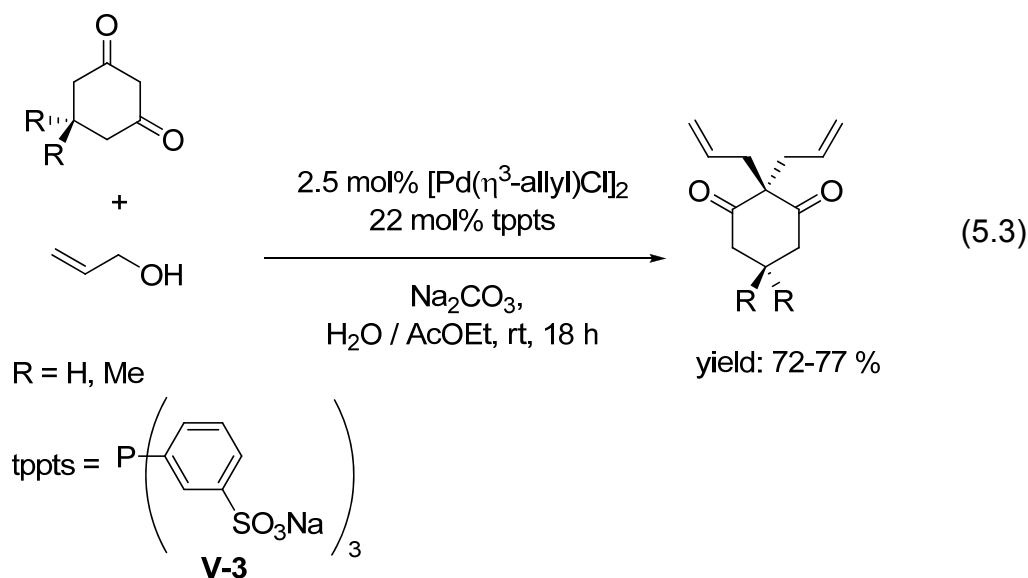
Cyclic 1,3-diketones such as dimedone (**V-1**, 5,5-dimethylcyclohexane-1,3-dione) exist in  $\text{CDCl}_3$  in two forms, which are in equilibrium (see Equation 5.1). In MeOD solution the equilibrium is completely shifted to the enol tautomer, which is presumably stabilized by hydrogen bonding.<sup>[3]</sup>



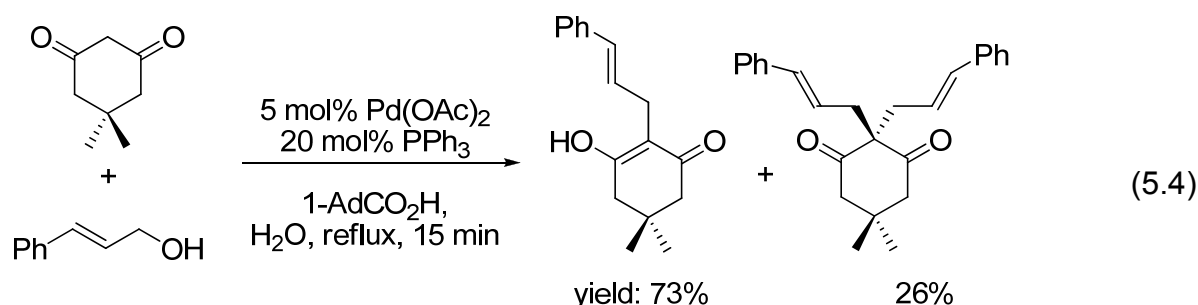
The allylation of different cyclic 1,3-diketones with allyl acetate can be catalyzed by a palladium(II) precursor, **V-2**, as shown in Equation 5.2.<sup>[4]</sup> The active catalyst in this reaction is generated in situ and is thought to involve palladium(0) nanoparticles and additional reagents (tetrabutylammonium bromide and potassium carbonate) are required to afford the products. The products are obtained in high yields by refluxing the reaction mixture for ca. 7 hours.



Changing the allyl substrate, from allyl acetate to allyl alcohol affords the products in slightly lower yield, and requires stirring for 18 hours (Equation 5.3).<sup>[5]</sup> The reaction proceeds under basic conditions (addition of sodium carbonate) and a relatively large quantity of an additional phosphorus containing ligand, **V-3**, is necessary.



Gan and co-workers have reported a palladium/carboxylic acid catalyzed allylation of dimedone with cinnamyl alcohol in water (Equation 5.4).<sup>[6]</sup> The reaction proceeds rapidly, however elevated temperature and a substantial amount of the acid are required. Only the linear products are obtained, which is not unusual for palladium, and the ratio of mono- to di-allylated product is moderate with 2:1.



For more examples of transition metal catalyzed allylation of cyclic 1,3-diketones see Curran<sup>[7]</sup>, Ikariya<sup>[8]</sup>, Itoh<sup>[9]</sup> and Sinou<sup>[10]</sup>.

## 5.2. Results and Discussion

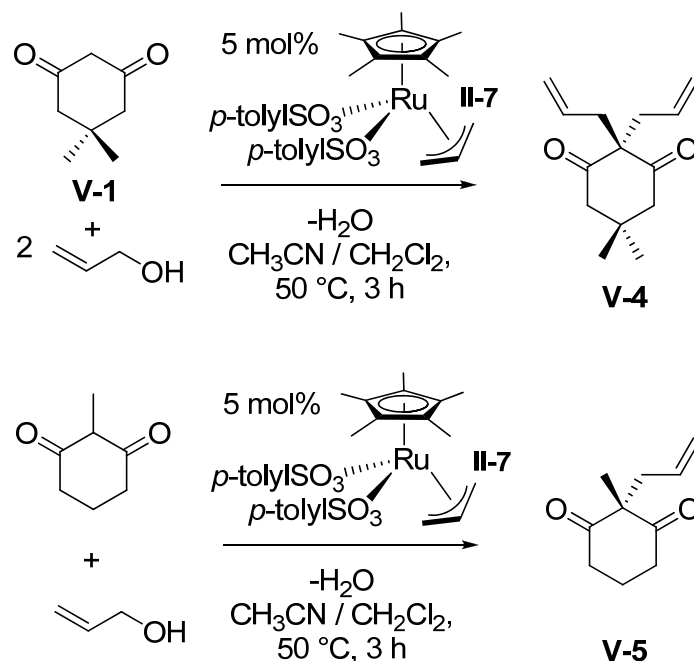
In an attempt to improve the reaction rate and the regioselectivity of the reactions, we have carried out several catalytic allylation reactions of cyclic 1,3-diketones with different allyl alcohols using a ruthenium(IV)-allyl catalyst.

### 5.2.1. Allylation of Cyclic 1,3-Diketones with Allyl Alcohol

The ruthenium catalyst **II-7** easily affords the products of the allylation of a variety of cyclic 1,3-diketones using  $\text{CH}_2=\text{CHCH}_2\text{OH}$  as substrate, without acid, base or other additives (Scheme 5.1 and Table 5.1).

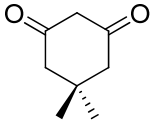
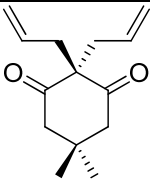
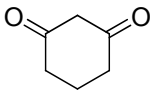
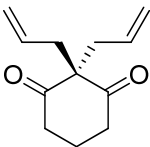
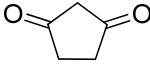
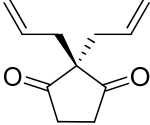
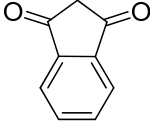
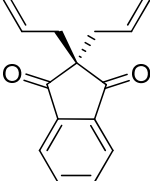
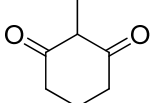
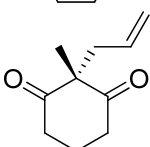
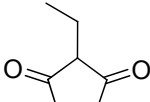
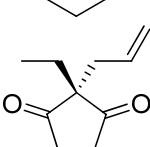
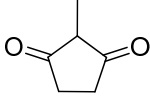
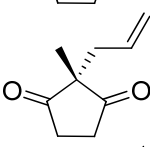
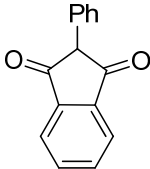
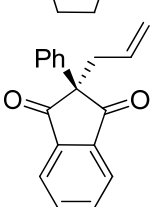
The reaction of the diketones not substituted at the 2-position results exclusively in the double allylated products in greater than 90% yield; e.g compound **V-4** in the Scheme 5.1 and entries 1-4 in Table 5.1.

Further, one can smoothly add an allyl function to an existing tertiary carbon centre (at the 2-position), and this is shown by compound **V-5** in the Scheme 5.1 and entries 5-8 in Table 5.1. The yields are essentially quantitative and the values shown are for isolated yields, after column chromatography.



**Scheme 5.1.** Shows the allylation reactions of cyclic 1,3-diketones to the products **V-4** and **V-5**, respectively.

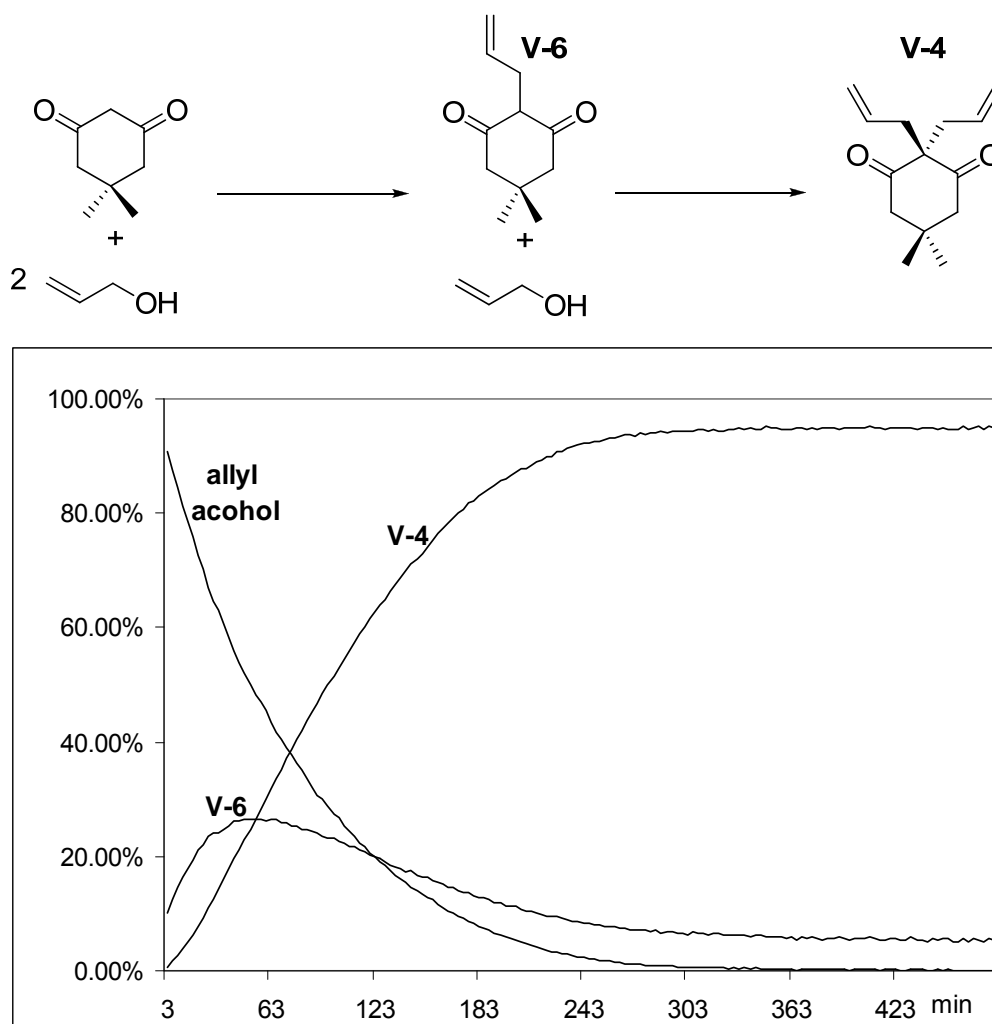
**Table 5.1.** Allylation of 1,3-diketones with  $\text{CH}_2=\text{CHCH}_2\text{OH}$  using **II-7**.

Entry <sup>[a]</sup>	Nucleophile	Product	Yield [%] <sup>[b]</sup>
1			97
2			92
3			88
4 <sup>[c]</sup>			89
5			96
6			92
7			98
8			96

[a] Reaction conditions: MeCN (0.8 ml),  $\text{CH}_2\text{Cl}_2$  (3.3 ml), diketone (0.80 mmol),  $\text{CH}_2=\text{CHCH}_2\text{OH}$  (0.85 mmol or 1.65 mmol), **II-7** (0.04 mmol = 5 mol%), 50 °C. [b] Yield of product isolated after purification by chromatography. [c] 16 h at 50 °C.

Figure 5.1 gives an overview of the development of the double-allylation compound, **V-4**, as a function of time using  $\text{CH}_2=\text{CHCH}_2\text{OH}$ . From this figure, one can deduce that the rate of the second allylation for this relatively small alcohol is similar to that of

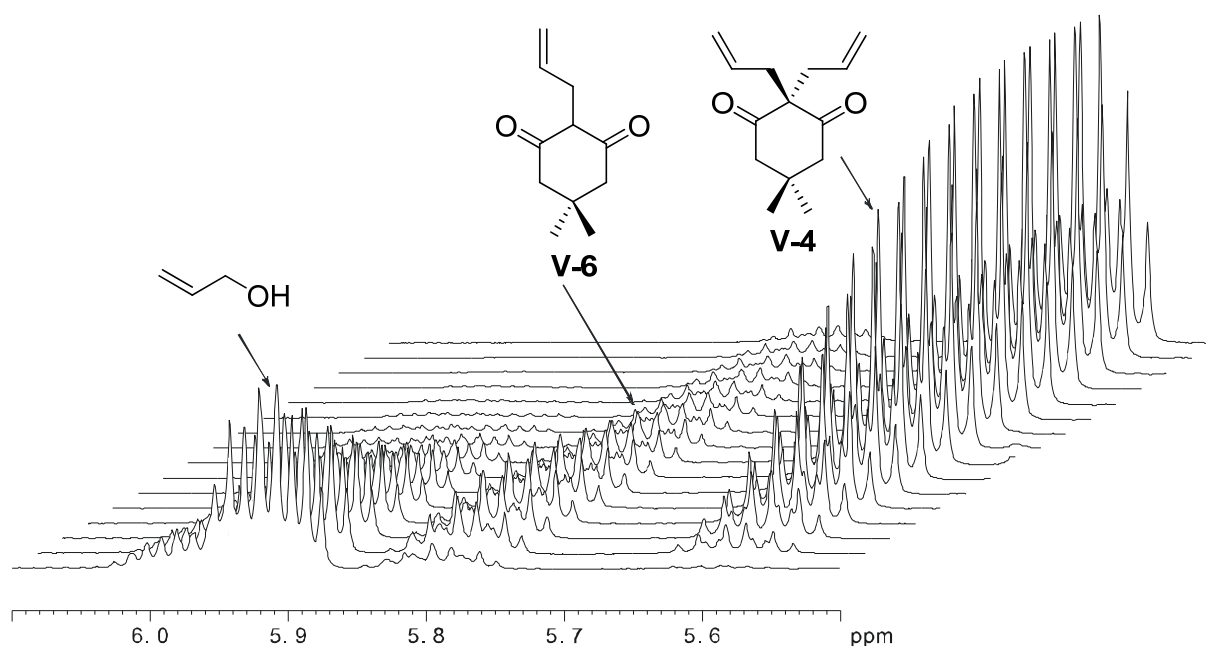
the rate for the first allylation so that a high yield of the mono-allyl product **V-6** is difficult to obtain.



**Figure 5.1.** An overview of the development of double-allylation, giving **V-4**, and the mono-allylation product **V-6** as a function of time at rt. The double-allylation and mono-allylation compounds grow in at similar rates. The decreasing curve represents the concentration of allyl alcohol as a function of time.

Figure 5.2 gives an overview of the recorded spectra for the development of the double-allyl product, **V-4**, the partial appearance of the mono-allyl product, **V-6** and the disappearance of the allyl alcohol as a function of time at ambient temperature.

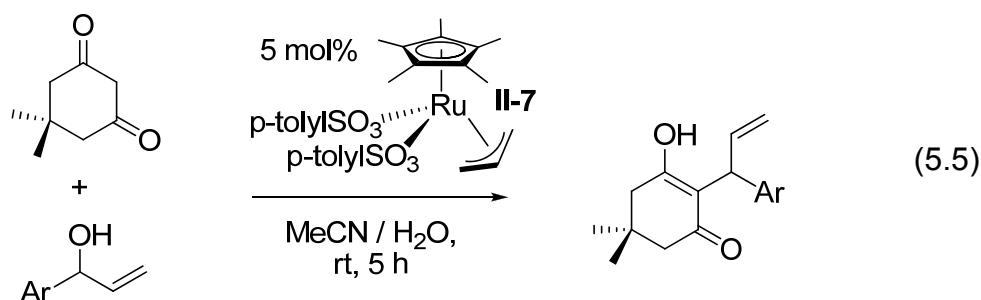




**Figure 5.2.** An overview of the recorded spectra for the development of the double-allyl product, **V-4**, the partial appearance of the mono-allyl product, **V-6** and the disappearance of the allyl alcohol as a function of time at rt (500 MHz,  $\text{CD}_2\text{Cl}_2/\text{CD}_3\text{CN}$ ).

### 5.2.2. Allylation of Dimedone with Several Aryl Allyl Alcohols

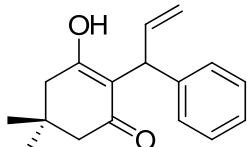
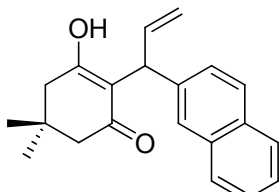
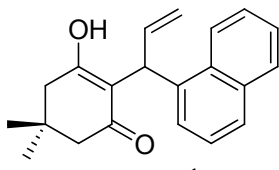
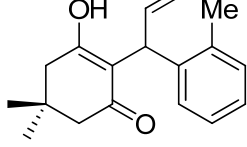
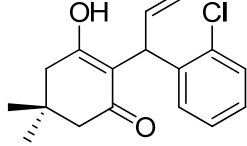
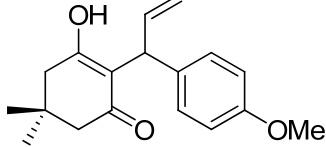
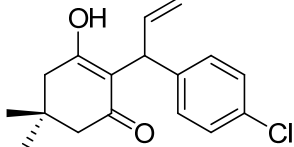
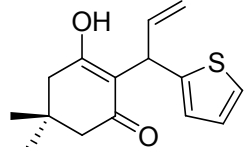
Interestingly catalyst **II-7** regioselectively *mono-allylates* dimedone using a series of substituted aryl allyl alcohols as substrates, under relatively mild conditions (see Equation 5.5).



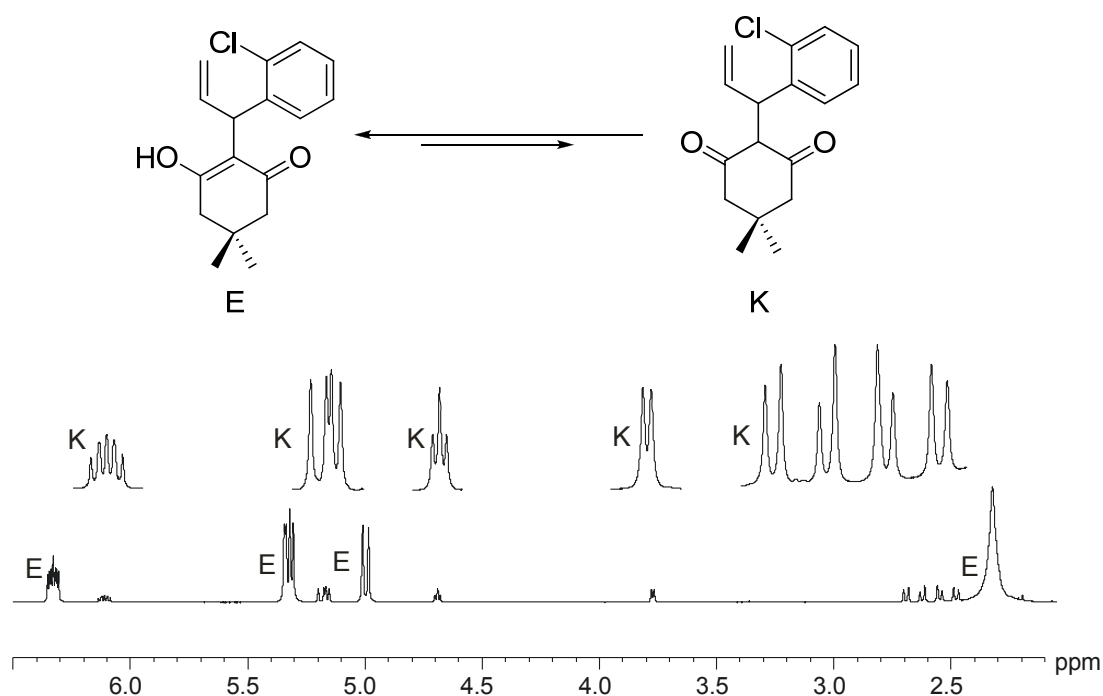
The yields shown in Table 5.2 are for isolated products, after recrystallization. Based on NMR data, the conversion to the desired product is of the order of 90%. The reactions proceed smoothly at ambient temperature and are complete in a few hours. In chloroform solution the organic products exist as a mixture of the enol and diketone forms (Figure 5.3 represents an example for the product from entry 5). For the characterization of the products, their NMR spectra were measured in  $\text{DMF-d}_7$ , in

which the enol form dominates and therefore show this product in the Table (see Equation 5.5 and Figure 5.4). The OH resonance of the enol form is clearly visible at  $\delta = 10.73$  ppm.

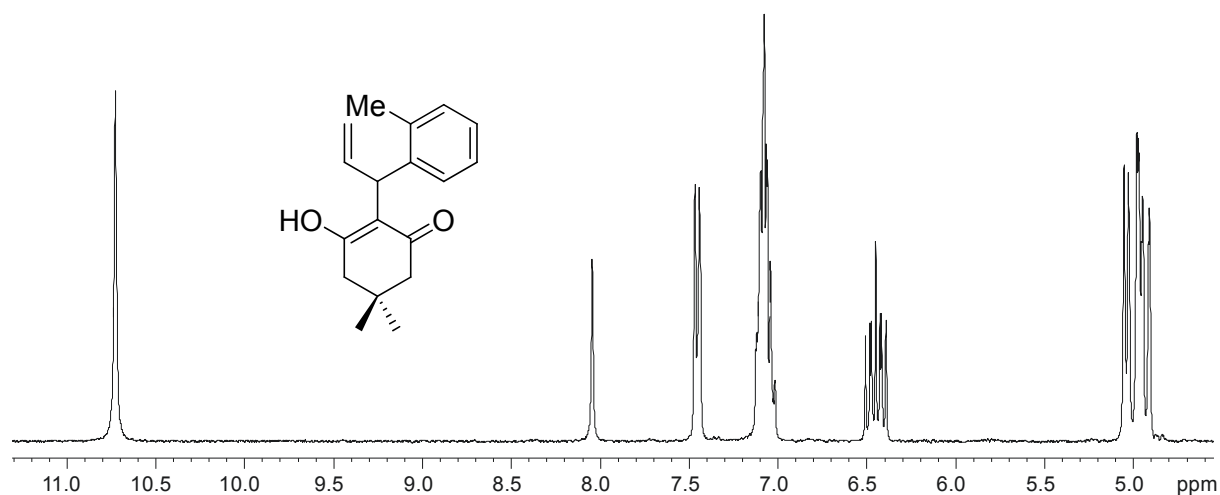
**Table 5.2.** Mono-allylation of dimedone with  $\text{ArCH(OH)CH=CH}_2$  catalyzed by **II-7**.

Entry <sup>[a]</sup>	Ar	Product	Yield [%] <sup>[b]</sup>
1	Ph		78
2	2-naphthyl		79
3	1-naphthyl		70
4	<i>o</i> -Me-C <sub>6</sub> H <sub>4</sub> -		77
5	<i>o</i> -Cl-C <sub>6</sub> H <sub>4</sub> -		75
6	<i>p</i> -MeO-C <sub>6</sub> H <sub>4</sub> -		73
7	<i>p</i> -Cl-C <sub>6</sub> H <sub>4</sub> -		62
8	1-thiophenyl		77

[a] Reaction conditions: MeCN (1.6 ml), H<sub>2</sub>O (1.6 ml), diketone (0.65 mmol),  $\text{ArCH(OH)CH=CH}_2$  (0.68 mmol), **II-7** (0.03 mmol = 5 mol%), rt, 5 h. [b] Yield of product isolated after purification by crystallization.



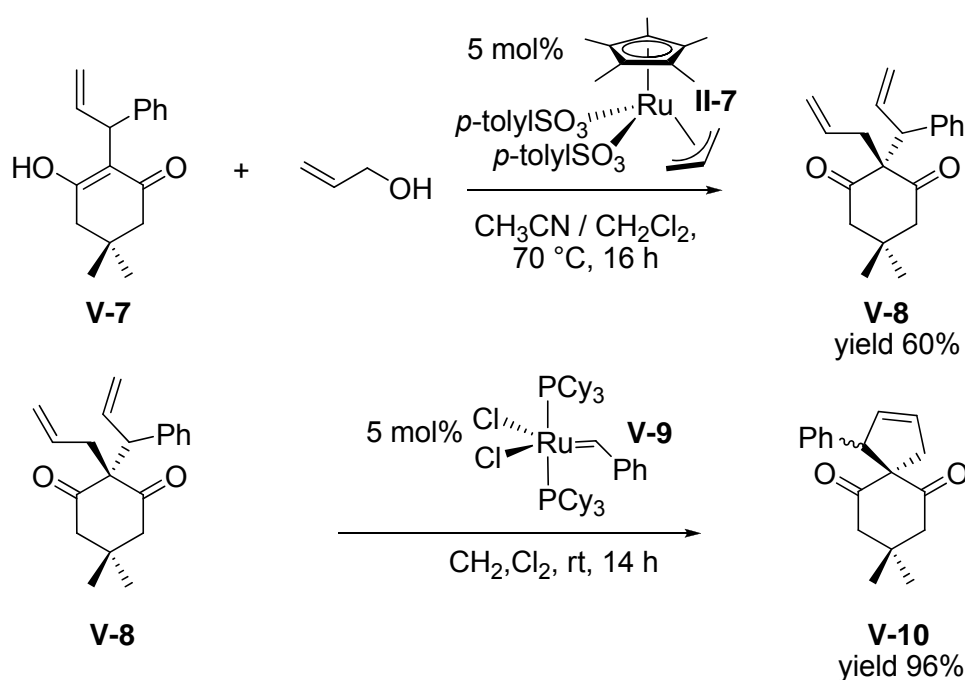
**Figure 5.3.** Section of the  $^1\text{H-NMR}$  spectrum of the product derived from dimedone and the allyl alcohol,  $o\text{-Cl-C}_6\text{H}_4\text{CH(OH)CH=CH}_2$ . **E** represents the enol tautomer and **K** the ketone tautomer, which are in equilibrium in a  $\text{CDCl}_3$  solution at rt. The resonances stem from the methylene and allyl protons of **E** and **K**, respectively (700 MHz,  $\text{CDCl}_3$ ).



**Figure 5.4.** Section of the  $^1\text{H-NMR}$  spectrum of the product derived from dimedone and the allyl alcohol,  $(o\text{-tolyl})\text{CH(OH)CH=CH}_2$ . The resonance at  $\delta = 10.73$  ppm stems from the OH group of the enol. There are three signals (two from the vinyl group  $\text{CH=CH}_2$  and the aliphatic CH) in the region around  $\delta = 5.0$  ppm. The residual CHO of the solvent appears at ca  $\delta = 8.04$  ppm (300 MHz,  $\text{DMF-d}_7$ ).

For this type of 1,3-diketone substrate, we know of no other catalyst that is completely regioselective or even specific for the mono-allyl product. Both of these characteristics are unique. Further, note that although literature palladium<sup>[8]</sup> and ruthenium<sup>[11]</sup> catalysts can convert allyl alcohols into allyl ethers, there is essentially no *di-allyl ether formed* under our reaction conditions (acetonitrile/water), although acid is present. This is yet another form of selectivity that presumably, arises from the relatively mild reaction conditions.

In a second catalysed step, the mono-allylated product **V-7** can then be treated with, e.g., allyl alcohol, to afford a mixed bis-allyl product such as **V-8**, in 60% yield. We have ring-closed<sup>[4]</sup> that compound with Grubb's first generation metathesis catalyst **V-9**, to give an asymmetric spirane derivative, **V-10** in 96% yield (see Scheme 5.2).



**Scheme 5.2.** Shows the double allylation of compound **V-7**, followed by a ring closing reaction to give the spirane product **V-10**.

### 5.3. Conclusions

Summarizing this brief chapter, because it readily accommodates allyl alcohols as substrate, the ruthenium(IV)-allyl catalyst **II-7** represents an efficient "green" alternative in that it does not waste the leaving group. Further, the reactions take place under mild conditions and no additives of any kind are required. The catalyst is

sufficiently fast such that the desired products are formed before the alcohol can react with acid to form di-allyl ether.

For substituted allyl alcohols, whereas palladium catalysts afford mixtures of mono- and di-allyl products, ruthenium catalyst **II-7** is capable of both regioselectivity and mono-allylation of the 1,3-diketone substrates reported. We know of no other catalyst that is both so selective and specific for the mono-allyl product.

One of these mono-allylated products is shown to undergo a second allylation with allyl alcohol, followed by a ring closing reaction to give a asymmetrical spirane product.

#### 5.4. References

- [1] I. W. J. Still, G. W. Kutney, *The Journal of Organic Chemistry* **1981**, *46*, 4911-4914.
- [2] A. W. Fort, *The Journal of Organic Chemistry* **1981**, *26*, 765-767.
- [3] J. Clayden, N. Greeves, S. Warren, P. Wothers, *Organic Chemistry*, Oxford University Press, **2001**.
- [4] B. C. Ranu, K. Chattopadhyay, L. Adak, *Organic Letters* **2007**, *9*, 4595-4598.
- [5] H. Kinoshita, H. Shinokubo, K. Oshima, *Organic Letters* **2004**, *6*, 4085-4088.
- [6] K.-H. Gan, C.-J. Jhong, S.-C. Yang, *Tetrahedron* **2008**, *64*, 1204-1212.
- [7] C. E. Schwartz, D. P. Curran, *Journal of the American Chemical Society* **2002**, *112*, 9272-9284.
- [8] Y. Kayaki, T. Koda, T. Ikariya, *The Journal of Organic Chemistry* **2004**, *69*, 2595-2597.
- [9] Y. Yamamoto, Y.-i. Nakagai, K. Itoh, *Chemistry - A European Journal* **2004**, *10*, 231-236.
- [10] S. Sigismondi, D. Sinou, *Journal of Molecular Catalysis A: Chemical* **1997**, *116*, 289-296.
- [11] H. Saburi, s. Tanaka, M. Kitamura, *Angew. Chem. Int. Ed. Engl.* **2005**, *44*, 1730.

**6.**

**Experimental**

## 6.1. General

### 6.1.1. Techniques and Chemicals

All air- or moisture-sensitive manipulations were carried out under a nitrogen atmosphere using standard *Schlenk* techniques. *Schlenks* were heated in an oven (150 °C) and then dried under vacuum. Anhydrous solvents, when needed, were dried over an appropriate drying agent and then distilled under nitrogen. Pentane, hexane, Et<sub>2</sub>O, THF, toluene were distilled over Na / benzophenone, CH<sub>2</sub>Cl<sub>2</sub> over CaH<sub>2</sub>, acetone over Drierite® and CH<sub>3</sub>CN over P<sub>2</sub>O<sub>5</sub> and stored under nitrogen. CD<sub>3</sub>CN, DMF-d<sub>7</sub>, CDCl<sub>3</sub> and CD<sub>3</sub>NO<sub>2</sub> were dried over molecular sieves and stored under nitrogen. Acetone-d<sub>6</sub> and CD<sub>2</sub>Cl<sub>2</sub> were distilled (bulb-to-bulb) over Drierite® and CaH<sub>2</sub>, respectively, and stored under nitrogen. For flash chromatography technical grade solvents were used.

### 6.1.2. Analytical Techniques and Instruments

**Flash Chromatography:** *Fluka Silica Gel* 60: particle size 40-63 µm.

**NMR spectra:** <sup>1</sup>H-, <sup>13</sup>C-, and 2D-NMR spectra were recorded with Bruker DPX-250, 300, 400, 500, and 700 MHz spectrometers at room temperature (if not indicated differently). Chemical shifts (δ) are given in ppm and referenced to TMS as an external standard for <sup>1</sup>H- and <sup>13</sup>C-NMR spectra. To specify the signal multiplicity, the following abbreviations are used: s = singlet, d = doublet, t = triplet and m = multiplet.<sup>[1]</sup> Coupling constants *J* are given in Hertz (Hz). The <sup>1</sup>H-NOESY experiments were acquired using a standard three-pulse sequence and a mixing time of 600 ms. Diffusion measurements were made on 2 mmol/L solutions.

**Melting points (m.p.):** Were measured on a *Büchi-510* melting point apparatus. The temperatures are given in degree Celsius (°C) and are uncorrected.

**High resolution mass-spectra (MS):** High resolution EI- and MALDI-MS were measured by the MS-service of the Laboratory of Organic Chemistry (ETH Zürich).

**Elemental analyses (EA):** were performed by the Laboratory of Microelemental Analysis (ETH Zürich).

**Crystallography:** Data sets were obtained using a *Bruker SMART* Platform Diffractometer equipped with a CCD Detector (graphite monochromated Mo-Kα radiation, λ = 0.71073 Å) at low-temperature (usually -40 °C). The program SMART served for data collection and the integration was performed with the software



SAINT.<sup>[2]</sup> The structures were solved by Patterson and direct methods,<sup>[3]</sup> using the program WinGX.<sup>[4]</sup> All atoms except hydrogen atoms and atoms of disordered molecules were refined anisotropically. H-atoms were placed at calculated positions based on stereochemical considerations and refined according to the riding model. In the end an absorption correction was performed with the program SADABS.<sup>[5]</sup> The crystallographic data, R-values of the full-matrix least-squares refinements<sup>[3]</sup> and interatomic distances and angles are given in Tables in sub-Chapter 7.2.

**Computational Details.** The computational calculations were carried out by *Prof. Luis F. Veiros* from Portugal. The calculations were performed using the GAUSSIAN 03 software package,<sup>[6]</sup> and the PBE1PBE functional, without symmetry constraints.

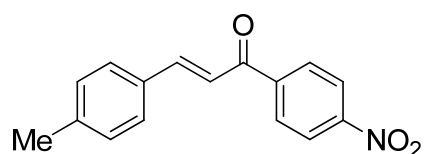
### 6.1.3. Synthesis of Substrates

Commercially available starting materials were purchased from commercial sources and used as received. (1*E*,4*E*)-1,5-Diphenylpenta-1,4-dien-3-ol,<sup>[7]</sup> 1,4-pentadien-3-yl-acetate,<sup>[8]</sup> 5-bromo-penta-1,3-diene,<sup>[9]</sup> PhCH(OCO<sub>2</sub><sup>t</sup>Bu)CHCH<sub>2</sub>,<sup>[10]</sup> (*E*)-1,2-Epoxy-4-phenylbut-3-ene<sup>[11]</sup> and allyl sulfonate ethers<sup>[12]</sup> were synthesized according to known literature procedures.

#### Synthesis of 1,3-di-aryl allyl ketone compounds.

The 1,3-di-aryl allyl ketones were synthesized according to a literature procedure for (*E*)-1-(4-nitrophenyl)-3-*p*-tolylprop-2-en-1-one.<sup>[13]</sup> These compounds were identified by their <sup>1</sup>H-NMR spectra.

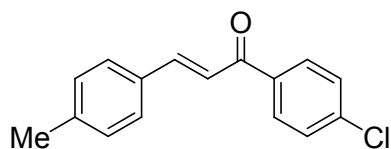
#### (*E*)-1-(*p*-nitrophenyl)-3-*p*-tolylprop-2-en-1-one.



NaOH (1.53 g, 38.5 mmol) was added to a suspension of *p*-nitroacetophenone (5.00 g, 30.3 mmol) in EtOH (20 mL) and H<sub>2</sub>O (16 mL). The resulting brown suspension was cooled in an ice-bath and then *p*-methylbenzaldehyde (3.5 mL, 30.3 mmol) was added over a period of 5 min. The reaction mixture was stirred at rt for 16 h, after which time a yellow solid has precipitated. The product was filtered off and recrystallized from EtOH / Et<sub>2</sub>O and then dried under vacuum to yield a yellow solid (6.04 g, 75%).

**<sup>1</sup>H-NMR** (300 MHz, CDCl<sub>3</sub>): δ: 8.39-8.35 (m, 2H), 8.18-8.14 (m, 2H), 7.85 (d, 1H, *J* = 16 Hz), 7.60-7.57 (m, 2H), 7.46 (d, 1H, *J* = 16 Hz), 7.29-7.26 (m, 2H), 2.44 (s, 3H).

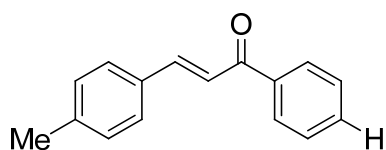
**(*E*)-1-(*p*-chlorophenyl)-3-*p*-tolylprop-2-en-1-one.**



NaOH (1.95 g, 48.9 mmol) was added to a suspension of *p*-chloroacetophenone (5.00 ml, 38.5 mmol) in EtOH (15 mL) and H<sub>2</sub>O (10 mL). The resulting yellow suspension was cooled in an ice-bath and then *p*-methylbenzaldehyde (4.5 mL, 38.5 mmol) was added drop wise over a period of 5 min. The reaction mixture was stirred at rt for 16 h, after which time a white solid has precipitated. The product was filtered off and then dried under vacuum to yield a white solid (9.04 g, 92%).

**<sup>1</sup>H-NMR** (300 MHz, CDCl<sub>3</sub>): δ: 8.00-7.97 (m, 2H), 7.82 (d, 1H, *J* = 16 Hz), 7.58-7.44 (m, 5H), 7.27-7.24 (m, 2H), 2.42 (s, 3H).

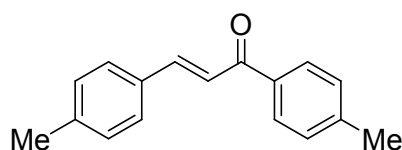
**(*E*)-1-phenyl-3-*p*-tolylprop-2-en-1-one.**



NaOH (4.20 g, 105.0 mmol) was added to a suspension of acetophenone (10.7 ml, 83.2 mmol) in EtOH (19 mL) and H<sub>2</sub>O (38 mL). The resulting yellow suspension was cooled in an ice-bath and then *p*-methylbenzaldehyde (10.8 mL, 83.2 mmol) was added drop wise over a period of 5 min. The reaction mixture was stirred at rt for 16 h, after which time a yellow solid has precipitated. The product was filtered off and then dried under vacuum to yield a yellow solid (18.20 g, 98%).

**<sup>1</sup>H-NMR** (300 MHz, CDCl<sub>3</sub>): δ: 8.05-8.02 (m, 2H), 7.82 (d, 1H, *J* = 16 Hz), 7.60-7.49 (m, 6H), 7.26-7.24 (m, 2H), 2.42 (s, 3H).

**(*E*)-1,3-di-*p*-tolylprop-2-en-1-one.**

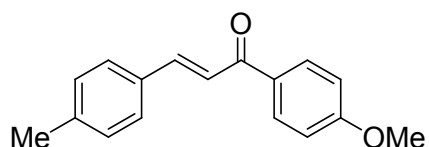


NaOH (1.90 g, 47.5 mmol) was added to a suspension of *p*-methylacetophenone (5.00 ml, 37.4 mmol) in EtOH (15 mL) and H<sub>2</sub>O (10 mL). The resulting yellow suspension was cooled in an ice-bath and then *p*-methylbenzaldehyde (4.4 mL, 37.4 mmol) was added drop wise over a period of 5 min. The reaction mixture was stirred

at rt for 16 h, after which time a white solid has precipitated. The product was filtered off and then dried under vacuum to yield a white solid (8.20 g, 91%).

<sup>1</sup>H-NMR (300 MHz, CDCl<sub>3</sub>): δ: 7.97-7.94 (m, 2H), 7.81 (d, 1H, *J* = 16 Hz), 7.58-7.49 (m, 3H), 7.33-7.33 (m, 4H), 2.46 (s, 3H), 2.42 (s, 3H).

### (*E*)-1-(*p*-methoxyphenyl)-3-*p*-tolylprop-2-en-1-one.



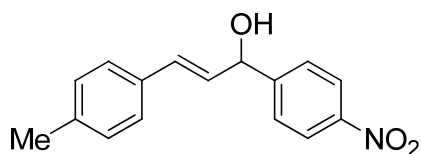
NaOH (1.35 g, 33.8 mmol) was added to a suspension of *p*-acetylanisol (4.00 g, 26.6 mmol) in EtOH (14 mL) and H<sub>2</sub>O (12 mL). The resulting yellow suspension was cooled in an ice-bath and then *p*-methylbenzaldehyde (10.8 mL, 83.2 mmol) was added drop wise over a period of 5 min. The reaction mixture was stirred at rt for 16 h, after which time a yellow solid has precipitated. The product was filtered off and then dried under vacuum to yield a yellow solid (5.87 g, 88%).

<sup>1</sup>H-NMR (300 MHz, CDCl<sub>3</sub>): δ: 8.08-8.04 (m, 2H), 7.81(d, 1H, *J* = 16 Hz), 7.58-7.50 (m, 3H), 7.28-7.23 (m, 2H), 7.02-6.99 (m, 2H), 3.91 (s, 3H), 2.42 (s, 3H).

### Synthesis of 1,3-di-aryl allyl alcohol compounds.

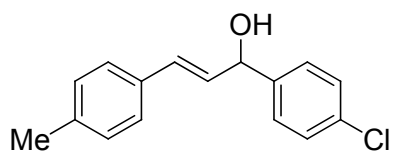
The 1,3-di-aryl allyl alcohols were synthesized according to a literature procedure for (*E*)-1-(4-nitrophenyl)-3-*p*-tolylprop-2-en-1-ol.<sup>[13]</sup> These compounds were identified by their <sup>1</sup>H-NMR spectra.

### (*E*)-1-(*p*-nitrophenyl)-3-*p*-tolylprop-2-en-1-ol (III-7a).



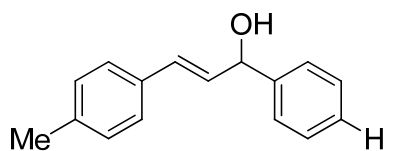
NaBH<sub>4</sub> (0.42 g, 11.2 mmol) was added in small portions to a stirred suspension of (*E*)-1-(*p*-nitrophenyl)-3-*p*-tolylprop-2-en-1-one (3.00 g, 11.2 mmol) in MeOH (18 mL). The mixture was stirred and gently heated until a clear solution resulted. This was diluted with a saturated aqueous sodium chloride solution (60 mL) and extracted with Et<sub>2</sub>O (3 x 30 mL). The extract was washed with H<sub>2</sub>O (3 x 30 mL), dried over Na<sub>2</sub>SO<sub>4</sub> and the solvent evaporated under vacuum. The product was recrystallized from pentane / Et<sub>2</sub>O and dried under vacuum to yield an orange solid (1.52 g, 50%).

<sup>1</sup>H-NMR (300 MHz, CDCl<sub>3</sub>): δ: 8.25-8.22 (m, 2H), 7.64-7.62 (m, 2H), 7.31-7.29 (m, 2H), 7.17-7.14 (m, 2H), 6.71 (d, 1H, *J* = 16 Hz), 6.26 (dd, 1H, *J*<sub>1</sub> = 16 Hz, *J*<sub>2</sub> = 7 Hz), 5.49 (dd, 1H, *J*<sub>1</sub> = 7 Hz, *J*<sub>2</sub> = 3 Hz), 2.36 (s, 3H), 2.22 (d, 1H, *J* = 3 Hz).

**(E)-1-(*p*-chlorophenyl)-3-*p*-tolylprop-2-en-1-ol (III-7b).**

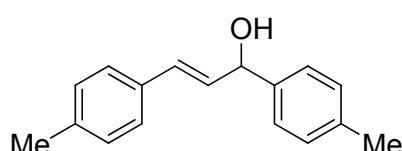
NaBH<sub>4</sub> (0.59 g, 15.6 mmol) was added in small portions to a stirred suspension of (*E*)-1-(*p*-chlorophenyl)-3-*p*-tolylprop-2-en-1-one (4.00 g, 15.6 mmol) in MeOH (30 mL). The mixture was stirred and gently heated until a clear solution resulted. This was diluted with a saturated aqueous sodium chloride solution (80 mL) and extracted with Et<sub>2</sub>O (3 x 30 mL). The extract was washed with H<sub>2</sub>O (3 x 30 mL), dried over Na<sub>2</sub>SO<sub>4</sub> and the solvent evaporated under vacuum. The product was dried under vacuum to yield a white solid (3.63 g, 90%).

<sup>1</sup>H-NMR (300 MHz, CDCl<sub>3</sub>): δ: 7.38-7.28 (m, 6H), 7.16-7.13 (m, 2H), 6.66 (d, 1H, *J* = 16 Hz), 6.30 (dd, 1H, *J*<sub>1</sub> = 16 Hz, *J*<sub>2</sub> = 7 Hz), 5.40-5.34 (m, 1H), 2.36 (s, 3H), 2.13-2.05 (m, 1H).

**(E)-1-phenyl-3-*p*-tolylprop-2-en-1-ol (III-7c).**

NaBH<sub>4</sub> (0.68 g, 18.0 mmol) was added in small portions to a stirred suspension of (*E*)-1-phenyl-3-*p*-tolylprop-2-en-1-one (4.00 g, 18.0 mmol) in MeOH (30 mL). The mixture was stirred and gently heated until a clear solution resulted. This was diluted with a saturated aqueous sodium chloride solution (80 mL) and extracted with Et<sub>2</sub>O (3 x 30 mL). The extract was washed with H<sub>2</sub>O (3 x 30 mL), dried over Na<sub>2</sub>SO<sub>4</sub> and the solvent evaporated under vacuum. The product was recrystallized from pentane / Et<sub>2</sub>O and dried under vacuum to yield a white solid (1.81 g, 45%).

<sup>1</sup>H-NMR (300 MHz, CDCl<sub>3</sub>): δ: 7.39-7.28 (m, 6H), 7.15-7.11 (m, 2H), 6.68 (d, 1H, *J* = 16 Hz), 6.36 (dd, 1H, *J*<sub>1</sub> = 16 Hz, *J*<sub>2</sub> = 7 Hz), 5.40 (dd, 1H, *J*<sub>1</sub> = 7 Hz, *J*<sub>2</sub> = 4 Hz), 2.35 (s, 3H), 2.01 (d, 1H, *J* = 4 Hz).

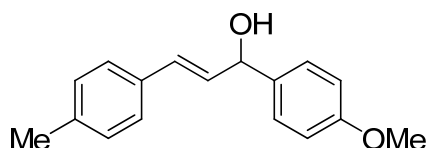
**(E)-1,3-di-*p*-tolylprop-2-en-1-ol (III-7d).**

NaBH<sub>4</sub> (0.32 g, 8.46 mmol) was added in small portions to a stirred suspension of (*E*)-1,3-di-*p*-tolylprop-2-en-1-one (2.00 g, 8.46 mmol) in MeOH (15 mL). The mixture was stirred and gently heated until a clear solution resulted. This was diluted with a saturated aqueous sodium chloride solution (40 mL) and extracted with Et<sub>2</sub>O (3 x 30 mL). The extract was washed with H<sub>2</sub>O (3 x 30 mL), dried over Na<sub>2</sub>SO<sub>4</sub> and the solvent evaporated under vacuum. The product was separated by

column chromatography on silica gel (hexane/EtOAc = 6:1) and dried under vacuum to yield a white solid (1.41 g, 70%).

<sup>1</sup>H-NMR (300 MHz, CDCl<sub>3</sub>): δ: 7.36-7.12 (m, 2H), 6.67 (d, 1H, *J* = 16 Hz), 6.35 (dd, 1H, *J*<sub>1</sub> = 16 Hz, *J*<sub>2</sub> = 6 Hz), 5.37-5.35 (m, 1H), 2.37 (s, 3H), 2.35 (s, 3H), 1.95 (d, 1H, *J* = 4 Hz).

**(*E*)-1-(*p*-methoxyphenyl)-3-*p*-tolylprop-2-en-1-ol.**



NaBH<sub>4</sub> (0.45 g, 11.9 mmol) was added in small portions to a stirred suspension of (*E*)-1-(*p*-methoxyphenyl)-3-*p*-tolylprop-2-en-1-one (3.00 g, 11.9 mmol) in MeOH (18 mL). The mixture was

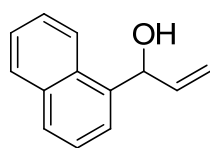
stirred and gently heated until a clear solution resulted. This was diluted with a saturated aqueous sodium chloride solution (60 mL) and extracted with Et<sub>2</sub>O (3 x 30 mL). The extract was washed with H<sub>2</sub>O (3 x 30 mL), dried over Na<sub>2</sub>SO<sub>4</sub> and the solvent evaporated under vacuum. The product was dried under vacuum to yield a viscous oil (2.86 g, 94 %).

<sup>1</sup>H-NMR (300 MHz, CDCl<sub>3</sub>): δ: 7.39-7.28 (m, 4H), 7.19-7.11 (m, 2H), 6.95-6.90 (m, 2H), 6.66 (d, 1H, *J* = 16 Hz), 6.35 (dd, 1H, *J*<sub>1</sub> = 16 Hz, *J*<sub>2</sub> = 7 Hz), 5.37-5.34 (m, 1H), 3.83 (s, 3H), 2.36 (s, 3H), 2.03-2.02 (m, 1H).

**Synthesis of ArCH(OH)CH=CH<sub>2</sub> (Ar = 1-naphtyl, 2-naphtyl, *o*-MeC<sub>6</sub>H<sub>4</sub>, *o*-ClC<sub>6</sub>H<sub>4</sub>, *o*-MeOC<sub>6</sub>H<sub>4</sub>, *p*-ClC<sub>6</sub>H<sub>4</sub>, *p*-MeOC<sub>6</sub>H<sub>4</sub>, 1-<sup>t</sup>Bu, 1-mesityl, 1-thiophenyl and 1-furyl).**

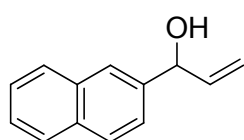
The substituted aryl allyl alcohols used in the allylation reaction were synthesized according to a modified literature procedure.<sup>[14]</sup> The modification consisted of performing the addition of vinylmagnesium bromide (1M in THF, 1.2 equivalents) at -78 °C within 15 min with subsequent stirring at r.t. for 15 min. The alcohols were isolated by distillation under vacuum. These compounds were identified by their <sup>1</sup>H-NMR spectra.

**1-(Naphthalen-1-yl)prop-2-en-1-ol.**

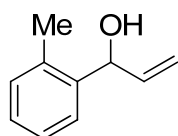


43% yield, viscous oil; b.p. 85 °C (10<sup>-1</sup> mbar);

<sup>1</sup>H-NMR (300 MHz, CDCl<sub>3</sub>): δ: 8.22 (d, 1H, *J* = 2 Hz), 7.92-7.82 (m, 2H), 7.66-7.47 (m, 4H), 6.33-6.22 (m, 1H), 6.22 (s, 1H), 5.48 (d, 1H, *J* = 16 Hz), 5.31 (d, 1H, *J* = 12 Hz), 2.16 (d, 1H, *J* = 4 Hz).

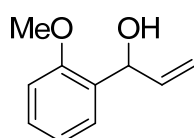
**1-(Naphthalen-2-yl)prop-2-en-1-ol.**52% yield, viscous oil; b.p. 90 °C (10<sup>-1</sup> mbar);

<sup>1</sup>H-NMR (300 MHz, CDCl<sub>3</sub>): δ: 7.86-7.85 (m, 4H), 7.52-7.47 (m, 3H), 6.21-6.10 (m, 1H), 5.47-5.41 (m, 2H), 5.27 (d, 1H, *J* = 10 Hz), 2.10 (d, 1H, *J* = 4 Hz).

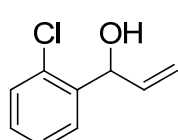
**1-*o*-Tolylprop-2-en-1-ol (IV-20).**

67% yield, viscous oil; b.p. 105 °C (20 mbar);

<sup>1</sup>H-NMR (250 MHz, CDCl<sub>3</sub>): δ: 7.24 (d, 1H, *J* = 9 Hz), 7.32-7.16 (m, 3H), 6.14-6.00 (m, 1H), 5.45-5.21 (m, 3H), 2.39 (s, 3H), 1.93 (d, 1H, *J* = 4 Hz).

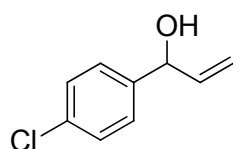
**1-(*o*-Methoxyphenyl)prop-2-en-1-ol (IV-21).**66% yield, viscous oil; b.p. 55 °C (10<sup>-1</sup> mbar);

<sup>1</sup>H-NMR (300 MHz, CDCl<sub>3</sub>): δ: 7.31-7.26 (m, 2H), 7.01-6.91 (m, 2H), 6.21-6.10 (m, 1H), 5.44 (t, 1H, *J* = 6 Hz), 5.33 (d, 1H, *J* = 17 Hz), 5.19 (d, 1H, *J* = 13 Hz), 3.88 (s, 3H), 2.83 (d, 1H, *J* = 4 Hz).

**1-(*o*-Chlorophenyl)prop-2-en-1-ol (IV-22).**

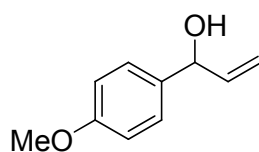
63 % yield, viscous oil; b.p. 110 °C (20 mbar);

<sup>1</sup>H-NMR (300 MHz, CDCl<sub>3</sub>): δ: 7.56 (d, 1H, *J* = 8 Hz), 7.38-7.22 (m, 3H), 6.12-6.01 (m, 1H), 5.67 (t, 1H, *J* = 5 Hz), 5.41 (d, 1H, *J* = 16 Hz), 5.25 (d, 1H, *J* = 10 Hz), 2.18 (d, 1H, *J* = 4 Hz).

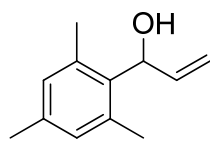
**1-(*p*-Chlorophenyl)prop-2-en-1-ol.**

59% yield, viscous oil; b.p. 115 °C (20 mbar);

<sup>1</sup>H-NMR (300 MHz, CDCl<sub>3</sub>): δ: 7.33 (s, 4H), 6.07-5.96 (m, 1H), 5.36 (d, 1H, *J* = 16 Hz), 5.24-5.19 (m, 2H), 2.19 (d, 1H, *J* = 4 Hz).

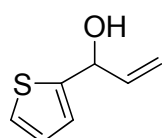
**1-(*p*-Methoxyphenyl)prop-2-en-1-ol.**60% yield, viscous oil; b.p. 60 °C (10<sup>-1</sup> mbar);

<sup>1</sup>H-NMR (300 MHz, CDCl<sub>3</sub>): δ: 7.31 (d, 2H, *J* = 8 Hz), 6.91 (d, 1H, *J* = 9 Hz), 6.12-6.01 (m, 1H), 5.35 (d, 1H, *J* = 16 Hz), 5.23-5.18 (m, 2H), 3.82 (s, 3H), 2.03 (d, 1H, *J* = 4 Hz).

**1-Mesitylprop-2-en-1-ol.**

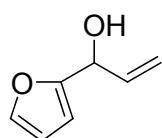
53% yield, viscous oil; b.p. 125 °C (20 mbar);

<sup>1</sup>H-NMR (300 MHz, CDCl<sub>3</sub>): δ: 6.86 (s, 2H), 6.25-6.12 (m, 1H), 5.73 (s, 1H), 5.28-5.16 (m, 2H), 2.41 (s, 6H), 2.29 (s, 3H), 1.87 (d, 1H, *J* = 4 Hz).

**1-(Thiophen-2-yl)prop-2-en-1-ol.**

column chromatography on silica gel (pentane/Et<sub>2</sub>O = 7:3) 65% yield, viscous oil;

<sup>1</sup>H-NMR (300 MHz, CDCl<sub>3</sub>): δ: 7.31-7.28 (m, 1H), 7.02-6.99 (m, 2H), 6.21-6.10 (m, 1H), 5.47-5.41 (m, 2H), 5.28 (d, 1H, *J* = 10 Hz), 2.14 (d, 1H, *J* = 4 Hz).

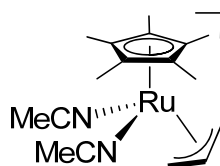
**1-(Furan-2-yl)prop-2-en-1-ol.**

67% yield, viscous oil; b.p. 70 °C (20 mbar);

<sup>1</sup>H-NMR (250 MHz, CDCl<sub>3</sub>): δ: 7.43 (s, 1H), 6.37 (d, 1H, *J* = 3 Hz), 6.28 (d, 1H, *J* = 3 Hz), 6.29-6.09 (m, 1H), 5.45 (d, 1H, *J* = 16 Hz), 5.32 (d, 1H, *J* = 10 Hz), 5.25 (t, 1H, *J* = 6 Hz), 2.18 (d, 1H, *J* = 4 Hz).

## 6.2. Chapter 2: Synthesis and Characterisation of new Ruthenium-Cp\* Complexes

[Ru(Cp\*)(MeCN)<sub>3</sub>](PF<sub>6</sub>)<sub>2</sub>,<sup>[15]</sup> [RuCp\*(η<sup>3</sup>-PhCHCHCH<sub>2</sub>)(MeCN)<sub>2</sub>](PF<sub>6</sub>)<sub>2</sub>,<sup>[16]</sup> [RuCp\*(η<sup>3</sup>-Phenylallyl)(DMF)<sub>2</sub>](PF<sub>6</sub>)<sub>2</sub><sup>[16]</sup> and [Ru(η<sup>3</sup>-C<sub>3</sub>H<sub>5</sub>)Cl<sub>2</sub>(Cp\*)]<sup>[17]</sup> were synthesized according to known literature procedures.

**Synthesis of [Ru(η<sup>3</sup>-C<sub>3</sub>H<sub>5</sub>)(Cp\*)(MeCN)<sub>2</sub>](PF<sub>6</sub>)<sub>2</sub> (II-6).**

Toluene (110 mL) was added to an MeCN solution (110 mL) of [Ru(η<sup>3</sup>-C<sub>3</sub>H<sub>5</sub>)Cl<sub>2</sub>(Cp\*)] (0.565 g, 1.62 mmol) and AgPF<sub>6</sub> (1.640 g, 6.49 mmol). The reaction mixture was stirred at room temperature for 20 h, after which time the solution was

evaporated under vacuum. The resulting residue was dissolved in acetone (5 mL) and filtered through Celite. After evaporation of the solvent the resulting solid was washed with acetone (2 x 5 mL). The filtrate was evaporated under vacuum, and the residue washed with water (3 x 5 mL) to remove the remaining AgPF<sub>6</sub>. After the

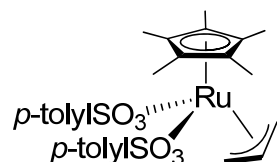
mixture was dried under vacuum, the crude product was again dissolved in acetone (5 mL), filtered through Celite, evaporated and dried under vacuum to afford a brown solid (0.990 g, 94%).

**$^1\text{H-NMR}$**  (400 MHz, acetone- $d_6$ ):  $\delta$ : 5.98 (tt, 1H,  $J_1 = 11$  Hz,  $J_2 = 6$  Hz, C- $H_{\text{central}}$ ), 4.80 (d, 2H,  $J = 6$  Hz, C- $H_{\text{syn}}$ ), 3.33 (d, 2H,  $J = 11$  Hz, C- $H_{\text{anti}}$ ), 2.72 (s, 6H, MeCN), 2.02 (s, 15H,  $\text{C}_5\text{Me}_5$ ). See also Table N1.

**$^{13}\text{C-NMR}$**  (100 MHz, acetone- $d_6$ ):  $\delta$ : 135.2 (MeCN), 111.7 ( $\text{C}_5\text{Me}_5$ ), 101.4 ( $\text{C}_{\text{central}}$ ), 73.6 ( $\text{C}_{\text{terminal}}$ ), 10.5 ( $\text{C}_5\text{Me}_5$ ), 5.3 (MeCN). See also Table N1.

**Elemental analysis (%)**: calcd. for  $\text{C}_{17}\text{H}_{26}\text{F}_{12}\text{N}_2\text{P}_2\text{Ru}$ : C 31.44, H 4.04, N 4.31; found: C 31.61, H 3.95, N 4.12.

**$[\text{Ru}(\eta^3\text{-C}_3\text{H}_5)(\text{Cp}^*)(p\text{-MeC}_6\text{H}_4\text{SO}_3)_2]$  (II-7).**



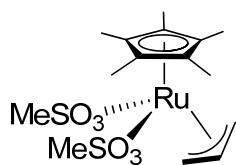
Toluene (16 mL) was added to an  $\text{CH}_3\text{CN}$  solution (16 mL) of  $[\text{Ru}(\eta^3\text{-C}_3\text{H}_5)\text{Cl}_2(\text{Cp}^*)]$  (0.084 g, 0.24 mmol) and  $p\text{-MeC}_6\text{H}_4\text{SO}_3\text{Ag}$  (0.134 g, 0.48 mmol). The reaction mixture was stirred at room temperature for 17 h after which time the solution was evaporated under vacuum. The resulting residue was dissolved in  $\text{CH}_2\text{Cl}_2$  (3 mL) and filtered. After evaporation of the solvent, the resulting solid was washed with cold (0 °C) THF (3 x 1 mL) and dried under vacuum to afford an orange solid (0.103 g, 69%). An acetone solution of this solid was then layered with  $\text{Et}_2\text{O}$  and stored at -6 °C, to afford crystals of **II-7** suitable for X-ray diffraction.

**$^1\text{H-NMR}$**  (400 MHz,  $\text{CD}_2\text{Cl}_2$ ):  $\delta$ : 7.56 (d, 4H,  $J = 8$  Hz, C- $H_{\text{tosyl}}$ ), 7.13 (d, 4H,  $J = 8$  Hz, C- $H_{\text{tosyl}}$ ), 6.22 (tt, 1H,  $J_1 = 10$  Hz,  $J_2 = 6$  Hz, C- $H_{\text{central}}$ ), 5.30 (d, 2H,  $J = 6$  Hz, C- $H_{\text{syn}}$ ), 2.83 (d, 2H,  $J = 10$  Hz, C- $H_{\text{anti}}$ ), 2.39 (s, 6H, Me), 1.66 (s, 15H,  $\text{C}_5\text{Me}_5$ ). See also Table N2.

**$^{13}\text{C-NMR}$**  (100 MHz,  $\text{CD}_2\text{Cl}_2$ ):  $\delta$ : 142.5 ( $\text{C}_{\text{tosyl}}$ ), 140.9 ( $\text{C}_{\text{tosyl}}$ ), 128.9 ( $\text{C}_{\text{tosyl}}$ ), 125.9 ( $\text{C}_{\text{tosyl}}$ ), 108.8 ( $\text{C}_5\text{Me}_5$ ), 100.1 ( $\text{C}_{\text{central}}$ ), 66.7 ( $\text{C}_{\text{terminal}}$ ), 21.1 (Me), 9.8 ( $\text{C}_5\text{Me}_5$ ). See also Table N2.

**Elemental analysis (%)**: calcd. for  $\text{C}_{27}\text{H}_{34}\text{O}_6\text{RuS}_2$ : C, 52.33; H, 5.53. Found: C, 52.05; H, 5.52.



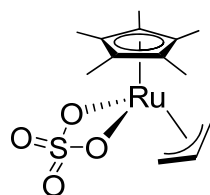
**[Ru( $\eta^3$ -C<sub>3</sub>H<sub>5</sub>)(Cp\*)(MeSO<sub>3</sub>)<sub>2</sub>] (II-8).**

Toluene (19 mL) was added to an CH<sub>3</sub>CN solution (19 mL) of [Ru( $\eta^3$ -C<sub>3</sub>H<sub>5</sub>)Cl<sub>2</sub>(Cp\*)] (0.100 g, 0.29 mmol) and MeSO<sub>3</sub>Ag (0.117 g, 0.58 mmol). The reaction mixture was stirred at room temperature for 14 h after which time the solution was evaporated under vacuum. The resulting residue was dissolved in CH<sub>2</sub>Cl<sub>2</sub> (3 mL) and filtered. After evaporation of the solvent the resulting solid was washed with cold (0 °C) THF (2 x 1 mL) and dried under vacuum to afford an orange solid (0.093 g, 69%).

<sup>1</sup>H-NMR (300 MHz, CD<sub>2</sub>Cl<sub>2</sub>):  $\delta$ : 6.43 (tt, 1H,  $J_1 = 10$  Hz,  $J_2 = 6$  Hz, C- $H_{central}$ ), 5.05 (d, 2H,  $J = 6$  Hz, C- $H_{syn}$ ), 2.86 (d, 2H,  $J = 10$  Hz, C- $H_{anti}$ ), 2.73 (s, 6H, Me), 1.64 (s, 15H, C<sub>5</sub>Me<sub>5</sub>). See also Table N3.

<sup>13</sup>C-NMR (75 MHz, CD<sub>2</sub>Cl<sub>2</sub>):  $\delta$ : 108.6 (C<sub>5</sub>Me<sub>5</sub>), 100.0 (C<sub>central</sub>), 67.7 (C<sub>terminal</sub>), 41.6 (Me), 9.5 (C<sub>5</sub>Me<sub>5</sub>). See also Table N3.

**Elemental analysis (%)**: calcd. for C<sub>15</sub>H<sub>26</sub>O<sub>6</sub>RuS<sub>2</sub>: C, 38.53; H, 5.60. Found: C, 39.33; H, 5.63.

**Synthesis of [Ru( $\eta^3$ -C<sub>3</sub>H<sub>5</sub>)(Cp\*)( $\kappa^2$ -SO<sub>4</sub>)] (II-9).**

Ag<sub>2</sub>SO<sub>4</sub> (0.488 g, 1.29 mmol) was added to an CH<sub>3</sub>CN solution (30 mL) of [Ru( $\eta^3$ -C<sub>3</sub>H<sub>5</sub>)Cl<sub>2</sub>(Cp\*)] (0.15 g, 0.43 mmol). The reaction mixture was stirred at room temperature for 18 h, after which time the solution was evaporated under vacuum. The resulting residue was dissolved in CH<sub>2</sub>Cl<sub>2</sub> and filtered through Celite. The filtrate was evaporated and the residue was dried under vacuum. This sequence was repeated twice to yield a light brown solid (0.143 g, 89%). A CH<sub>2</sub>Cl<sub>2</sub> solution of this solid was then layered with Et<sub>2</sub>O and stored at -6 °C, to afford crystals of **II-9** suitable for X-ray diffraction.

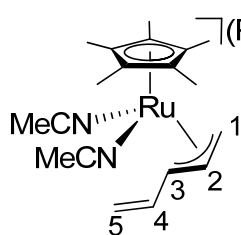
<sup>1</sup>H-NMR (500 MHz, CD<sub>2</sub>Cl<sub>2</sub>):  $\delta$ : 5.23 (tt, 1H,  $J_1 = 11$  Hz,  $J_2 = 7$  Hz, C- $H_{central}$ ), 4.03 (d, 2H,  $J = 7$  Hz, C- $H_{syn}$ ), 2.63 (d, 2H,  $J = 11$  Hz, C- $H_{anti}$ ), 1.65 (s, 15H, C<sub>5</sub>Me<sub>5</sub>). See also Table N4.

<sup>13</sup>C-NMR (125 MHz, CD<sub>2</sub>Cl<sub>2</sub>):  $\delta$ : 107.3 (C<sub>5</sub>Me<sub>5</sub>), 101.5 (C<sub>central</sub>), 65.6 (C<sub>terminal</sub>), 9.3 (C<sub>5</sub>Me<sub>5</sub>). See also Table N4.

**Elemental analysis (%)**: calcd. for C<sub>13</sub>H<sub>20</sub>O<sub>4</sub>SRu: C 41.81, H 5.40; found: C 41.33, H 5.36.

**HR MALDI-MS**: calcd for [MH<sup>+</sup>] 375.0198, found 375.0198.

**[Ru( $\eta^3$ -CH<sub>2</sub>CHCHCH=CH<sub>2</sub>)(Cp\*)(MeCN)<sub>2</sub>](PF<sub>6</sub>)(BF<sub>4</sub>) (II-15).**



1,4-Pentadien-3-ol (0.010 g, 0.119 mmol) and HBF<sub>4</sub>·Et<sub>2</sub>O (0.016 g, 0.099 mmol) was added to a solution of [Ru(Cp\*)(MeCN)<sub>3</sub>](PF<sub>6</sub>) (0.050 g, 0.099 mmol) in CH<sub>3</sub>CN (6 mL) containing 4Å MS. The resulting red suspension was stirred at room temperature for 30 min, after which time the suspension was filtered, and then slowly concentrated under vacuum. The crude red solid was washed with Et<sub>2</sub>O (2 x 2 mL) and dried under vacuum to afford the mixture (0.050 g, 82%, 2:1 ratio of the Cp\*-signals) as an orange solid. The major product was identified as **II-15**.

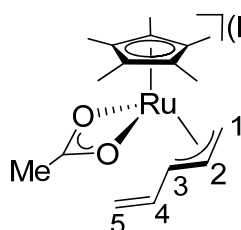
**<sup>1</sup>H-NMR** (500 MHz, CD<sub>3</sub>CN): δ: 6.39 (dt, 1H, *J*<sub>1</sub> = 17 Hz, *J*<sub>2</sub> = 10 Hz, C-4-*H*), 6.04 (d, 1H, *J* = 10 Hz, C-5-*H*<sub>cis</sub>), 5.99 (d, 1H, *J* = 17 Hz C-5-*H*<sub>trans</sub>), 5.86 (dt, 1H, *J*<sub>1</sub> = 11 Hz, *J*<sub>2</sub> = 7 Hz, C-2-*H*), 4.54 (d, 1H, *J* = 7 Hz, C-1-*H*<sub>syn</sub>), 4.29 (t, 1H, *J* = 11 Hz, C-3-*H*), 2.94 (d, 1H, *J* = 11 Hz, C-1-*H*<sub>anti</sub>), 1.75 (s, 15H, C<sub>5</sub>Me<sub>5</sub>), MeCN not detectable because of the exchange with CD<sub>3</sub>CN. See also Table N5.

**<sup>13</sup>C-NMR** (125 MHz, CD<sub>3</sub>CN): δ: 135.7 (C-4), 129.1 (C-5), 108.9 (C<sub>5</sub>Me<sub>5</sub>), 98.6 (C-3), 97.0 (C-2), 67.4 (C-1), 9.1 (C<sub>5</sub>Me<sub>5</sub>). See also Table N5.

The second component (not completely characterized) was shown by detailed NMR studies to contain an  $\eta^5$ -C<sub>5</sub>H<sub>7</sub>-fragment with 7 protons in the ratio 2:2:2:1 and is reasonably an "U" shaped fragment.

**<sup>1</sup>H-NMR** (500 MHz, CD<sub>3</sub>CN): δ: 4.90 (m, 2H, C-2-*H*), 4.40 (t, 1H, *J* = 12, C-3-*H*), 4.03 (d, 2H, *J* = 7 Hz C-1-*H*<sub>syn</sub>), 3.13 (d, 2H, *J* = 16 Hz, C-1-*H*<sub>anti</sub>), 1.71 (s, 30H, C<sub>5</sub>Me<sub>5</sub>), MeCN not detectable because of the exchange with CD<sub>3</sub>CN. **<sup>13</sup>C-NMR** (125 MHz, CD<sub>3</sub>CN): δ: 129.0 (C-3), 99.8 (C<sub>5</sub>Me<sub>5</sub>), 61.5 (C-1), 9.2 (C<sub>5</sub>Me<sub>5</sub>), C-2 not detectable.

**Synthesis of [Ru( $\kappa^2$ -O<sub>2</sub>CMe)( $\eta^3$ -CH<sub>2</sub>CHCHCH=CH<sub>2</sub>)(Cp\*)]PF<sub>6</sub> (II-17).**



1,4-Pentadien-3-yl acetate (28.8 μL, 0.228 mmol) was added to a solution of [Ru(Cp\*)(MeCN)<sub>3</sub>](PF<sub>6</sub>) (0.100 g, 0.198mmol) in CH<sub>2</sub>Cl<sub>2</sub> (8 mL). The resulting reddish solution was stirred at room temperature for 30 min. The solution volume was reduced under vacuum, and hexane was added, precipitating a brown-yellow powder. The solid was washed with hexane (2 x 3 mL) and dried under vacuum to yield a yellow solid (0.105 g, 98 %). A dichloromethane solution of

this solid was then layered with diethyl ether and stored at  $-32\text{ }^{\circ}\text{C}$ , to afford crystals of **II-17** suitable for X-ray diffraction.

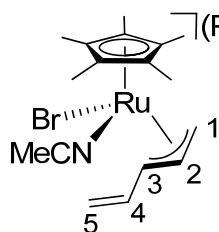
$^1\text{H-NMR}$  (400 MHz,  $\text{CD}_2\text{Cl}_2$ ):  $\delta$ : 6.08 (dt, 1H,  $J_1 = 17\text{ Hz}$ ,  $J_2 = 10\text{ Hz}$ , C-4-*H*), 5.75 (d, 1H,  $J = 10\text{ Hz}$ , C-5-*H*<sub>cis</sub>), 5.71 (d, 1H,  $J = 17\text{ Hz}$ , C-5-*H*<sub>trans</sub>), 5.47 (dt, 1H,  $J_1 = 10\text{ Hz}$ ,  $J_2 = 6\text{ Hz}$ , C-2-*H*), 4.46 (d, 1H,  $J = 6\text{ Hz}$ , C-1-*H*<sub>syn</sub>), 4.05 (t, 1H,  $J = 10\text{ Hz}$ , C-3-*H*), 3.01 (d, 1H,  $J = 10\text{ Hz}$ , C-1-*H*<sub>anti</sub>), 1.92 (s, 3H,  $\kappa^2\text{-O}_2\text{CMe}$ ), 1.55 (s, 15H,  $\text{C}_5\text{Me}_5$ ). See also Table N6.

$^{13}\text{C-NMR}$  (100 MHz,  $\text{CD}_2\text{Cl}_2$ ):  $\delta$ : 194.5 ( $\kappa^2\text{-O}_2\text{CMe}$ ), 135.6 (C-4), 124.1 (C-5), 107.1 ( $\text{C}_5\text{Me}_5$ ), 103.6 (C-2), 88.5 (C-3), 66.7 (C-1), 25.6 ( $\kappa^2\text{-O}_2\text{CMe}$ ), 9.0 ( $\text{C}_5\text{Me}_5$ ). See also Table N6.

**Elemental analysis (%)**: calcd for  $\text{C}_{17}\text{H}_{25}\text{O}_2\text{F}_6\text{PRu}$ : C 40.24, H 4.97; found: C 40.19, H 5.09.

**HR MALDI-MS**: calcd. for  $[\text{C}_{17}\text{H}_{25}\text{O}_2\text{Ru}^+]$  363.0893, found 363.0893 ( $[(\text{M-PF}_6)^+]$ ).

#### Synthesis of $[\text{Ru}(\eta^3\text{-CH}_2\text{CHCHCH}=\text{CH}_2)\text{Br}(\text{Cp}^*)(\text{MeCN})]\text{PF}_6$ (**II-18**).

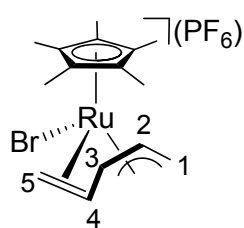


5-Bromopenta-1,3-diene (0.0525 g, 0.357 mmol) was added to a solution of  $[\text{Ru}(\text{Cp}^*)(\text{MeCN})_3](\text{PF}_6)$  (0.150 g, 0.297 mmol) in  $\text{CH}_2\text{Cl}_2$  (8 mL). The resulting red-brown solution was stirred at room temperature for 30 min, after which time the solution was filtered, and then slowly concentrated under vacuum. The brown crude solid was washed with hexane (2 x 3 mL) and dissolved in  $\text{CH}_2\text{Cl}_2$  (9 mL). Addition of hexane (4.5 mL) afforded a yellow precipitate, which was collected by filtration. The filtrate was evaporated and the remaining brown solid was dissolved in  $\text{CH}_2\text{Cl}_2$  and layered with  $\text{Et}_2\text{O}$  at  $-32\text{ }^{\circ}\text{C}$  to afford crystals of **II-18** suitable for X-ray diffraction.

$^1\text{H-NMR}$  (300 MHz,  $\text{CD}_3\text{NO}_2$ ):  $\delta$ : 6.27 (dt, 1H,  $J_1 = 17\text{ Hz}$ ,  $J_2 = 10\text{ Hz}$ , C-4-*H*), 5.79 (d, 1H,  $J = 17\text{ Hz}$ , C-5-*H*<sub>trans</sub>), 5.82 (d, 1H,  $J = 10\text{ Hz}$ , C-5-*H*<sub>cis</sub>), 5.43 (dt, 1H,  $J_1 = 10\text{ Hz}$ ,  $J_2 = 6\text{ Hz}$ , C-2-*H*), 4.54 (d, 1H,  $J = 6\text{ Hz}$ , C-5-*H*<sub>syn</sub>), 3.82 (t, 1H,  $J = 10\text{ Hz}$ , C-3-*H*), 2.56-2.54 (m, 4H,  $\text{MeCN}$  and C-1-*H*<sub>anti</sub>), 1.73 (s, 15H,  $\text{C}_5\text{Me}_5$ ). See also Table N7.

$^{13}\text{C-NMR}$  (75 MHz,  $\text{CD}_3\text{NO}_2$ ):  $\delta$ : 136.2 (C-4), 124.3 (C-5), 106.1 ( $\text{C}_5\text{Me}_5$ ), 95.8 (C-2), 87.4 (C-3), 65.8 (C-1), 8.3 ( $\text{C}_5\text{Me}_5$ ), 3.1 ( $\text{MeCN}$ ),  $\text{C}_{\text{nitrile}}$  not detectable. If one redissolves the crystals of **II-18**, a mixture of **II-18** and **II-22** is obtained. See also Table N7.

### Synthesis of $[\text{Ru}(\eta^5\text{-S-CH}_2\text{CHCHCH=CH}_2)\text{Br}(\text{Cp}^*)]\text{PF}_6$ (**II-22**).



5-Bromopenta-1,3-diene (0.0525 g, 0.357 mmol) was added to a solution of  $[\text{Ru}(\text{Cp}^*)(\text{MeCN})_3](\text{PF}_6)$  (0.150 g, 0.297 mmol) in  $\text{CH}_2\text{Cl}_2$  (8 mL). The resulting red-brown solution was stirred at room temperature for 30 min, after which time the solution was filtered, and then slowly concentrated under vacuum. The brown

crude solid was washed with hexane (2 x 3 mL) and dissolved in  $\text{CH}_2\text{Cl}_2$  (9 mL). Addition of hexane (4.5 mL) afforded a yellow precipitate, which was collected by filtration and dried under vacuum to yield a yellow solid (0.113 g, 72%). A  $\text{CH}_2\text{Cl}_2$  solution of this solid was then layered with hexane and stored at  $-6^\circ\text{C}$ , to afford crystals of **II-22** suitable for X-ray diffraction.

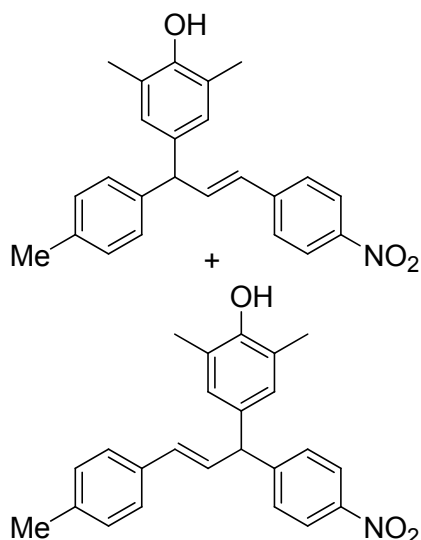
**$^1\text{H-NMR}$**  (700 MHz,  $\text{CD}_3\text{NO}_2$ , 243 K):  $\delta$ : 5.39 (ddd, 1H,  $J_1 = 12$  Hz,  $J_2 = 8$  Hz,  $J_3 = 6$  Hz, C-2-*H*), 4.90 (t, 1H,  $J = 7$  Hz, C-3-*H*), 4.43 (d, 1H,  $J = 7$  Hz, C-5-*H*<sub>cis</sub>), 4.26 (dd, 1H,  $J_1 = 7$  Hz,  $J_2 = 3$  Hz, C-1-*H*<sub>syn</sub>), 4.13 (d, 1H,  $J = 12$  Hz, C-5-*H*<sub>trans</sub>), 4.07 (dd, 1H,  $J_1 = 12$  Hz,  $J_2 = 3$  Hz, C-1-*H*<sub>anti</sub>), 3.86 (dt, 1H,  $J_1 = 12$  Hz,  $J_2 = 7$  Hz, C-4-*H*), 1.98 (s, 15H,  $\text{C}_5\text{Me}_5$ ). See also Table N8.

**$^{13}\text{C-NMR}$**  (176 MHz,  $\text{CD}_3\text{NO}_2$ , 243 K):  $\delta$ : 109.4 ( $\text{C}_5\text{Me}_5$ ), 107.4 (C-2), 100.6 (C-4), 90.9 (C-3), 78.0 (C-5), 68.6 (C-1), 9.3 ( $\text{C}_5\text{Me}_5$ ). See also Table N8.

**Elemental analysis (%)**: calcd. for  $\text{C}_{15}\text{H}_{22}\text{BrF}_6\text{PRu}$ : C 34.10, H 4.20, Br 15.13; found: C 34.41, H 4.29, Br 15.01.

### 6.3. Chapter 3: Allylation of Phenol Derivatives

#### Mixture of (*E*)-2,6-dimethyl-4-(3-(*p*-nitrophenyl)-1-*p*-tolylallyl)phenol and (*E*)-2,6-dimethyl-4-(1-(*p*-nitrophenyl)-3-*p*-tolylallyl)phenol (III-8a).



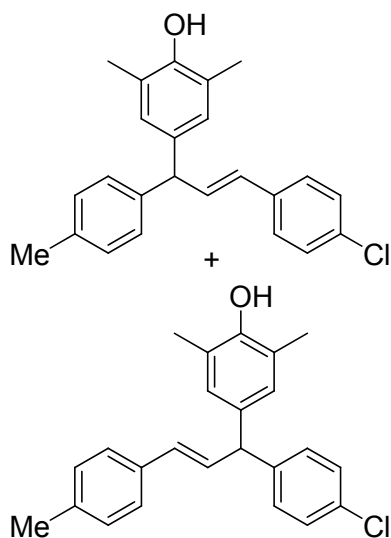
2,6-Dimethylphenol (32.5 mg, 0.266 mmol) was added to an acetonitrile solution (2 mL) of (*E*)-1-(*p*-nitrophenyl)-3-*p*-tolylprop-2-en-1-ol (71.6 mg, 0.266 mmol) and [Ru( $\eta^3$ -PhCHCHCH<sub>2</sub>)Cp\*(DMF)<sub>2</sub>](PF<sub>6</sub>)<sub>2</sub>, (**I-39**) (6.4 mg, 0.008 mmol). The resulting brown suspension was stirred at 80 °C for 16 h. Filtration through silica gel and subsequent washing of the silica gel with EtOAc removed the ruthenium-catalyst. The mixed solvent was then evaporated to afford the crude product as a yellow powder. This material was washed with hexane and dried under vacuum to afford a yellow solid as a mixture of isomers (148 mg, 72%).

<sup>1</sup>H-NMR and <sup>13</sup>C-NMR see Table N9.

**Elemental analysis (%)**: calcd. for C<sub>24</sub>H<sub>23</sub>NO<sub>3</sub>: C, 77.19; H, 6.21; N, 3.75. Found: C, 76.52; H, 6.18; N, 3.83.

**HR EI-MS**: calcd. for [C<sub>24</sub>H<sub>23</sub>NO<sub>3</sub><sup>+</sup>] 373.1673, found 373.1672.

#### Mixture of (*E*)-4-(3-(*p*-chlorophenyl)-1-*p*-tolylallyl)-2,6-dimethylphenol and (*E*)-4-(1-(*p*-chlorophenyl)-3-*p*-tolylallyl)-2,6-dimethylphenol (III-8b).



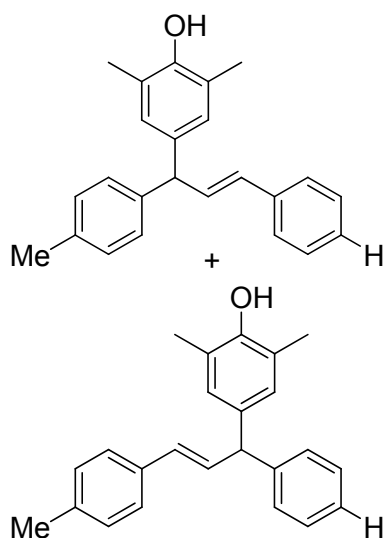
2,6-Dimethylphenol (43.3 mg, 0.355 mmol) was added to an acetonitrile solution (4 mL) of (*E*)-1-(*p*-chlorophenyl)-3-*p*-tolylprop-2-en-1-ol (91.8 mg, 0.355 mmol) and [Ru( $\eta^3$ -PhCHCHCH<sub>2</sub>)Cp\*(DMF)<sub>2</sub>](PF<sub>6</sub>)<sub>2</sub>, (**I-39**) (8.0 mg, 0.010 mmol). The resulting brown suspension was stirred at 80 °C for 16 h. Filtration through silica gel and subsequent washing of the silica gel with EtOAc removed the ruthenium-catalyst. The mixed solvent was then evaporated to afford the crude product as a yellow oil. This material was separated by

column chromatography on silica gel. (Hexane / Et<sub>2</sub>O = 10:1). The product was dried under vacuum to afford an orange solid as a mixture of isomers (101 mg, 81%).

<sup>1</sup>H-NMR and <sup>13</sup>C-NMR see Table N10.

HR EI-MS: calcd. for [C<sub>24</sub>H<sub>23</sub>ClO<sup>+</sup>] 362.1432, found 362.1432.

**Mixture of (*E*)-2,6-dimethyl-4-(3-phenyl-1-*p*-tolylallyl)phenol and (*E*)-2,6-dimethyl-4-(1-phenyl-3-*p*-tolylallyl)phenol (III-8c).**



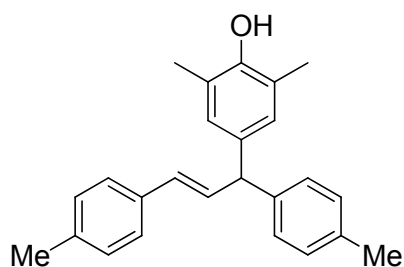
2,6-Dimethylphenol (48.7 mg, 0.399 mmol) was added to an acetonitrile solution (4 mL) of (*E*)-1-phenyl-3-*p*-tolylprop-2-en-1-ol (89.5 mg, 0.399 mmol) and [Ru( $\eta^3$ -PhCHCHCH<sub>2</sub>)Cp\*(DMF)<sub>2</sub>] (PF<sub>6</sub>)<sub>2</sub>, (**I-39**) (9.0 mg, 0.011 mmol). The resulting brown suspension was stirred at 80 °C for 16 h. Filtration through silica gel and subsequent washing of the silica gel with EtOAc removed the ruthenium-catalyst. The mixed solvent was then evaporated to afford the crude product as a yellow oil. This material was separated by column chromatography on silica gel (Hexane / Et<sub>2</sub>O = 10:1).

The product was dried under vacuum to afford a red solid as a mixture of isomers (94 mg, 72%).

<sup>1</sup>H-NMR and <sup>13</sup>C-NMR see Table N11.

HR EI-MS: calcd. for [C<sub>24</sub>H<sub>24</sub>O<sup>+</sup>] 328.1822, found 328.1823.

**(*E*)-4-(1,3-di-*p*-tolylallyl)-2,6-dimethylphenol (III-8d).**



2,6-Dimethylphenol (43.2 mg, 0.355 mmol) was added to an acetonitrile solution (4 mL) of (*E*)-1,3-di-*p*-tolylprop-2-en-1-ol (91.8 mg, 0.355 mmol) and [Ru( $\eta^3$ -PhCHCHCH<sub>2</sub>)Cp\*(DMF)<sub>2</sub>] (PF<sub>6</sub>)<sub>2</sub>, (**I-39**) (8.0 mg, 0.010 mmol). The resulting brown suspension was stirred at 80 °C for 16 h. Filtration through silica gel and subsequent washing of the silica gel with EtOAc removed the ruthenium-catalyst. The mixed solvent was then evaporated to afford the crude product as a yellow oil. This material was separated by column chromatography on silica gel (Hexane / Et<sub>2</sub>O = 10:1). The product was dried under vacuum to afford an orange solid (57 mg, 47%).

**<sup>1</sup>H-NMR** (500 MHz, CDCl<sub>3</sub>): δ: 7.32 (d, 2H, *J* = 8 Hz), 7.20-7.12 (m, 6H), 6.89 (s, 2H), 6.63 (dd, 1H, *J*<sub>1</sub> = 16 Hz, *J*<sub>2</sub> = 8 Hz), 6.34 (d, 1H, *J* = 16 Hz), 4.77 (d, 1H, *J* = 8 Hz), 4.56 (s, 1H), 2.38 (s, 3H), 2.37 (s, 3H), 2.26 (s, 6H). See also Table N12.

**<sup>13</sup>C-NMR** (75 MHz, CDCl<sub>3</sub>): δ: 151.1, 141.6, 137.3, 136.1, 135.9, 135.2, 132.7, 131.0, 129.6, 129.5, 129.1, 128.8, 126.4, 123.3, 53.3, 21.6, 21.4, 16.4. See also Table N12.

**HR EI-MS**: calcd. for [C<sub>25</sub>H<sub>26</sub>O<sup>+</sup>] 342.1978, found 342.1980.

#### 6.4. Chapter 4: Allylation of Indoles

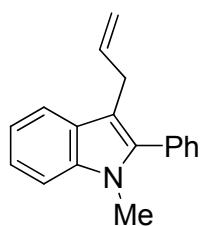
##### A typical procedure for NMR-monitored allylation of indoles or pyrroles.

Indole or pyrrole (0.07 mmol) was added to an CD<sub>3</sub>CN solution (0.5 mL) of allylic alcohol (0.07 mmol) and [Ru( $\eta^3$ -C<sub>3</sub>H<sub>5</sub>)(Cp\*)(MeCN)<sub>2</sub>](PF<sub>6</sub>)<sub>2</sub> (**I-28**) (0.0023 g, 0.035 mmol) in an oven-dried NMR tube, and the mixture was monitored at ambient temperature. As an alternative to [Ru( $\eta^3$ -C<sub>3</sub>H<sub>5</sub>)(Cp\*)(MeCN)<sub>2</sub>](PF<sub>6</sub>)<sub>2</sub> one can use [Ru(Cp\*)(MeCN)<sub>3</sub>]PF<sub>6</sub> (0.035 mmol) together with *p*-toluene-sulfonic or camphorsulfonic acid (0.035 mmol), respectively.

##### A typical preparative procedure for 3-allylation of indoles.

Indole (1 mmol) was added to an CH<sub>3</sub>CN solution (5 mL) of allylic alcohol (1 mmol) and [Ru( $\eta^3$ -C<sub>3</sub>H<sub>5</sub>)(Cp\*)(MeCN)<sub>2</sub>](PF<sub>6</sub>)<sub>2</sub> (**II-6**) (0.0325 g, 0.05 mmol). After stirring at room temperature the reaction mixture was evaporated at 40 °C under vacuum and separated by column chromatography on silica gel.

##### 3-Allyl-1-methyl-2-phenyl-1*H*-indole.<sup>[18]</sup>

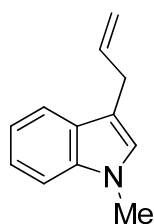


Et<sub>2</sub>O; 97% yield, viscous oil;

**<sup>1</sup>H-NMR** (500 MHz, CDCl<sub>3</sub>): δ: 7.66 (d, 1H, *J* = 8 Hz), 7.43-7.67 (m, 5H), 7.38 (d, 1H, *J* = 8 Hz), 7.29 (t, 1H, *J* = 8 Hz), 7.17 (t, 1H, *J* = 7 Hz), 6.03-6.08 (m, 1H), 5.01-5.10 (m, 2H), 3.65 (s, 3H), 3.48 (d, 2H, *J* = 6 Hz).

**<sup>13</sup>C-NMR** (125 MHz, CDCl<sub>3</sub>): δ: 138.3, 138.1, 137.5, 132.0, 130.7, 128.5, 128.1, 128.0, 121.9, 119.4, 119.3, 114.7, 110.8, 109.5, 31.0, 29.4.

**HR EI-MS**: calcd. for [C<sub>18</sub>H<sub>17</sub>N<sup>+</sup>] 247.1356, found 247.1355.

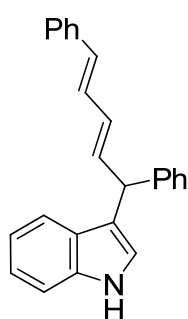
**3-Allyl-1-methyl-1*H*-indole.<sup>[19]</sup>**

Et<sub>2</sub>O; 93% yield, viscous oil;

**<sup>1</sup>H-NMR** (500 MHz, CDCl<sub>3</sub>): δ: 7.64 (d, 1H, *J* = 8 Hz), 7.36-7.24 (m, 2H), 7.15 (t, 1H, *J* = 7 Hz), 6.89 (s, 1H), 6.18-6.04 (m, 1H), 5.26-5.09 (m, 2H), 3.70 (s, 3H), 3.57 (d, 2H, *J* = 7 Hz).

**<sup>13</sup>C-NMR** (125 MHz, CDCl<sub>3</sub>): δ: 137.6, 137.5, 128.0, 126.5, 121.6, 119.2, 118.7, 115.0, 112.9, 109.2, 32.6, 29.8.

**HR EI-MS:** calcd. for [C<sub>12</sub>H<sub>13</sub>N<sup>+</sup>] 171.1043, found 171.1044.

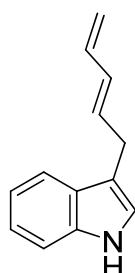
**3-((2*E*,4*E*)-1,5-diphenylpenta-2,4-dienyl)-1*H*-indole.**

Hexane / CH<sub>2</sub>Cl<sub>2</sub> = 1:1; 85% yield, very viscous oil;

**<sup>1</sup>H-NMR** (500 MHz, CDCl<sub>3</sub>): δ: 8.02 (br s, 1H), 7.49 (d, 1H, *J* = 8 Hz), 7.44-7.23 (m, 12H), 7.11 (t, 1H, *J* = 8 Hz), 6.93 (s, 1H), 6.92 (dd, 1H, *J*<sub>1</sub> = 14 Hz, *J*<sub>2</sub> = 12 Hz), 6.51 (d, 1H, *J* = 16 Hz), 6.41 (dd, 1H, *J*<sub>1</sub> = 16 Hz, *J*<sub>2</sub> = 7 Hz), 6.31 (dd, 1H, *J*<sub>1</sub> = 15 Hz, *J*<sub>2</sub> = 11 Hz), 5.13 (d, 1H, *J* = 8 Hz).

**<sup>13</sup>C-NMR** (125 MHz, CDCl<sub>3</sub>): δ: 143.7, 137.8, 137.3, 137.0, 131.7, 131.5, 129.3, 128.91, 128.86, 128.80, 128.76, 127.6, 126.7, 126.6, 122.9, 122.5, 120.2, 119.8, 199.0, 111.4, 46.4.

**HR EI-MS:** calcd. for [C<sub>25</sub>H<sub>21</sub>N<sup>+</sup>] 335.1669, found 335.1667.

**(*E*)-3-(penta-2,4-dienyl)-1*H*-indole.**

Pentane / CH<sub>2</sub>Cl<sub>2</sub> = 10:1; 45% yield, viscous oil;

**<sup>1</sup>H-NMR** (300 MHz, CDCl<sub>3</sub>): δ: 7.95 (br s, 1H), 7.61 (d, 1H, *J* = 8 Hz), 7.38 (d, 1H, *J* = 8 Hz), 7.22 (t, 1H, *J* = 7 Hz), 7.16 (t, 1H, *J* = 8 Hz), 7.01 (s, 1H), 6.47-6.34 (m, 1H), 6.28-6.20 (m, 1H), 6.05-5.95 (m, 1H), 5.13 (d, 1H, *J* = 17 Hz), 5.00 (d, 1H, *J* = 10 Hz), 3.59 (d, 2H, *J* = 7 Hz).

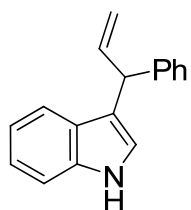
**<sup>13</sup>C-NMR** (75 MHz, CDCl<sub>3</sub>): δ: 137.1, 136.4, 133.5, 131.6, 127.4, 122.1, 121.7, 119.3, 119.1, 115.3, 114.5, 111.1, 28.5.

**HR EI-MS:** calcd. for [C<sub>13</sub>H<sub>13</sub>N<sup>+</sup>] 183.1043, found 183.1037.

**3-(1-Phenylallyl)-1*H*-indole and 3-cinnamyl-1*H*-indole.**

Pentane / CH<sub>2</sub>Cl<sub>2</sub>, gradient from 10:1 to 2:1; 64% and 26% yield, respectively.



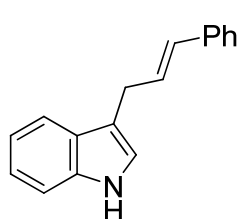
**3-(1-Phenylallyl)-1H-indole.**

Transparent oil;

**$^1\text{H-NMR}$**  (500 MHz,  $\text{CDCl}_3$ ):  $\delta$ : 7.86 (br s, 1H), 7.56 (d, 1H,  $J = 8$  Hz), 7.44-7.34 (m, 6H), 7.31 (t, 1H,  $J = 8$  Hz), 7.18 (t, 1H,  $J = 8$  Hz), 6.91 (s, 1H), 6.50 (m, 1H), 5.35 (d, 1H,  $J = 10$  Hz), 5.23 (d, 1H,  $J = 18$  Hz), 5.11 (d, 1H,  $J = 7$  Hz).

**$^{13}\text{C-NMR}$**  (125 MHz,  $\text{CDCl}_3$ ):  $\delta$ : 143.5, 140.8, 136.9, 128.73, 128.65, 127.1, 126.6, 122.8, 122.3, 120.1, 119.6, 118.7, 115.8, 111.4, 47.3.

**HR EI-MS**: calcd. for  $[\text{C}_{17}\text{H}_{15}\text{N}^{+}]$  233.1199, found 233.1191.

**3-Cinnamyl-1H-indole.**<sup>[20]</sup>

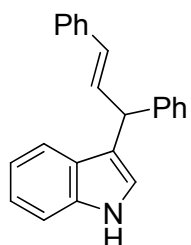
White solid;

**$^1\text{H-NMR}$**  (300 MHz,  $\text{CDCl}_3$ ):  $\delta$ : 7.98 (br s, 1H), 7.68 (d, 1H,  $J = 8$  Hz), 7.41-7.13 (m, 8H), 7.06 (s, 1H), 6.61-6.50 (m, 2H), 3.72 (d, 2H,  $J = 6$  Hz).

**$^{13}\text{C-NMR}$**  (75 MHz,  $\text{CDCl}_3$ ):  $\delta$ : 29.1, 111.2, 114.8, 119.3, 119.5,

121.9, 122.2, 126.3, 127.1, 127.6, 128.6, 129.4, 130.6, 136.6, 137.9.

**HR EI-MS**: calcd. for  $[\text{C}_{17}\text{H}_{15}\text{N}^{+}]$  233.1199, found 233.1196.

**(E)-3-(1,3-diphenylallyl)-1H-indole.**<sup>[21]</sup> $\text{CH}_2\text{Cl}_2$ ; 91% yield, white solid;

**$^1\text{H-NMR}$**  (300 MHz,  $\text{CDCl}_3$ ):  $\delta$ : 7.98 (br s, 1H), 7.48 (d, 1H,  $J = 8$  Hz), 7.42-7.19 (m, 12H), 7.07 (t, 1H,  $J = 8$  Hz), 6.94 (s, 1H), 6.78 (dd, 1H,  $J_1 = 16$  Hz,  $J_2 = 7$  Hz), 6.49 (d, 1H,  $J = 16$  Hz), 5.17 (d, 1H,  $J = 8$  Hz).

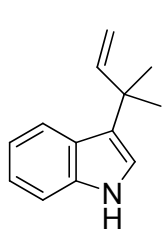
**$^{13}\text{C-NMR}$**  (75 MHz,  $\text{CDCl}_3$ ):  $\delta$ : 143.7, 137.9, 137.0, 132.9, 130.9,

128.83, 128.82, 128.76, 127.5, 127.2, 126.72, 126.67, 122.9, 122.4, 120.2, 119.8, 119.1, 111.4, 46.5.

**Mixture of 3-(1,1-dimethyl-allyl)-1H-indole and 3-(3-methyl-but-2-enyl)-1H-indole.**

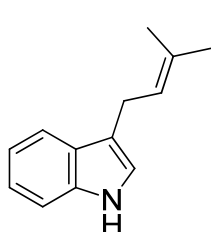
Pentane /  $\text{CH}_2\text{Cl}_2$ , gradient from 10:1 to 2:1; 75% yield, mixture ratio 13:1, viscous oil.

**HR EI-MS**: calcd. for  $[\text{C}_{13}\text{H}_{15}\text{N}^{+}]$  185.1204, found 185.1202.

**3-(1,1-Dimethyl-allyl)-1H-indole.**<sup>[22]</sup>

<sup>1</sup>H-NMR (400 MHz, CDCl<sub>3</sub>): δ: 7.85 (br s, 1H), 7.76 (d, 1H, *J* = 8 Hz), 7.34 (d, 1H, *J* = 8 Hz), 7.19 (t, 1H, *J* = 8 Hz), 7.10 (t, 1H, *J* = 8 Hz), 6.96 (s, 1H), 6.17 (dd, 1H, *J*<sub>1</sub> = 17 Hz, *J*<sub>2</sub> = 10 Hz), 5.11 (d, 1H, *J* = 17 Hz), 5.06 (d, 1H, *J* = 10 Hz), 1.55 (s, 6H).

<sup>13</sup>C-NMR (100 MHz, CDCl<sub>3</sub>): δ: <sup>13</sup>C NMR: δ: 147.9, 137.2, 126.1, 124.0, 121.7, 121.5, 120.2, 119.0, 111.3, 110.8, 37.6, 28.2.

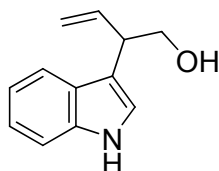
**3-(3-Methyl-but-2-enyl)-1H-indole.**<sup>[22]</sup>

<sup>1</sup>H-NMR (400 MHz, CDCl<sub>3</sub>): δ: 7.56 (d, 1H, *J* = 9 Hz), 6.89 (s, 1H), 5.43 (t, 1H, *J* = 8 Hz), 3.47 (d, 2H, *J* = 7 Hz), 1.79 (s, 6H).

<sup>13</sup>C-NMR: couldn't identify, because of overlap.

**2-(1H-Indol-3-yl)-but-3-en-1-ol and (E)-4-(1H-indol-3-yl)-but-2-en-1-ol.**

Hexane / EtOAc, gradient from 10:1 to 2:1; 34% and 16% yield, respectively.

**2-(1H-Indol-3-yl)-but-3-en-1-ol.**

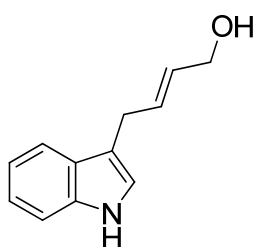
Viscous oil;

<sup>1</sup>H-NMR (400 MHz, CDCl<sub>3</sub>): δ: 8.28 (br s, 1H), 7.70 (d, 1H, *J* = 8 Hz), 7.37 (d, 1H, *J* = 8 Hz), 7.26 (t, 1H, *J* = 8 Hz), 7.18 (t, 1H, *J* = 8 Hz), 7.02 (s, 1H), 6.18-6.10 (m, 1H), 5.31 (d, 1H, *J* = 17 Hz), 5.27

(d, 1H, *J* = 10 Hz), 4.04-3.87 (m, 3H), 2.02 (br s, 1H).

<sup>13</sup>C-NMR (100 MHz, CDCl<sub>3</sub>): δ: 138.3, 136.6, 126.7, 122.3, 121.9, 119.5, 119.4, 116.7, 114.7, 111.5, 65.3, 44.1.

HR EI-MS: calcd. for [C<sub>12</sub>H<sub>13</sub>NO<sup>+</sup>] 187.0992, found 187.0992.

**(E)-4-(1H-Indol-3-yl)-but-2-en-1-ol.**

Viscous oil;

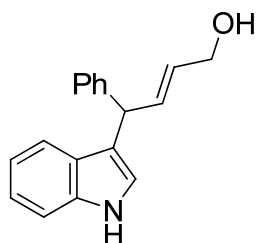
<sup>1</sup>H-NMR (400 MHz, CDCl<sub>3</sub>): δ: 8.02 (br s, 1H), 7.62 (d, 1H, *J* = 8 Hz), 7.38 (d, 1H, *J* = 8 Hz), 7.22 (t, 1H, *J* = 8 Hz), 7.14 (t, 1H, *J* = 8 Hz), 7.00 (s, 1H), 6.00-5.94 (m, 1H), 5.84-5.78 (m, 1H), 4.15 (d, 1H, *J* = 6 Hz), 3.55 (d, 1H, *J* = 6 Hz), 1.63 (br s, 1H).

<sup>13</sup>C-NMR (100 MHz, CDCl<sub>3</sub>): δ: 136.4, 131.6, 129.7, 127.3, 122.0, 121.6, 119.3, 119.0, 114.4, 111.1, 63.6, 28.2.

HR EI-MS: calcd. for [C<sub>12</sub>H<sub>13</sub>NO<sup>+</sup>] 187.0992, found 187.0991.

**(E)-4-(1H-Indol-3-yl)-4-phenylbut-2-en-1-ol and (E)-2-(1H-indol-3-yl)-4-phenylbut-3-en-1-ol.**

Hexane / EtOAc, gradient from 10:1 to 2:1; 44 and 24% yield, respectively.

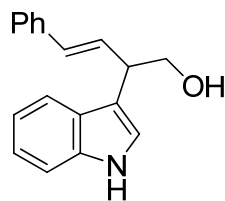
**(E)-4-(1H-Indol-3-yl)-4-phenylbut-2-en-1-ol.**

Viscous oil;

**<sup>1</sup>H-NMR** (300 MHz, CDCl<sub>3</sub>): δ: 8.03 (br s, 1H), 7.42-7.17 (m, 8H), 7.05 (t, 1H, *J* = 8 Hz), 6.91 (s, 1H), 5.73 (dt, 1H, *J*<sub>1</sub> = 15 Hz, *J*<sub>2</sub> = 6 Hz), 6.26 (dd, 1H, *J*<sub>1</sub> = 15 Hz, *J*<sub>2</sub> = 8 Hz), 5.00 (d, 1H, *J* = 8 Hz), 4.20 (d, 2H, *J* = 6 Hz), 1.40 (br s, 1H).

**<sup>13</sup>C-NMR** (75 MHz, CDCl<sub>3</sub>): δ: 143.2, 136.7, 134.4, 130.0, 128.4, 128.3, 126.7, 126.4, 122.4, 122.1, 119.7, 119.4, 118.5, 111.1, 63.5, 45.6.

**HR EI-MS:** calcd. for [C<sub>12</sub>H<sub>13</sub>NO<sup>+</sup>] 263.1305, found 263.1303.

**(E)-2-(1H-Indol-3-yl)-4-phenylbut-3-en-1-ol.**

Viscous oil;

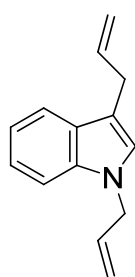
**<sup>1</sup>H-NMR** (300 MHz, CDCl<sub>3</sub>): δ: 8.12 (br s, 1H), 7.71 (d, 1H, *J* = 8 Hz), 7.43-7.12 (m, 9H), 6.64 (d, 1H, *J* = 16 Hz), 6.53 (dd, 1H, *J*<sub>1</sub> = 16 Hz, *J*<sub>2</sub> = 6 Hz), 4.01-3.99 (m, 3H), 1.70 (br s, 1H).

**<sup>13</sup>C-NMR** (75 MHz, CDCl<sub>3</sub>): δ: 137.5, 136.7, 131.8, 129.8, 128.5, 127.4, 126.6, 126.3, 122.4, 121.8, 119.6, 119.4, 114.9, 111.4, 65.7, 65.7.

**HR EI-MS:** calcd. for [C<sub>12</sub>H<sub>13</sub>NO<sup>+</sup>] 263.1305, found 263.1305.

**A typical preparative procedure for 1,3-diallylation of indoles.**

Indole (0.35 mmol) was added to an acetonitrile solution (2.5 mL) of allyl alcohol (1.4 mmol) and [Ru( $\eta^3$ -C<sub>3</sub>H<sub>5</sub>)(Cp\*)(MeCN)<sub>2</sub>](PF<sub>6</sub>)<sub>2</sub>, (**II-6**) (0.0114 g, 0.018 mmol). The reaction mixture was stirred for 16 h at room temperature and then the solvent was evaporated at 40 °C under vacuum and the products were separated by column chromatography on silica gel.

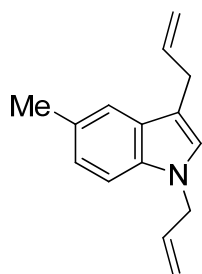
**1,3-Diallyl-1*H*-indole.**<sup>[23]</sup>

Pentane / CH<sub>2</sub>Cl<sub>2</sub> = 5:1; 76% yield transparent oil;

<sup>1</sup>H-NMR (400 MHz, CDCl<sub>3</sub>): δ: 7.69 (d, 1H, *J* = 8 Hz), 7.37 (d, 1H, *J* = 8 Hz), 7.29 (t, 1H, *J* = 8 Hz), 7.19 (t, 1H, *J* = 8 Hz), 6.96 (s, 1H), 6.22-6.12 (m, 1H), 6.11-6.01 (m, 1H), 5.28-5.15 (m, 4H), 4.74 (m, 2H), 3.61 (d, 2H, *J* = 6 Hz).

<sup>13</sup>C-NMR (100 MHz, CDCl<sub>3</sub>): δ: 137.7, 136.9, 134.0, 128.4, 125.8, 121.9, 119.6, 119.2, 117.4, 115.4, 113.7, 109.8, 49.0, 30.1.

HR EI-MS: calcd. for [C<sub>14</sub>H<sub>15</sub>N<sup>+</sup>] 197.1199, found 197.1199.

**1,3-Diallyl-5-methyl-1*H*-indole.**

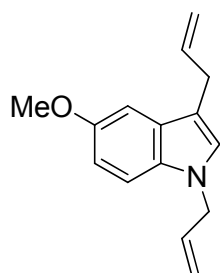
CH<sub>2</sub>Cl<sub>2</sub>; 86% yield, yellowish oil;

<sup>1</sup>H-NMR (300 MHz, CDCl<sub>3</sub>): δ: 7.39 (s, 1H), 7.20 (d, 1H, *J* = 8 Hz), 7.05 (d, 1H, *J* = 8 Hz), 6.87 (s, 1H), 6.16-5.93 (m, 2H), 5.21-5.07 (m, 4H), 4.67 (d, 2H, *J* = 5 Hz), 3.51 (d, 2H, *J* = 6 Hz), 2.48 (s, 3H).

<sup>13</sup>C-NMR (75 MHz, CDCl<sub>3</sub>): δ: 137.9, 135.4, 134.1, 128.6, 128.4,

125.9, 123.5, 119.2, 117.3, 115.3, 113.1, 109.6, 49.0, 30.1, 21.8.

HR EI-MS: calcd. for [C<sub>15</sub>H<sub>17</sub>N<sup>+</sup>] 211.1356, found 211.1356.

**1,3-Diallyl-5-methoxy-1*H*-indole.**

CH<sub>2</sub>Cl<sub>2</sub>; 79% yield transparent liquid;

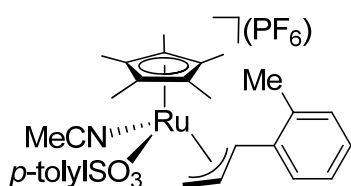
<sup>1</sup>H-NMR (300 MHz, CDCl<sub>3</sub>): δ: 7.24 (d, 1H, *J* = 9 Hz), 7.10 (s, 1H), 6.94 (d, 1H, *J* = 8 Hz), 6.92 (s, 1H), 6.20-5.96 (m, 2H), 5.26-5.12 (m, 4H), 4.68 (d, 2H, *J* = 5 Hz), 3.92 (s, 3H), 3.55 (d, 2H, *J* = 6 Hz).

<sup>13</sup>C-NMR (75 MHz, CDCl<sub>3</sub>): δ: 154.0, 137.7, 134.1, 132.3, 128.6,

126.4, 117.3, 115.3, 113.0, 112.0, 110.6, 101.5, 56.2, 49.1, 30.1.

HR EI-MS: calcd. for [C<sub>15</sub>H<sub>17</sub>NO<sup>+</sup>] 227.1305, found 227.1305.

**Attempt to synthesize [Ru(η<sup>3</sup>-*o*-MeC<sub>6</sub>H<sub>4</sub>CHCHCH<sub>2</sub>)(Cp\*)(*p*-MeC<sub>6</sub>H<sub>4</sub>-SO<sub>3</sub>)(MeCN)] PF<sub>6</sub>.**



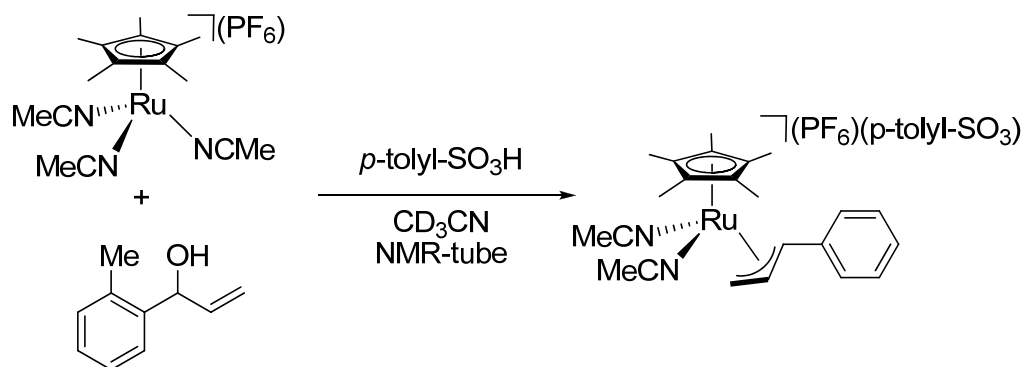
1-(*o*-Tolyl)prop-2-en-1-ol (17.6 mg, 0.119 mmol) was added to an CH<sub>3</sub>CN solution (2.5 mL) of [Ru(Cp\*)(CH<sub>3</sub>CN)<sub>3</sub>]PF<sub>6</sub> (60 mg, 0.119 mmol) and *p*-

toluenesulfonic acid monohydrate (22.6 mg, 0.119 mmol). The resulting orange solution was stirred at room temperature for 30 min, after which time the solution was concentrated under vacuum. The resulting crude material was washed two times with Et<sub>2</sub>O and then dried to afford 87 mg of an orange solid. This solid is not completely soluble in CD<sub>2</sub>Cl<sub>2</sub> and we estimate that 60-65% of the material is [Ru( $\eta^3$ -o-MeC<sub>6</sub>H<sub>4</sub>CHCHCH<sub>2</sub>)(Cp\*)(*p*-MeC<sub>6</sub>H<sub>4</sub>-SO<sub>3</sub>)(MeCN)]<sup>+</sup>.

**<sup>1</sup>H-NMR** (700 MHz, CD<sub>2</sub>Cl<sub>2</sub>):  $\delta$ : 7.90 (d, 1H, *J* = 8 Hz, C-*H*<sub>arom.</sub>), 7.62 (1H, overlap), 7.60 (d, 2H, *J* = 8 Hz, C-*H*<sub>tosyl.</sub>), 7.39 (t, 1H, *J* = 8 Hz C-*H*<sub>arom.</sub>), 7.35 (d, 1H, *J* = 6 Hz, C-*H*<sub>arom.</sub>), 7.29 (d, 2H, *J* = 8 Hz, C-*H*<sub>tosyl.</sub>), 6.81 (ddd, 1H, *J*<sub>1</sub> = 12 Hz, *J*<sub>2</sub> = 11 Hz, *J*<sub>3</sub> = 7 Hz, C-*H*<sub>central</sub>), 5.34 (d, 1H, *J* = 12 Hz, Ph-C-*H*<sub>anti</sub>), 4.46 (d, 1H, *J* = 7 Hz, C<sub>terminal</sub>-*H*<sub>syn</sub>), 3.25 (d, 1H, *J* = 11 Hz, C<sub>terminal</sub>-*H*<sub>anti</sub>), 2.42 (s, 3H, Me<sub>tosyl.</sub>), 2.35 (s, 3H, Me), 2.28 (s, 3H, MeCN), 1.70 (s, 15H, C<sub>5</sub>Me<sub>5</sub>). See also Table N13.

**<sup>13</sup>C-NMR** (176 MHz, CD<sub>2</sub>Cl<sub>2</sub>):  $\delta$ : 141.7 (C<sub>tosyl.</sub>), 141.3 (C<sub>tosyl.</sub>), 139.8 (C<sub>arom.</sub>), 139.7 (C<sub>arom.</sub>), 133.4 (MeCN), 132.7 (C<sub>arom.</sub>), 131.7 (C<sub>arom.</sub>), 129.6 (C<sub>arom.</sub>), 129.2 (C<sub>tosyl.</sub>), 126.7 (C<sub>arom.</sub>), 125.6 (C<sub>tosyl.</sub>), 106.4 (C<sub>5</sub>Me<sub>5</sub>), 101.9 (Ph-C), 97.2 (C<sub>central</sub>), 67.9 (C<sub>terminal</sub>), 21.4 (Me<sub>tosyl.</sub>), 20.3 (Me), 9.8 (C<sub>5</sub>Me<sub>5</sub>), 4.5 (MeCN). See also Table N13.

**Oxidative addition reactions of *o*-Me-C<sub>6</sub>H<sub>4</sub>-CH(OH)CH=CH<sub>2</sub> with *p*-MeC<sub>6</sub>H<sub>4</sub>SO<sub>3</sub>H and [Ru(Cp\*)(MeCN)<sub>3</sub>]PF<sub>6</sub> monitored by NMR spectroscopy.**

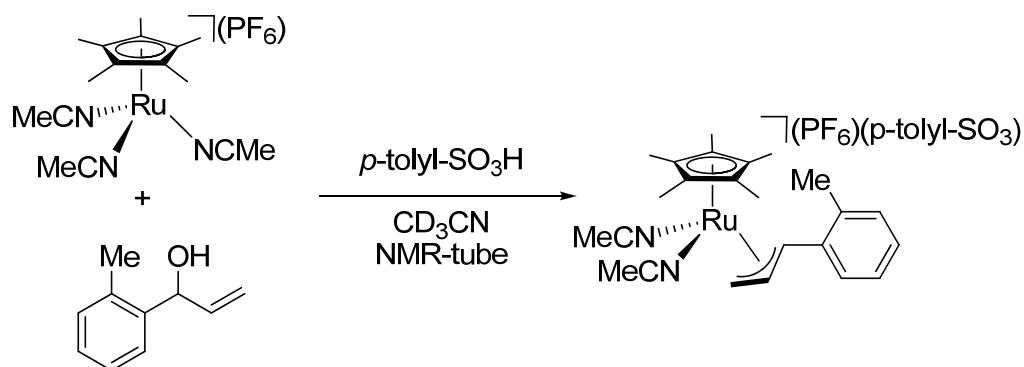


1-(*o*-Tolyl)prop-2-en-1-ol (8.8 mg, 0.059 mmol) was added to an CD<sub>3</sub>CN solution (0.5 mL) of [Ru(Cp\*)(MeCN)<sub>3</sub>]PF<sub>6</sub> (30 mg, 0.059 mmol) and *p*-toluenesulfonic acid monohydrate (11.3 mg, 0.059 mmol) in an NMR-tube.

**<sup>1</sup>H-NMR** (300 MHz, CD<sub>3</sub>CN):  $\delta$ : 7.85 (d, 1H, *J* = 9 Hz, C-*H*<sub>arom.</sub>), 7.64 (d, 2H, *J* = 8 Hz, C-*H*<sub>tosyl.</sub>), 7.61 (t, 1H, *J* = 7 Hz, C-*H*<sub>arom.</sub>), 7.38-7.34 (m, 2H, C-*H*<sub>arom.</sub>), 7.21 (d, 2H, *J* = 8 Hz, C-*H*<sub>tosyl.</sub>), 6.38-6.28 (m, 1H, C-*H*<sub>central</sub>), 5.49 (d, 1H, *J* = 12 Hz, Ph-C-*H*<sub>anti</sub>), 4.64 (d, 1H, *J* = 6 Hz, C<sub>terminal</sub>-*H*<sub>syn</sub>), 3.13 (d, 1H, *J* = 10 Hz, C<sub>terminal</sub>-*H*<sub>anti</sub>), 2.36 (brs, 6H, 2 x Me), 1.76 (s, 15H, C<sub>5</sub>Me<sub>5</sub>).

$^{13}\text{C-NMR}$  (75 MHz,  $\text{CD}_3\text{CN}$ ):  $\delta$ : 132.5 ( $C_{\text{arom.}}$ ), 132.3 ( $C_{\text{arom.}}$ ), 130.1 ( $C_{\text{arom.}}$ ), 128.7 ( $C_{\text{tosyl.}}$ ), 126.8 ( $C_{\text{arom.}}$ ), 125.9 ( $C_{\text{tosyl.}}$ ), 107.6 ( $C_5\text{Me}_5$ ), 107.1 (Ph-C), 95.2 ( $C_{\text{central}}$ ), 64.3 ( $C_{\text{terminal}}$ ), 20.4 (Me), 19.8 (Me), 9.3 ( $C_5\text{Me}_5$ ), MeCN not detectable and quaternary C-chemicals shifts are neglected.

**Oxidative addition reactions of  $\text{PhCH}(\text{OH})\text{CH}=\text{CH}_2$  with  $p\text{-MeC}_6\text{H}_4\text{SO}_3\text{H}$  and  $[\text{Ru}(\text{Cp}^*)(\text{MeCN})_3]\text{PF}_6$  monitored by NMR spectroscopy.**

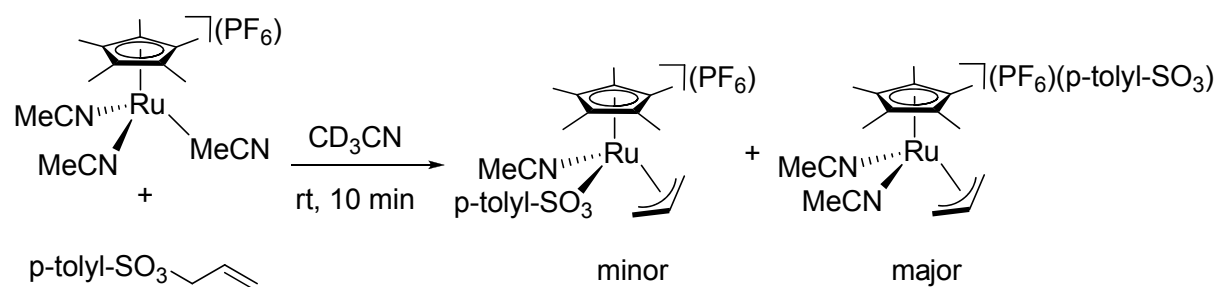


$\alpha$ -Vinylbenzyl alcohol (8.08 mg, 0.059 mmol) was added to an  $\text{CD}_3\text{CN}$  solution (0.5 mL) of  $[\text{Ru}(\text{Cp}^*)(\text{MeCN})_3]\text{PF}_6$  (30 mg, 0.059 mmol) and  $p$ -toluenesulfonic acid monohydrate (11.3 mg, 0.059 mmol) in an NMR-tube.

$^1\text{H-NMR}$  (700 MHz,  $\text{CD}_3\text{CN}$ ):  $\delta$ : 7.73 (d, 2H,  $J = 8$  Hz,  $C\text{-}H_{\text{arom.}}$ ), 7.69 (t, 1H,  $J = 7$  Hz,  $C\text{-}H_{\text{arom.}}$ ), 7.66 (d, 2H,  $J = 8$  Hz,  $C\text{-}H_{\text{tosyl.}}$ ), 7.50 (t, 2H,  $J = 8$  Hz,  $C\text{-}H_{\text{arom.}}$ ), 7.21 (d, 2H,  $J = 8$  Hz,  $C\text{-}H_{\text{tosyl.}}$ ), 6.43-6.39 (m, 1H,  $C\text{-}H_{\text{central}}$ ), 5.01 (d, 1H,  $J = 12$  Hz, Ph-C- $H_{\text{anti}}$ ), 4.62 (d, 1H,  $J = 6$  Hz,  $C_{\text{terminal}}\text{-}H_{\text{syn}}$ ), 3.10 (d, 1H,  $J = 10$  Hz,  $C_{\text{terminal}}\text{-}H_{\text{anti}}$ ), 2.37 (s, 3H, Me), 1.75 (s, 15H,  $C_5\text{Me}_5$ ).

$^{13}\text{C-NMR}$  (176 MHz,  $\text{CD}_3\text{CN}$ ):  $\delta$ : 132.2 ( $C_{\text{arom.}}$ ), 130.7 ( $C_{\text{arom.}}$ ), 128.6 ( $C_{\text{tosyl.}}$ ), 126.2 ( $C_{\text{arom.}}$ ), 125.8 ( $C_{\text{tosyl.}}$ ), 108.1 ( $C_5\text{Me}_5$ ), 102.9 (Ph-C), 93.6 ( $C_{\text{central}}$ ), 65.8 ( $C_{\text{terminal}}$ ), 20.4 (Me), 9.0 ( $C_5\text{Me}_5$ ), MeCN not detectable and quaternary C-chemicals shifts are neglected.

### Oxidative addition reactions of allyl tosylate with $[\text{Ru}(\text{Cp}^*)(\text{MeCN})_3]\text{PF}_6$ monitored by NMR spectroscopy.



Allyl tosylate (12.6 mg, 0.059 mmol) was added to an  $\text{CD}_3\text{CN}$  solution (0.5 mL) of  $[\text{Ru}(\text{Cp}^*)(\text{MeCN})_3]\text{PF}_6$  (30 mg, 0.059 mmol) in an NMR-tube and the spectra were recorded. The major and minor products were identified as  $[\text{Ru}(\eta^3\text{-C}_3\text{H}_5)(\text{Cp}^*)(\text{MeCN})_2]^{2+}$  and  $[\text{Ru}(\eta^3\text{-C}_3\text{H}_5)(\text{Cp}^*)(p\text{-MeC}_6\text{H}_4\text{SO}_3)(\text{MeCN})]^+$ , respectively. The  $^1\text{H}$ - and  $^{13}\text{C}$ - chemical shifts for these two products couldn't identify completely, because of signal overlap. Further, small quantities (about 5% or less) of several other  $\eta^3$ -allyl species are present.

#### major compound:

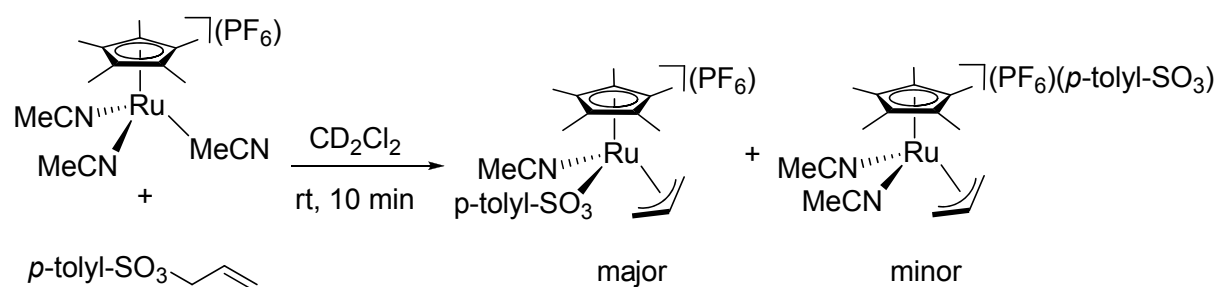
$^1\text{H-NMR}$  (500 MHz,  $\text{CD}_3\text{CN}$ ):  $\delta$ : 7.63 (d, 2H,  $J = 8$  Hz,  $\text{C-H}_{\text{tosyl}}$ ), 7.21 (d, 2H,  $J = 8$  Hz,  $\text{C-H}_{\text{tosyl}}$ ), 5.78-5.74 (m, 1H,  $\text{C-H}_{\text{central}}$ ), 4.56 (d, 2H,  $J = 6$  Hz,  $\text{C-H}_{\text{syn}}$ ), 3.02 (d, 2H,  $J = 10$  Hz,  $\text{C-H}_{\text{anti}}$ ), 2.38 (s, 3H,  $\text{Me}_{\text{tosyl}}$ ), 1.80 (s, 15H,  $\text{C}_5\text{Me}_5$ ).

$^{13}\text{C-NMR}$  (125 MHz,  $\text{CD}_3\text{CN}$ ):  $\delta$ : 128.8 ( $\text{C}_{\text{tosyl}}$ ), 126.1 ( $\text{C}_{\text{tosyl}}$ ), 110.3 ( $\text{C}_5\text{Me}_5$ ), 99.9 ( $\text{C}_{\text{central}}$ ), 72.2 ( $\text{C}_{\text{terminal}}$ ), 20.7 ( $\text{Me}_{\text{tosyl}}$ ), 9.3 ( $\text{C}_5\text{Me}_5$ ).

#### minor compound:

$^1\text{H-NMR}$  (500 MHz,  $\text{CD}_3\text{CN}$ ):  $\delta$ : 7.58 (d, 2H,  $J = 8$  Hz,  $\text{C-H}_{\text{tosyl}}$ ), 7.29 (d, 2H,  $J = 8$  Hz,  $\text{C-H}_{\text{tosyl}}$ ), 6.14-6.07 (m, 1H,  $\text{C-H}_{\text{central}}$ ), 4.60 (dd, 1H,  $J_1 = 6$  Hz,  $J_2 = 3$  Hz,  $\text{C-H}_{\text{syn}}$ ), 4.45 (dd, 1H,  $J_1 = 6$  Hz,  $J_2 = 3$  Hz,  $\text{C-H}_{\text{syn}}$ ), 3.28 (d, 1H,  $J = 10.5$  Hz,  $\text{C-H}_{\text{anti}}$ ), 2.82 (d, 1H,  $J = 10.2$  Hz,  $\text{C-H}_{\text{anti}}$ ), 2.40 (s, 3H,  $\text{Me}_{\text{tosyl}}$ ), 1.67 (s, 15H,  $\text{C}_5\text{Me}_5$ ).

$^{13}\text{C-NMR}$  (125 MHz,  $\text{CD}_3\text{CN}$ ):  $\delta$ : 129.5 ( $\text{C}_{\text{tosyl}}$ ), 125.9 ( $\text{C}_{\text{tosyl}}$ ), 109.8 ( $\text{C}_5\text{Me}_5$ ), 100.3 ( $\text{C}_{\text{central}}$ ), 74.2 ( $\text{C}_{\text{terminal}}$ ), 67.6 ( $\text{C}_{\text{terminal}}$ ), 20.8 ( $\text{Me}_{\text{tosyl}}$ ), 9.4 ( $\text{C}_5\text{Me}_5$ ).



Allyl tosylate (12.6 mg, 0.059 mmol) was added to a  $\text{CD}_2\text{Cl}_2$  solution (0.5 mL) of  $[\text{Ru}(\text{Cp}^*)(\text{MeCN})_3]\text{PF}_6$  (30 mg, 0.059 mmol) in an NMR-tube and the spectra were recorded. The major and minor products were identified as  $[\text{Ru}(\eta^3\text{-C}_3\text{H}_5)(\text{Cp}^*)(p\text{-MeC}_6\text{H}_4\text{SO}_3)(\text{MeCN})]^+$  and  $[\text{Ru}(\eta^3\text{-C}_3\text{H}_5)(\text{Cp}^*)(\text{MeCN})_2]^{2+}$ , respectively. The  $^1\text{H}$ - and  $^{13}\text{C}$ - chemical shifts for these two products couldn't identify completely, because of signal overlap. Further, small quantities (about 5% or less) of several other  $\eta^3$ -allyl species are present.

**major compound:**

$^1\text{H-NMR}$  (500 MHz,  $\text{CD}_2\text{Cl}_2$ ):  $\delta$ : 7.59 (d, 2H,  $J = 8$  Hz,  $\text{C-H}_{\text{tosyl}}$ ), 7.27 (d, 2H,  $J = 8$  Hz,  $\text{C-H}_{\text{tosyl}}$ ), 6.28-6.19 (m, 1H,  $\text{C-H}_{\text{central}}$ ), 4.58 (dd, 1H,  $J_1 = 7$  Hz,  $J_2 = 3$  Hz,  $\text{C-H}_{\text{syn}}$ ), 4.52 (dd, 1H,  $J_1 = 6$  Hz,  $J_2 = 3$  Hz,  $\text{C-H}_{\text{syn}}$ ), 3.19 (d, 1H,  $J = 11$  Hz,  $\text{C-H}_{\text{anti}}$ ), 2.75 (d, 1H,  $J = 11$  Hz,  $\text{C-H}_{\text{anti}}$ ), 2.60 (s, 3H,  $\text{MeCN}$ ), 2.42 (s, 3H,  $\text{Me}_{\text{tosyl}}$ ), 1.72 (s, 15H,  $\text{C}_5\text{Me}_5$ ).

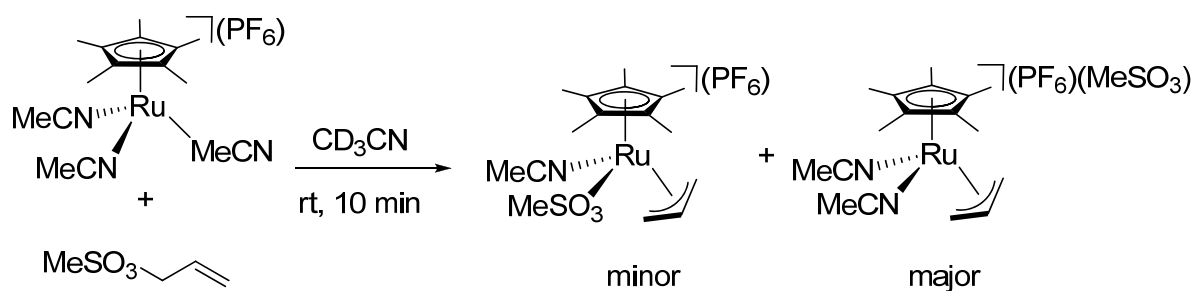
$^{13}\text{C-NMR}$  (125 MHz,  $\text{CD}_2\text{Cl}_2$ ):  $\delta$ : 129.5 ( $\text{C}_{\text{tosyl}}$ ), 125.8 ( $\text{C}_{\text{tosyl}}$ ), 109.2 ( $\text{C}_5\text{Me}_5$ ), 100.5 ( $\text{C}_{\text{central}}$ ), 75.0 ( $\text{C}_{\text{terminal}}$ ), 67.3 ( $\text{C}_{\text{terminal}}$ ), 21.4 ( $\text{Me}_{\text{tosyl}}$ ), 5.0 ( $\text{MeCN}$ ), 9.9 ( $\text{C}_5\text{Me}_5$ ).

**minor compound:**

$^1\text{H-NMR}$  (500 MHz,  $\text{CD}_2\text{Cl}_2$ ):  $\delta$ : 5.94-5.82 (m, 1H,  $\text{C-H}_{\text{central}}$ ), 5.30 (d, 2H,  $J = 7$  Hz,  $\text{C-H}_{\text{syn}}$ ), 2.84 (d, 2H,  $J = 11$  Hz,  $\text{C-H}_{\text{anti}}$ ), 1.64 (s, 15H,  $\text{C}_5\text{Me}_5$ ).

$^{13}\text{C-NMR}$  (125 MHz,  $\text{CD}_2\text{Cl}_2$ ):  $\delta$ : 100.5 ( $\text{C}_{\text{central}}$ ), 66.9 ( $\text{C}_{\text{terminal}}$ ).

**Oxidative addition reactions of allyl mesylate with  $[\text{Ru}(\text{Cp}^*)(\text{MeCN})_3]\text{PF}_6$ .**



Allyl mesylate (8.1mg, 0.059 mmol) was added to an  $\text{CD}_3\text{CN}$  solution (0.5 mL) of  $[\text{Ru}(\text{Cp}^*)(\text{MeCN})_3]\text{PF}_6$  (30 mg, 0.059 mmol) in an NMR-tube and the spectra were recorded. The major and minor products were identified as  $[\text{Ru}(\eta^3\text{-C}_3\text{H}_5)(\text{Cp}^*)(\text{MeCN})_2]^{2+}$  and  $[\text{Ru}(\eta^3\text{-C}_3\text{H}_5)(\text{Cp}^*)(\text{MeSO}_3)(\text{MeCN})]^+$ , respectively. The  $^1\text{H}$ - and  $^{13}\text{C}$ - chemical shifts for these two products couldn't identify completely, because of signal overlap. Further, small quantities (about 5% or less) of several other  $\eta^3$ -allyl species are present.



**major compound:**

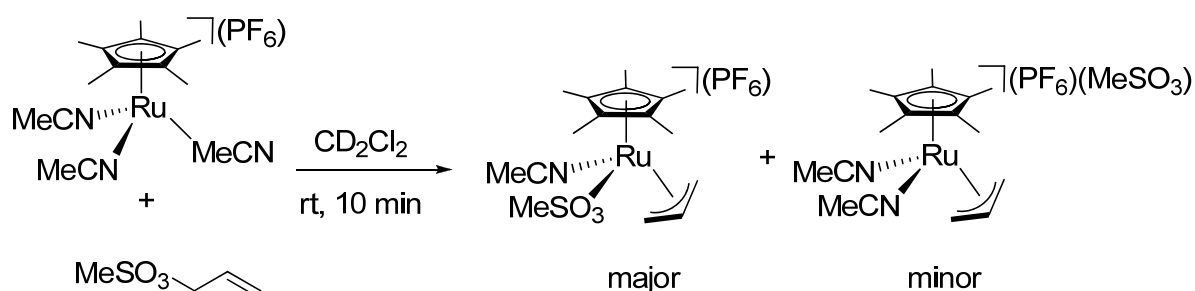
$^1\text{H-NMR}$  (500 MHz,  $\text{CD}_3\text{CN}$ ):  $\delta$ : 5.79-5.74 (m, 1H,  $C\text{-}H_{\text{central}}$ ), 4.58 (d, 2H,  $J = 7$  Hz,  $C\text{-}H_{\text{syn}}$ ), 3.05 (d, 2H,  $J = 11$  Hz,  $C\text{-}H_{\text{anti}}$ ), 2.66 (s, 3H,  $\text{Me}_{\text{mesyl}}$ ), 1.82 (s, 15H,  $\text{C}_5\text{Me}_5$ ).

$^{13}\text{C-NMR}$  (125 MHz,  $\text{CD}_3\text{CN}$ ):  $\delta$ : 110.2 ( $\text{C}_5\text{Me}_5$ ), 99.9 ( $C_{\text{central}}$ ), 72.2 ( $C_{\text{terminal}}$ ), 39.2 ( $\text{Me}_{\text{mesyl}}$ ), 9.4 ( $\text{C}_5\text{Me}_5$ ).

**minor compound:**

$^1\text{H-NMR}$  (500 MHz,  $\text{CD}_3\text{CN}$ ): 6.16-6.09 (m, 1H,  $C\text{-}H_{\text{central}}$ ), 4.59 (overlap,  $C\text{-}H_{\text{syn}}$ ), 4.43 (dd, 1H,  $J_1 = 6$  Hz,  $J_2 = 3$  Hz,  $C\text{-}H_{\text{syn}}$ ), 3.24 (overlap,  $C\text{-}H_{\text{anti}}$ ), 2.80 (d, 1H,  $J = 11$  Hz,  $C\text{-}H_{\text{anti}}$ ), 2.69 (s, 3H,  $\text{Me}_{\text{mesyl}}$ ), 1.69 (s, 15H,  $\text{C}_5\text{Me}_5$ ).

$^{13}\text{C-NMR}$  (125 MHz,  $\text{CD}_3\text{CN}$ ):  $\delta$ : 109.6 ( $\text{C}_5\text{Me}_5$ ), 100.2 ( $C_{\text{central}}$ ), 74.3 ( $C_{\text{terminal}}$ ), 67.1 ( $C_{\text{terminal}}$ ), 41.6 ( $\text{Me}_{\text{mesyl}}$ ), 9.3 ( $\text{C}_5\text{Me}_5$ ).



Allyl mesylate (8.1mg, 0.059 mmol) was added to a  $\text{CD}_2\text{Cl}_2$  solution (0.5 mL) of  $[\text{Ru}(\text{Cp}^*)(\text{MeCN})_3]\text{PF}_6$  (30 mg, 0.059 mmol) in an NMR-tube and the spectra were recorded. The major and minor products were identified as  $[\text{Ru}(\eta^3\text{-C}_3\text{H}_5)(\text{Cp}^*)(p\text{-MeSO}_3)(\text{MeCN})]^+$  and  $[\text{Ru}(\eta^3\text{-C}_3\text{H}_5)(\text{Cp}^*)(\text{MeCN})_2]^{2+}$ , respectively. The  $^1\text{H}$ - and  $^{13}\text{C}$ -chemical shifts for these two products couldn't identify completely, because of signal overlap. Further, small quantities (about 5% or less) of several other  $\eta^3$ -allyl species are present.

**major compound:**

$^1\text{H-NMR}$  (500 MHz,  $\text{CD}_2\text{Cl}_2$ ):  $\delta$ : 6.25-6.18 (m, 1H,  $C\text{-}H_{\text{central}}$ ), 4.60 (dd, 1H,  $J_1 = 7$  Hz,  $J_2 = 3$  Hz,  $C\text{-}H_{\text{syn}}$ ), 4.48 (dd, 1H,  $J_1 = 6$  Hz,  $J_2 = 3$  Hz,  $C\text{-}H_{\text{syn}}$ ), 3.18 (d, 1H,  $J = 11$  Hz,  $C\text{-}H_{\text{anti}}$ ), 2.73 (d, 1H,  $J = 10$  Hz,  $C\text{-}H_{\text{anti}}$ ), 2.78 (s, 3H,  $\text{Me}_{\text{mesyl}}$ ), 2.60 (s, 3H,  $\text{MeCN}$ ), 1.75 (s, 15H,  $\text{C}_5\text{Me}_5$ ).

$^{13}\text{C-NMR}$  (125 MHz,  $\text{CD}_2\text{Cl}_2$ ):  $\delta$ : 109.6 ( $\text{C}_5\text{Me}_5$ ), 100.3 ( $C_{\text{central}}$ ), 75.1 ( $C_{\text{terminal}}$ ), 67.2 ( $C_{\text{terminal}}$ ), 42.3 ( $\text{Me}_{\text{mesyl}}$ ), 5.0 ( $\text{MeCN}$ ), 9.8 ( $\text{C}_5\text{Me}_5$ ).

**minor compound:**

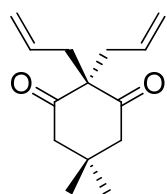
$^1\text{H-NMR}$  (500 MHz,  $\text{CD}_2\text{Cl}_2$ ):  $\delta$ : 6.48-6.42 (m, 1H,  $\text{C-H}_{\text{central}}$ ), 5.05 (d, 2H,  $J = 7$  Hz,  $\text{C-H}_{\text{syn}}$ ), 2.88 (d, 2H,  $J = 11$  Hz,  $\text{C-H}_{\text{anti}}$ ), 1.65 (s, 15H,  $\text{C}_5\text{Me}_5$ ).

$^{13}\text{C-NMR}$  (125 MHz,  $\text{CD}_2\text{Cl}_2$ ):  $\delta$ : 109.0 ( $\text{C}_5\text{Me}_5$ ), 100.5 ( $\text{C}_{\text{central}}$ ), 68.0 ( $\text{C}_{\text{terminal}}$ ) 9.9 ( $\text{C}_5\text{Me}_5$ ).

**6.5. Chapter 5: Allylation of Cyclic 1,3-Diketones****A typical preparative procedure for allylation of 1,3-diketones with  $\text{CH}_2=\text{CHCH}_2\text{OH}$ .**

1,3-Diketone (0.80 mmol) was added to an  $\text{CH}_3\text{CN}$  solution (0.8 mL) of allyl alcohol (0.85 mmol or 1.65 mmol) and  $[\text{Ru}(\eta^3\text{-C}_3\text{H}_5)(\text{Cp}^*)(p\text{-MeC}_6\text{H}_4\text{SO}_3)_2]$ , (**II-7**) (0.025 g, 0.04 mmol). After addition of  $\text{CH}_2\text{Cl}_2$  (3.3 ml) the reaction mixture was stirred for 3 h at 50 °C, then evaporated under vacuum and the product separated by column chromatography on silica gel.

These products are all known compounds and were identified by comparison of their spectroscopic data ( $^1\text{H}$  and  $^{13}\text{C}$  NMR) and HR EI-MS.

**2,2-Diallyl-5,5-dimethylcyclohexane-1,3-dione.**<sup>[24]</sup>

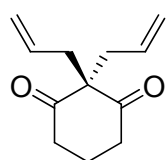
Hexane / EtOAc = 6:1; 97% yield, viscous oil;

$^1\text{H-NMR}$  (300 MHz,  $\text{CDCl}_3$ ):  $\delta$ : 5.67-5.55 (m, 2H), 5.14-5.07 (m, 4H), 2.56 (s, 4H), 2.52 (d, 4H,  $J = 8$  Hz), 1.00 (s, 6H).

$^{13}\text{C-NMR}$  (75 MHz,  $\text{CDCl}_3$ ):  $\delta$ : 208.7, 132.4, 119.4, 68.0, 52.1, 38.9,

30.7, 28.8.

**HR EI-MS:** calcd. for  $[\text{C}_{14}\text{H}_{20}\text{O}_2]^{++}$  220.1458, found 220.1459.

**2,2-Diallylcyclohexane-1,3-dione.**<sup>[25]</sup>

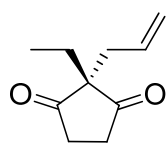
Hexane / EtOAc = 6:1; 92% yield, viscous oil;

$^1\text{H-NMR}$  (300 MHz,  $\text{CDCl}_3$ ):  $\delta$ : 5.61-5.50 (m, 2H), 5.08-5.03 (m, 4H), 2.58-2.52 (m, 8H), 1.98-1.91 (m, 2H).

$^{13}\text{C-NMR}$  (75 MHz,  $\text{CDCl}_3$ ):  $\delta$ : 210.3, 132.4, 119.4, 68.3, 40.9, 40.0,

16.4.

**HR EI-MS:** calcd. for  $[\text{C}_{12}\text{H}_{16}\text{O}_2]^{++}$  192.1145, found 192.1147.

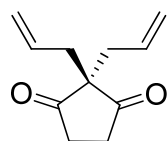
**2-Allyl-2-ethylcyclopentane-1,3-dione.**<sup>[26]</sup>

Hexane / EtOAc = 6:1; 92% yield, viscous oil;

<sup>1</sup>H-NMR (300 MHz, CDCl<sub>3</sub>): δ: 5.64-5.50 (m, 1H), 5.08-5.03 (m, 2H), 2.67 (brs, 4H), 2.36 (d, 2H, *J* = 8 Hz), 1.71 (q, 2H, *J* = 8 Hz), 0.79 (t, 3H, *J* = 8 Hz).

<sup>13</sup>C-NMR (75 MHz, CDCl<sub>3</sub>): δ: 216.9, 131.6, 119.7, 61.8, 39.2, 36.4, 28.2, 9.1.

HR EI-MS: calcd. for [C<sub>10</sub>H<sub>14</sub>O<sub>2</sub><sup>++</sup>] 166.0988, found 166.0990.

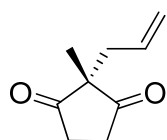
**2,2-Diallylcyclopentane-1,3-dione.**<sup>[27]</sup>

Hexane / EtOAc = 6:1; 88% yield, viscous oil;

<sup>1</sup>H-NMR (300 MHz, CDCl<sub>3</sub>): δ: 5.64-5.50 (m, 2H), 5.09-5.04 (m, 4H), 2.63 (brs, 4H), 2.38 (d, 4H, *J* = 8 Hz).

<sup>13</sup>C-NMR (75 MHz, CDCl<sub>3</sub>): δ: 216.4, 131.3, 120.0, 61.2, 39.4, 36.4.

HR EI-MS: calcd. for [C<sub>11</sub>H<sub>14</sub>O<sub>2</sub><sup>++</sup>] 178.0988, found 178.0989.

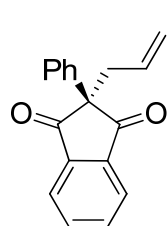
**2-Allyl-2-methylcyclopentane-1,3-dione.**<sup>[26]</sup>

Hexane / EtOAc = 6:1; 98% yield, viscous oil;

<sup>1</sup>H-NMR (300 MHz, CDCl<sub>3</sub>): δ: 5.64-5.53 (m, 1H), 5.09-5.04 (m, 2H), 2.82-2.63 (m, 4H), 2.35 (d, 2H, *J* = 8 Hz), 1.12 (s, 3H).

<sup>13</sup>C-NMR (75 MHz, CDCl<sub>3</sub>): δ: 216.2, 131.5, 119.8, 56.7, 40.0, 35.4, 18.8.

HR EI-MS: calcd. for [C<sub>9</sub>H<sub>12</sub>O<sub>2</sub><sup>++</sup>] 152.0832, found 152.0830.

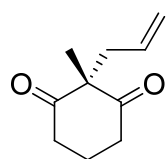
**2-Allyl-2-phenylindene-1,3-dione.**<sup>[28]</sup>

Hexane / EtOAc = 6:1; 98% yield, viscous oil;

<sup>1</sup>H-NMR (500 MHz, CDCl<sub>3</sub>): δ: 8.05-8.03 (m, 2H), 7.88-7.86 (m, 2H), 7.45 (d, 2H, *J* = 5 Hz), 7.35-7.26 (m, 3H), 5.62-5.56 (m, 1H), 5.15 (d, 1H, *J* = 10 Hz), 4.96 (d, 1H, *J* = 6 Hz), 3.06 (d, 2H, *J* = 4 Hz).

<sup>13</sup>C-NMR (125 MHz, CDCl<sub>3</sub>): δ: 201.5, 142.5, 137.0, 136.3, 132.2, 129.2, 128.2, 127.3, 123.9, 124.0, 120.4, 62.6, 40.5.

HR EI-MS: calcd. for [C<sub>18</sub>H<sub>14</sub>O<sub>2</sub><sup>++</sup>] 262.0988, found 262.0992.

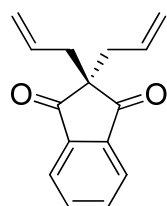
**2-Allyl-2-methylcyclohexane-1,3-dione.**<sup>[29]</sup>

Hexane / EtOAc = 6:1; 96% yield, viscous oil;

**<sup>1</sup>H-NMR** (300 MHz, CDCl<sub>3</sub>): δ: 5.63-5.54 (m, 1H), 5.10-5.05 (m, 2H), 2.68 -2.64 (m, 4H), 2.54 (d, 2H, *J* = 8 Hz), 2.05-1.87 (m, 2H), 1.25 (s, 3H).

**<sup>13</sup>C-NMR** (75 MHz, CDCl<sub>3</sub>): δ: 209.8, 132.2, 119.2, 65.2, 41.3, 38.2, 19.5, 17.5.

**HR EI-MS:** calcd. for [C<sub>10</sub>H<sub>14</sub>O<sub>2</sub><sup>+</sup>] 166.0988, found 166.0989.

**2,2-diallyl-1H-indene-1,3(2H)-dione.**<sup>[28]</sup>

Hexane / EtOAc = 6:1; 89% yield, viscous oil;

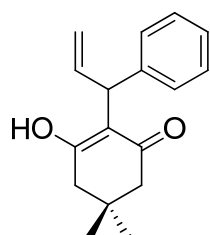
**<sup>1</sup>H-NMR** (300 MHz, CDCl<sub>3</sub>): δ: 7.97-7.93 (m, 2H), 7.86-7.82 (m, 2H), 5.54-5.40 (m, 1H), 5.03 (d, 2H, *J* = 17 Hz), 4.89 (d, 2H, *J* = 10 Hz), 2.55 (d, 4H, *J* = 8 Hz).

**<sup>13</sup>C-NMR** (75 MHz, CDCl<sub>3</sub>): δ: 203.3, 142.23, 135.7, 131.4, 123.0, 119.5, 58.3, 38.8.

**HR EI-MS:** calcd. for [C<sub>15</sub>H<sub>14</sub>O<sub>2</sub><sup>+</sup>] 226.0988, found 226.0983.

**A typical preparative procedure for allylation of 1,3-diketones with ArCH(OH)CH=CH<sub>2</sub> (Ar = Ph, 1-naphtyl, 2-naphtyl, *o*-MeC<sub>6</sub>H<sub>4</sub>, *o*-ClC<sub>6</sub>H<sub>4</sub>, *p*-MeOC<sub>6</sub>H<sub>4</sub>, *p*-ClC<sub>6</sub>H<sub>4</sub> or 1-thiophenyl).**

1,3-Diketone (0.84 mmol) was added to an acetonitrile solution (1.6 mL) of ArCH(OH)CH=CH<sub>2</sub> (0.68 mmol) and [Ru( $\eta^3$ -C<sub>3</sub>H<sub>5</sub>)(Cp<sup>\*</sup>)(*p*-CH<sub>3</sub>C<sub>6</sub>H<sub>4</sub>SO<sub>3</sub>)<sub>2</sub>], (**II-7**) (0.020 g, 0.03 mmol). After addition of H<sub>2</sub>O (1.6 ml) the reaction mixture was stirred for 5 h at room temperature, then evaporated under vacuum. Addition of EtOAc followed by filtration through silica gel removed the ruthenium catalyst. The crude material was crystallized from EtOAc, Et<sub>2</sub>O or hexane solutions at -40 °C. At ambient temperature the <sup>13</sup>C spectra in DMF-d<sub>7</sub> of all of the enol forms show only an average of the C-O and C=O signals.

**3-Hydroxy-5,5-dimethyl-2-(1-phenylallyl)cyclohex-2-enone.**

Crystallized from EtOAc; 78 % yield, white solid; m.p. 129-130 °C;

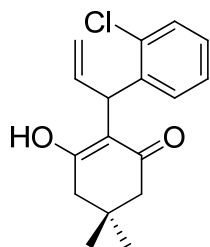
**<sup>1</sup>H-NMR** (300 MHz, DMF-d<sub>7</sub>): δ: 11.0 (brs, 1H) 7.47-7.28 (m, 5H), 6.83-6.71 (m, 1H), 5.28-5.14 (m, 3H), 2.54 (brs, 4H), 1.23 (s, 6H).

**<sup>13</sup>C-NMR** (75 MHz, DMF-d<sub>7</sub>): δ: 184.0, 144.6, 140.4, 127.9, 127.7,

125.4, 116.2, 114.4, 47.2, 43.9, 32.0, 27.9.

**HR EI-MS:** calcd. for  $[C_{17}H_{20}O_2]^{+}$  256.1458, found 256.1463.

### 2-(1-(*o*-Chlorophenyl)allyl)-3-hydroxy-5,5-dimethylcyclohex-2-enone.



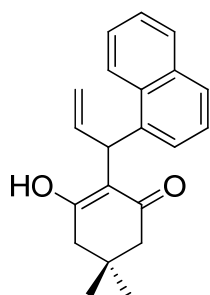
Crystallized from EtOAc; 75 % yield, white solid; m.p. 169-170 °C;

**$^1H$ -NMR** (300 MHz, DMF- $d_7$ ):  $\delta$ : 10.8 (brs, 1H), 7.56 (d, 1H,  $J = 8$  Hz), 7.36-7.17 (m, 3H), 6.40-6.31 (m, 1H), 5.22 (d, 1H,  $J = 7$  Hz), 5.06-4.98 (m, 2H), 2.34 (brs, 4H), 1.05 (s, 6H).

**$^{13}C$ -NMR** (75 MHz, DMF- $d_7$ ):  $\delta$ : 141.9, 139.1, 133.5, 131.3, 129.1, 127.4, 126.4, 114.5, 114.1, 47.3, 41.7, 31.8, 27.9, C-O not observed.

**HR EI-MS:** calcd. for  $[C_{17}H_{19}ClO_2]^{+}$  290.1068, found 290.1057.

### 3-Hydroxy-5,5-dimethyl-2-(1-(naphthalen-1-yl)allyl)cyclohex-2-enone.



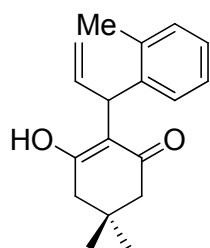
Crystallized from EtOAc; 70 % yield, white solid; m.p. 165-166 °C;

**$^1H$ -NMR** (300 MHz, DMF- $d_7$ ):  $\delta$ : 11.0 (brs, 1H), 8.37-7.58 (m, 7H), 6.81-6.70 (m, 1H), 5.82 (d, 1H,  $J = 7$  Hz), 5.32-5.26 (m, 2H), 2.56-2.43 (m, 4H), 1.15 (s, 6H).

**$^{13}C$ -NMR** (75 MHz, DMF- $d_7$ ):  $\delta$ : 140.2, 139.9, 133.9, 132.2, 128.6, 126.6, 126.2, 125.5, 125.2, 125.1, 124.4, 115.8, 113.8, 47.1, 40.3, 31.7, 27.7, C-O not observed.

**HR EI-MS:** calcd. for  $[C_{21}H_{22}O_2]^{+}$  306.1614, found 306.1618.

### 3-Hydroxy-5,5-dimethyl-2-(1-*o*-tolylallyl)cyclohex-2-enone.

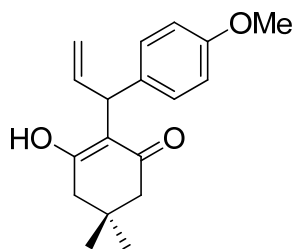


Crystallized from EtOAc; 77 % yield, white solid; m.p. 151-152 °C;

**$^1H$ -NMR** (300 MHz, DMF- $d_7$ ):  $\delta$ : 10.7 (brs, 1H), 7.46 (d, 1H,  $J = 7$  Hz), 7.12-7.04 (m, 3H), 6.51-6.39 (m, 1H), 5.05-4.91 (m, 3H), 2.35-2.32 (m, 7H), 1.04 (s, 6H).

**$^{13}C$ -NMR** (75 MHz, DMF- $d_7$ ):  $\delta$ : 142.6, 140.8, 136.2, 129.9, 129.2, 125.6, 125.4, 115.6, 112.9, 47.6, 41.5, 31.8, 27.9, 19.3, C-O not observed.

**HR EI-MS:** calcd. for  $[C_{18}H_{22}O_2]^{+}$  270.1614, found 270.1612.

**3-Hydroxy-2-(1-(*p*-methoxyphenyl)allyl)-5,5-dimethylcyclohex-2-enone.**

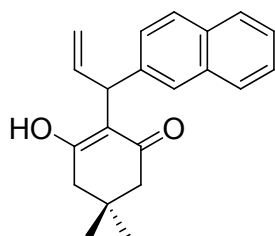
Crystallized from EtOAc; 73 % yield, white solid; m.p. 126-127;

<sup>1</sup>H-NMR (300 MHz, DMF-d<sub>7</sub>): δ: 10.8 (brs, 1H), 7.19 (d, 2H, *J* = 8 Hz), 6.83 (d, 2H, *J* = 8 Hz), 6.63-6.51 (m, 1H), 5.07-4.89 (m, 3H), 3.77 (s, 3H), 2.35 (brs, 4H), 1.05 (s, 6H).

<sup>13</sup>C-NMR (75 MHz, DMF-d<sub>7</sub>): δ: 157.6, 140.7, 136.3, 128.5,

116.2, 113.8, 113.2, 54.8, 47.1, 43.1, 31.8, 27.8, C-O not observed.

HR EI-MS: calcd. for [C<sub>18</sub>H<sub>22</sub>O<sub>3</sub><sup>+</sup>] 286.1563, found 286.1563.

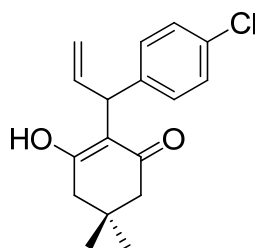
**3-Hydroxy-5,5-dimethyl-2-(1-(naphthalene-2-yl)allyl)cyclohex-2-enone.**

Crystallized from EtOAc; 79 % yield, white solid; m.p. 121-123 °C;

<sup>1</sup>H-NMR (300 MHz, DMF-d<sub>7</sub>): δ: 10.9 (brs, 1H), 7.86-7.44 (m, 7H), 6.80-6.68 (m, 1H), 5.22-5.15 (m, 3H), 2.42 (brs, 4H), 1.10 (s, 6H).

<sup>13</sup>C-NMR (75 MHz, DMF-d<sub>7</sub>): δ: 143.0, 140.0, 133.6, 132.0, 127.6, 127.5, 127.2, 126.8, 125.8, 125.3, 125.1, 115.9, 114.6, 47.0, 43.9, 31.8, 27.8, C-O not observed.

HR EI-MS: calcd. for [C<sub>21</sub>H<sub>22</sub>O<sub>2</sub><sup>+</sup>] 306.1614, found 306.1613.

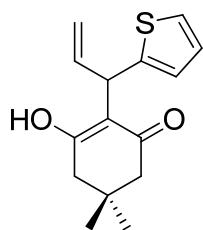
**2-(1-(*p*-chlorophenyl)allyl)-3-hydroxy-5,5-dimethylcyclohex-2-enone.**

Crystallized from Et<sub>2</sub>O / Hexane; 62 % yield, white solid; m.p. m.p. 135-137 °C;

<sup>1</sup>H-NMR (300 MHz, DMF-d<sub>7</sub>): δ: 10.9 (brs, 1H), 7.33-7.26 (m, 4H), 6.56-6.47 (m, 1H), 5.121-4.93 (m, 3H), 2.36 (brs, 4H), 1.05 (s, 6H).

<sup>13</sup>C-NMR (75 MHz, DMF-d<sub>7</sub>): δ: 183.3, 143.6, 139.6, 130.3, 129.3, 127.7, 115.5, 114.6, 47.0, 43.1, 31.8, 27.7.

HR EI-MS: calcd. for [C<sub>17</sub>H<sub>19</sub>ClO<sub>2</sub><sup>+</sup>] 290.1068, found 290.1068.

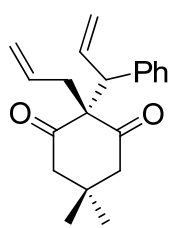
**3-Hydroxy-5,5-dimethyl-2-(1-(thiophen-2-yl)allyl)cyclohex-2-enone.**

Crystallized from Et<sub>2</sub>O; 77 % yield, white solid; m.p. m.p. 131-132 °C;

<sup>1</sup>H-NMR (300 MHz, DMF-d<sub>7</sub>): δ: 11.2 (brs, 1H), 7.42 (d, 1H, *J* = 5 Hz), 7.09-7.07 (m, 1H), 6.96-6.94 (m, 1H), 6.96-6.94 (m, 1H), 6.80-6.68 (m, 1H), 5.31-5.17 (m, 3H), 2.53 (brs, 4H), 1.24 (s, 6H).

<sup>13</sup>C-NMR (75 MHz, DMF-d<sub>7</sub>): δ: 182.6, 148.7, 140.0, 126.4, 123.3, 123.0, 116.0, 114.3, 47.0, 39.9, 31.8, 27.8.

HR EI-MS: calcd. for [C<sub>15</sub>H<sub>18</sub>O<sub>2</sub>S<sup>+</sup>] 262.1022, found 262.1022.

**Synthesis of 2-allyl-5,5-dimethyl-2-(1-phenylallyl)cyclohexane-1,3-dione (V-5).**

3-Hydroxy-5,5-dimethyl-2-(1-phenylallyl)cyclohex-2-enone (0.80 mmol)

was added to an CH<sub>3</sub>CN solution (0.8 mL) of allyl alcohol (0.88 mmol) and [Ru( $\eta^3$ -C<sub>3</sub>H<sub>5</sub>)(Cp<sup>\*</sup>)(*p*-MeC<sub>6</sub>H<sub>4</sub>SO<sub>3</sub>)<sub>2</sub>], (**II-7**) (0.025 g, 0.04 mmol).

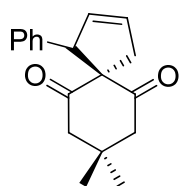
After addition of CH<sub>2</sub>Cl<sub>2</sub> (3.4 ml) the reaction mixture was refluxed for 16 h at 70°, then evaporated under vacuum and separated by column

chromatography on silica gel (Hexane / EtOAc gradient from 8:1 to 6:1). The product was dried under vacuum to afford a very viscous oil (140 mg, 60 %).

<sup>1</sup>H-NMR (700 MHz, CDCl<sub>3</sub>): δ: 7.29 (t, 2H, *J*<sub>1</sub> = 8 Hz, *J*<sub>2</sub> = 7 Hz), 7.24 (t, 1H, *J*<sub>1</sub> = 8 Hz, *J*<sub>2</sub> = 7 Hz), 7.08 (d, 2H, *J*<sub>1</sub> = 8 Hz), 6.32 (dt, 1H, *J*<sub>1</sub> = 17 Hz, *J*<sub>2</sub> = 11 Hz), 5.58-5.54 (m, 1H), 5.21 (dd, 1H, *J*<sub>1</sub> = 1 Hz, *J*<sub>2</sub> = 11 Hz), 5.13 (d, 1H, *J* = 17 Hz), 5.07 (dd, 1H, *J*<sub>1</sub> = 18 Hz, *J*<sub>2</sub> = 1 Hz), 5.00 (dd, 1H, *J*<sub>1</sub> = 11 Hz, *J*<sub>2</sub> = 1 Hz), 3.77 (d, 1H, *J* = 11 Hz), 2.66 (dd, 1H, *J*<sub>1</sub> = 13 Hz, *J*<sub>2</sub> = 7 Hz), 2.58 (dd, 1H, *J*<sub>1</sub> = 13 Hz, *J*<sub>2</sub> = 7 Hz), 2.42 (dd, 1H, *J*<sub>1</sub> = 15 Hz, *J*<sub>2</sub> = 2 Hz), 2.38-2.36 (m, 2H), 2.06 (d, 1H, *J* = 15 Hz), 0.85 (s, 3H), 0.77 (s, 3H).

<sup>13</sup>C-NMR (176 MHz, CDCl<sub>3</sub>): δ: 209.7, 209.3, 139.2, 135.5, 133.4, 129.2, 128.5, 127.5, 119.5, 118.5, 71.3, 57.8, 54.3, 54.0, 37.5, 30.4, 30.1, 28.1.

HR EI-MS: calcd. for [C<sub>20</sub>H<sub>24</sub>O<sub>2</sub><sup>+</sup>] 296.1771, found 296.1773.

**Synthesis of 8,8-dimethyl-1-phenylspiro[4.5]dec-2-ene-6,10-dione (V-7)**

A mixture of 2-allyl-5,5-dimethyl-2-(1-phenylallyl)cyclohexane-1,3-dione (0.11 mmol) and Grubb's catalyst

(bis(tricyclohexylphosphine)benzylidene ruthenium(IV) dichloride) (5 mg, 0.006 mmol) in dry CH<sub>2</sub>Cl<sub>2</sub> (4 ml) was stirred at rt for 14 h under

N<sub>2</sub> atmosphere. The reaction mixture was evaporated under vacuum and separated

by column chromatography on silica gel (Hexane / EtOAc = 6:1). The product was dried under vacuum to afford a white solid (29 mg, 96 %, m.p. 135-136 °C).

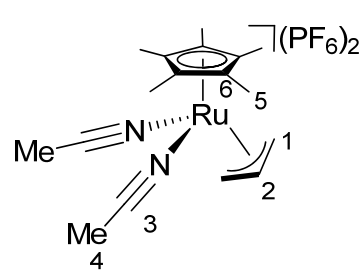
**<sup>1</sup>H-NMR** (700 MHz, CDCl<sub>3</sub>): δ: 7.30-7.27 (m, 3H), 7.13 (d, 2H,  $J_1 = 7$  Hz), 6.02-6.00 (m, 1H), 5.38-5.36 (m, 1H), 4.14 (d, 1H,  $J = 1$  Hz), 3.25 (dd, 1H,  $J_1 = 17$  Hz,  $J_1 = 3$  Hz), 3.05-3.01 (m, 2H), 2.51 (dd, 1H,  $J_1 = 15$  Hz,  $J_1 = 3$  Hz), 2.02 (dd, 1H,  $J_1 = 15$  Hz,  $J_1 = 3$  Hz), 1.74 (d, 1H,  $J = 15$  Hz), 1.04 (s, 3H), 0.76 (s, 3H).

**<sup>13</sup>C-NMR** (176 MHz, CDCl<sub>3</sub>): δ: 207.0, 206.1, 138.8, 131.6, 129.2, 128.6, 128.4, 128.0, 75.8, 63.1, 53.8, 51.6, 34.0, 30.6, 30.1, 26.7.

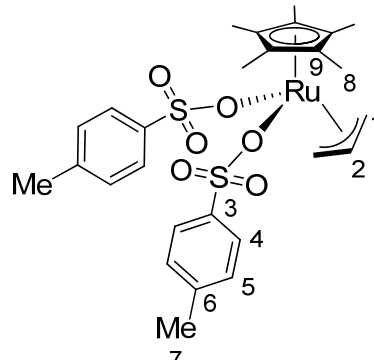
**HR EI-MS**: calcd. for [C<sub>18</sub>H<sub>20</sub>O<sub>2</sub>]<sup>++</sup> 268.1458, found 268.1456.

## 6.6. NMR Tables

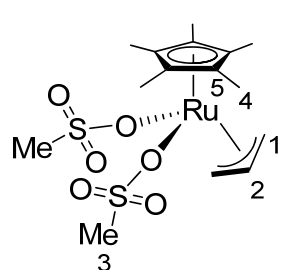
**Table N1.** <sup>1</sup>H- and <sup>13</sup>C-NMR data for [Ru(η<sup>3</sup>-C<sub>3</sub>H<sub>5</sub>)(Cp\*)(MeCN)<sub>2</sub>](PF<sub>6</sub>)<sub>2</sub> (**II-6**) in acetone-d<sub>6</sub> at rt.

	Position	δ( <sup>1</sup> H) [ppm]	<sup>3</sup> J <sub>HH</sub> [Hz]	δ( <sup>13</sup> C) [ppm]
	1 <sub>syn</sub>	4.80	6	73.6
	1 <sub>anti</sub>	3.33	11	73.6
	2	5.98	11, 6	101.4
	3	-	-	135.2
	4	2.72	-	5.3
	5	2.02	-	10.5
	6	-	-	11.7

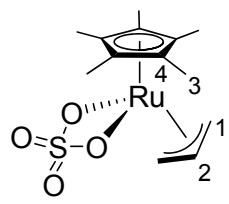


**Table N2.**  $^1\text{H}$ - and  $^{13}\text{C}$ -NMR data for  $[\text{Ru}(\eta^3\text{-C}_3\text{H}_5)(\text{Cp}^*)(p\text{-MeC}_6\text{H}_4\text{SO}_3)_2]$  (**II-7**) in  $\text{CD}_2\text{Cl}_2$  at rt.


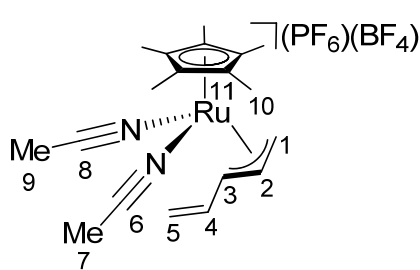
Position	$\delta(^1\text{H})$ [ppm]	$^3J_{\text{HH}}$ [Hz]	$\delta(^{13}\text{C})$ [ppm]
1 <sub>syn</sub>	5.30	6	66.7
1 <sub>anti</sub>	2.83	10	66.7
2	6.22	10, 6	100.1
3	-	-	142.5
4	7.56	-	125.9
5	7.13	-	128.9
6	-	-	140.9
7	2.39	-	21.1
8	1.66	-	9.8
9	-	-	108.8

**Table N3.**  $^1\text{H}$ - and  $^{13}\text{C}$ -NMR data for  $[\text{Ru}(\eta^3\text{-C}_3\text{H}_5)(\text{Cp}^*)(\text{MeSO}_3)_2]$  (**II-8**) in  $\text{CD}_2\text{Cl}_2$  at rt.


Position	$\delta(^1\text{H})$ [ppm]	$^3J_{\text{HH}}$ [Hz]	$\delta(^{13}\text{C})$ [ppm]
1 <sub>syn</sub>	5.05	6	67.6
1 <sub>anti</sub>	2.86	10	67.6
2	6.43	10, 6	100.0
3	2.73	-	41.6
4	1.64	-	9.5
5	-	-	108.6

**Table N4.**  $^1\text{H}$ - and  $^{13}\text{C}$ -NMR data for  $[\text{Ru}(\eta^3\text{-C}_3\text{H}_5)(\text{Cp}^*)(\kappa^2\text{-SO}_4)]$  (**II-9**) in  $\text{CD}_2\text{Cl}_2$  at rt.


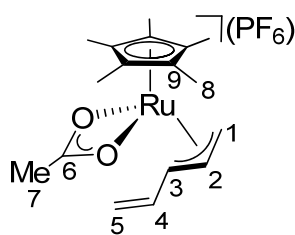
Position	$\delta(^1\text{H})$ [ppm]	$^3J_{\text{HH}}$ [Hz]	$\delta(^{13}\text{C})$ [ppm]
1 <sub>syn</sub>	4.03	7	65.6
1 <sub>anti</sub>	2.63	11	65.6
2	5.23	11, 7	101.5
3	1.65	-	9.3
4	-	-	107.3

**Table N5.**  $^1\text{H}$ - and  $^{13}\text{C}$ -NMR data for  $[\text{Ru}(\eta^3\text{-CH}_2\text{CHCHCH}=\text{CH}_2)(\text{Cp}^*)(\text{MeCN})_2](\text{PF}_6)(\text{BF}_4)$  (**II-15**) in  $\text{CD}_3\text{CN}$  at rt.


Position	$\delta(^1\text{H})$ [ppm]	$^3J_{\text{HH}}$ [Hz]	$\delta(^{13}\text{C})$ [ppm]
1 <sub>syn</sub>	4.54	7	67.4
1 <sub>anti</sub>	2.94	11	67.4
2	5.86	11, 7	97.0
3	4.29	11	98.6
4	6.39	17, 10	135.7
5 <sub>cis</sub>	6.04	10	129.1
5 <sub>trans</sub>	5.99	17	129.1
6	*	-	*
7	*	-	*
8	*	-	*
9	*	-	*
10	1.75	-	9.1
11	-	-	108.9

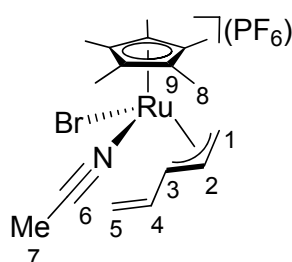
\* exchange with  $\text{CD}_3\text{CN}$

**Table N6.**  $^1\text{H}$ - and  $^{13}\text{C}$ -NMR data for  $[\text{Ru}(\kappa^2\text{-O}_2\text{CMe})(\eta^3\text{-CH}_2\text{CHCHCH}=\text{CH}_2)(\text{Cp}^*)]\text{PF}_6$  (**II-17**) in  $\text{CD}_2\text{Cl}_2$  at rt.



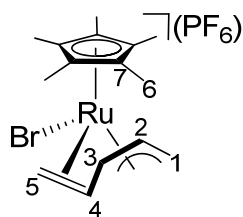
Position	$\delta(^1\text{H})$ [ppm]	$^3J_{\text{HH}}$ [Hz]	$\delta(^{13}\text{C})$ [ppm]
1 <sub>syn</sub>	4.46	6	66.7
1 <sub>anti</sub>	3.01	10	66.7
2	6.47	10, 6	103.6
3	4.05	10	88.5
4	6.08	17, 10	135.6
5 <sub>cis</sub>	5.75	10,	124.1
5 <sub>trans</sub>	5.71	17	124.1
6	-	-	194.5
7	1.92	-	25.6
8	1.55	-	9.0
9	-	-	107.1

**Table N7.**  $^1\text{H}$ - and  $^{13}\text{C}$ -NMR data for  $[\text{Ru}(\eta^3\text{-CH}_2\text{CHCHCH}=\text{CH}_2)\text{Br}(\text{Cp}^*)](\text{MeCN})\text{PF}_6$  (**II-18**) in  $\text{CD}_3\text{NO}_2$  at rt.



Position	$\delta(^1\text{H})$ [ppm]	$^3J_{\text{HH}}$ [Hz]	$\delta(^{13}\text{C})$ [ppm]
1 <sub>syn</sub>	4.54	6	65.8
1 <sub>anti</sub>	2.56	overlap	65.8
2	5.43	10, 6	95.8
3	3.82	10	87.4
4	6.27	17, 10	136.2
5 <sub>cis</sub>	5.82	10	124.3
5 <sub>trans</sub>	5.79	17	124.3
6	-	-	?
7	2.54	-	3.1
8	1.73	-	8.3
9	-	-	106.1

**Table N8.**  $^1\text{H}$ - and  $^{13}\text{C}$ -NMR data for  $[\text{Ru}(\eta^5\text{-S-CH}_2\text{CHCHCH}=\text{CH}_2)\text{Br}(\text{Cp}^*)]\text{PF}_6$  (**II-22**) in  $\text{CD}_3\text{NO}_2$  at rt.



Position	$\delta(^1\text{H})$ [ppm]	$^3J_{\text{HH}}$ [Hz]	$\delta(^{13}\text{C})$ [ppm]
1 <sub>syn</sub>	4.26	8, 3	68.6
1 <sub>anti</sub>	4.07	12, 3	68.6
2	5.39	12, 7, 6	107.4
3	4.90	7	90.9
4	3.86	12, 7	100.6
5 <sub>syn</sub>	4.43	7	78.0
5 <sub>anti</sub>	4.13	12	78.0
6	1.98	-	9.3
7	-	-	109.4

**Table N9.**  $^1\text{H}$ - and  $^{13}\text{C}$ -NMR data for (*E*)-2,6-dimethyl-4-(3-(*p*-nitrophenyl)-1-*p*-tolylallyl)phenol and (*E*)-2,6-dimethyl-4-(1-(*p*-nitrophenyl)-3-*p*-tolylallyl)phenol (**III-8a**) in  $\text{CD}_3\text{Cl}$  at rt.

Position	major		minor	
	$\delta(^1\text{H})$ [ppm]	$\delta(^{13}\text{C})$ [ppm]	$\delta(^1\text{H})$ [ppm]	$\delta(^{13}\text{C})$ [ppm]
1	-	x	-	x
2	7.13	x	8.20	124.0
3	7.13	x	7.43	129.8
4	-	x	-	x
5	4.80	53.7	4.87	53.7
6	6.86	193.3	6.56	130.7
7	6.40	129.5	6.33	132.6
8	-	144.3	-	x
9	7.51	127.1	7.24	126.7
10	8.19	124.4	7.13	x
11	-	147.4	-	x
12	-	x	-	x
13	6.85	138.8	x	x
14	-	x	-	x
15	2.25	16.4	2.25	16.4
16	-	151.4	-	151.4
17	4.60	-	4.63	-
18	2.37	21.5	2.37	21.6

x overlap

**Table N10.**  $^1\text{H}$ - and  $^{13}\text{C}$ -NMR data for (*E*)-4-(3-(*p*-chlorophenyl)-1-*p*-tolylallyl)-2,6-dimethylphenol and (*E*)-4-(1-(*p*-chlorophen-yl)-3-*p*-tolylallyl)-2,6-dimethylphenol (**III-8b**) in  $\text{CD}_3\text{Cl}$  at rt.

Position	major		minor	
	$\delta(^1\text{H})$ [ppm]	$\delta(^{13}\text{C})$ [ppm]	$\delta(^1\text{H})$ [ppm]	$\delta(^{13}\text{C})$ [ppm]
1	-	x	-	x
2	x	x	x	x
3	x	x	x	x
4	-	x	-	x
5	4.75	53.1	4.75	52.8
6	6.64	134.0	6.56	x
7	6.29	129.5	6.30	131.2
8	-	x	-	x
9	x	x	x	x
10	x	x	x	x
11	-	x	-	x
12	-	x	-	x
13	6.86	x		x
14	-	123.2	-	123.2
15	2.24	16.0	2.24	16.0
16	-	x	-	x
17	4.55	-	4.56	-
18	2.36	21.0	2.36	21.2

x overlap

**Table N11.**  $^1\text{H}$ - and  $^{13}\text{C}$ -NMR data for (*E*)-2,6-dimethyl-4-(3-phenyl-1-*p*-tolylallyl)phenol and (*E*)-2,6-dimethyl-4-(1-phenyl-3-*p*-tolylallyl)phenol (**III-8c**) in  $\text{CD}_3\text{Cl}$  at rt.

Position	minor		major	
	$\delta(^1\text{H})$ [ppm]	$\delta(^{13}\text{C})$ [ppm]	$\delta(^1\text{H})$ [ppm]	$\delta(^{13}\text{C})$ [ppm]
1	-	x	-	x
2	7.15	x	x	x
3	7.28	x	7.17	x
4	-	x	-	x
5	4.79	53.9	4.76	53.5
6	6.63	132.5	6.66	133.7
7	6.32	131.2	6.36	131.0
8	-	x	-	x
9	7.32	x	7.42	x
10	7.14	x	7.33	x
11	-	x	-	x
12	-	x	-	x
13	6.88	129.0	6.88	129.0
14	-	123.3	-	123.3
15	2.34	16.4	2.34	16.4
16	-	151.2	-	151.2
17	x	-	x	-
18	2.35	21.4	2.34	21.6
19	x	x	x	x

x overlap

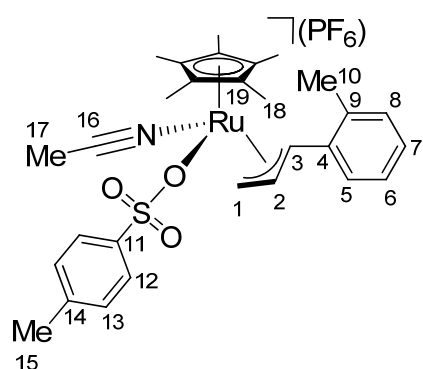
**Table N12.**  $^1\text{H}$ - and  $^{13}\text{C}$ -NMR data for (E)-4-(1,3-di-*p*-tolylallyl)-2,6-dimethylphenol (**III-8d**) in  $\text{CD}_3\text{Cl}$  at rt.

Position	$\delta(^1\text{H})$ [ppm]	$\delta(^{13}\text{C})$ [ppm]
1	-	x
2	x	x
3		x
4	-	x
5	4.77	53.2
6	6.63	130.6
7	6.34	132.4
8	-	x
9		x
10		x
11	-	x
12	-	x
13	6.89	128.6
14	-	x
15	2.26	16.4
16	-	151.1
17	4.56	-
18	2.38 or 2.37	21.4 or 21.6
19	2.37 or 2.38	21.6 or 21.4

x overlap



**Table N13.**  $^1\text{H}$ - and  $^{13}\text{C}$ -NMR data for  $[\text{Ru}(\eta^3\text{-}o\text{-MeC}_6\text{H}_4\text{CHCHCH}_2)(\text{Cp}^*)(\text{MeCN})(p\text{-MeC}_6\text{H}_4\text{-SO}_3)]\text{PF}_6$  in  $\text{CD}_2\text{Cl}_2$  at rt.



Position	$\delta(^1\text{H})$ [ppm]	$^3J_{\text{HH}}$ [Hz]	$\delta(^{13}\text{C})$ [ppm]
1 <sub>syn</sub>	4.46	7	67.9
1 <sub>anti</sub>	3.25	11	67.9
2	6.81	12, 11, 7	97.2
3	5.34	12	101.9
4	-	-	139.7
5	7.90	8	129.6
6	7.39	8	126.7
7	7.62	?	131.7
8	7.35	8	132.7
9	-	-	139.8
10	2.35	-	20.3
11	-	-	141.3
12	7.6	8	125.6
13	7.29	8	129.2
14	-	-	141.7
15	2.42	-	41.4
16	-	-	133.4
17	2.28	-	4.5
18	1.70	-	9.8
19	-	-	106.4

**6.7. References**

- [1] E. Pretsch, T. Clerc, J. Seibl, W. Simon, *Strukturaufklärung organischer Verbindungen*, Springer Verlag, **1990**.
- [2] SAINT, v. 6.01; Bruker AXS, Inc., Madison, **2001**, p. Software for CCD diffractometers.
- [3] G. M. Sheldrick, in *SHELXLS-97*, University of Göttingen, Göttingen, Germany, **1997**.
- [4] L. Farrugia, *Journal of Applied Crystallography* **1999**, *32*, 837-838.
- [5] R. Blessing, *Acta Crystallographica Section A* **1995**, *51*, 33-38.
- [6] M. J. T. Frisch, G. W.; Schlegel, H. B.; Scuseria, G. E.; Robb, J. R. M. M. A.; Cheeseman, J. A., Jr.; Vreven, T.; Kudin, K., J. C. M. N.; Burant, J. M.; Iyengar, S. S.; Tomasi, J.; Barone, V.; B. C. Mennucci, M.; Scalmani, G.; Rega, N.; Petersson, G. A.; H. H. Nakatsuji, M.; Ehara, M.; Toyota, K.; Fukuda, R.; Hasegawa, J.; M. N. Ishida, T.; Honda, Y.; Kitao, O.; Nakai, H.; Klene, M.; Li, J. E. H. X.; Knox, H. P.; Cross, J. B.; Adamo, C.; Jaramillo, J.; R. S. Gomperts, R. E.; Yazyev, O.; Austin, A. J.; Cammi, R.; C. O. Pomelli, J. W.; Ayala, P. Y.; Morokuma, K.; Voth, G. A.; P. D. Salvador, J. J.; Zakrzewski, V. G.; Dapprich, S.; Daniels, M. C. F. A. D.; Strain, O.; Malick, D. K.; Rabuck, A. D.; K. F. Raghavachari, J. B.; Ortiz, J. V.; Cui, Q.; Baboul, A. G.; S. C. Clifford, J.; Stefanov, B. B.; Liu, G.; Liashenko, A.; Piskorz, I. M. P.; Komaromi, R. L.; Fox, D. J.; Keith, T.; Al-Laham, M. A.; C. Y. N. Peng, A.; Challacombe, M.; Gill, P. M. W.; Johnson, W. W. B.; Chen, M. W.; Gonzalez, C.; Pople, J. A. , Gaussian 03, Revision C.02; Gaussian, Inc., Wallingford, CT, **2004**.
- [7] A. Bayer, J. S. Svendsen, *European Journal of Organic Chemistry* **2001**, *2001*, 1769-1780.
- [8] Y. I. M. Nilsson, P. G. Andersson, J. E. Baeckvall, *Journal of the American Chemical Society* **1993**, *115*, 6609-6613.
- [9] G. Prévost, P. Miginiac, L. Miginiac-Groizeleau, *Bull. Soc. Chim. Fr.* **1964**, 2485-2492.
- [10] B. M. Trost, P. L. Fraise, Z. T. Ball, *Angewandte Chemie International Edition* **2002**, *41*, 1059-1061.

- [11] I. C. Cotterill, M. C. Shelton, D. E. W. Machermer, D. P. Henderson, E. J. Toone, *J. Chem. Soc. Perkin Trans. 1* **1998**, 1335 - 1342.
- [12] W. D. Emmons, A. F. Ferris, *Journal of the American Chemical Society* **2002**, *75*, 2257-2257.
- [13] A. M. Easton, M. J. A. Habib, J. Park, W. E. Watts, *J. Chem. Soc., Perkin Trans. 2* **1972**, 2290-2229.
- [14] A. Briot, C. Baehr, R. Brouillard, A. Wagner, C. Mioskowski, *The Journal of Organic Chemistry* **2004**, *69*, 1374-1377.
- [15] B. Steinmetz, W. A. Schenk, *Organometallics* **1999**, *18*, 943-946.
- [16] I. Fernández, R. Hermatschweiler, F. Breher, P. S. Pregosin, L. F. Veiros, M. J. Calhorda, *Angewandte Chemie International Edition* **2006**, *45*, 6386-6391.
- [17] H. Nagashima, K. Mukai, Y. Shiota, K. Ara, K. Itoh, H. Suzuki, N. Oshima, Y. Morooka, *Organometallics* **1985**, *4*, 1314-1315.
- [18] G. Babu, A. Orita, J. Otera, *Organic Letters* **2005**, *7*, 4641-4643.
- [19] O. Tsukasa, T. Masanao, *Journal Heterocyclic Chemistry* **1987**, *24*, 377-386.
- [20] S. Cacchi, G. Fabrizi, P. Pace, *The Journal of Organic Chemistry* **1998**, *63*, 1001-1011.
- [21] M. Bandini, A. Melloni, A. Umani-Ronchi, *Organic Letters* **2004**, *6*, 3199-3202.
- [22] S. Araki, S.-I. Manabe, Y. Butsugan, *Bulletin of the Chemical Society of Japan* **1984**, *57*, 1433-1434.
- [23] G. J. Bodwell, J. Li, *Organic Letters* **2001**, *4*, 127-130.
- [24] M. A. Lapitskaya, K. K. Pivnitskii, *Zhurnal Organicheskoi Khimii* **1990**, *26*, 1926-1929.
- [25] S. Kotha, E. Manivannan, T. Ganesh, N. Sreenivasachary, A. Deb, *Synlett* **1999**, *1999*, 1618-1620.
- [26] H. Schick, H. Schwarz, A. Finger, S. Schwarz, *Tetrahedron* **1982**, *38*, 1279-1283.
- [27] C. E. Schwartz, D. P. Curran, *Journal of the American Chemical Society* **2002**, *112*, 9272-9284.
- [28] M. Braun, R. Veith, *Tetrahedron Letters* **1986**, *27*, 179-182.
- [29] R. Thennati, P. Namasivayam, *S. Communications*, **1993**, *22*, 3095-3108.



**7.**

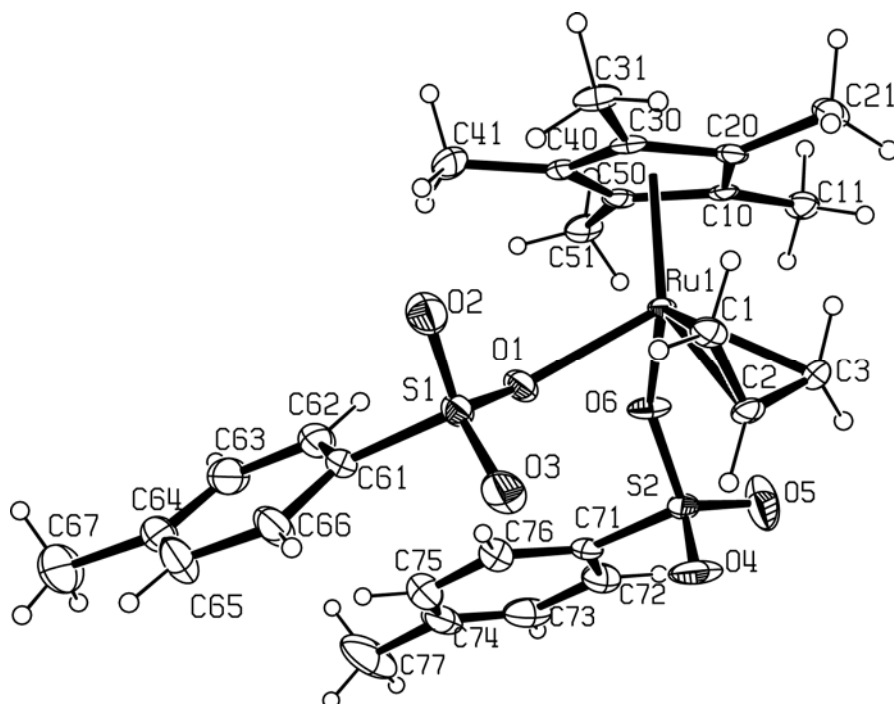
**Appendix**

**7.1. Abbreviations**

*	stereogenic center
°C	degree Celsius
μ	micro
Å	Ångström
Ac	acetyl
ADMET	acyclic diene polymerization
Ar	aryl
b	branched
b.p.	boiling point
BINAP	2,2'-bis(diphenylphosphino)-1,1'-binaphthyl
BINOL	1,1'-binaphthyl-2,2'-diol
Bn	benzyl
byp	bipyridine
CALB	candida antarctica lipase B
cat.	catalyst
Cbz	carboxybenzyl
CHCl <sub>3</sub>	chloroform
CM	cross metathesis
COD	1,5-cyclooctadiene
COT	1,3,5-cyclooctatriene
Cp	cyclopentadienyl
Cp*	1,2,3,4,5-pentamethylcyclopentadienyl
DMF	dimethylformamide
dppe	1,2-bis(diphenylphosphino)ethane
DPPent	bis(diphenylphosphino)pentane
EA	elemental analysis
EI-MS	electron impact mass spectroscopy
Eq.	equivalents
Et	ethyl
Et <sub>2</sub> O	diethyl ether
h	hours
Hz	Hertz

h $\nu$	irradiation
i.e.	in example
<sup>i</sup> Pr	isopropyl
l	linear
L	litre
LUMO	lowest unoccupied molecular orbital
m.p.	melting point
Me	methyl
MeCN	acetonitrile
MeNO <sub>2</sub>	nitromethane
Mes	mesitylene
min	minutes
MS	mass spectroscopy
<sup>n</sup> Bu	butyl
NMR	nuclear magnetic mesonance
NOESY	nuclear Overhauser spectroscopy
NPA	natural population analysis
<i>o</i> -	<i>ortho</i> -
ORTEP	oak ridge thermal ellipsoid plot
<i>p</i> -	<i>para</i> -
PGSE	pulsed gradient spin echo
Ph	phenyl
ppm	parts per million
RCM	ring closing metathesis
ROMP	ring opening metathesis
rt	room temperature
TBAB	tetrabutylammonium bromide
TBDPS	<i>tert</i> -butyldimethylsilyl
<sup>t</sup> Bu	<i>tert</i> -butyl
Tf	trifluoromethylsulfonyl
THF	Tetrahydrofuran
TMS	Tetramethylsilane
tppts	3,3',3''-Phosphinidynetris(benzenesulfonic acid)trisodium salt
WI	Wiberg indices

## 7.2. Crystallographic Data and Tables

**[Ru( $\eta^3$ -C<sub>3</sub>H<sub>5</sub>)(Cp\*)(*p*-MeC<sub>6</sub>H<sub>4</sub>SO<sub>3</sub>)<sub>2</sub>] (II-7)**

**Figure A.1.** ORTEP representation of [Ru( $\eta^3$ -C<sub>3</sub>H<sub>5</sub>)(Cp\*)(*p*-MeC<sub>6</sub>H<sub>4</sub>SO<sub>3</sub>)<sub>2</sub>] (thermal ellipsoids are drawn at 30% probability).

**Table A.1.** Experimental Data for the X-ray Study of [Ru( $\eta^3$ -C<sub>3</sub>H<sub>5</sub>)(Cp\*)(*p*-MeC<sub>6</sub>H<sub>4</sub>SO<sub>3</sub>)<sub>2</sub>]

Empirical formula	C <sub>30</sub> H <sub>40</sub> O <sub>7</sub> RuS <sub>2</sub>	
Formula weight	677.81	
Temperature	223(2) K	
Wavelength	0.71073 Å	
Crystal system	Monoclinic	
Space group	P2 <sub>1</sub>	
Unit cell dimensions	a = 8.1350(10) Å	α = 90°.
	b = 12.229(2) Å	β = 98.1100(10)°.
	c = 16.238(2) Å	γ = 90°.
Volume	1599.2(4) Å <sup>3</sup>	
Z	2	
Density (calculated)	1.408 Mg/m <sup>3</sup>	



Absorption coefficient	0.663 mm <sup>-1</sup>
F(000)	704
Crystal size	0.84 x 0.36 x 0.10 mm <sup>3</sup>
Theta range for data collection	1.27 to 33.51°.
Index ranges	-12<=h<=12, -18<=k<=18, -25<=l<=24
Reflections collected	22958
Independent reflections	11275 [R(int) = 0.0416]
Refinement method	Full-matrix least-squares on F <sup>2</sup>
Data / restraints / parameters	11275 / 1 / 371
Goodness-of-fit on F <sup>2</sup>	1.054
Final R indices [I>2sigma(I)]	R1 = 0.0493, wR2 = 0.0971
R indices (all data)	R1 = 0.0812, wR2 = 0.1121

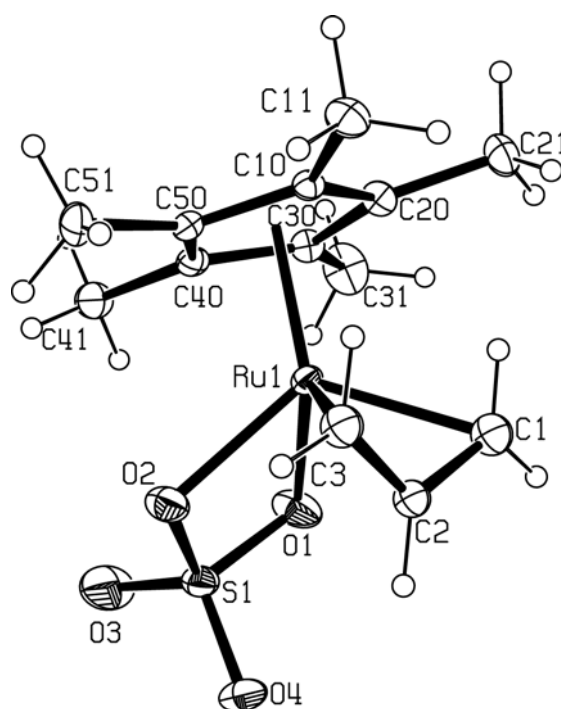
**Table A.2.** Bond Lengths [Å] and Angles [°] for [Ru( $\eta^3$ -C<sub>3</sub>H<sub>5</sub>)(Cp\*)(*p*-MeC<sub>6</sub>H<sub>4</sub>SO<sub>3</sub>)<sub>2</sub>]

Ru(1)-C(2)	2.135(3)	C(40)-C(50)	1.398(6)
Ru(1)-O(6)	2.144(3)	C(40)-C(41)	1.489(7)
Ru(1)-O(1)	2.154(4)	C(50)-C(51)	1.496(7)
Ru(1)-C(10)	2.173(4)	C(61)-C(62)	1.371(7)
Ru(1)-C(1)	2.185(4)	C(61)-C(66)	1.387(7)
Ru(1)-C(20)	2.196(3)	C(62)-C(63)	1.388(7)
Ru(1)-C(3)	2.213(4)	C(63)-C(64)	1.383(10)
Ru(1)-C(30)	2.228(4)	C(64)-C(65)	1.362(10)
Ru(1)-C(50)	2.265(5)	C(64)-C(67)	1.526(8)
Ru(1)-C(40)	2.313(4)	C(65)-C(66)	1.408(8)
S(1)-O(3)	1.434(3)	C(71)-C(72)	1.371(7)
S(1)-O(2)	1.454(3)	C(71)-C(76)	1.390(7)
S(1)-O(1)	1.474(4)	C(72)-C(73)	1.420(8)
S(1)-C(61)	1.778(4)	C(73)-C(74)	1.360(10)
S(2)-O(5)	1.413(5)	C(74)-C(75)	1.366(9)
S(2)-O(4)	1.446(4)	C(74)-C(77)	1.526(8)
S(2)-O(6)	1.490(3)	C(75)-C(76)	1.387(8)
S(2)-C(71)	1.768(4)	C(4)-C(5)	1.460(12)
O(7)-C(5)	1.203(11)	C(5)-C(6)	1.467(12)
C(1)-C(2)	1.396(6)	C(2)-Ru(1)-O(6)	95.31(14)
C(2)-C(3)	1.402(6)	C(2)-Ru(1)-O(1)	90.57(15)
C(10)-C(20)	1.429(6)	O(6)-Ru(1)-O(1)	77.69(12)
C(10)-C(50)	1.457(7)	C(2)-Ru(1)-C(10)	126.53(15)
C(10)-C(11)	1.491(6)	O(6)-Ru(1)-C(10)	92.85(15)
C(20)-C(30)	1.444(6)	O(1)-Ru(1)-C(10)	142.64(16)
C(20)-C(21)	1.504(5)	C(2)-Ru(1)-C(1)	37.69(15)
C(30)-C(40)	1.439(7)	O(6)-Ru(1)-C(1)	130.77(15)
C(30)-C(31)	1.487(6)	O(1)-Ru(1)-C(1)	87.14(16)

C(10)-Ru(1)-C(1)	123.93(16)	O(6)-S(2)-C(71)	102.8(2)
C(2)-Ru(1)-C(20)	109.29(14)	S(1)-O(1)-Ru(1)	134.4(2)
O(6)-Ru(1)-C(20)	130.65(16)	S(2)-O(6)-Ru(1)	137.8(2)
O(1)-Ru(1)-C(20)	141.01(15)	C(2)-C(1)-Ru(1)	69.2(2)
C(10)-Ru(1)-C(20)	38.18(16)	C(1)-C(2)-C(3)	114.7(3)
C(1)-Ru(1)-C(20)	89.06(16)	C(1)-C(2)-Ru(1)	73.1(2)
C(2)-Ru(1)-C(3)	37.56(16)	C(3)-C(2)-Ru(1)	74.2(2)
O(6)-Ru(1)-C(3)	85.21(16)	C(2)-C(3)-Ru(1)	68.2(2)
O(1)-Ru(1)-C(3)	123.35(16)	C(20)-C(10)-C(50)	106.3(4)
C(10)-Ru(1)-C(3)	91.10(17)	C(20)-C(10)-C(11)	128.4(4)
C(1)-Ru(1)-C(3)	64.8(2)	C(50)-C(10)-C(11)	124.4(4)
C(20)-Ru(1)-C(3)	89.27(16)	C(20)-C(10)-Ru(1)	71.8(2)
C(2)-Ru(1)-C(30)	121.27(16)	C(50)-C(10)-Ru(1)	74.3(2)
O(6)-Ru(1)-C(30)	143.30(15)	C(11)-C(10)-Ru(1)	127.1(3)
O(1)-Ru(1)-C(30)	102.92(15)	C(10)-C(20)-C(30)	108.8(3)
C(10)-Ru(1)-C(30)	64.10(17)	C(10)-C(20)-C(21)	124.9(4)
C(1)-Ru(1)-C(30)	85.56(16)	C(30)-C(20)-C(21)	125.7(4)
C(20)-Ru(1)-C(30)	38.09(16)	C(10)-C(20)-Ru(1)	70.1(2)
C(3)-Ru(1)-C(30)	121.17(17)	C(30)-C(20)-Ru(1)	72.2(2)
C(2)-Ru(1)-C(50)	163.88(16)	C(21)-C(20)-Ru(1)	130.7(2)
O(6)-Ru(1)-C(50)	82.31(15)	C(40)-C(30)-C(20)	106.9(4)
O(1)-Ru(1)-C(50)	104.38(16)	C(40)-C(30)-C(31)	126.4(4)
C(10)-Ru(1)-C(50)	38.26(17)	C(20)-C(30)-C(31)	126.0(4)
C(1)-Ru(1)-C(50)	146.88(17)	C(40)-C(30)-Ru(1)	74.8(2)
C(20)-Ru(1)-C(50)	62.33(15)	C(20)-C(30)-Ru(1)	69.8(2)
C(3)-Ru(1)-C(50)	126.38(18)	C(31)-C(30)-Ru(1)	128.1(3)
C(30)-Ru(1)-C(50)	61.76(17)	C(50)-C(40)-C(30)	108.8(5)
C(2)-Ru(1)-C(40)	155.15(17)	C(50)-C(40)-C(41)	126.2(6)
O(6)-Ru(1)-C(40)	107.95(16)	C(30)-C(40)-C(41)	125.1(5)
O(1)-Ru(1)-C(40)	86.05(15)	C(50)-C(40)-Ru(1)	70.3(3)
C(10)-Ru(1)-C(40)	62.33(17)	C(30)-C(40)-Ru(1)	68.3(2)
C(1)-Ru(1)-C(40)	117.47(18)	C(41)-C(40)-Ru(1)	127.7(3)
C(20)-Ru(1)-C(40)	61.72(15)	C(40)-C(50)-C(10)	109.0(5)
C(3)-Ru(1)-C(40)	150.22(17)	C(40)-C(50)-C(51)	127.1(5)
C(30)-Ru(1)-C(40)	36.88(17)	C(10)-C(50)-C(51)	123.9(5)
C(50)-Ru(1)-C(40)	35.54(16)	C(40)-C(50)-Ru(1)	74.1(3)
O(3)-S(1)-O(2)	113.2(3)	C(10)-C(50)-Ru(1)	67.5(2)
O(3)-S(1)-O(1)	113.6(2)	C(51)-C(50)-Ru(1)	124.7(3)
O(2)-S(1)-O(1)	111.4(2)	C(62)-C(61)-C(66)	120.3(4)
O(3)-S(1)-C(61)	107.4(2)	C(62)-C(61)-S(1)	121.8(3)
O(2)-S(1)-C(61)	107.0(2)	C(66)-C(61)-S(1)	117.9(4)
O(1)-S(1)-C(61)	103.5(2)	C(61)-C(62)-C(63)	120.1(5)
O(5)-S(2)-O(4)	114.4(3)	C(64)-C(63)-C(62)	120.7(6)
O(5)-S(2)-O(6)	113.1(3)	C(65)-C(64)-C(63)	119.0(5)
O(4)-S(2)-O(6)	111.1(2)	C(65)-C(64)-C(67)	120.1(7)
O(5)-S(2)-C(71)	107.1(2)	C(63)-C(64)-C(67)	120.9(7)
O(4)-S(2)-C(71)	107.3(2)	C(64)-C(65)-C(66)	121.5(6)

C(61)-C(66)-C(65)	118.5(6)	C(73)-C(74)-C(77)	119.2(7)
C(72)-C(71)-C(76)	119.8(4)	C(75)-C(74)-C(77)	122.4(7)
C(72)-C(71)-S(2)	121.2(4)	C(74)-C(75)-C(76)	122.0(6)
C(76)-C(71)-S(2)	118.9(4)	C(75)-C(76)-C(71)	119.4(5)
C(71)-C(72)-C(73)	119.0(6)	O(7)-C(5)-C(4)	123.2(11)
C(74)-C(73)-C(72)	121.4(6)	O(7)-C(5)-C(6)	117.9(9)
C(73)-C(74)-C(75)	118.5(5)	C(4)-C(5)-C(6)	118.9(9)

**[Ru( $\eta^3$ -C<sub>3</sub>H<sub>5</sub>)(Cp\*)( $\kappa^2$ -SO<sub>4</sub>)] (II-9)**



**Figure A.2.** ORTEP representation of [Ru( $\eta^3$ -C<sub>3</sub>H<sub>5</sub>)(Cp\*)( $\kappa^2$ -SO<sub>4</sub>)] (thermal ellipsoids are drawn at 30% probability).

**Table A.3.** Experimental Data for the X-ray Study of [Ru( $\eta^3$ -C<sub>3</sub>H<sub>5</sub>)(Cp\*)( $\kappa^2$ -SO<sub>4</sub>)]

Empirical formula	C <sub>13</sub> H <sub>20</sub> O <sub>4</sub> RuS
Formula weight	373.42
Temperature	233(2) K
Wavelength	0.71073 Å
Crystal system	Orthorhombic
Space group	<i>P</i> 2 <sub>1</sub> 2 <sub>1</sub> 2 <sub>1</sub>
Unit cell dimensions	<i>a</i> = 8.4076(13) Å $\alpha$ = 90°.

	$b = 11.6192(18) \text{ \AA}$	$\beta = 90^\circ$
	$c = 14.515(2) \text{ \AA}$	$\gamma = 90^\circ$
Volume	1418.0(4) $\text{\AA}^3$	
Z	4	
Density (calculated)	1.749 $\text{Mg/m}^3$	
Absorption coefficient	1.259 $\text{mm}^{-1}$	
F(000)	760	
Crystal size	0.50 x 0.34 x 0.06 $\text{mm}^3$	
Theta range for data collection	2.25 to 33.64°.	
Index ranges	-12<=h<=12, -17<=k<=17, -22<=l<=21	
Reflections collected	20859	
Independent reflections	5209 [R(int) = 0.0375]	
Refinement method	Full-matrix least-squares on F <sup>2</sup>	
Data / restraints / parameters	5209 / 0 / 173	
Goodness-of-fit on F <sup>2</sup>	1.022	
Final R indices [I>2sigma(I)]	R1 = 0.0393, wR2 = 0.0837	
R indices (all data)	R1 = 0.0551, wR2 = 0.0900	

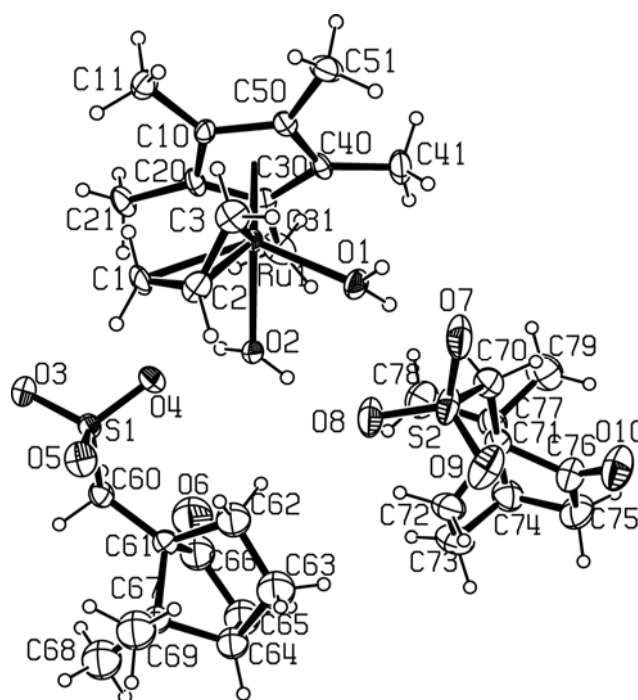
**Table A.4.** Bond Lengths [ $\text{\AA}$ ] and Angles [ $^\circ$ ] for  $[\text{Ru}(\eta^3\text{-C}_3\text{H}_5)(\text{Cp}^*)(\kappa^2\text{-SO}_4)]$

Ru(1)-O(2)	2.103(3)	C(30)-C(40)	1.432(5)
Ru(1)-O(1)	2.108(3)	C(30)-C(31)	1.489(5)
Ru(1)-C(3)	2.139(10)	C(40)-C(50)	1.437(5)
Ru(1)-C(2)	2.163(6)	C(40)-C(41)	1.504(4)
Ru(1)-C(40)	2.173(3)	C(50)-C(51)	1.491(4)
Ru(1)-C(1)	2.181(8)	O(2)-Ru(1)-O(1)	66.86(10)
Ru(1)-C(50)	2.188(3)	O(2)-Ru(1)-C(3)	89.7(3)
Ru(1)-C(30)	2.211(3)	O(1)-Ru(1)-C(3)	117.6(3)
Ru(1)-C(10)	2.251(3)	O(2)-Ru(1)-C(2)	83.8(2)
Ru(1)-C(20)	2.276(4)	O(1)-Ru(1)-C(2)	92.1(2)
S(1)-O(3)	1.429(3)	C(3)-Ru(1)-C(2)	26.0(3)
S(1)-O(4)	1.437(3)	O(2)-Ru(1)-C(40)	92.83(12)
S(1)-O(1)	1.518(3)	O(1)-Ru(1)-C(40)	94.79(14)
S(1)-O(2)	1.527(3)	C(3)-Ru(1)-C(40)	145.6(3)
C(1)-C(2)	1.400(10)	C(2)-Ru(1)-C(40)	170.4(2)
C(2)-C(3)	1.396(10)	O(2)-Ru(1)-C(1)	117.8(2)
C(10)-C(20)	1.431(4)	O(1)-Ru(1)-C(1)	91.0(2)
C(10)-C(50)	1.445(5)	C(3)-Ru(1)-C(1)	49.1(4)
C(10)-C(11)	1.493(5)	C(2)-Ru(1)-C(1)	37.6(3)
C(20)-C(30)	1.428(5)	C(40)-Ru(1)-C(1)	148.5(2)
C(20)-C(21)	1.493(5)	O(2)-Ru(1)-C(50)	92.48(13)

---

O(1)-Ru(1)-C(50)	129.65(16)	O(2)-S(1)-Ru(1)	49.68(10)
C(3)-Ru(1)-C(50)	107.1(3)	S(1)-O(1)-Ru(1)	96.77(13)
C(2)-Ru(1)-C(50)	132.5(2)	S(1)-O(2)-Ru(1)	96.70(13)
C(40)-Ru(1)-C(50)	38.49(12)	C(2)-C(1)-Ru(1)	70.5(4)
C(1)-Ru(1)-C(50)	137.7(2)	C(3)-C(2)-C(1)	116.4(7)
O(2)-Ru(1)-C(30)	126.03(14)	C(3)-C(2)-Ru(1)	76.3(4)
O(1)-Ru(1)-C(30)	91.32(14)	C(1)-C(2)-Ru(1)	71.9(4)
C(3)-Ru(1)-C(30)	141.9(3)	C(2)-C(3)-Ru(1)	67.2(4)
C(2)-Ru(1)-C(30)	148.4(2)	C(20)-C(10)-C(50)	107.7(3)
C(40)-Ru(1)-C(30)	38.11(12)	C(20)-C(10)-C(11)	125.6(4)
C(1)-Ru(1)-C(30)	111.0(2)	C(50)-C(10)-C(11)	126.0(3)
C(50)-Ru(1)-C(30)	63.62(11)	C(20)-C(10)-Ru(1)	72.5(2)
O(2)-Ru(1)-C(10)	125.24(11)	C(50)-C(10)-Ru(1)	68.64(18)
O(1)-Ru(1)-C(10)	153.77(13)	C(11)-C(10)-Ru(1)	131.9(2)
C(3)-Ru(1)-C(10)	87.3(3)	C(30)-C(20)-C(10)	108.3(3)
C(2)-Ru(1)-C(10)	111.4(2)	C(30)-C(20)-C(21)	126.3(3)
C(40)-Ru(1)-C(10)	63.49(11)	C(10)-C(20)-C(21)	125.1(4)
C(1)-Ru(1)-C(10)	100.5(2)	C(30)-C(20)-Ru(1)	68.96(19)
C(50)-Ru(1)-C(10)	37.96(14)	C(10)-C(20)-Ru(1)	70.6(2)
C(30)-Ru(1)-C(10)	62.58(13)	C(21)-C(20)-Ru(1)	131.3(3)
O(2)-Ru(1)-C(20)	153.75(12)	C(20)-C(30)-C(40)	108.4(3)
O(1)-Ru(1)-C(20)	121.48(12)	C(20)-C(30)-C(31)	124.8(4)
C(3)-Ru(1)-C(20)	104.9(3)	C(40)-C(30)-C(31)	126.8(4)
C(2)-Ru(1)-C(20)	118.59(19)	C(20)-C(30)-Ru(1)	73.95(19)
C(40)-Ru(1)-C(20)	62.78(12)	C(40)-C(30)-Ru(1)	69.52(17)
C(1)-Ru(1)-C(20)	87.9(2)	C(31)-C(30)-Ru(1)	123.7(3)
C(50)-Ru(1)-C(20)	62.65(13)	C(30)-C(40)-C(50)	107.8(2)
C(30)-Ru(1)-C(20)	37.08(14)	C(30)-C(40)-C(41)	126.5(3)
C(10)-Ru(1)-C(20)	36.86(11)	C(50)-C(40)-C(41)	125.6(3)
O(3)-S(1)-O(4)	113.54(19)	C(30)-C(40)-Ru(1)	72.37(17)
O(3)-S(1)-O(1)	111.3(2)	C(50)-C(40)-Ru(1)	71.30(17)
O(4)-S(1)-O(1)	110.9(2)	C(41)-C(40)-Ru(1)	124.0(2)
O(3)-S(1)-O(2)	110.7(2)	C(40)-C(50)-C(10)	107.8(3)
O(4)-S(1)-O(2)	110.3(2)	C(40)-C(50)-C(51)	126.9(4)
O(1)-S(1)-O(2)	99.26(14)	C(10)-C(50)-C(51)	125.2(3)
O(3)-S(1)-Ru(1)	127.79(14)	C(40)-C(50)-Ru(1)	70.21(16)
O(4)-S(1)-Ru(1)	118.67(14)	C(10)-C(50)-Ru(1)	73.40(18)
O(1)-S(1)-Ru(1)	49.85(11)	C(51)-C(50)-Ru(1)	123.7(2)

**[Ru( $\eta^3$ -C<sub>3</sub>H<sub>5</sub>)(Cp\*)(H<sub>2</sub>O)<sub>2</sub>](camphor-SO<sub>3</sub>)<sub>2</sub> (II-14)**



**Figure A.3.** ORTEP representation of [Ru( $\eta^3$ -C<sub>3</sub>H<sub>5</sub>)(Cp\*)(H<sub>2</sub>O)<sub>2</sub>](camphor-SO<sub>3</sub>)<sub>2</sub> (thermal ellipsoids are drawn at 30% probability).

**Table A.5.** Experimental Data for the X-ray Study of [Ru( $\eta^3$ -C<sub>3</sub>H<sub>5</sub>)(Cp\*)(H<sub>2</sub>O)<sub>2</sub>](camphor-SO<sub>3</sub>)<sub>2</sub>

Empirical formula	C <sub>33</sub> H <sub>54</sub> O <sub>10</sub> RuS <sub>2</sub>	
Formula weight	847.71	
Temperature	230(2) K	
Wavelength	0.71073 Å	
Crystal system	Monoclinic	
Space group	<i>P</i> 2 <sub>1</sub>	
Unit cell dimensions	a = 6.8961(3) Å	α = 90°.
	b = 16.7105(7) Å	β = 97.8180(10)°.
	c = 17.5960(7) Å	γ = 90°.
Volume	2008.87(15) Å <sup>3</sup>	
Z	2	
Density (calculated)	1.401 Mg/m <sup>3</sup>	
Absorption coefficient	0.556 mm <sup>-1</sup>	
F(000)	888	
Crystal size	0.80 x 0.28 x 0.24 mm <sup>3</sup>	

Theta range for data collection	1.17 to 26.39°.
Index ranges	-8<=h<=8, -20<=k<=20, -21<=l<=22
Reflections collected	20331
Independent reflections	8250 [R(int) = 0.0490]
Refinement method	Full-matrix least-squares on F <sup>2</sup>
Data / restraints / parameters	8250 / 104 / 454
Goodness-of-fit on F <sup>2</sup>	1.019
Final R indices [I>2sigma(I)]	R1 = 0.0405, wR2 = 0.0999
R indices (all data)	R1 = 0.0523, wR2 = 0.1086

**Table A.6.** Bond Lengths [Å] and Angles [°] for [Ru( $\eta^3$ -C<sub>3</sub>H<sub>5</sub>)(Cp\*)(H<sub>2</sub>O)<sub>2</sub>](camphor-SO<sub>3</sub>)<sub>2</sub>

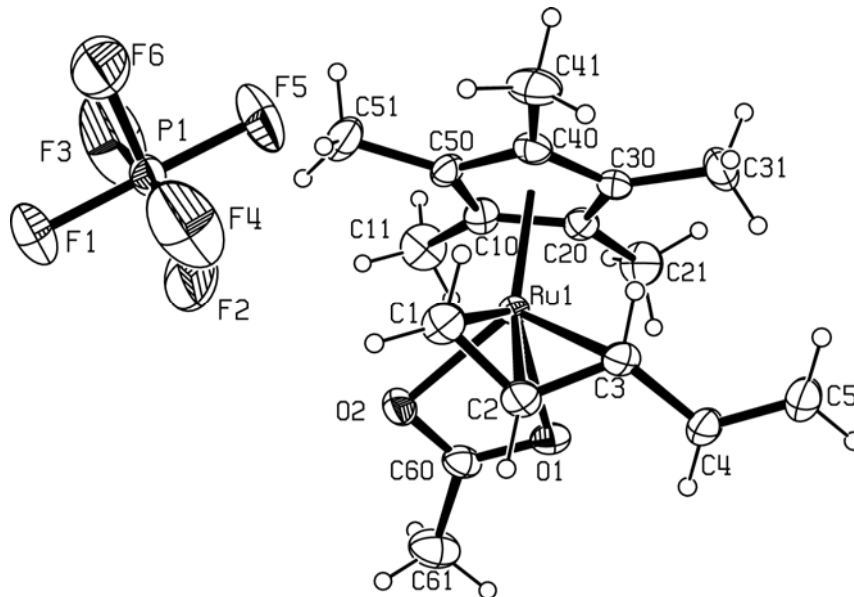
Ru(1)-C(2)	2.114(4)	C(64)-C(67)	1.544(10)
Ru(1)-O(1)	2.119(3)	C(65)-C(66)	1.531(12)
Ru(1)-O(2)	2.141(3)	C(66)-O(6)	1.224(11)
Ru(1)-C(50)	2.173(5)	C(67)-C(69)	1.491(11)
Ru(1)-C(10)	2.179(5)	C(67)-C(68)	1.541(11)
Ru(1)-C(3)	2.183(4)	O(3)-S(1)	1.461(4)
Ru(1)-C(20)	2.189(5)	O(4)-S(1)	1.452(3)
Ru(1)-C(1)	2.199(5)	O(5)-S(1)	1.446(4)
Ru(1)-C(40)	2.279(5)	C(70)-C(71)	1.516(7)
Ru(1)-C(30)	2.283(3)	C(70)-S(2)	1.795(7)
C(1)-C(2)	1.421(8)	C(71)-C(76)	1.506(7)
C(2)-C(3)	1.407(8)	C(71)-C(72)	1.558(7)
C(10)-C(20)	1.424(8)	C(71)-C(77)	1.558(7)
C(10)-C(50)	1.445(5)	C(72)-C(73)	1.546(9)
C(10)-C(11)	1.489(8)	C(73)-C(74)	1.499(9)
C(20)-C(30)	1.417(8)	C(74)-C(75)	1.530(9)
C(20)-C(21)	1.518(7)	C(74)-C(77)	1.538(8)
C(30)-C(40)	1.437(8)	C(75)-C(76)	1.517(8)
C(30)-C(31)	1.509(6)	C(76)-O(10)	1.210(7)
C(40)-C(50)	1.439(8)	C(77)-C(79)	1.502(8)
C(40)-C(41)	1.465(8)	C(77)-C(78)	1.518(9)
C(50)-C(51)	1.500(8)	O(7)-S(2)	1.471(5)
C(60)-C(61)	1.525(9)	O(8)-S(2)	1.457(4)
C(60)-S(1)	1.80(2)	O(9)-S(2)	1.419(5)
C(61)-C(66)	1.452(11)	C(2)-Ru(1)-O(1)	85.88(18)
C(61)-C(67)	1.549(9)	C(2)-Ru(1)-O(2)	86.02(19)
C(61)-C(62)	1.596(11)	O(1)-Ru(1)-O(2)	79.02(13)
C(62)-C(63)	1.542(12)	C(2)-Ru(1)-C(50)	126.3(2)
C(63)-C(64)	1.537(12)	O(1)-Ru(1)-C(50)	100.32(17)
C(64)-C(65)	1.513(12)	O(2)-Ru(1)-C(50)	147.72(17)

C(2)-Ru(1)-C(10)	109.7(2)	C(20)-C(10)-Ru(1)	71.4(3)
O(1)-Ru(1)-C(10)	137.98(18)	C(50)-C(10)-Ru(1)	70.4(4)
O(2)-Ru(1)-C(10)	138.73(18)	C(11)-C(10)-Ru(1)	130.4(4)
C(50)-Ru(1)-C(10)	38.79(12)	C(30)-C(20)-C(10)	109.4(4)
C(2)-Ru(1)-C(3)	38.2(2)	C(30)-C(20)-C(21)	124.6(6)
O(1)-Ru(1)-C(3)	79.4(2)	C(10)-C(20)-C(21)	125.4(5)
O(2)-Ru(1)-C(3)	120.95(16)	C(30)-C(20)-Ru(1)	75.2(3)
C(50)-Ru(1)-C(3)	90.10(19)	C(10)-C(20)-Ru(1)	70.6(3)
C(10)-Ru(1)-C(3)	89.4(2)	C(21)-C(20)-Ru(1)	128.1(4)
C(2)-Ru(1)-C(20)	123.5(2)	C(20)-C(30)-C(40)	108.2(3)
O(1)-Ru(1)-C(20)	150.59(17)	C(20)-C(30)-C(31)	127.7(6)
O(2)-Ru(1)-C(20)	101.24(18)	C(40)-C(30)-C(31)	124.2(6)
C(50)-Ru(1)-C(20)	63.8(2)	C(20)-C(30)-Ru(1)	68.0(3)
C(10)-Ru(1)-C(20)	38.1(2)	C(40)-C(30)-Ru(1)	71.5(3)
C(3)-Ru(1)-C(20)	122.7(2)	C(31)-C(30)-Ru(1)	125.8(3)
C(2)-Ru(1)-C(1)	38.4(2)	C(30)-C(40)-C(50)	107.2(4)
O(1)-Ru(1)-C(1)	120.90(16)	C(30)-C(40)-C(41)	127.5(5)
O(2)-Ru(1)-C(1)	79.21(19)	C(50)-C(40)-C(41)	125.2(5)
C(50)-Ru(1)-C(1)	125.4(2)	C(30)-C(40)-Ru(1)	71.8(2)
C(10)-Ru(1)-C(1)	90.0(2)	C(50)-C(40)-Ru(1)	67.2(3)
C(3)-Ru(1)-C(1)	66.7(3)	C(41)-C(40)-Ru(1)	128.7(4)
C(20)-Ru(1)-C(1)	87.54(19)	C(40)-C(41)-H(41A)	109.5
C(2)-Ru(1)-C(40)	161.9(2)	C(40)-C(41)-H(41B)	109.5
O(1)-Ru(1)-C(40)	89.78(17)	C(40)-C(50)-C(10)	108.3(5)
O(2)-Ru(1)-C(40)	110.38(18)	C(40)-C(50)-C(51)	123.7(5)
C(50)-Ru(1)-C(40)	37.6(2)	C(10)-C(50)-C(51)	127.2(6)
C(10)-Ru(1)-C(40)	63.2(2)	C(40)-C(50)-Ru(1)	75.2(3)
C(3)-Ru(1)-C(40)	123.8(2)	C(10)-C(50)-Ru(1)	70.8(4)
C(20)-Ru(1)-C(40)	62.26(12)	C(51)-C(50)-Ru(1)	128.2(4)
C(1)-Ru(1)-C(40)	149.30(19)	C(61)-C(60)-S(1)	120.5(12)
C(2)-Ru(1)-C(30)	157.3(2)	C(66)-C(61)-C(60)	115.3(10)
O(1)-Ru(1)-C(30)	114.5(2)	C(66)-C(61)-C(67)	101.8(7)
O(2)-Ru(1)-C(30)	88.05(14)	C(60)-C(61)-C(67)	118.5(9)
C(50)-Ru(1)-C(30)	62.54(17)	C(66)-C(61)-C(62)	101.1(7)
C(10)-Ru(1)-C(30)	62.57(19)	C(60)-C(61)-C(62)	118.1(9)
C(3)-Ru(1)-C(30)	150.48(15)	C(67)-C(61)-C(62)	99.1(6)
C(20)-Ru(1)-C(30)	36.9(2)	C(63)-C(62)-C(61)	102.8(7)
C(1)-Ru(1)-C(30)	118.9(2)	C(64)-C(63)-C(62)	105.0(8)
C(40)-Ru(1)-C(30)	36.7(2)	C(65)-C(64)-C(63)	104.4(8)
C(2)-C(1)-Ru(1)	67.6(3)	C(65)-C(64)-C(67)	105.1(7)
C(3)-C(2)-C(1)	116.8(5)	C(63)-C(64)-C(67)	99.2(7)
C(3)-C(2)-Ru(1)	73.6(2)	C(64)-C(65)-C(66)	100.1(8)
C(1)-C(2)-Ru(1)	74.0(3)	O(6)-C(66)-C(61)	127.9(9)
C(2)-C(3)-Ru(1)	68.3(3)	O(6)-C(66)-C(65)	122.1(10)
C(20)-C(10)-C(50)	106.8(5)	C(61)-C(66)-C(65)	110.0(8)
C(20)-C(10)-C(11)	126.6(5)	C(69)-C(67)-C(68)	107.1(8)
C(50)-C(10)-C(11)	125.9(6)	C(69)-C(67)-C(64)	114.4(7)



C(68)-C(67)-C(64)	111.1(7)	C(73)-C(74)-C(75)	106.8(6)
C(69A)-C(67)-C(61)	115.9(7)	C(73)-C(74)-C(77)	104.8(5)
C(68)-C(67)-C(61)	112.3(7)	C(75)-C(74)-C(77)	102.7(5)
C(64)-C(67)-C(61)	95.9(6)	C(76)-C(75)-C(74)	101.3(5)
O(5)-S(1)-O(4)	112.9(2)	O(10)-C(76)-C(71)	126.7(5)
O(5)-S(1)-O(3)	112.6(2)	O(10)-C(76)-C(75)	126.3(6)
O(4)-S(1)-O(3)	112.4(2)	C(71)-C(76)-C(75)	106.7(5)
O(5)-S(1)-C(60)	109.0(7)	C(79)-C(77)-C(78)	110.2(6)
O(4)-S(1)-C(60)	107.0(7)	C(79)-C(77)-C(74)	114.3(6)
O(3)-S(1)-C(60)	102.2(4)	C(78)-C(77)-C(74)	112.6(5)
C(71)-C(70)-S(2)	116.7(4)	C(79)-C(77)-C(71)	113.0(5)
C(76)-C(71)-C(70)	114.1(5)	C(78)-C(77)-C(71)	112.7(5)
C(76)-C(71)-C(72)	102.9(5)	C(74)-C(77)-C(71)	93.2(4)
C(70)-C(71)-C(72)	118.3(5)	O(9)-S(2)-O(8)	114.8(3)
C(76)-C(71)-C(77)	99.9(4)	O(9)-S(2)-O(7)	112.9(3)
C(70)-C(71)-C(77)	117.1(5)	O(8)-S(2)-O(7)	110.6(2)
C(72)-C(71)-C(77)	102.0(4)	O(9)-S(2)-C(70)	108.6(3)
C(73)-C(72)-C(71)	104.4(5)	O(8)-S(2)-C(70)	107.0(3)
C(74)-C(73)-C(72)	102.1(5)	O(7)-S(2)-C(70)	101.8(3)

**[Ru( $\kappa^2$ -O<sub>2</sub>CMe)( $\eta^3$ -CH<sub>2</sub>CHCH=CH<sub>2</sub>)(Cp<sup>\*</sup>)]PF<sub>6</sub> (II-17)**



**Figure A.4.** ORTEP representation of [Ru( $\kappa^2$ -O<sub>2</sub>CMe)( $\eta^3$ -CH<sub>2</sub>CHCH=CH<sub>2</sub>)(Cp<sup>\*</sup>)]PF<sub>6</sub> (thermal ellipsoids are drawn at 30% probability).

**Table A.7.** Experimental Data for the X-ray Study of  $[\text{Ru}(\kappa^2\text{-O}_2\text{CMe})(\eta^3\text{-CH}_2\text{CHCHCH}=\text{CH}_2)(\text{Cp}^*)]\text{PF}_6$ 

Empirical formula	$\text{C}_{17}\text{H}_{25}\text{F}_6\text{O}_2\text{PRu}$		
Formula weight	507.41		
Temperature	233(2) K		
Wavelength	0.71073 Å		
Crystal system	Monoclinic		
Space group	$P2_1$		
Unit cell dimensions	$a = 9.0768(7)$ Å	$\alpha = 90^\circ$ .	
	$b = 8.3752(6)$ Å	$\beta = 95.8600(10)^\circ$ .	
	$c = 13.2634(9)$ Å	$\gamma = 90^\circ$ .	
Volume	1003.01(13) Å <sup>3</sup>		
Z	2		
Density (calculated)	1.680 Mg/m <sup>3</sup>		
Absorption coefficient	0.924 mm <sup>-1</sup>		
F(000)	512		
Crystal size	0.40 x 0.34 x 0.05 mm <sup>3</sup>		
Theta range for data collection	1.54 to 33.57°.		
Index ranges	-13 ≤ h ≤ 13, -12 ≤ k ≤ 13, -20 ≤ l ≤ 20		
Reflections collected	7597		
Independent reflections	3582 [R(int) = 0.0247]		
Refinement method	Full-matrix least-squares on F <sup>2</sup>		
Data / restraints / parameters	3582 / 1 / 250		
Goodness-of-fit on F <sup>2</sup>	1.018		
Final R indices [I > 2σ(I)]	R1 = 0.0350, wR2 = 0.0690		
R indices (all data)	R1 = 0.0558, wR2 = 0.0744		

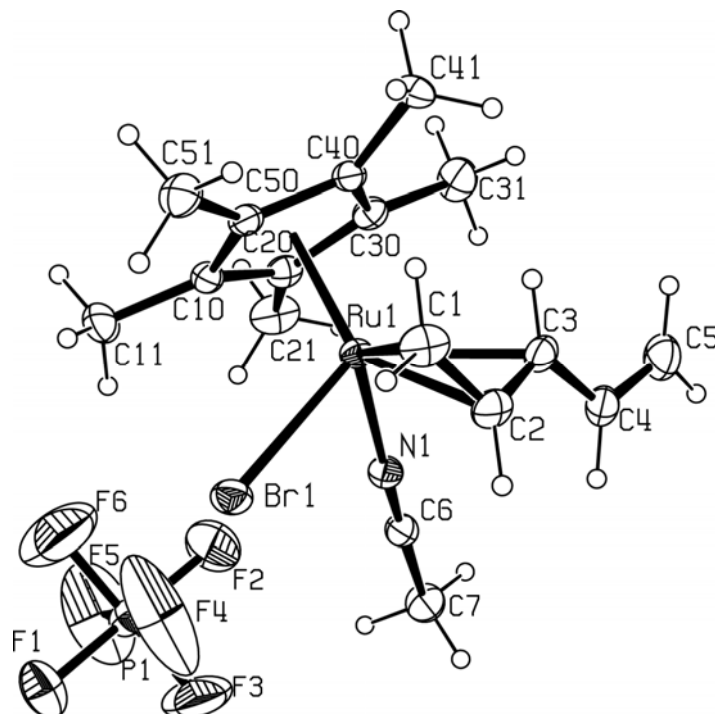
**Table A.8.** Bond Lengths [Å] and Angles [°] for  $[\text{Ru}(\kappa^2\text{-O}_2\text{CMe})(\eta^3\text{-CH}_2\text{CHCHCH}=\text{CH}_2)(\text{Cp}^*)]\text{PF}_6$ 

Ru(1)-C(2)	2.123(6)	Ru(1)-C(30)	2.236(7)
Ru(1)-O(2)	2.139(4)	Ru(1)-C(20)	2.243(5)
Ru(1)-O(1)	2.147(3)	Ru(1)-C(3)	2.260(7)
Ru(1)-C(50)	2.183(4)	Ru(1)-C(60)	2.511(5)
Ru(1)-C(1)	2.195(8)	P(1)-F(3)	1.532(6)
Ru(1)-C(10)	2.205(5)	P(1)-F(4)	1.549(8)
Ru(1)-C(40)	2.223(5)	P(1)-F(2)	1.554(5)

P(1)-F(6)	1.561(5)	C(40)-Ru(1)-C(30)	36.6(2)
P(1)-F(5)	1.583(6)	C(2)-Ru(1)-C(20)	152.1(2)
P(1)-F(1)	1.584(4)	O(2)-Ru(1)-C(20)	117.45(16)
O(1)-C(60)	1.275(7)	O(1)-Ru(1)-C(20)	89.9(2)
O(2)-C(60)	1.285(7)	C(50)-Ru(1)-C(20)	62.73(17)
C(1)-C(2)	1.409(12)	C(1)-Ru(1)-C(20)	150.9(3)
C(2)-C(3)	1.397(12)	C(10)-Ru(1)-C(20)	37.00(18)
C(3)-C(4)	1.500(9)	C(40)-Ru(1)-C(20)	61.88(19)
C(4)-C(5)	1.338(9)	C(30)-Ru(1)-C(20)	37.1(2)
C(10)-C(20)	1.412(7)	C(2)-Ru(1)-C(3)	37.0(3)
C(10)-C(50)	1.435(7)	O(2)-Ru(1)-C(3)	118.0(2)
C(10)-C(11)	1.492(8)	O(1)-Ru(1)-C(3)	89.14(18)
C(20)-C(30)	1.425(9)	C(50)-Ru(1)-C(3)	131.6(2)
C(20)-C(21)	1.513(7)	C(1)-Ru(1)-C(3)	64.0(3)
C(30)-C(40)	1.401(9)	C(10)-Ru(1)-C(3)	149.7(3)
C(30)-C(31)	1.498(9)	C(40)-Ru(1)-C(3)	95.2(2)
C(40)-C(50)	1.449(7)	C(30)-Ru(1)-C(3)	87.6(3)
C(40)-C(41)	1.497(7)	C(20)-Ru(1)-C(3)	115.2(3)
C(50)-C(51)	1.498(7)	C(2)-Ru(1)-C(60)	86.2(2)
C(60)-C(61)	1.488(8)	O(2)-Ru(1)-C(60)	30.78(16)
C(2)-Ru(1)-O(2)	85.2(2)	O(1)-Ru(1)-C(60)	30.51(19)
C(2)-Ru(1)-O(1)	87.4(3)	C(50)-Ru(1)-C(60)	121.91(17)
O(2)-Ru(1)-O(1)	61.29(19)	C(1)-Ru(1)-C(60)	102.8(3)
C(2)-Ru(1)-C(50)	132.4(2)	C(10)-Ru(1)-C(60)	96.25(17)
O(2)-Ru(1)-C(50)	100.71(16)	C(40)-Ru(1)-C(60)	158.87(17)
O(1)-Ru(1)-C(50)	136.90(17)	C(30)-Ru(1)-C(60)	139.3(2)
C(2)-Ru(1)-C(1)	38.0(3)	C(20)-Ru(1)-C(60)	105.04(18)
O(2)-Ru(1)-C(1)	83.6(3)	C(3)-Ru(1)-C(60)	105.6(2)
O(1)-Ru(1)-C(1)	118.7(3)	F(3)-P(1)-F(4)	176.1(6)
C(50)-Ru(1)-C(1)	95.2(2)	F(3)-P(1)-F(2)	88.0(6)
C(2)-Ru(1)-C(10)	169.1(2)	F(4)-P(1)-F(2)	88.3(6)
O(2)-Ru(1)-C(10)	91.39(16)	F(3)-P(1)-F(6)	89.5(6)
O(1)-Ru(1)-C(10)	100.09(19)	F(4)-P(1)-F(6)	94.2(6)
C(50)-Ru(1)-C(10)	38.18(19)	F(2)-P(1)-F(6)	177.5(6)
C(1)-Ru(1)-C(10)	131.3(2)	F(3)-P(1)-F(5)	92.8(4)
C(2)-Ru(1)-C(40)	113.2(2)	F(4)-P(1)-F(5)	88.8(5)
O(2)-Ru(1)-C(40)	137.59(17)	F(2)-P(1)-F(5)	91.9(4)
O(1)-Ru(1)-C(40)	150.5(2)	F(6)-P(1)-F(5)	88.3(4)
C(50)-Ru(1)-C(40)	38.38(19)	F(3)-P(1)-F(1)	88.9(4)
C(1)-Ru(1)-C(40)	89.0(3)	F(4)-P(1)-F(1)	89.6(4)
C(10)-Ru(1)-C(40)	63.14(19)	F(2)-P(1)-F(1)	88.8(4)
C(2)-Ru(1)-C(30)	121.6(3)	F(6)-P(1)-F(1)	91.1(4)
O(2)-Ru(1)-C(30)	153.1(2)	F(5)-P(1)-F(1)	178.2(3)
O(1)-Ru(1)-C(30)	114.9(3)	C(60)-O(1)-Ru(1)	90.7(3)
C(50)-Ru(1)-C(30)	62.8(2)	C(60)-O(2)-Ru(1)	90.8(3)
C(1)-Ru(1)-C(30)	117.4(2)	C(2)-C(1)-Ru(1)	68.2(4)
C(10)-Ru(1)-C(30)	62.4(2)	C(3)-C(2)-C(1)	114.6(7)

C(3)-C(2)-Ru(1)	76.8(4)	C(40)-C(30)-Ru(1)	71.2(3)
C(1)-C(2)-Ru(1)	73.7(4)	C(20)-C(30)-Ru(1)	71.7(3)
C(2)-C(3)-C(4)	119.7(6)	C(31)-C(30)-Ru(1)	130.0(5)
C(2)-C(3)-Ru(1)	66.2(4)	C(30)-C(40)-C(50)	107.9(5)
C(4)-C(3)-Ru(1)	113.5(4)	C(30)-C(40)-C(41)	126.3(6)
C(2)-C(3)-H(3A)	120.1	C(50)-C(40)-C(41)	125.6(5)
C(5)-C(4)-C(3)	120.1(5)	C(30)-C(40)-Ru(1)	72.2(4)
C(20)-C(10)-C(50)	108.1(4)	C(50)-C(40)-Ru(1)	69.3(3)
C(20)-C(10)-C(11)	126.2(5)	C(41)-C(40)-Ru(1)	128.1(4)
C(50)-C(10)-C(11)	125.7(5)	C(10)-C(50)-C(40)	107.0(4)
C(20)-C(10)-Ru(1)	73.0(3)	C(10)-C(50)-C(51)	124.9(5)
C(50)-C(10)-Ru(1)	70.1(3)	C(40)-C(50)-C(51)	127.7(5)
C(11)-C(10)-Ru(1)	122.6(4)	C(10)-C(50)-Ru(1)	71.7(3)
C(10)-C(20)-C(30)	108.3(5)	C(40)-C(50)-Ru(1)	72.3(3)
C(10)-C(20)-C(21)	125.8(5)	C(51)-C(50)-Ru(1)	127.2(4)
C(30)-C(20)-C(21)	125.9(5)	O(1)-C(60)-O(2)	117.2(4)
C(10)-C(20)-Ru(1)	70.0(3)	O(1)-C(60)-C(61)	120.3(5)
C(30)-C(20)-Ru(1)	71.2(3)	O(2)-C(60)-C(61)	122.5(5)
C(21)-C(20)-Ru(1)	125.0(4)	O(1)-C(60)-Ru(1)	58.8(2)
C(40)-C(30)-C(20)	108.7(5)	O(2)-C(60)-Ru(1)	58.4(2)
C(40)-C(30)-C(31)	126.0(7)	C(61)-C(60)-Ru(1)	179.1(5)
C(20)-C(30)-C(31)	124.7(6)		

**[Ru( $\eta^3$ -CH<sub>2</sub>CHCHCH=CH<sub>2</sub>)Br(Cp\*)(MeCN)]PF<sub>6</sub> (II-18)**



**Figure A.5.** ORTEP representation of [Ru( $\eta^3$ -CH<sub>2</sub>CHCHCH=CH<sub>2</sub>)Br(Cp\*)(MeCN)]PF<sub>6</sub> (thermal ellipsoids are drawn at 30% probability).

**Table A.9.** Experimental Data for the X-ray Study of  $[\text{Ru}(\eta^3\text{-CH}_2\text{CHCHCH}=\text{CH}_2)\text{Br}(\text{Cp}^*)(\text{MeCN})]\text{PF}_6$ 

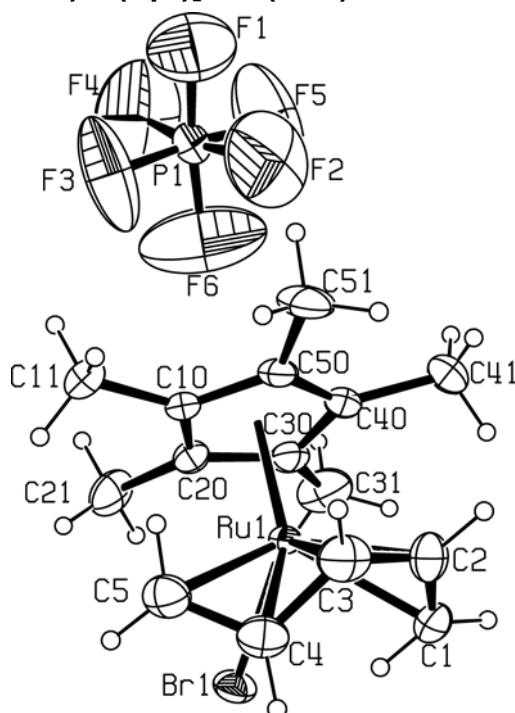
Empirical formula	$\text{C}_{17}\text{H}_{25}\text{BrF}_6\text{NPRu}$		
Formula weight	612.51		
Temperature	223(2) K		
Wavelength	0.71073 Å		
Crystal system	Monoclinic		
Space group	$P2_1/c$		
Unit cell dimensions	$a = 8.2925(10)$ Å	$\alpha = 90^\circ$ .	
	$b = 15.354(2)$ Å	$\beta = 94.660(10)^\circ$ .	
	$c = 17.775(2)$ Å	$\gamma = 90^\circ$ .	
Volume	2255.8(5) Å <sup>3</sup>		
Z	4		
Density (calculated)	1.804 Mg/m <sup>3</sup>		
Absorption coefficient	2.594 mm <sup>-1</sup>		
F(000)	1214		
Crystal size	0.44 x 0.30 x 0.25 mm <sup>3</sup>		
Theta range for data collection	1.76 to 33.75°.		
Index ranges	-12 ≤ h ≤ 12, -23 ≤ k ≤ 22, -26 ≤ l ≤ 27		
Reflections collected	33139		
Independent reflections	8250 [R(int) = 0.0335]		
Refinement method	Full-matrix least-squares on F <sup>2</sup>		
Data / restraints / parameters	8250 / 0 / 267		
Goodness-of-fit on F <sup>2</sup>	1.023		
Final R indices [I > 2σ(I)]	R1 = 0.0467, wR2 = 0.1190		
R indices (all data)	R1 = 0.0753, wR2 = 0.1346		

**Table A.10.** Bond Lengths [Å] and Angles [°] for  $[\text{Ru}(\eta^3\text{-CH}_2\text{CHCHCH}=\text{CH}_2)\text{Br}(\text{Cp}^*)(\text{MeCN})]\text{PF}_6$ 

Ru(1)-N(1)	2.080(3)	Ru(1)-C(20)	2.273(3)
Ru(1)-C(2)	2.159(4)	Ru(1)-C(3)	2.299(4)
Ru(1)-C(50)	2.182(3)	Ru(1)-Br(1)	2.5522(5)
Ru(1)-C(40)	2.209(3)	Ru(1)-C(6)	3.205(4)
Ru(1)-C(1)	2.220(4)	P(1)-F(3)	1.481(5)
Ru(1)-C(30)	2.237(3)	P(1)-F(4)	1.490(5)
Ru(1)-C(10)	2.250(3)	P(1)-F(6)	1.508(6)

P(1)-F(5)	1.514(6)	C(50)-Ru(1)-C(20)	62.66(13)
P(1)-F(1)	1.572(4)	C(40)-Ru(1)-C(20)	62.28(13)
P(1)-F(2)	1.588(4)	C(1)-Ru(1)-C(20)	148.77(14)
C(1)-C(2)	1.404(6)	C(30)-Ru(1)-C(20)	36.93(14)
C(2)-C(3)	1.404(6)	C(10)-Ru(1)-C(20)	36.54(14)
C(3)-C(4)	1.455(6)	N(1)-Ru(1)-C(3)	82.54(13)
C(4)-C(5)	1.315(7)	C(2)-Ru(1)-C(3)	36.54(16)
C(6)-N(1)	1.126(5)	C(50)-Ru(1)-C(3)	127.29(14)
C(6)-C(7)	1.451(5)	C(40)-Ru(1)-C(3)	92.27(13)
C(10)-C(20)	1.418(5)	C(1)-Ru(1)-C(3)	64.09(16)
C(10)-C(50)	1.447(5)	C(30)-Ru(1)-C(3)	88.24(14)
C(10)-C(11)	1.489(5)	C(10)-Ru(1)-C(3)	150.19(14)
C(20)-C(30)	1.429(5)	C(20)-Ru(1)-C(3)	118.66(15)
C(20)-C(21)	1.496(5)	N(1)-Ru(1)-Br(1)	82.45(9)
C(30)-C(40)	1.439(5)	C(2)-Ru(1)-Br(1)	89.55(12)
C(30)-C(31)	1.497(5)	C(50)-Ru(1)-Br(1)	93.75(10)
C(40)-C(50)	1.437(5)	C(40)-Ru(1)-Br(1)	130.51(9)
C(40)-C(41)	1.484(5)	C(1)-Ru(1)-Br(1)	81.25(13)
C(50)-C(51)	1.495(5)	C(30)-Ru(1)-Br(1)	148.16(10)
C(52)-C(53)	0.611(12)	C(10)-Ru(1)-Br(1)	86.16(9)
C(52)-C(54)	0.734(14)	C(20)-Ru(1)-Br(1)	114.01(10)
C(52)-C(55)	1.798(17)	C(3)-Ru(1)-Br(1)	123.58(11)
C(53)-C(55)	1.49(2)	N(1)-Ru(1)-C(6)	0.97(11)
C(54)-C(55)	1.205(17)	C(2)-Ru(1)-C(6)	90.27(13)
N(1)-Ru(1)-C(2)	89.91(14)	C(50)-Ru(1)-C(6)	143.32(12)
N(1)-Ru(1)-C(50)	143.62(13)	C(40)-Ru(1)-C(6)	139.33(11)
C(2)-Ru(1)-C(50)	126.35(15)	C(1)-Ru(1)-C(6)	124.89(13)
N(1)-Ru(1)-C(40)	140.29(13)	C(30)-Ru(1)-C(6)	101.60(11)
C(2)-Ru(1)-C(40)	108.96(14)	C(10)-Ru(1)-C(6)	105.33(12)
C(50)-Ru(1)-C(40)	38.21(13)	C(20)-Ru(1)-C(6)	85.11(11)
N(1)-Ru(1)-C(1)	124.31(14)	C(3)-Ru(1)-C(6)	82.30(12)
C(2)-Ru(1)-C(1)	37.37(16)	Br(1)-Ru(1)-C(6)	83.36(7)
C(50)-Ru(1)-C(1)	90.38(15)	F(3)-P(1)-F(4)	89.1(6)
C(40)-Ru(1)-C(1)	86.92(14)	F(3)-P(1)-F(6)	179.4(4)
N(1)-Ru(1)-C(30)	102.55(13)	F(4)-P(1)-F(6)	91.2(6)
C(2)-Ru(1)-C(30)	121.56(15)	F(3)-P(1)-F(5)	93.3(6)
C(50)-Ru(1)-C(30)	63.45(13)	F(4)-P(1)-F(5)	176.7(6)
C(40)-Ru(1)-C(30)	37.77(12)	F(6)-P(1)-F(5)	86.4(6)
C(1)-Ru(1)-C(30)	118.47(15)	F(3)-P(1)-F(1)	93.1(3)
N(1)-Ru(1)-C(10)	105.58(13)	F(4)-P(1)-F(1)	86.9(3)
C(2)-Ru(1)-C(10)	163.20(15)	F(6)-P(1)-F(1)	87.5(4)
C(50)-Ru(1)-C(10)	38.08(13)	F(5)-P(1)-F(1)	95.3(3)
C(40)-Ru(1)-C(10)	62.90(12)	F(3)-P(1)-F(2)	87.2(3)
C(1)-Ru(1)-C(10)	125.84(15)	F(4)-P(1)-F(2)	89.8(3)
C(30)-Ru(1)-C(10)	62.10(13)	F(6)-P(1)-F(2)	92.3(4)
N(1)-Ru(1)-C(20)	85.81(13)	F(5)-P(1)-F(2)	88.0(4)
C(2)-Ru(1)-C(20)	155.18(16)	F(1)-P(1)-F(2)	176.7(3)

C(2)-C(1)-Ru(1)	69.0(2)	C(20)-C(30)-C(31)	125.9(4)
C(1)-C(2)-C(3)	117.4(4)	C(40)-C(30)-C(31)	125.5(4)
C(1)-C(2)-Ru(1)	73.7(2)	C(20)-C(30)-Ru(1)	72.9(2)
C(3)-C(2)-Ru(1)	77.2(2)	C(40)-C(30)-Ru(1)	70.05(19)
C(2)-C(3)-C(4)	123.6(4)	C(31)-C(30)-Ru(1)	130.0(3)
C(2)-C(3)-Ru(1)	66.3(2)	C(50)-C(40)-C(30)	107.8(3)
C(4)-C(3)-Ru(1)	121.4(3)	C(50)-C(40)-C(41)	126.6(3)
C(2)-C(3)-H(3A)	118.2	C(30)-C(40)-C(41)	125.0(3)
C(5)-C(4)-C(3)	123.9(5)	C(50)-C(40)-Ru(1)	69.87(19)
N(1)-C(6)-C(7)	177.9(4)	C(30)-C(40)-Ru(1)	72.18(19)
N(1)-C(6)-Ru(1)	1.8(2)	C(41)-C(40)-Ru(1)	130.8(3)
C(7)-C(6)-Ru(1)	177.4(3)	C(40)-C(50)-C(10)	107.5(3)
C(6)-N(1)-Ru(1)	177.2(3)	C(40)-C(50)-C(51)	126.3(3)
C(20)-C(10)-C(50)	108.0(3)	C(10)-C(50)-C(51)	125.6(3)
C(20)-C(10)-C(11)	126.0(4)	C(40)-C(50)-Ru(1)	71.93(19)
C(50)-C(10)-C(11)	125.8(4)	C(10)-C(50)-Ru(1)	73.50(19)
C(20)-C(10)-Ru(1)	72.6(2)	C(51)-C(50)-Ru(1)	126.3(3)
C(50)-C(10)-Ru(1)	68.42(19)	C(53)-C(52)-C(54)	31.4(15)
C(11)-C(10)-Ru(1)	129.0(3)	C(53)-C(52)-C(55)	50.9(15)
C(10)-C(20)-C(30)	108.8(3)	C(54)-C(52)-C(55)	28.4(12)
C(10)-C(20)-C(21)	125.8(4)	C(52)-C(53)-C(55)	110.5(17)
C(30)-C(20)-C(21)	125.4(4)	C(52)-C(54)-C(55)	134.7(19)
C(10)-C(20)-Ru(1)	70.82(19)	C(54)-C(55)-C(53)	10.9(9)
C(30)-C(20)-Ru(1)	70.17(19)	C(54)-C(55)-C(52)	16.9(8)
C(21)-C(20)-Ru(1)	126.4(3)	C(53)-C(55)-C(52)	18.6(5)
C(20)-C(30)-C(40)	107.9(3)		

**[Ru( $\eta^5$ -S-CH<sub>2</sub>CHCHCH=CH<sub>2</sub>)Br(Cp\*)]PF<sub>6</sub> (II-22)**

**Figure A.6.** ORTEP representation of [Ru( $\eta^5$ -S-CH<sub>2</sub>CHCHCH=CH<sub>2</sub>)Br(Cp\*)]PF<sub>6</sub> (thermal ellipsoids are drawn at 30% probability).

**Table A.11.** Experimental Data for the X-ray Study of [Ru( $\eta^5$ -S-CH<sub>2</sub>CHCHCH=CH<sub>2</sub>)Br(Cp\*)]PF<sub>6</sub>

Empirical formula	C <sub>15</sub> H <sub>22</sub> BrF <sub>6</sub> PRu	
Formula weight	528.28	
Temperature	233(2) K	
Wavelength	0.71073 Å	
Crystal system	Monoclinic	
Space group	<i>P2<sub>1</sub>/c</i>	
Unit cell dimensions	a = 19.0427(12) Å	$\alpha = 90^\circ$ .
	b = 12.7307(8) Å	$\beta = 115.158(2)^\circ$ .
	c = 16.7370(11) Å	$\gamma = 90^\circ$ .
Volume	3672.6(4) Å <sup>3</sup>	
Z	8	
Density (calculated)	1.911 Mg/m <sup>3</sup>	
Absorption coefficient	3.168 mm <sup>-1</sup>	
F(000)	2080	
Crystal size	0.40 x 0.20 x 0.20 mm <sup>3</sup>	



Theta range for data collection	1.18 to 28.28°.
Index ranges	-25<=h<=25, -16<=k<=16, -22<=l<=22
Reflections collected	42110
Independent reflections	9106 [R(int) = 0.0826]
Refinement method	Full-matrix least-squares on F <sup>2</sup>
Data / restraints / parameters	9106 / 528 / 443
Goodness-of-fit on F <sup>2</sup>	1.016
Final R indices [I>2sigma(I)]	R1 = 0.0536, wR2 = 0.1467
R indices (all data)	R1 = 0.0912, wR2 = 0.1660

**Table A.12.** Bond Lengths [Å] and Angles [°] for [Ru( $\eta^5$ -S-CH<sub>2</sub>CHCHCH=CH<sub>2</sub>)Br(Cp<sup>\*</sup>)]PF<sub>6</sub>

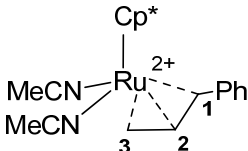

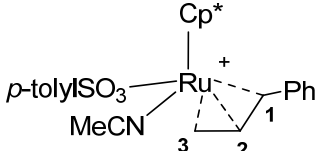
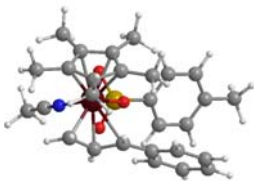
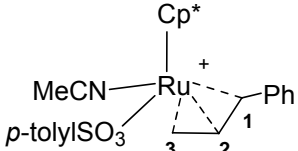
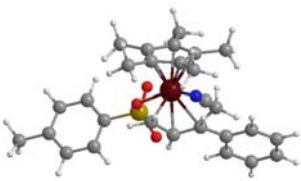
Ru(1)-C(4)	2.152(7)	C(50)-C(51)	1.485(10)
Ru(1)-C(3)	2.152(8)	C(2)-Ru(1)-C(3)	39.8(3)
Ru(1)-C(30)	2.190(7)	C(4)-Ru(1)-C(30)	173.1(3)
Ru(1)-C(2)	2.216(7)	C(3)-Ru(1)-C(30)	146.9(3)
Ru(1)-C(40)	2.221(6)	C(4)-Ru(1)-C(2)	67.8(3)
Ru(1)-C(20)	2.240(6)	C(3)-Ru(1)-C(2)	36.9(3)
Ru(1)-C(50)	2.241(6)	C(30)-Ru(1)-C(2)	118.8(3)
Ru(1)-C(1)	2.258(7)	C(4)-Ru(1)-C(40)	148.6(3)
Ru(1)-C(10)	2.273(6)	C(3)-Ru(1)-C(40)	109.6(3)
Ru(1)-C(5)	2.302(7)	C(30)-Ru(1)-C(40)	37.5(3)
Ru(1)-Br(1)	2.5288(8)	C(2)-Ru(1)-C(40)	89.8(3)
P(1)-F(4)	1.440(9)	C(4)-Ru(1)-C(20)	136.6(3)
P(1)-F(3)	1.446(8)	C(3)-Ru(1)-C(20)	147.8(3)
P(1)-F(5)	1.450(12)	C(30)-Ru(1)-C(20)	37.9(2)
P(1)-F(6)	1.475(13)	C(2)-Ru(1)-C(20)	151.4(3)
P(1)-F(1)	1.488(10)	C(40)-Ru(1)-C(20)	61.6(3)
P(1)-F(2)	1.511(10)	C(4)-Ru(1)-C(50)	120.1(3)
C(5)-C(4)	1.344(11)	C(3)-Ru(1)-C(50)	92.6(3)
C(4)-C(3)	1.465(11)	C(30)-Ru(1)-C(50)	62.9(3)
C(3)-C(2)	1.385(13)	C(2)-Ru(1)-C(50)	95.3(3)
C(1)-C(5)	1.429(12)	C(40)-Ru(1)-C(50)	37.3(3)
C(10)-C(50)	1.401(9)	C(20)-Ru(1)-C(50)	61.1(2)
C(10)-C(20)	1.400(10)	C(4)-Ru(1)-C(1)	79.2(3)
C(10)-C(11)	1.498(10)	C(3)-Ru(1)-C(1)	67.6(3)
C(20)-C(30)	1.438(9)	C(30)-Ru(1)-C(1)	104.9(3)
C(20)-C(21)	1.506(10)	C(2)-Ru(1)-C(1)	37.2(3)
C(30)-C(40)	1.419(11)	C(40)-Ru(1)-C(1)	96.5(3)
C(30)-C(31)	1.502(11)	C(20)-Ru(1)-C(1)	140.9(3)
C(40)-C(50)	1.428(11)	C(50)-Ru(1)-C(1)	121.4(3)
C(40)-C(41)	1.509(10)	C(4)-Ru(1)-C(10)	116.0(3)

---

C(3)-Ru(1)-C(10)	111.7(3)	C(4)-C(5)-Ru(1)	66.4(4)
C(30)-Ru(1)-C(10)	62.1(2)	C(5)-C(4)-C(3)	114.0(7)
C(2)-Ru(1)-C(10)	129.1(3)	C(5)-C(4)-Ru(1)	78.7(4)
C(40)-Ru(1)-C(10)	61.0(2)	C(3)-C(4)-Ru(1)	70.1(4)
C(20)-Ru(1)-C(10)	36.1(2)	C(2)-C(3)-C(4)	117.5(8)
C(50)-Ru(1)-C(10)	36.2(2)	C(2)-C(3)-Ru(1)	74.1(5)
C(1)-Ru(1)-C(10)	156.6(3)	C(4)-C(3)-Ru(1)	70.1(4)
C(4)-Ru(1)-C(5)	34.9(3)	C(3)-C(2)-C(1)	121.5(8)
C(3)-Ru(1)-C(5)	63.8(3)	C(3)-C(2)-Ru(1)	69.0(4)
C(30)-Ru(1)-C(5)	139.9(3)	C(1)-C(2)-Ru(1)	73.0(4)
C(2)-Ru(1)-C(5)	99.0(3)	C(2)-C(1)-Ru(1)	69.8(4)
C(40)-Ru(1)-C(5)	140.5(3)	C(50)-C(10)-C(20)	108.9(6)
C(20)-Ru(1)-C(5)	102.0(3)	C(50)-C(10)-C(11)	126.1(7)
C(50)-Ru(1)-C(5)	103.3(3)	C(20)-C(10)-C(11)	124.5(6)
C(1)-Ru(1)-C(5)	113.7(3)	C(50)-C(10)-Ru(1)	70.7(3)
C(10)-Ru(1)-C(5)	84.5(3)	C(20)-C(10)-Ru(1)	70.6(3)
C(4)-Ru(1)-Br(1)	86.0(2)	C(11)-C(10)-Ru(1)	130.8(5)
C(3)-Ru(1)-Br(1)	120.2(2)	C(10)-C(20)-C(30)	108.5(6)
C(30)-Ru(1)-Br(1)	88.94(19)	C(10)-C(20)-C(21)	126.6(6)
C(2)-Ru(1)-Br(1)	115.6(2)	C(30)-C(20)-C(21)	124.5(7)
C(40)-Ru(1)-Br(1)	124.5(2)	C(10)-C(20)-Ru(1)	73.2(4)
C(20)-Ru(1)-Br(1)	85.14(17)	C(30)-C(20)-Ru(1)	69.2(4)
C(50)-Ru(1)-Br(1)	146.12(19)	C(21)-C(20)-Ru(1)	129.1(5)
C(1)-Ru(1)-Br(1)	82.1(2)	C(40)-C(30)-C(20)	106.3(6)
C(10)-Ru(1)-Br(1)	115.26(17)	C(40)-C(30)-C(31)	126.4(7)
C(5)-Ru(1)-Br(1)	85.9(2)	C(20)-C(30)-C(31)	126.5(8)
F(4)-P(1)-F(3)	93.9(8)	C(40)-C(30)-Ru(1)	72.4(4)
F(4)-P(1)-F(5)	82.5(9)	C(20)-C(30)-Ru(1)	72.9(4)
F(3)-P(1)-F(5)	172.1(9)	C(31)-C(30)-Ru(1)	127.6(5)
F(4)-P(1)-F(6)	93.8(10)	C(30)-C(40)-C(50)	108.6(6)
F(3)-P(1)-F(6)	89.0(10)	C(30)-C(40)-C(41)	123.5(8)
F(5)-P(1)-F(6)	84.3(11)	C(50)-C(40)-C(41)	127.6(8)
F(4)-P(1)-F(1)	95.4(9)	C(30)-C(40)-Ru(1)	70.1(4)
F(3)-P(1)-F(1)	91.9(9)	C(50)-C(40)-Ru(1)	72.1(4)
F(5)-P(1)-F(1)	95.4(9)	C(41)-C(40)-Ru(1)	127.6(5)
F(6)-P(1)-F(1)	170.7(10)	C(10)-C(50)-C(40)	107.5(7)
F(4)-P(1)-F(2)	167.9(9)	C(10)-C(50)-C(51)	127.2(8)
F(3)-P(1)-F(2)	97.2(8)	C(40)-C(50)-C(51)	124.7(7)
F(5)-P(1)-F(2)	87.0(9)	C(10)-C(50)-Ru(1)	73.2(3)
F(6)-P(1)-F(2)	91.3(9)	C(40)-C(50)-Ru(1)	70.6(3)
F(1)-P(1)-F(2)	79.4(8)	C(51)-C(50)-Ru(1)	128.8(6)

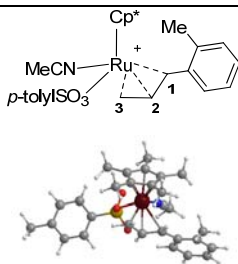
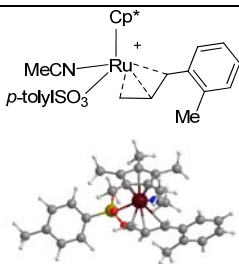
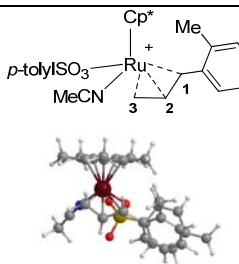
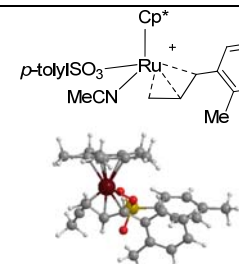
## 7.3. Computational Details

**Table A.13.** Optimized structures and selected metric and electronic parameters for complexes  $[\text{Ru}(\eta^3\text{-PhCH}_2\text{CHCH})(\text{Cp}^*)(p\text{-MeC}_6\text{H}_4\text{SO}_3)_{1-n}(\text{MeCN})_n]^{\text{n}+}$  ( $n = 0-1$ ).

	 	 	 
	IV-25	IV-26a	IV-26b
$C_{\text{Ru}}$	0.400	0.498	0.497
$C_{\text{C1}}$	-0.098	-0.141	-0.167
$C_{\text{C2}}$	-0.283	-0.269	-0.263
$C_{\text{C3}}$	-0.422	-0.444	-0.423
$C_{\text{allyl}}$	0.490	0.361	0.350
$d_{\text{Ru-C1}}/\text{Å}$	2.578	2.452	2.414
$d_{\text{Ru-C2}}/\text{Å}$	2.232	2.182	2.178
$d_{\text{Ru-C3}}/\text{Å}$	2.176	2.162	2.164
$\text{WI}_{\text{Ru-C1}}$	0.244	0.291	0.338
$\text{WI}_{\text{Ru-C2}}$	0.238	0.261	0.253
$\text{WI}_{\text{Ru-C3}}$	0.487	0.522	0.489

**C:** NPA charge; **WI:** Wiberg index (bond strength indicator); **d:** bond length.

**Table A.14.** Optimized structures and selected metric and electronic parameters for complexes  $[\text{Ru}(\eta^3\text{-}o\text{-MeC}_6\text{H}_4\text{CH}_2\text{CHCH})(\text{Cp}^*)(p\text{-MeC}_6\text{H}_4\text{SO}_3)(\text{MeCN})]^+$ .

	 <b>IV-27a</b>	 <b>IV-27b</b>	 <b>IV-27c</b>	 <b>IV-27d</b>
$C_{\text{Ru}}$	0.494	0.497	0.500	0.507
$C_{\text{C1}}$	-0.147	-0.156	-0.121	-0.130
$C_{\text{C2}}$	-0.271	-0.270	-0.281	-0.279
$C_{\text{C3}}$	-0.428	-0.424	-0.449	-0.449
$C_{\text{allyl}}$	0.376	0.361	0.377	0.359
$d_{\text{Ru-C1}}/\text{\AA}$	2.506	2.448	2.544	2.526
$d_{\text{Ru-C2}}/\text{\AA}$	2.194	2.184	2.198	2.206
$d_{\text{Ru-C3}}/\text{\AA}$	2.154	2.158	2.150	2.148
$\text{WI}_{\text{Ru-C1}}$	0.298	0.318	0.259	0.261
$\text{WI}_{\text{Ru-C2}}$	0.244	0.248	0.257	0.248
$\text{WI}_{\text{Ru-C3}}$	0.495	0.497	0.531	0.539
$C_{\text{Ru}}$	0.494	0.497	0.500	0.507

**C:** NPA charge; **WI:** Wiberg index (bond strength indicator); **d:** bond length.

## 7.4. Curriculum Vitae

Name:	Stefan Gruber
Date of Birth:	February 14 <sup>th</sup> , 1982
Nationality:	Swiss
Citizenship:	St. Niklaus (VS)
1989 – 1995	Primarschule in St. Niklaus (VS) (primary school)
1995 – 1997	Orientierungsschule in St. Niklaus (VS) (secondary school)
1997 – 2002	Kollegium Spiritus Sanctus in Brig (VS) (high school)
2002	Matura Typus C (high school degree in natural sciences)
2002 – 2006	B.Sc. Degree in Chemistry, ETH Zürich
2005 – 2006	M.Sc. Degree in Chemistry, ETH Zürich
2006 – 2009	Doctoral Thesis at ETH Zürich: “Ruthenium(IV) Catalyzed Allylation Using Allyl Alcohols as Substrates” under the supervision of Prof. P. S. Pregosin.